HIGHWAY RESEARCH RECORD

Number 239

Design and Performance of Pavement Systems

12 Reports

Subject Area

25 Pavement Design
26 Pavement Performance

HIGHWAY RESEARCH BOARD

DIVISION OF ENGINEERING NATIONAL RESEARCH COUNCIL
NATIONAL ACADEMY OF SCIENCES—NATIONAL ACADEMY OF ENGINEERING

Washington, D.C., 1968

Publication 1626

Price: $7.00

Available from

Highway Research Board
National Academy of Sciences
2101 Constitution Avenue
Washington, D.C. 20418

Department of Design

W. B. Drake, Chairman
Kentucky Department of Highways, Lexington

HIGHWAY RESEARCH BOARD STAFF

L. F. Spaine

PAVEMENT DIVISION

Milton E. Harr, Chairman
Purdue University, Lafayette, Indiana

COMMITTEE ON RIGID PAVEMENT DESIGN
(As of December 31, 1967)

F. H. Scrivner, Chairman
Texas Transportation Institute, College Station

Henry Aaron	W. Ronald Hudson, Secy.	Ernest T. Perkins
Phillip P. Brown	F. N. Hveem	Thomas B. Pringle
John E. Burke	W. H. Jacobs	M. D. Shelby
B. E. Colley	Wallace J. Liddle	W. T. Spencer
E. A. Finney	B. Franklin McCullough	William Van Breemen
Phil Fordyce	Phillip L. Melville	K. B. Woods
W. S. Housel		

COMMITTEE ON FLEXIBLE PAVEMENT DESIGN
(As of December 31, 1967)

Stuart Williams, Chairman
Bureau of Public Roads, Washington, D.C.

A. C. Benkelman	Frank B. Hennion	Frank P. Nichols, Jr.
John A. Bishop	Raymond C. Herner	R. L. Peyton
W. H. Campen	W. S. Housel	E. Guy Robbins
Bonner S. Coffman	Wallace J. Liddle	Donald R. Schwartz
Robert A. Crawford	R. E. Livingston	Emery L. Shaw
James M. Desmond	Alfred W. Maner	George B. Sherman
W. B. Drake	Chester McDowell	Eugene L. Skok, Jr.
Charles R. Foster	C. E. Minor	John H. Swanberg
John M. Griffith	Carl L. Monismith	B. A. Vallerga

COMMITTEE ON COMPOSITE PAVEMENT DESIGN
(As of December 31, 1967)

James H. Havens, Chairman
Kentucky Department of Highways, Lexington

Ernest J. Barenberg	Thomas B. Pringle	Russell N. Sharpe
Richard D. Barksdale	George W. Ring, III	John H. Swanberg
Karl H. Dunn	Robert L. Schiffman	William Van Breemen
Edward L. Kawala, Secy.	Donald R. Schwartz	Eldon J. Yoder
R. Ian Kingham	F. H. Scrivner	Ernest Zube
R. E. Livingston		

COMMITTEE ON THEORY OF PAVEMENT DESIGN
(As of December 31, 1967)

Aleksandar S. Vesic, Chairman
Duke University, Durham, North Carolina

W. F. Abercrombie	William J. Kenis, Sr.	Robert L. Schiffman
Richard G. Ahlvin	Carl L. Monismith	G. Y. Sebastyan
Eugene Y. Huang	R. G. Packard	James F. Shook
W. Ronald Hudson	William H. Perloff	Nai C. Yang

Foreword

Pavements have been important engineering structures throughout the history of modern man. Adequate roads made the Roman Empire great in its day, while the lack of good pavement in others made effective travel difficult and retarded development.

Within the last 20 years there has been a growing awareness among highway engineers of the need for more reliable methods for the design of pavement structures. This awareness has been reflected in a growing research program, including the AASHO Road Test, and has brought into sharper focus the true breadth of the problem. We have been aware for a number of years of the many complex pieces that act together in the pavement. Because of limitations in funding and the diversity of support in pavement research, our efforts have been fractionated into many diverse parts. This has been true not just in pavement design and research but in many other areas of civil engineering.

Within the past five years there has been a growing awareness of the need for an integrated approach in attacking complex civil engineering problems. This has resulted in the application of systems engineering techniques. The term "systems engineering" means many things to many people. Basically, however, it involves a unified systematic approach to a problem, recognizing the complex interrelations and feedback between the parts. It also brings out the important need to establish some type of criterion for judging the acceptability of the system.

As you can see by its title, "Design and Performance of Pavement Systems," the work in this RECORD recognizes the pavement as a system to some extent. Two of the papers, by Hutchinson and Haas and by Yang, discuss the system as a whole and make an attempt to put it into perspective. The other papers deal with specific important pieces of the system and by their very nature illustrate the breadth and complexity of the problems facing us.

The publication under the same cover of a variety of papers concerning pavement, ranging from prestressed concrete research to work with emulsified asphalt bases, is a desirable way to remind us of the complexity of the problem. I hope that this trend will continue. As you read the articles herein, keep in mind the relationship of that particular work to the total problem. All of us can then strive to relate our developments for more immediate application directly to the pavement system.

—W. R. Hudson

Contents

A Systems Analysis of the Highway Pavement Design Process

B. G. HUTCHINSON, Associate Professor of Civil Engineering,
University of Waterloo, and
R. C. G. HAAS, Assistant Professor of Engineering, Carleton University, Ottawa

•INVESTMENTS in highway and street systems represent a considerable portion of our national productive effort. A state of imperfect technology coupled with the high expenditures involved has generated a continually increasing amount of research into various aspects of the road transport activity. A significant amount of this effort has been directed toward developing a fundamental understanding of the behavior of highway pavements and the use of this information in their design.

The pavement design problem has been recognized as a major area of research by the U.S. Bureau of Public Roads in formulating its National Program of Research and Development in Highway Transportation (1). This program sets forth three broad problem areas of the highest priority to highway transportation. It attempts to recognize the technological and administrative aspects of each problem area by stating that the basis for support of individual projects will include importance, possible benefits, probability of success, usefulness, and uniqueness.

The actual application of these criteria to such areas as highway pavement research has a very subjective basis. It appears to place a major emphasis on the technological aspects of the problem without attempting to evaluate the economic implications or the probable payoff from investments of research resources in the technological subproblems identified. In addition, the problem statements are oriented toward the existing philosophy of pavement design, which fails to recognize explicitly the progressive nature of pavement deterioration or the age at which failure occurs. This prevents the optimization of capital investments and maintenance costs with respect to pavement types and component material alternatives.

This paper attempts to recognize in an explicit manner both the technological and economic attributes of pavements that are pertinent to their design. It demonstrates that a true rationalization of the highway pavement design process is best achieved through a comprehensive application of systems engineering principles. The principal objectives of the paper are (a) to provide a systems analysis of the highway pavement design process and to define each of the elements of this process; (b) to suggest methods for organizing existing information on each of these elements, to explore the deficiencies of available information, and to suggest methods for the systematic collection of information, its storage, retrieval, and analysis; and (c) to provide some preliminary discussion relating to a sensitivity analysis of the pavement design process, which will provide an ordering of the probable payoff that is likely to accrue from information generated on the various subproblems.

The paper is essentially divided into two major sections. In the first section, existing design procedures are reviewed and the current philosophy of pavement design and the deficiencies of these methods are discussed. A comprehensive systems analysis of the highway pavement design process is described in the second section, along with some of the requirements pertinent to a sensitivity analysis of the process.

Paper sponsored by Committee on Theory of Pavement Design and presented at the 47th Annual Meeting.

EXISTING DESIGN PROCEDURES

The principal objective of a highway pavement is to provide for the safe and efficient passage of highway vehicles across natural land forms under all climatic conditions. This objective may be accomplished by a large number of different types of pavement. The principal task of the engineer charged with pavement design is to select the pavement strategy that is the most economical to construct and maintain throughout the specified design period and provides adequate levels of service.

The existing design procedures for highway pavements are all oriented toward a specific pavement technology. Separate design procedures exist for conventional flexible pavements, pavements incorporating stabilized base courses, rigid pavements, and so on. Their formal development is limited to an analysis of certain technological features of each principal pavement type. A common design framework does not exist that permits the systematic evaluation of a variety of design alternatives and that allows the designer to proceed to the selection of the most economical pavement strategy.

A Classification of Procedures

Figure 1 provides a concise summary of the evolution of design methods for flexible pavements and indicates in a general way the principal features and limitations of these methods. Figure 2 provides a similar summary of the evolution of design methods for rigid pavements and emphasizes some of the advancements in technology that have characterized all approaches.

The general approach to pavement design from the turn of the century to the Second World War consisted essentially of using standard pavement sections and evaluating their actual field performance in terms of "satisfactory" and "unsatisfactory." However, higher vehicle speeds, greater loads, and increased traffic volumes indicated to a number of highway agencies the need for some form of objective structural design method. This need was reinforced during the war when higher quality airfield pavements were required to accommodate the heavier wheel loads and traffic volumes generated by the war. In addition, greater emphasis was placed on the development of specifications for controlling the quality of paving materials.

In the 1950's the theoretical approaches to pavement structural design began to be consolidated and their relation to the in-service behavior of pavements explored. The late 1950's and early 1960's produced the first comprehensive efforts at evaluating the validity of pavement design procedures through the systematic observation of the performance of full-scale pavements.

The AASHO Road Test (2), which was completed in the early 1960's, was intended to have a significant impact on current design methods. Unfortunately, the accelerated nature of this experiment and the dominant influence of traffic masked the effects of the climatic environment on pavement performance.

The Special Committee on Pavement Design and Evaluation of the Canadian Good Roads Association initiated probably the most comprehensive and systematic field study of pavement behavior yet undertaken, about 10 years ago. The principal findings of this Committee are well described in the literature (3, 4, 5). The investigation has provided the first systematic information on failure age and its relation to pavement structural design, traffic loadings and climatic conditions.

Deficiencies of Current Procedures

The principal limitations of current pavement design techniques that prevent a complete rationalization of the design process include the following:

1. The primary mechanisms of pavement failure and the processes of secondary deterioration are imperfectly understood;
2. The implications of new and significantly different pavement materials can only be evaluated after several years of field performance data are available;
3. The transfer of pavement performance data from one geographic locality to another is at present a very subjective operation;

METHODS	FEATURES	LIMITATIONS
A METHODS BASED ON "JUDGEMENT" Examples: Most Can. & U.S. Urban Centers; Ont. Dept. of Hwys.	Attempt to prevent failure. Simple and quick in application. Negligible design costs.	(1)No provisions in method for economic comparisons of pavement type alternatives (A,B,C,D,E,F,G). (2)Weak, subjective link between design and performance evaluation (A,B,C,D,E,F). (3)Failure to recognize effect of layers (A,B,C). (4)Environmental effects accounted for in only a very subjective manner (A,B,C,D,E,F). (5)Failure to account for effect of repeated loads on pavement deterioration (A,B,C,D,F). (6)Variations in construction quality not adequately accounted for (A,B,C,D,E,F). (7)Failure to recognize progressive nature of pvt. deterioration by considering only failure or non-failure condition (A,B,C,D,E,F). (8)No distinction between static or moving nature of loads (A,B,C,D). (9)Inadequate recognition of seasona strength variation of subgrades (A,B,C,D,F). (10)Simulation of in-service material behaviour not adequately evaluated in laboratory testing (A,B,C,D,F).
B METHODS BASED ON SIMPLE STRENGTH TESTS Examples: CBR or Modified CBR Method; U.S. Corps of Eng., Wyoming	Attempt to prevent failure. Simple equip. & proced. for meas. subgrade and base properties. Empirical correl. with pavement thickness.	
C METHODS BASED ON SOIL FORMULA Examples: Group Index Methods; Can. Fed. D.P.W., U.S. F.A.A. Method.	Attempt to prevent failure. Simple soil classif. tests to assign mean expected strength values to subgrade. Empirical link with pavement thickness.	
D METHODS BASED ON TRIAXIAL TEST Examples: Kansas Method, Texas Method, Calif. Method.	Attempt to prevent failure. Test values can be used in stability analysis of pavement components and subgrade.	
E METHODS BASED ON PLATE BEARING TEST Examples: U.S. Navy Method, Can. D.O.T. Method.	Attempt to prevent failure by limiting deflec. Full-scale testing of subgrade and pvt. structure reaction to load.	
F METHODS BASED ON STRUCTURAL ANALYSIS OF LAYERED SYSTEMS Examples: Burmister's Method, Shell 3-Layer Method.	Attempt to control or avoid failure mechanisms. Objective analysis to predict stresses and strains at any point in pavement or subgrade.	
G METHODS BASED ON STATISTICAL EVALUATION OF PAVEMENT PERFORMANCE Examples: Design Eqn. From AASHO Test, CGRA Design Guide.	Attempt to measure performance v. age relations and to control failure age by limiting deflections. Full-scale testing and evaluation	

1900 1910 1920 1930 1940 1950 1960 1967

Figure 1. Classification of the approaches to flexible pavement design.

METHODS	Features	Limitations
METHODS BASED ON "JUDGMENT"	Group A methods are characterized by attempts to prevent failure and are simple in application. Group B methods attempt to control or avoid failure mechanisms and generally incorporate fatigue criteria. Group C methods attempt to measure performance-age relationships and to produce predictive models of these. Some of the most marked features of all groups have recently consisted of advances in design and construction technology that include the following: 1.Machines with automatic controls. 2.Central-mixing plants. 3.Slip form pavers. 4.Mechanical placing of reinforcement 5.Dowel placing machines. 6.New joint forming techniques. 7.New curing compounds.	(1)No provisions in method for economic comparisons of pavement type alternatives (A,B,C). (2)Weak, subjective link between design and performance eval. (A,B) (3)Variations in construction quality not adequately accounted for (A,B). (4)Failure to recognize progressive nature of pavement deterioration by considering only failure or non-failure condition (A,B). (5)Environmental effects accounted for in only a very subjective manner (A,B). (6)No provisions in method for economic comparisons of alternative joint designs (A,B,C).
METHODS BASED ON STRUCTURAL ANALYSIS OF STRESSES AND DEFLECTIONS		
METHODS BASED ON STATISTICAL EVALUATION OF PAVEMENT PERFORMANCE		

1900 1920 1940 1960 1967

Figure 2. Classification of the approaches to rigid pavement design.

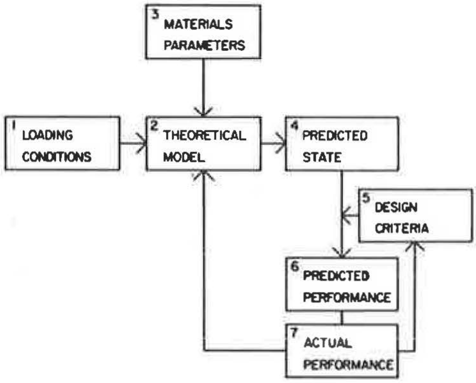

Figure 3. Structure of existing design procedures.

4. Pavement construction procedures and the natural heterogeneity of paving materials produce wide variations in the "quality" of the finished pavement, and current design procedures are unable to account for probable variations in this quality;

5. Laboratory methods of evaluating pavement material components in a manner that accurately simulates in-service time-temperature-age-stress-strain behavior are in a primitive state of development;

6. The optimization of initial capital and maintenance costs between alternative pavement types is impossible because of the lack of systematic information on performance;

7. The implications of changes in legal axle loads cannot be evaluated insofar as optimizing pavement investments in relation to the most efficient vehicle weights are concerned; and

8. Cost data for the various types of paving materials are not readily available for economic analyses of alternate pavement designs.

This listing indicates in a general manner a number of the factors retarding the development of a truly rational pavement design process. The literature contains many references to "rational" pavement design methods where the author implies that this involves accurate predictions of stresses and strains in various parts of the layered system through the use of structural analysis techniques. This paper uses the word "rational" in its broadest sense and implies that any rational method must consider not only the technological behavior of a pavement but also its economic characteristics.

Figures 1 and 2 summarize some of the principal limitations of current design procedures. While the models of pavement behavior underlying the various methods of design differ in detail, the basic philosophy underlying these methods is essentially the same and may be conveyed in the form shown in Figure 3. This diagram attempts to show that the constant interaction between the actual behavior of highway pavements and the models formulated to explain observed field behavior has stimulated the gradual evolution of design procedures.

Implicit in these current models of pavement behavior is the assumption that they are perfectly reliable predictors of actual pavement behavior, or at least some critical stress or strain condition within a pavement. The design criteria, which may be expressed either implictly or explictly as limiting deflections, stresses, and so on, are assumed to be absolutely indicative of failure conditions. In other words, the use of these design criteria implies either satisfactory or unsatisfactory pavement performance.

Pavement failure results from a progressive deterioration in pavement serviceability, which begins at the time a pavement is placed in service. The attributes of highway pavements of ultimate interest to the pavement design engineer are their probable failure ages and the cost streams necessary to achieve these service lives. With existing pavement design procedures, the relationship of the design criteria to probable service lives of pavements is based on subjective considerations rather than systematically collected evidence on field performance. In other words, in terms of Figure 3 the relationships between steps 4, 5, and 6 have not been formally established. The design criteria for highway pavements must not be viewed as ends in themselves but simply as a means to the prediction of failure age.

The current approaches based on the statistical analysis of the performance of actual pavements have measured failure ages directly and related these measurements to structural design, traffic loads, and climatic conditions. The major deficiency of these approaches is that it is difficult to generalize the results and use them for new pavement types for which little performance data are available. Their principal contribution arises from the information they give on the expected lives of pavement types that are currently

used. In this sense they do provide the pavement design engineer with the type of information required to optimize the capital and maintenance costs of pavements.

A HIGHWAY PAVEMENT DESIGN PROCESS

The need for a comprehensive formulation of a highway pavement design process that provides for the integration of both the technological and economic attributes of highway pavements has been discussed previously. An appropriate way of structuring any engineering design process is to organize it into six major phases: problem definition, solution generation, solution analysis, solution evaluation and optimization, implementation, and performance measurement.

The systems analysis of the highway pavement design process described in this section is subdivided into these six major phases.

Problem Definition

The problem definition phase can be further broken down into six major components, which are (a) objectives, (b) inputs, (c) outputs, (d) constraints, (e) cost function, and (f) decision criterion.

Objectives—The principal objectives to be fulfilled by a highway pavement are of an economic and social nature and may be expressed as follows:

1. To provide a pavement of adequate serviceability throughout its design life,
2. To provide pavements capable of permitting operating speeds and wheel loads of vehicles at levels that maximize the economic and social benefits to society of highway transportation, and
3. To minimize the total expenditures consumed by the provision of pavements.

In general, higher overall pavement serviceability qualities can be provided throughout a highway system by the expenditure of larger sums of money on pavements. Higher wheel loads and higher operating speeds can be permitted only through the expenditure of such larger sums of money. These three objectives therefore tend to be contradictory and ideally a procedure is required which will permit improvements in objectives 1 and 2 to be "traded-off" against increased expenditures.

At present it is impossible to approach such a trade-off in any rational manner. Minimum acceptable standards must be established for pavement serviceability, wheel loads, and operating speeds. These standards are based on the highway authority's interpretation of what proportion of their resources the public is willing to allocate to the achieving of such attributes in a highway system, relative to the resources they are willing to devote to other objectives such as education, recreation facilities, and so on. The pavement designer must then attempt to minimize the expenditures consumed by the provision of pavements within the constraints established by these standards.

The pavement design process, however, must be structured in a manner that allows the implications of changes in these standards to be explored. For example, in the future the pavement design engineer will no doubt be called on to predict the cost implications of providing pavements with minimum pavement serviceability levels that are capable of handling operating speeds of 100 mph instead of the current 60-70 mph. He will also be required to predict the cost implications of increases in legal axle loads.

Pavement Performance—Unlike many other types of engineering systems, highway pavements undergo significant physical deterioration during relatively short life spans. The progressive nature of such deterioration and the age at which pavement failure occurs are of paramount importance to the pavement design engineer. The fundamental operating characteristic of a highway pavement is its pavement serviceability-age history. A hypothetical pavement serviceability-age history for a flexible pavement is shown in Figure 4.

This history is defined in terms of three basic variables: the pavement serviceability (S), the pavement serviceability level at which pavement failure occurs (S^*), and the ages (A) at which S^* occurs. The history shown implies that one or more resur-

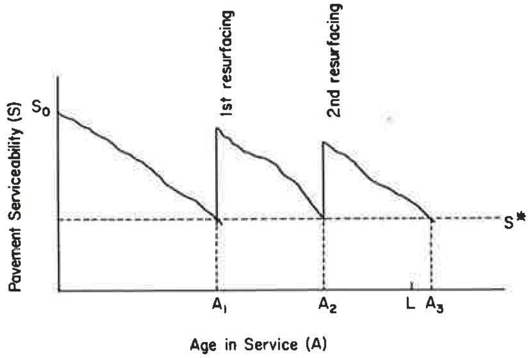

S = pavement serviceability
S_o = pavement serviceability at time of construction
S^* = failure level of pavement serviceability
A_1 = age at 1st resurfacing
A_2 = age at 2nd resurfacing
A_3 = age at failure of 2nd resurfacing
L = design life over which pavement strategies are compared

Figure 4. Generalized serviceability profile of highway pavements.

facings of the pavement occur during its life. The design life over which the economic characteristics of pavements will be compared is designated by the symbol L.

When a vehicle travels along a highway pavement, motions are generated in the body of the vehicle that are a function of the suspension characteristics of the vehicle, the speed of the vehicle, and the roughness of the highway pavement. The motion and vibration of the vehicle induce a response in the human occupants such as discomfort and fatigue and in some cases physiological damage.

Figure 5 (a) illustrates the components of this problem in terms of pavement roughness (r), vehicular characteristics (v), speed of the vehicle (p), vibration of the vehicle (m), and human response to this motion (h). Figure 5 (b) attempts to recognize the complexity of this problem and suggests by means of the matrix that the vehicular vibration generated by each combination of roughness r_i and vehicular class v_j will induce a set of human responses $\{h_{ij}\}$ for a fixed vehicular speed.

The problem facing the highway engineer is essentially one of averaging these human response measures to arrive at a single index that characterizes the extent to which a particular pavement section is serving the traveling public. This index, which must possess at least an interval scale status, has been called pavement serviceability and is shown in Figure 5 (b) as S_i. Terms used in Figures 4 and 5 are defined as follows in the sense in which they are used in this paper:

Pavement Roughness (r): the distortion of the pavement surface from the geometry of the designed pavement surface; this distortion may result from deficiencies in the original construction and permanent distortions induced by vehicular wheel loads and climatic conditions.

Pavement Serviceability (S): the average magnitude of human response to motion generated in highway vehicles by pavement roughness at a specified vehicular speed.

Failure Serviceability (S*): the level of pavement serviceability at which pavements are no longer considered to provide an adequate surface for the passage of vehicles at desired speeds.

Pavement Performance: the pavement serviceability-age history of a pavement.

The current procedure most commonly used for estimating pavement serviceability is that developed at the AASHO Road Test (2) in which a present serviceability rating is estimated subjectively. The validity of this procedure in estimating pavement serviceability depends on the subjective estimating abilities of the pavement raters and their facility to recognize each of the components classified in the matrix of Figure 5 (b).

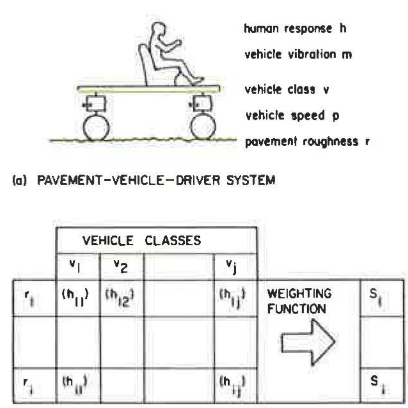

Figure 5. Components of pavement serviceability.

Hutchinson (6) has pointed out that if pavement serviceability measures are to be manipulated statistically, as they have been in the analysis of the AASHO Road Test data and in the CGRA studies (3), then they must achieve at least an interval scale status of measurement. In addition, if these measurements are to be used over longer periods of time and transmitted between various highway jurisdictions, then it would seem appropriate that the unit of measurement be stable and reliable.

It might be argued that a knowledge of the complete pavement serviceability-age history is not required and that only the failure ages need to be known. However, unless the total histories are known, it is impossible to evaluate such things as the cost implications of increasing the minimum acceptable level of pavement serviceability S*. Also, if a valid link is to be established between theoretical models of pavement behavior, cumulative damage theories, and pavement serviceability, then it is essential to have a precise knowledge of the pavement serviceability-age history. One further requirement of the pavement serviceability measure indicated by this discussion is that S* must be established independently of S.

The principles of subjective rating scale construction described by Hutchinson (6) indicate that the subjective units used by a pavement rater to express present serviceability ratings are highly dependent upon the spectrum of pavement serviceabilities to which the pavement rater has been exposed. In other words, the rating units actually used by a rater in a jurisdiction with a relatively narrow range of pavement serviceabilities will be quite different from the unit established by a rater in a jurisdiction with a wide range of actual pavement serviceabilities.

In addition, the fact that the level at which a pavement is no longer considered to serve the traveling public satisfactorily was observed to be equal to a present serviceability rating of 2. 5 (7) cannot be considered a fundamental characteristic of highway pavements. This observation could have been predicted from a knowledge of the characteristics of subjective rating scales without conducting any field experiments. It is well known that raters tend to gauge their feelings by scaling up and scaling down from some mean condition represented by the verbal cue average.

It must be re-emphasized that present subjective rating procedures used to estimate pavement serviceability do not provide measurements in a form that can be validly used for statistical manipulation or to explore the implications of changes in the level of S at which S* is considered to occur. S* is not independently established with present procedures. If significant advances are to be made in the measurement of pavement serviceability then S must be estimated from objective measures of human response. Hutchinson (25) has reported a preliminary attempt to measure human response to vehicular motion by a tracking test. At the present time the level of S at which S* is considered to occur must be established arbitrarily just in the same way that other highway standards are established.

Input Factors—The specification of the inputs to a highway pavement involves the identification of all those factors external to pavements that contribute to decrements in pavement serviceability. While many factors such as wheel loads, climatic factors, subgrade characteristics, and so on are known to influence pavement behavior, it is difficult to specify these factors in any quantitative manner. This difficulty arises from the existing lack of knowledge on the fundamental mechanisms of pavement deterioration. The manner in which these input factors are specified must be conditioned by the way in which this information is to be used. There is no justification for attempting to predict the loading spectrum to which a highway pavement might be subjected unless it is possible to use this information.

A primary factor that contributes to the deterioration of pavements in Canada and the Northern United States is the distortion of the pavement surface induced by frost action. The CGRA pavement evaluation studies (4) have indicated that flexible pavements that are structurally adequate with respect to traffic loads and located on light clay subgrades will deteriorate to an unacceptable level of pavement serviceability in about 15 years simply from the influence of climatic factors.

Differential frost heaving of a subgrade soil is influenced by a large number of factors, among which are the rate and degree of soil freezing, groundwater conditions,

SUBGRADE CLASSES

1. Rock
2. Well graded granular
3. Poorly graded granular
4. Silty sands and gravels
5. Silts
6. Low-medium plastic clays
7. Highly plastic clays
8. Peat

DRAINAGE CLASSES

1. Good
2. Imperfect
3. Poor

TRAFFIC CLASSES

1. Less than 1000 A.D.T.
2. 1000 - 3000
3. Greater than 3000

RAINFALL CLASSES

1. 30" per year
2. 40"

FREEZING INDEX CLASSES

1. Less than 1000 degree days
2. 1000 - 1500
3. 1500 - 2000
4. 2000 - 2500
5. Greater than 2500

Figure 6. Environmental classification.

minor variations in soil texture, pavement thickness, and so on. The pertinent climatic factors at a particular location can only be estimated in a statistical sense, yet frost heaving is a function of, among other factors, the specific temperature regime rather than some annual average statistic.

Shields and Dacyszyn (8) have reported one of the few systematic studies of the seasonal variation in strength of flexible pavements. The study examined the seasonal strength characteristics of some 24 pavement sections in Alberta that were observed over a period of five years. They concluded that "seasonal strength variation in flexible pavements is a widely fluctuating value which cannot as yet be related directly to pavement strength characteristics or to generalized climatic statistics. It would appear that these variations and fluctuations are greatly influenced by micro-climatic features which would require intensive evaluation and detailed analysis for control purposes."

Similar comments could also be made about other factors, such as the specification of probable traffic loads. It is only realistic for the pavement design engineer to classify the environmental factors in a relatively coarse manner. It would be meaningless at this stage to attempt to predict precisely the probable distributions of axle loads, climatic conditions, the properties of component materials, and so on, since the pavement design engineer cannot use this information. A similar approach is followed in structural design procedures in which general zones of earthquake intensity, snow loadings, wind loadings, and so on are established. A more detailed discussion of the factors influencing pavement performance is given in a subsequent portion of this paper.

A number of environmental classes have been established for the analysis of some Ontario pavement performance data, which are described later in this paper. These classes were based on a consideration of the following environmental factors: subgrade soil classification, freezing index, precipitation, drainage, and traffic conditions. The particular subclasses identified within each of the factors are shown in Figure 6.

Pavement Output—The pertinent output characteristics of a highway pavement have already been conveyed in Figure 4. Ultimately, the pavement design engineer is concerned only with two variables—the ages A at which S* occurs. With this knowledge and information on the cost stream required to produce the predicted pavement serviceability-age history, the designer is in a position to compute the cost characteristics of each of the alternatives.

Different pavement designs commonly involve expenditures of resources at various points in time as well as having different failure ages. In order to provide a common basis for the comparison of the economic properties of designs, a standard time base, or design life L, must be selected.

Constraints—The design constraints may be defined as those factors that limit the extent of feasible pavement designs. One constraint on the behavior of pavements has already been established—the minimum acceptable level of pavement serviceability, S*.

A second constraint is the magnitude of the interest rate used for the calculation of the annual costs. While many public authorities do not presently execute formal economic analyses of highway investments, the importance of such aids to public enterprise decision-making has been recognized and they are becoming used more widely. A question of fundamental importance in their use is the magnitude of the interest rate to be used in the calculations.

Many analysts have argued that no interest should be used in the evaluation of investments financed from current revenues and that interest rates should only be used in the evaluation of investments financed from borrowed capital. However, it is now generally accepted that a representative market interest rate should be included in all economic evaluations whether current revenues or borrowed capital are involved.

The financial resources of public authorities are currently allocated by means of a budgetary constraint imposed by the body politic. The prevalent opinion seems to be that, because of the large role assumed by the so-called intangibles associated with public operations, this allocation can only be achieved subjectively.

There are a number of well-known deficiencies in this type of approach and Alder (9) argues that the overall choice of the quantity of resources to allocate to highway transportation can be made only as a reflection of the sum of numerous individual projects that are judged to be sound. Kuhn (10) further points out that, for these individual economic evaluations to be meaningful, an interest rate representative of the current market rate must be included whether the financing is supplied from current revenues or borrowed capital. He points out that the interest rate is the only mechanism that provides a basis for the allocation of resources between the public and private sectors of the economy.

The third constraint that should be imposed on the pavement design process is also an economic constraint and is a maximum limit on the expected annual cost of the optimal pavement strategy. This maximum limit must be established from a consideration of the economic characteristics of the overall highway project, of which the pavement structure is only one element.

Cost Function—The cost function is simply a device that relates the output characteristics of pavements (i.e., failure age and capital costs) to the primary design objective, which has been established as the minimization of costs. The following cost function has been suggested by Baldock (11):

$$AC = CRF_L \left[C + E_1 (PWF_A) + E_2 \left(PWF_{A_r} \right) - \left(1 - \frac{y}{x} \right) (E_1 \text{ or } E_2)\, PWF_{A_r} \right] + M \quad (1)$$

in which

- AC = annual cost of a 2-lane mile of pavement and shoulders,
- CRF_L = capital recovery factor for a design life of L years and a specified interest rate,
- C = initial capital cost of pavement and shoulders per mile,
- A = failure age of the initial pavement (years),
- A_r = failure age of first resurfacing measured from the original time of construction (years),
- PWF = present worth factor for A or A_r years and the specified interest rate,
- E_1 = first resurfacing cost per mile,
- E_2 = second resurfacing cost per mile,
- y = number of years from time of last resurfacing to the end of design life period, i.e., ($L - A$ or A_r),
- x = estimated life of last resurfacing (years), and
- M = average annual maintenance cost per mile.

In order to predict the expected annual cost for each of the pavement strategies under consideration the design engineer must establish (a) capital costs, (b) failure age of the initial pavement, (c) failure ages of the resurfacings, (d) costs of the resurfacings, (e) interest rate, and (f) maintenance costs.

Decision Criterion—Since the objectives and the cost function are one-dimensional, the decision criterion is straightforward and may be concisely stated: select that pavement strategy with the minimum expected annual cost in dollars.

Figure 7 summarizes the problem definition phase by illustrating the interrelationships between the six components described.

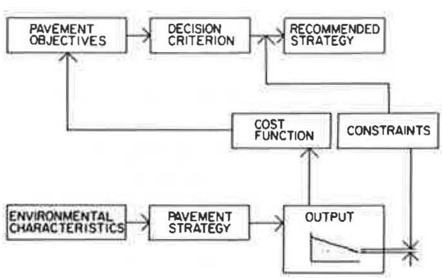

Figure 7. Components of the problem definition phase.

Solution Generation

There are a large number of potential solutions to a specific pavement design problem. These range from pavement strategies that have been used a large number of times and whose probable performance characteristics are well known, through to relatively new types of pavements for which very little performance information is available. The designs may consist of various types of portland cement concrete, asphaltic concrete surface courses supported by a variety of granular base courses and stabilized base courses, composite pavements, and so on.

Two general classes of potential solutions are established in this investigation, (a) standard pavement strategy, and (b) new pavement strategy. These two classes have been identified primarily as an aid to the analytical phase of the design process. Standard pavement strategy may be defined as a design type for specified environmental service conditions whose failure age distribution is known from accumulated relative frequency data on its performance. New pavement strategy may be defined as a pavement design type for which no prior experience or for which only limited evidence is available for specified environmental service conditions.

It is beyond the scope of this paper to list the possible pavement strategies that might be used as solutions to a pavement design problem. It is sufficient to state that at this stage of the pavement design process the pavement designer is faced with an array of possible solutions and he must select one of these strategies. The designer can assemble capital and maintenance costs fairly easily, but the problem is to predict the expected failure age in order to compute the expected annual cost of each strategy.

Solution Analysis

A method of approach for analyzing the two broad classes of highway pavements that are currently used is developed in this section. In addition, an approach to new pavement strategies is also described.

Flexible Pavements—It has been established previously that the principal technological problem is to predict the serviceability-age history for any pavement design alternative being considered. Typically, the conventional flexible pavement used by most authorities consists of a three-layer system with an asphaltic concrete surface course, a granular-type base course, and a subbase course of lower quality granular material. The principal objective of this phase of the design process is to generate sufficient information to allow the pavement designer to make a choice between overall pavement types. The selection of the most economical detailed design option within this overall pavement type is executed in the evaluation and optimization phase.

It has also been established that current flexible pavement design procedures do not permit serviceability-age histories to be predicted. However, the CGRA pavement evaluation studies do permit the serviceability-age histories to be predicted for standard pavement strategies. A number of regression models have been established for the Canada-wide data but difficulty has been experienced in arriving at a general model. Hutchinson (12) has examined the Ontario pavement performance data in an attempt to examine its usefulness for direct application to pavement design.

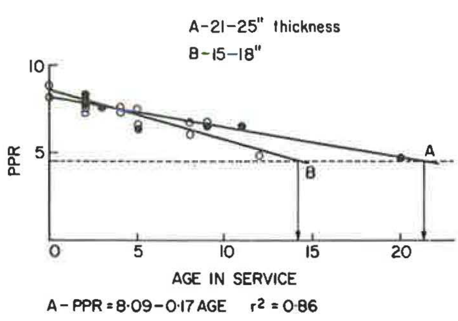

Figure 8. Pavement performance trends (pavements subjected to similar environmental conditions).

Available Ontario performance data have been sorted into common environmental classes of the type discussed previously and trends between present performance rating and the age in service has been plotted in the form shown in Figure 8. Pavement designs have been separated only in terms of total pavement thickness.

Lines were fitted to those serviceability-age histories for which sufficient data were

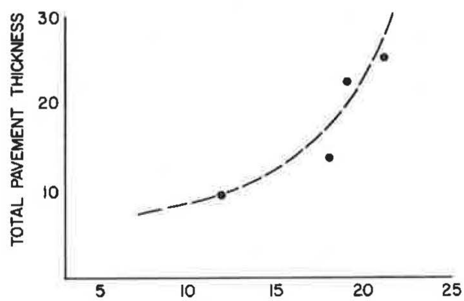

Figure 9. Thickness vs failure age for a particular environmental class.

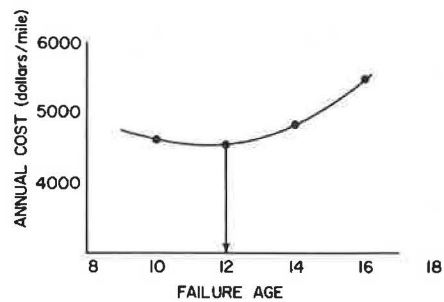

Figure 10. Annual cost curve for various pavement thicknesses.

available. In all other instances the serviceability-age trends were hand-fitted to the data subject to the constraint that the maximum value of the present performance rating at age 0 is equal to 8.5. This initial value is suggested by the field rating studies conducted by highway departments across Canada on many newly constructed pavement sections. The mean failure age in years has been scaled from the performance trend lines of this type at a present performance rating equal to 4.5 and used to prepare diagrams of the type shown in Figure 9. It must be emphasized that the thicknesses shown in

TABLE 1

ANNUAL COST COMPUTATIONS

TOTAL THICKNESS	FAILURE AGE	PWF_A	INITIAL[1] CAPITAL COST	RESURFACING COST	ANNUAL COST
9	10	0.5584	47,520	19,738	4,580
9.5	12	0.4970	49,456	20,534	4,560
11	14	0.4423	55,264	21,364	4,866
13.5	16	0.3937	65,944	22,228	5,492

1 - 2 x 12' lanes plus 2 x 10' shoulders

2 - thickness 1½" and price compounded @ 2% per annum to account for price increase plus 15% engineering and supervision costs

Assumptions

L = 25 years; i = 5%; X = 15 years

H_1 = 3", H_2 = 6" and H_3 = variable

Costs

asphaltic concrete surface course 3" thickness = $1.50/sq.yd.

granular base course 6" thickness = $0.95/sq.yd.

subbase course = $0.15/sq.yd./inch thickness

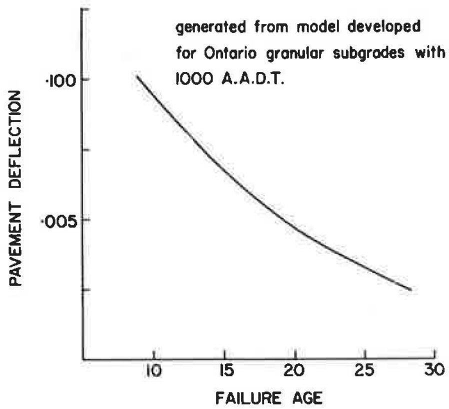

Figure 11. Deflection-age trend.

Figure 9 are total pavement thicknesses and consist of various combinations of surface course, base course, and subbase course thicknesses.

The information conveyed in Figure 9 can now be used to established a first estimate of the most appropriate total pavement thickness. Equation 1 can be used along with the type of information shown in Figure 9 to compute an annual cost curve as a function of failure age (or total pavement thickness). A typical set of computations is given in Table 1 and the information is summarized in Figure 10. This annual cost-failure age curve indicates that a total pavement thickness of about 10 inches would be the optimal design thickness for minimum annual cost and the expected life of the initial pavement would be 12 years. This optimality exists only for the cost information contained in Table 1 and the thickness-age relation of Figure 9. Different capital costs, resurfacing costs, thickness-age relation, etc., would of course change the optimal pavement thickness.

The preliminary analyses of the CGRA pavement evaluation data have shown that the surface deflections of flexible pavements are valid indicators of their relative strengths. Figure 11 shows a relationship that has been generated from the preliminary performance equations developed in this study. In addition, Meyerhof (13) has examined the relationship between the total pavement thickness and deflection for the CGRA data and the results of this study are shown in Figure 12.

Meyerhof suggests that, for normal flexible pavement thicknesses and from considerations of elastic theory, the theoretical relationship between the surface deflection and thickness may be expressed by

$$d \cdot D = C \tag{2}$$

in which

- d = surface deflection,
- D = total pavement thickness, and
- C = a constant for the standard CGRA Benkelman beam test,

and by

$$C = \frac{0.52\ W}{E_S^3\ n}$$

in which

- W = wheel load,
- E_S = subgrade modulus of elasticity, and
- n = the modular ratio of pavement to subgrade.

The deflection-thickness curves for various values of C are shown in Figure 12 and Meyerhof suggests the following average values:

Subgrade Type	C
Gravel	0.30
Sand	0.35
Silt	0.50
Clay	0.60
Peat	1.5-2.5

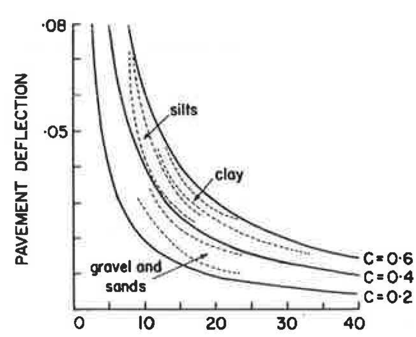

Figure 12. Deflection-thickness trends.

If relationships of the type shown in Figures 11 and 12 are available for a given environmental class, then they may be used along with cost data to arrive at an estimate of the optimal pavement thickness in the same manner as the information contained in Figure 9 was used.

The analytical framework described may be used to arrive at the optimal conventional flexible pavement strategy using the type of information obtained in the Canadian pavement evaluation studies.

The use of the surface deflection as an indicator of pavement strength is more sensitive than thickness since it also expresses some of the quality characteristics of the component materials. However, a large number of factors influence serviceability trends in flexible pavements.

Rigid Pavements—Very little systematic performance information is available for rigid pavements. The primary design variables that influence rigid pavement performance are slab thickness, the nature of the reinforcement, the joint designs, subbase properties, and subgrade properties.

Adequate performance data on rigid pavements with a variety of design variables are not currently available in Canada and an explicit procedure for arriving at the optimal rigid pavement design cannot be established. However, it would be a simple matter to calculate the annual costs associated with each rigid pavement design variation from capital cost estimates and failure-age predictions.

Factors Influencing Pavement Serviceability Changes—It has been established that the ultimate rationalization of the highway pavement design process is dependent upon a quantitative understanding of the rate of decrease in pavement serviceability with age in service. The prediction of this rate of change of serviceability must be based on an understanding of the factors causing the deterioration, their relative influence in a particular area or situation, and any interactions between these variables that influence the degree and rate of deterioration.

Figures 13 and 14 summarize the factors known to influence the performance of flexible and rigid pavements respectively. These flow charts do not attempt to indicate the relative importance of the variables but simply to classify them. The degree to which any of these factors, or combinations of factors, contribute to a loss in pavement serviceability is influenced by the climatic environment, quality of construction, and traffic at a particular location.

The diagrams show three main visible manifestations of pavement distress, which are further subdivided into a number of possible varieties. Since these classes of distress, in many cases, do not remain in their original or primary state, some of the possible consequences are shown. This secondary deterioration can often be much more detrimental to performance and in many cases may conceal the initial cause. It may also be responsible in certain cases for some confusion in field investigations of pavement failure mechanisms. Some of the factors identified in Figures 13 and 14 need to be further subdivided for a truly comprehensive picture of the pavement deterioration problem.

At the present time there is no generally accepted method for surveying pavement condition and classifying the various types of distress, and their relative importance in a particular area, as to the overall performance of a pavement. Research efforts have often tended to concentrate on factors that may be analytically complex but whose influence on pavement deterioration may be relatively minor.

The second step then, following the qualitative and comprehensive recognition of all the factors influencing performance, is broadly one of measurement and the development of techniques for the storage and retrieval of this information. The basic problem is to develop appropriate measurement techniques and to decide which are the most important factors in a particular jurisdiction. It is important that these techniques be developed not as ends within themselves but as useful means of providing information to predictive models of pavement performance. As previously pointed out, such models have been developed in Canada for rural highway conditions; however, they have a number of limitations, including applicability to most urban conditions. The format of the best of these models shows "age" as the most influential variable (14). This term en-

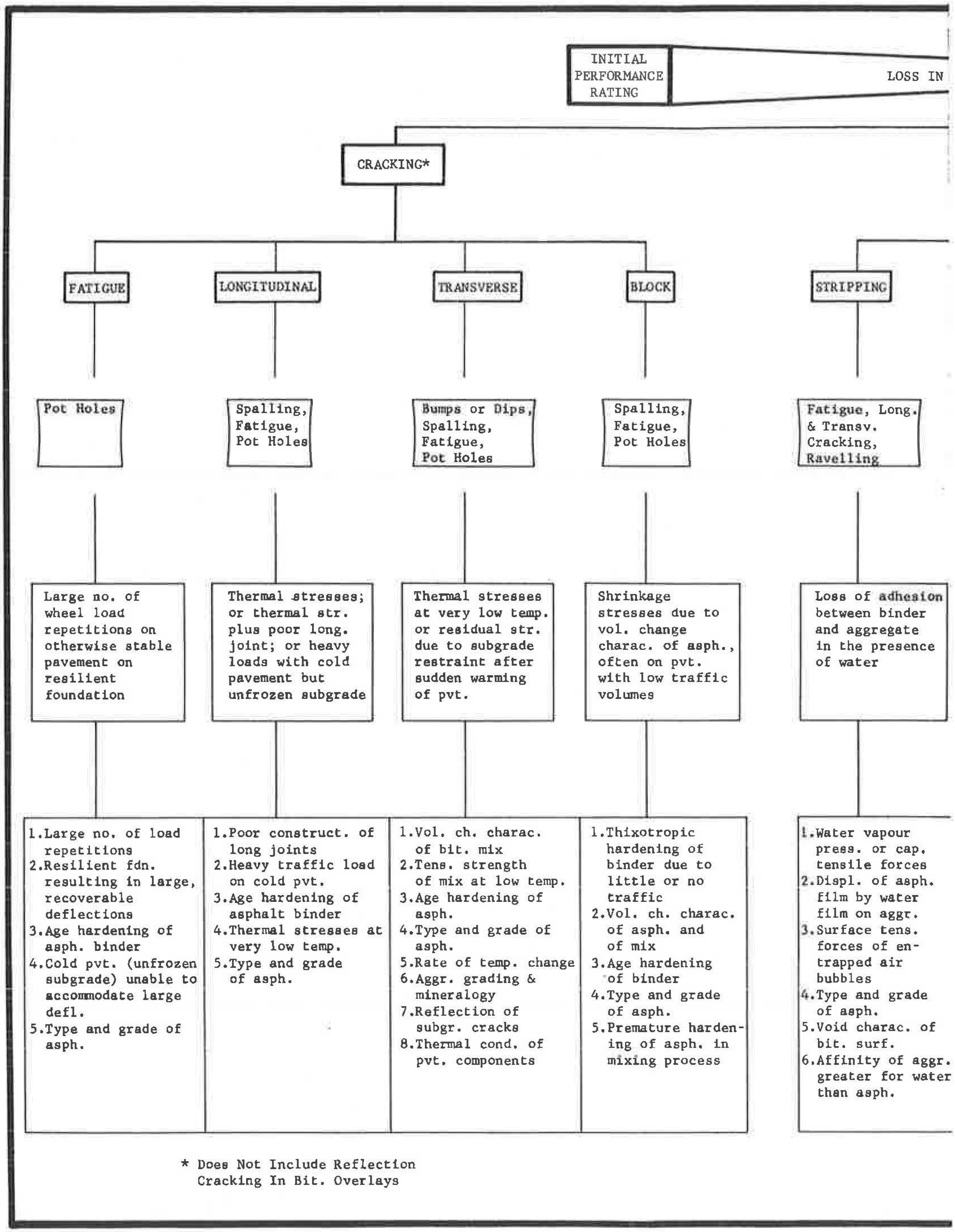

Figure 13. Qualitative representation of factors affecting flexible pavement performance.

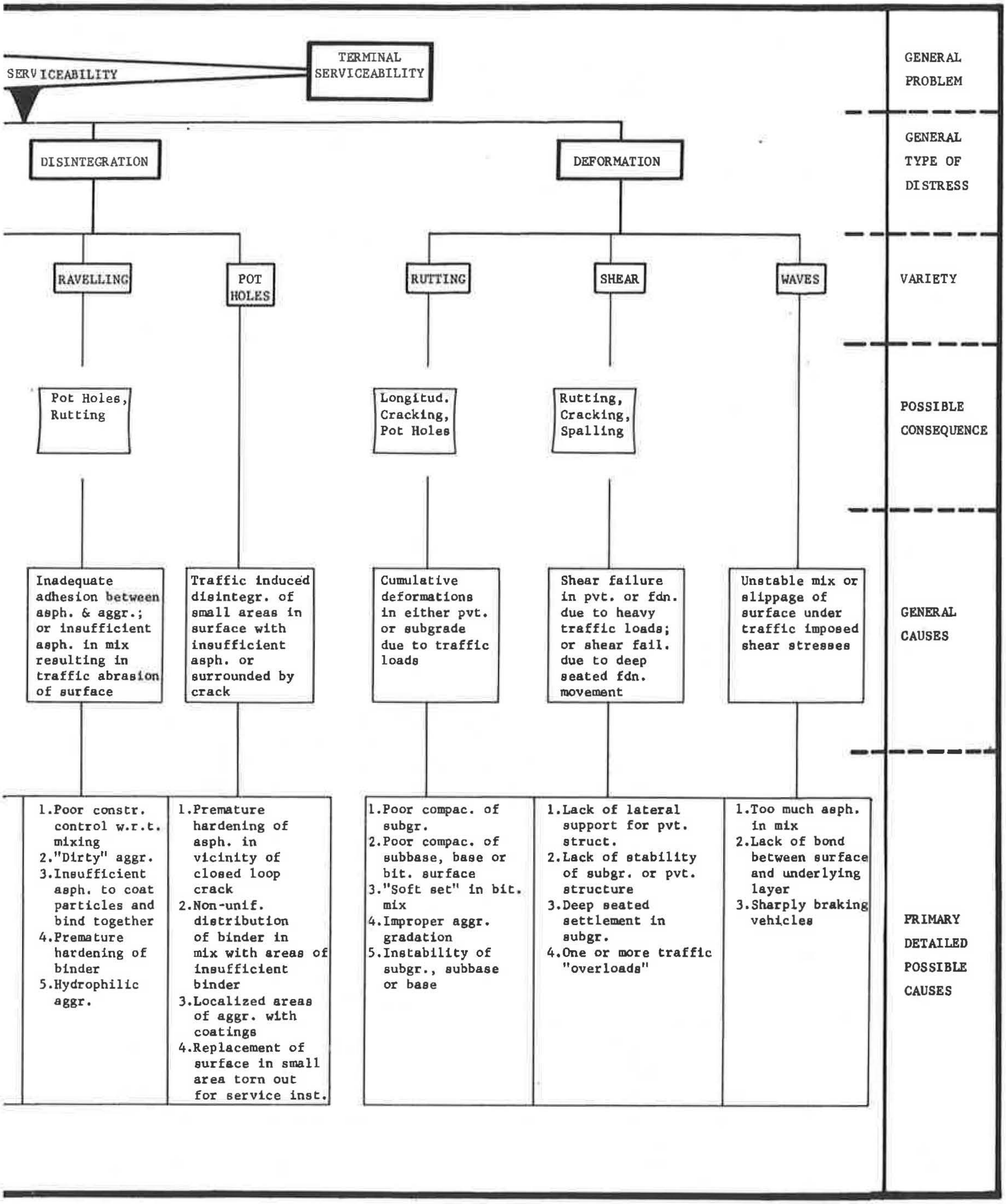

SERVICEABILITY
TERMINAL SERVICEABILITY
GENERAL PROBLEM
DISINTEGRATION
DEFORMATION
GENERAL TYPE OF DISTRESS
RAVELLING
POT HOLES
RUTTING
SHEAR
WAVES
VARIETY
Pot Holes, Rutting
Longitud. Cracking, Pot Holes
Rutting, Cracking, Spalling
POSSIBLE CONSEQUENCE
Inadequate adhesion between asph. & aggr.; or insufficient asph. in mix resulting in traffic abrasion of surface
Traffic induced disintegr. of small areas in surface with insufficient asph. or surrounded by crack
Cumulative deformations in either pvt. or subgrade due to traffic loads
Shear failure in pvt. or fdn. due to heavy traffic loads; or shear fail. due to deep seated fdn. movement
Unstable mix or slippage of surface under traffic imposed shear stresses
GENERAL CAUSES
1.Poor constr. control w.r.t. mixing 2."Dirty" aggr. 3.Insufficient asph. to coat particles and bind together 4.Premature hardening of binder 5.Hydrophilic aggr.
1.Premature hardening of asph. in vicinity of closed loop crack 2.Non-unif. distribution of binder in mix with areas of insufficient binder 3.Localized areas of aggr. with coatings 4.Replacement of surface in small area torn out for service inst.
1.Poor compac. of subgr. 2.Poor compac. of subbase, base or bit. surface 3."Soft set" in bit. mix 4.Improper aggr. gradation 5.Instability of subgr., subbase or base
1.Lack of lateral support for pvt. struct. 2.Lack of stability of subgr. or pvt. structure 3.Deep seated settlement in subgr. 4.One or more traffic "overloads"
1.Too much asph. in mix 2.Lack of bond between surface and underlying layer 3.Sharply braking vehicles
PRIMARY DETAILED POSSIBLE CAUSES

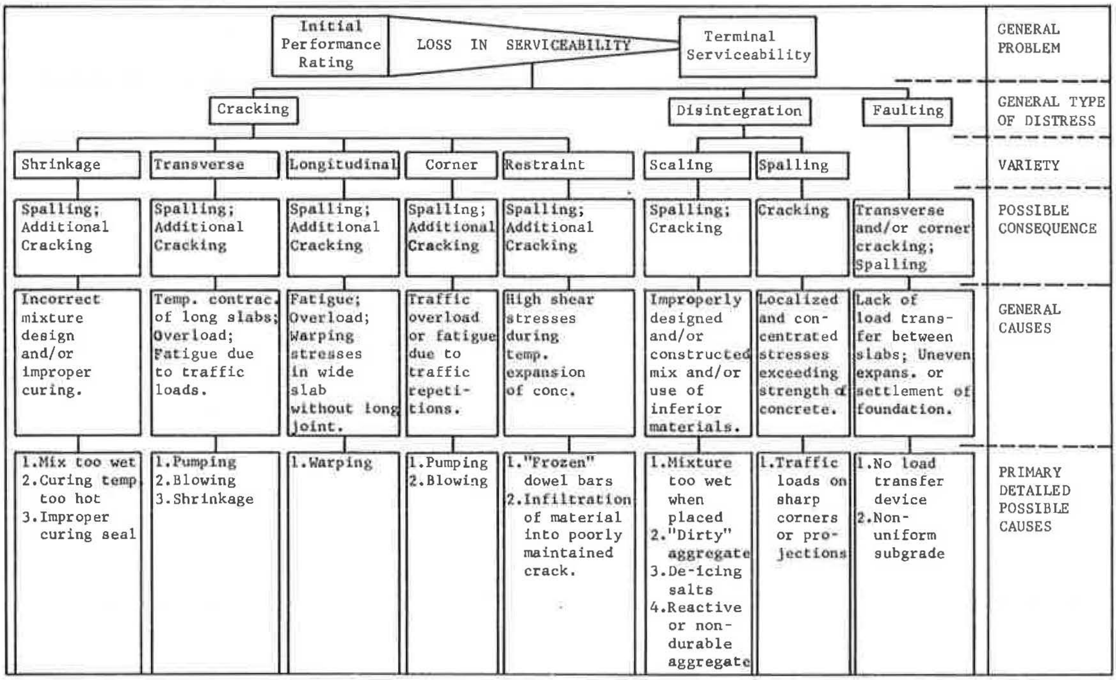

Figure 14. Qualitative representation of factors affecting rigid pavement performance.

compasses a number of the more detailed performance factors previously pointed out, which could ideally be incorporated into more precise predictive models if sufficient information were available.

The third broad step involved in progressing toward a comparative evaluation of all performance factors consists of investigating causal mechanisms of pavement distress. These investigations should be concerned with estimating the effects of various factors on the performance of the pavement structure, for a probable range of behavior. In addition, such investigations should be integrated with economic analyses of the potential payoff involved in being able to control any one factor. This type of approach can provide for optimum allocations of research and development funds. The current general situation of incomplete information makes such idealized comparisons impossible but in some cases allows the development of a sort of priority rating scheme based on subjective predictions of potential payoff. An example of this is the widespread incidence of transverse cracking of flexible pavements in Western Canada and the recent intensive research efforts in three prairie provinces (15, 16, 17, 18). Here, it was apparent that the secondary effects of transverse cracking were in many cases resulting in very rapid losses of serviceability for the pavements involved. It was further apparent that control of such deterioration could result in very substantial savings.

While the foregoing example is one in which large savings are possible without formal economic analysis of expected payoff, the probable payoffs on other performance factor evaluation and control are often not so apparent and require a greater degree of objectivity for rational decision-making. This includes the situation previously discussed where micro-climatic conditions control the performance of individual sections and data on certain factors in effect cannot be used by the designer.

New Pavement Strategies—The procedure previously described provides a basis for the analysis of those pavement strategies for which adequate performance information is available. The review of the information available in Ontario on the performance of

conventional flexible and rigid pavements indicated that this information was generally inadequate with the exception of a few environmental classes.

Two general classes of highway pavement have been identified in the Solution Generation phase. The basis for discrimination between these classes was stated to be the availability of performance data but a specified classification criterion was not established. Two additional procedures are required for the Solution Analysis phase. First, a rule must be developed that will permit a pavement to be classified as a standard pavement strategy or a new pavement strategy. Second, an overall framework is required that will permit new pavement strategies to be compared with standard pavement strategies in order to select the best course of action for a specific pavement design problem. A unified approach to both of these problems is developed in the following based on certain principles of Bayesian decision theory. The principles of Bayesian decision theory pertinent to this formulation have been reviewed by Hutchinson previously (19) and the following developments assume a knowledge of this information.

It has been pointed out that the failure age of the pavement strategy operating within a particular environmental class must be regarded as a random variable and this variable may be assumed to be normally distributed. In the procedure formulated for the selection of the optimum conventional flexible pavement design, it has been assumed that the expected or average value of the particular failure age distribution was adequate for analytical purposes. This is in fact an oversimplification, since the cost function is a nonlinear function of failure age.

The essential requirement involved in the analysis of new pavement strategies is to predict the failure age distribution, or the parameters of the distribution for the particular strategy. It is pertinent to consider in a general way how information on a new pavement strategy might be accumulated.

In the first instance preliminary laboratory tests and analysis may be performed to explore some of the implications of the new design but ultimately the probable failure age must be estimated from some very meager objective evidence or estimated subjectively. If the new design is judged to be superior when compared with the best standard design, then actual performance data can be accumulated with each successive implementation of the new design. Field performance meansurements involve the expenditure of significant amounts of resources and the problem is to establish the point at which the continued measurement of performance is no longer justified economically.

The essence of this problem when conveyed in terms of Bayesian decision principles can be conveyed in the form of a tree diagram as shown in Figure 15. The meanings of the symbols used are as follows:

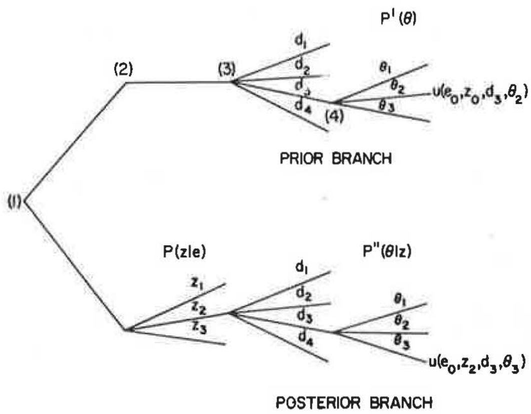

Figure 15. Simple decision tree.

d_0 = the decision to implement the new pavement strategy;

d_1 = the decision not to implement the new pavement strategy, which implies the use of the optimal pavement strategy;

θ = the state of nature that is a particular failure age;

e_0 = a dummy experiment, which conveys that no performance measurement is performed;

e_1 = performance measurement executed, which implies that the new pavement strategy should be implemented for trial;

z = the outcome of the new pavement strategy trial, which is its failure age;

u_t = the negative of the annual cost associated with the particular sequence of events expressed in the

brackets; e.g., $u_t(e_1, z_2, d_0, \theta_2)$ is the annual cost associated with the decision to measure first the performance, observe an outcome z_2 of this experiment, select a strategy d_0, and, finally, observe a failure age θ_2;

$P'(\theta)$ = the prior probability of occurrence of each possible failure age;

$P(z/e)$ = the probability of occurrence of each possible outcome of the experiment e;

$P''(\theta/z)$ = the posterior probability of occurrence of the failure age, given that the outcome of the experiment e is z; and

C_s = the negative of the annual cost of performance measurement.

The problem conveyed in Figure 15 can be described in general terms as follows. The designer is at node (1) and he must first decide whether to follow the prior branch and make an immediate choice between d_0 and d_1, or to postpone this choice by first implementing the new pavement strategy, measuring its performance, and on the basis of this new information making a choice between d_0 and d_1.

This type of problem can be approached by a method of analysis known as preposterior analysis, which is well described by Raiffa and Schlaifer (20). The essence of this method of analysis is that it provides a basis for evaluating the alternatives prior to actually implementing an experiment. The major features of this method of analysis are summarized in the following:

d' may be defined as the act that is optimal under the prior distribution of $\tilde{\theta}$:

$$E(\theta')\,[u_t(d', \theta)] \geq E(\theta')\,[u_t(d, \tilde{\theta})] \tag{3}$$

d_z may be defined as the act that is optimal under the posterior distribution of $\tilde{\theta}$, which has been determined by the outcome z of an experiment e:

$$E(\theta''|z)\,[u_t(d_z, \tilde{\theta})] = \max_d E(\theta''|z)\,[u_t(d, \tilde{\theta})] \tag{4}$$

If, instead of choosing the optimal prior act d' directly, the decision-maker performs an experiment e, observes an outcome z, and then chooses d_z he increases his terminal utility by

$$v_t(e, z) = E(\theta''|z)\,[u_t(d_z, \tilde{\theta})] - E(\theta''|z)\,[u_t(d', \tilde{\theta})] \tag{5}$$

$v_t(e, z)$ is termed the conditional value of the sample information z. Equation 5 can only be evaluated conditionally after a particular z has been observed. However, before z has been observed, the expected value of sample information can be computed from

$$v_t^*(e) = E(z|e)\,[v_t(e, \tilde{z})] \tag{6}$$

The economic significance of this quantity is that the expected terminal utility of a particular experiment is the expected utility of an immediate terminal action augmented by the expected value of sample information, which is

$$u_t^*(e) = u_t^*(e_0) + v_t^*(e) \tag{7}$$

The expected net gain of experimentation is defined as the expected value of sample information less the cost of obtaining it:

$$v^*(e) = v_t^*(e) - C_s \tag{8}$$

Analysis Process for New Pavement Strategies—These statistical decision principles can now be used to establish a systematic analysis process for new pavement strategies. This process is described as a sequence of steps:

1. List the expected annual cost of the optimal pavement strategy, AC_S.

2. List any observed failure ages for the new pavement strategy operating under the same environmental conditions and calculate the relative frequency of occurrence of each failure age. If prior evidence is not available, then these relative frequencies may be estimated subjectively.

3. Establish the cost function for the new pavement strategy in the form shown in Eq. 1. This is a straightforward procedure with the notable exception of the resurfacing costs expressed by the term E_1. This cost estimate must include not only the internal costs such as engineering and material costs but also the external costs to highway users that may result from the resurfacing operation. While the dollar value associated with these generally intangible costs is difficult to evaluate it is important that they be included in this manner in order to place the costs in their proper perspective. It is interesting to note certain comments by Moyer and Lampe (21) in this regard: ". . . in the selection of pavement type for urban freeways with traffic volumes ranging from 50,000 to 200,000 vehicles per day, portland cement concrete has generally been selected as the preferred pavement type in California because the traffic delays and accident hazards created by pavement repairs and resurfacing have been assumed to be much greater on asphalt concrete pavements than on portland cement concrete pavements. This study indicated that the magnitude and importance of the traffic delay and accident costs in the selection of pavement type for urban freeways has been greatly exaggerated. There is evident need for conducting factual studies to determine the true nature of these costs."

4. Calculate the expected value of sample information from

$$v_t^*(e) = E(z|e)\ \{E(\theta''|z)\ [u_t(d_z, \tilde{\theta})] - E(\theta''|z)\ [u_t(d', \tilde{\theta})]\} \tag{9}$$

5. If $v_t^*(e)$ is positive then the optimal prior act should be selected. (Remember that u_t is the negative of the annual cost.)

6. Calculate the annual cost of performance measurement and express it as C_s. If $v_t^*(e)$ is negative then execute performance if

$$|v_t^*(e)| \geq C_s \tag{10}$$

This implies that the new pavement strategy is selected for use even though it may not have been optimal with respect to immediate terminal action.

7. Calculate the expected utility of the new pavement strategy with respect to immediate terminal action:

$$u_t^*(e_0, d_0) = E(\theta''|z)\ [u_t(d_0, \theta)] \tag{12}$$

8. The new pavement strategy may be regarded as a standard pavement strategy if

$$u_t^*(e_0, d_0) \geq u_t^*(e, d_0) - C_s \tag{13}$$

Solution Evaluation and Optimization

At the completion of the solution analysis phase the pavement designer will have an estimate of the expected annual cost of each of the major types of pavement that he has considered. The objective of this phase is to explore the implications of the detailed design options that are possible within the most promising major design type.

This operation is particularly important for flexible pavements, in which equivalent strengths can be achieved by a large number of different combinations of layer thicknesses. The optimum combination is a function of the relative costs of the layer materials and their relative contributions to pavement strength.

For example, the layer equivalency equation developed at the AASHO Road Test (2) for flexible pavements,

$$D = 0.44D_1 + 0.14D_2 + 0.11D_3 \tag{14}$$

can be achieved by a large number of different combinations of layer thicknesses (subject to the constraints $D_1 \geq 2$ inches and $D_2 \geq 3$ inches). The optimum combination is a function of the relative cost of the layer materials and their relative contributions to pavement strength. If the cost data for each layer are given per inch of depth and per square yard of surface, and these might be, for example,

c_1 = \$0.50 per sq. yd. per inch of thickness,
c_2 = \$0.15 per sq. yd. per inch of thickness, and
c_3 = \$0.07 per sq. yd. per inch of thickness,

the total cost is given by

$$C = D_1 \cdot c_1 + D_2 \cdot c_2 + D_3 \cdot c_3$$

and the problem is to minimize C by selecting values for D_1, D_2, D_3 that will result in a specified thickness index D. This is a simple problem and may be solved by calculating the cost/contribution ratio for each layer:

layer 1: $\frac{0.50}{0.44} = 1.138$

layer 2: $\frac{0.15}{0.14} = 1.071$

layer 3: $\frac{0.07}{0.11} = 0.636$

Equation 14 demands that minimum thicknesses of 2 inches and 3 inches be used for the surface and base courses respectively. For the above conditions the remainder of the pavement should consist of layer 3 material since it possesses the minimum cost/contribution ratio.

More complex optimization techniques such as linear programming may be involved for other pavement types, such as rigid pavements, where various detailed design options may possess differential contributions to strength and relative costs.

Information Systems—The solution analysis phase of the systems process discussed in this paper is basically dependent on a certain amount of the appropriate evaluation data. Unfortunately, the required information systems are generally quite inadequate for the degree of sophistication we may desire for comparative analyses and in fact are in a very premature state of development, even for urban planning purposes. The first of these systems directly associated with the transportation field and using computer technology have come from the need to produce data for urban transportation planning models. However, as pointed out by Horwood (22), these have been generally ad hoc in nature and have been produced to satisfy their predominant purpose of traffic forecasting. Consequently, such approaches have produced very little "spin-off" in utilizing the information gathered for other purposes, largely because of the varied methods of organizing data and the attendant difficulties in processing. This type of situation applies to the field of highway pavements to an even greater degree but it appears that, because of the strong interest recently shown in development of urban data banks and the corresponding experience gained, plus the marked increases in computer operational capabilities, the development of highly flexible and sophisticated information systems for such purposes can soon become a distinct reality. It further appears that the professional groups charged with the attendant responsibilities must also be well versed in the statistical methodology of experimental design and analysis of variance and will provide a highly significant coordinating function within any one agency, such as a state or provincial highway department.

Before considering the basic requirements of an information system, it may be useful to list the major phases involved in considering the overall capability of such a system. In summary form these are

1. Proposed use of data,
2. Collecting the data,
3. Organizing the data,

4. Storing the data,
5. Retrieving the data, and
6. Analyzing the data.

When a decision has been made that some sort of automated storage and retrieval system is necessary for a highway agency to handle its planning, design, evaluation, cost, and maintenance data, then it immediately faces a series of basic questions which include the following:

1. What computer hardware equipment is required? This problem involves a variety of sub-problems and may in itself require a fairly detailed systems approach. It depends on such factors as the applicability and availability of the agency's current data-processing equipment, the quantity of information to be stored, the wide variety of available systems on the market, future requirements for data storage, software problems, available funds, availability of technical manpower, etc.
2. What purposes is the information to be used for? This is perhaps one of the most fundamental questions because it determines what data are to go into the system and what the analyses will be. If it is not adequately answered, the entire system can become most inefficient. In other words, as pointed out by Barraclough (23), a careful examination of the proposed use of each item of information must be made before a decision is reached to collect it.
3. What type of geocoding system is required? In the field of highway pavements, there can be little argument with the basic premise that some sort of locational identification of data is required. A number of systems are in current use or have been proposed for transportation planning, urban planning, and other purposes and have been discussed by Vance (24). His recommendation of the existing Universal Transverse Mercator Grid for use by transportation planners seems to be compatible with the highway pavement situation and the system could be used in a similar manner.
4. What type of query system is required? Querying refers to the techniques used to gain access to data in a variety of combinations, with efficiency. It is important that the system be developed for wide applicability and flexibility; otherwise each analysis will require its own specific retrieval technique. Horwood (22) has discussed the requirements of a good query system with respect to transportation planning and has stated, "A data handling procedure designed for ease of use is the single most important element of an information system." His comments are also significant to the data-programming requirements associated with the topic of this paper.
5. What type of output devices are required? Automatic graphic display of information is perhaps much more important to transportation and urban planning functions than to the highway pavement information system. However, a wide variety of relatively sophisticated graphic display subsystems are being developed and the possible applicability of these to producing plotted results of the stored data analyses warrants careful consideration.
6. What are the operational needs of the system? These requirements refer to day-to-day processing operations, production of output data at specific time intervals, generation of reports, and other functions.

The question of intended use of any item of stored data has been pointed out as fundamental to the problem of what data are to be stored. Barraclough (23) discusses some of the implications of either not getting required or sufficient data, or of getting unusable data, and goes on to present a long list of the sorts of items of information that might be desirable for land-use models. A similar listing for flexible pavement performance prediction models, with a sample in-depth listing of the transverse cracking factor (assuming that the appropriate objective measurement techniques have been developed) is presented, with the aid of Figure 13, for any particular evaluation section as follows:

1. Fatigue cracking
2. Longitudinal cracking
3. Transverse cracking (see detail)
4. Block cracking

5. Stripping disintegration
6. Raveling disintegration
7. Pot-hole disintegration
8. Rutting deformation
9. Shear deformation
10. Wave deformation
11. Gross pavement performance data
12. Traffic data
13. Environmental data
14. Construction data by variations in properties of as-placed specification items

    3a. Continuous temperature profile of pavement layer
    3b. Depth of frost penetration
    3c. Continuous precipitation record
    3d. Continuous recording strip to measure time of cracking
    3e. Continuously recorded stress and strain data
    3f. Void and density characteristics of the bituminous surface
    3g. Geotechnical characteristics of the subgrade
    3h. Volume, density, and moisture characteristics of the subgrade
    3i. Mineralogical characteristics of the pavement aggregates
    3j. Rheological characteristics of the binder at various age intervals
    3k. Rheological and tensile strength characteristics of the bituminous surfacing mixture at various age intervals
    3l. Rheological profile through the depth of the bituminous surface at various age intervals
    3m. Thermal conductivity and expansion-contraction characteristics of the bituminous surface
    3n. Amount of binder in the bituminous mixture
    3o. Gradation characteristics of the pavement aggregates
    3p. Source of binder for the bituminous surface mixture.

This in-depth listing could in some cases be further broken down into a number of sub-factors; in any case, it serves to illustrate the somewhat staggering array of information that might be collected. It further implies that an indiscriminate collection of such data would result in an information system of considerable complexity and great cost, in addition to the overwhelming efforts and costs associated with actually obtaining the required field and laboratory measurements. What is needed, then, is some sort of ordering system that establishes, say, first-order information, second-order information, and so on. The decision as to how specific items of data fit into the ordering system must be based on their relative influence on pavement performance. Such analyses of sensitivity, as previously discussed, depend on both technical and economic payoff considerations. Technical evaluations can often be very efficiently accomplished through carefully designed and controlled field experiments in which the pavement is a part of the regular highway system. An excellent example of this is the recent Saskatchewan field experiment on transverse cracking of flexible pavements in which it was concluded that asphalt source could significantly affect the degree of such cracking (17). Unfortunately, this type of planned experimentation has seen very limited use among highway agencies, although there are many situations where it could be employed to considerable advantage with very little additional expenditure during planning, design, construction, or operation.

Decisions as to what depth in the ordering system is to be used for data acquisition and storage depend on such factors as costs of obtaining the data, sensitivity of the model to the data, payoff involved in increased model sensitivity, and capability of the information system itself.

Implementation

A fundamental problem in the implementation phase of the highway pavement design process is to produce materials of a quality and homogeneity that are essentially in

agreement with the assumptions underlying the structural design of the pavement. The future performance of a pavement and its associated maintenance costs are directly related to the success in achieving these desired levels of quality.

Present quality control methods for highway paving materials are largely intuitive procedures conditioned by the construction engineers' experiences and the results of casual materials tests. In addition, the rationale underlying present highway materials specifications is largely arbitrary and frequently bears little relation to the actual capabilities of the various construction processes. Formal quality control procedures are required that are an integral part of the total highway pavement design process.

Very little systematic evidence has been obtained to illustrate the influence of the quality of construction on pavement performance. Wilkins (26) has shown for the Canadian pavement evaluation studies that minor areas of surface distress strongly influence the serviceability rating assigned to a pavement section. He has noted that if failure occurs in only 5 percent of a section the pavement is considered unacceptable as to serviceability and must be repaired or rehabilitated in spite of the fact that large areas of the pavement may have relatively high ratings. Economic implications of nonuniformity of construction indicate that the development of formal quality control procedures for construction probably has the greatest potential payoff of any area of the highway pavement design process.

SUMMARY AND CONCLUSIONS

The development of a rational highway pavement design process requires the ability to predict the pavement serviceability-age history of a potential highway pavement design under the expected traffic loadings, the climatic conditions, and the cost streams necessary to produce this serviceability profile. With the development of this capability the pavement designer is in a position to make a rational decision involving the selection of that design alternative which provides an adequate level of pavement serviceability throughout the design life and which is the most economic to construct and maintain.

Current approaches to pavement design do not formally recognize that a significant amount of physical deterioration can be tolerated in highway pavements and that this physical deterioration only has meaning with respect to the vehicles using a highway and their human occupants. In effect, they are oriented toward the concept of only satisfactory or unsatisfactory pavement performance.

Systematic field performance studies in Canada have indicated that pavements that are adequately proportioned to carry traffic loadings will deteriorate due to nonload associated factors. A quantitative understanding of the factors that induce this progressive deterioration in pavement serviceability is largely hindered by a lack of knowledge of the mechanics of pavement behavior.

A systems analysis of the highway pavement design process has been developed in this paper that attempts to recognize in a formal way both the technological and economic characteristics of highway pavements. The total process is broken down into its principal phases, which are problem definition, solution generation, solution analysis, evaluation and optimization, implementation, and performance assessment.

The current state of knowledge within each of these principal phases is reviewed and the relative importance of the deficiencies in knowledge discussed. The need for a properly designed data and retrieval system for field-performances studies is discussed and recommendations regarding such a system are set forth.

The primary deficiencies in current knowledge regarding pavement structures are considered to lie in the areas of field performance evaluation and quality control. In addition, the development of a comprehensive understanding of the nonload-associated causes of pavement deterioration and their relative effects on performance is essential to rationalizing the design process.

ACKNOWLEDGMENT

The studies on which this paper is based were supported by the National Research Council of Canada, the Ontario Department of Highways and the British American Research and Development Co.

REFERENCES

1. National Program of Research and Development in Highway Transportation. U.S. Bureau of Public Roads, Jan. 1967.
2. The AASHO Road Test: Report 5—Pavement Research. HRB Spec. Rept. 61E, 1962.
3. A Guide to the Structural Design of Flexible and Rigid Pavements in Canada. Canadian Good Roads Association, Sept. 1965.
4. Pavement Evaluation Studies in Canada. Proc. Internat. Conf. on Structural Design of Asphalt Pavements, Univ. of Michigan, 1962.
5. Field Performance Studies of Flexible Pavements in Canada. Proc. Internat. Conf. on Structural Design of Asphalt Pavements, Univ. of Michigan, 1967.
6. Hutchinson, B. G. Principles of Subjective Rating Scale Construction. Highway Research Record 46, p. 60-70, 1964.
7. Rogers, C. F., Cashell, H. D., and Irick, P. E. Nationwide Survey of Pavement Terminal Serviceability. Highway Research Record 42, p. 26-40, 1963.
8. Shields, B. P., and Dacyszyn, J. M. Seasonal Variations in Flexible Pavement Strength. Proc. Canadian Good Roads Association, 1965.
9. Alder, H. A. Economic Evaluation of Transport Projects. In Transport Investment and Economic Development (edited by G. Fromm). Brookings Institution, 1965.
10. Kuhn, T. E. Public Enterprise Economics and Transport Problems. Univ. of California Press, 1962.
11. Baldock, R. H. The Annual Cost of Highways. Highway Research Record 12, p. 91-111, 1963.
12. Hutchinson, B. G. The Use of Canadian Pavement Evaluation Data for Design. Proc. Canadian Good Roads Association, 1966.
13. Meyerhof, G. G. Preliminary Analysis of Benkelman Beam Deflections and Flexible Pavement Design. Proc. Canadian Good Roads Association, 1962.
14. Wilkins, E. B. Investigations of Pavement Design and Evaluation in Canada. Canadian Congress of Professional Engineers, Montreal, June 1967.
15. Shields, B. P., and Anderson, K. P. Some Aspects of Transverse Cracking in Asphalt Pavements. Proc. Canadian Tech. Asphalt Assoc., Vol. 9, 1964.
16. Anderson, K. O., Shields, B. P., and Dacyszyn, J. M. Cracking of Asphalt Pavements Due to Thermal Effects. Proc. AAPT, 1966.
17. Culley, R. W. Transverse Cracking of Flexible Pavements in Saskatchewan. Tech. Rept. 3, Sask. Dept. Highways, June 1966.
18. Highway Engineers Are Sorting Out the Variables in Asphalt Paving. Heavy Construction News, June 26, 1967.
19. Hutchinson, B. G. The Rationalization of Pavement Evaluation Decisions. Proc. Australian Road Research Board, 1966.
20. Raiffa, H., and Schlaifer, R. Applied Statistical Decision Theory. Harvard University Graduate School of Business Administration, 1961.
21. Moyer, R. A., and Lampe, J. E. A Study of Annual Costs of Flexible and Rigid Pavements for State Highways in California. Highway Research Record 77, p. 133-172, 1965.
22. Horwood, E. M. Urban Information Systems and Transportation Planning. Highway Research Record 194, p. 86-95, 1967.
23. Barraclough, R. E. Information for Land-Use Models. Highway Research Record 194, p. 1-14, 1967.
24. Vance, J. A. Geographical Data Coding Grid. Proc. Canadian Good Roads Association, 1966.
25. Hutchinson, B. G. The Measurement of Highway Pavement Performance. Proc. Internat. Conf. on Structural Design of Asphalt Pavements, Univ. of Michigan, 1967.
26. Wilkins, E. B. Effect of Strength Variations on Pavement Design. Proc. Canadian Good Roads Association, 1966.

Systems of Pavement Design and Analysis

NAI C. YANG, Civil Engineer, The Port of New York Authority

An analytical system is advanced for the design of new pavement based on the introduction of vehicle response as an important design parameter; the integration of design theories governing "rigid" and "flexible" pavements; and the tolerance of surface deformation and stress intensity in the pavement as well as in the subgrade. The system completely defies traditional design practice, but represents the collective work of theoreticians, practical engineers, material specialists, construction inspectors and maintenance crews. An even more important factor is the contribution of the pavement user who accepts the level of vehicle response and the one who pays the cost of construction.

•IN PRESENT engineering practice, pavement design methods tend to be divided into two groups: the empirical or statistical approach, and the theoretical analysis approach. Both have their own merits and drawbacks, and many good theories have been developed for pavement design using one or the other. However, when design problems are encountered for pavements of modern airports or superhighways, it will be found that present design practice is not adequate. First, the empirical and theoretical methods were, in most cases, developed independently. There is no correlation between them. Second, no pavement design theory includes the parameters of vehicle response, pavement roughness, maintenance, and riding criteria. Pavement theories developed in the early automobile age will not be adequate for today's jet aircraft and high-speed vehicle.

During the pavement tests for the redevelopment program at Newark Airport, extra efforts have been undertaken by the staff of The Port of New York Authority to obtain pertinent information that would contribute to the general knowledge of pavement engineering. The basis for the pavement design system proposed is the conclusions drawn from those tests. The statistical correlations deducted and at least part of the design analysis proposed are valid only for the subgrade, construction materials, and traffic pattern of the New York airports.

PURPOSE OF PAVEMENT CONSTRUCTION

Before going into the discussion of system analysis, it is appropriate to state the purpose of constructing pavement:

1. Safety: Pavements are built not only to support the vehicle load but also to perform under various traffic conditions. A vehicle can be operated on a dirt road as well as on a paved surface. The difference of vehicle operation is reflected by its dynamic response, speed limit, and, above all, the safety and comfort of the operator. In existing pavement design methods, strong emphasis has been given to the load-carrying capacity of the pavement, and practically no attention to the speed of the vehicle and its effect on the pavement performance. For instance, in airport construction there are three distinct areas where the pavement performs differently. For an identical pavement structure on uniform subgrade, the rutting at hard stand subject to static load is usually worse than the rutting of taxiways, and, in many cases, the performance of the runway portion of pavement is best. It can be seen that the load criteria of pavement design are not sufficient in modern pavement design.

Paper sponsored by Committee on Theory of Pavement Design and presented at the 47th Annual Meeting.

2. Maintenance: Experience shows that traffic can back up for several miles when a portion of highway pavement is under minor repair. If a major airport, such as John F. Kennedy Airport in New York, is undergoing minor runway maintenance, it can tie up air traffic at airports up to several thousand miles distant. The cost and inconvenience to a transportation system cannot be measured by the value of dollars. For the needs of today and tomorrow, the primary purpose of the pavement structure is not only to support the vehicle load but also to perform under various traffic conditions and survive within an anticipated service life. Therefore, the progressive deviation of pavement performance shall be mandatorily included in the pavement design system.

3. Economy: The ultimate goal of all engineering designs is the maximum utilization of material, equipment, and manpower, and to achieve the most economical solution. However, by introducing the factors of maintenance and traffic pattern into pavement design, the definition of the most economical solution should be modified to include the requirements of traffic safety and the frequency of maintenance. It becomes the prerequisite of modern pavement design that the standards of safety and maintenance be clearly specified for the type of pavement to be designed. It may be a long time before these standards can be established, but the system of pavement analysis proposed herein represents a first step in this direction.

BASIC ENGINEERING CONSIDERATIONS

There are several factors that will have a significant effect on the structural integrity of pavement construction. An understanding of these engineering considerations will lead to a sound judgment in the design concept.

Variability

A massive volume of road materials is always involved in the construction of pavements. The economical consideration will have a significant effect on the degree of variation for quality control and construction performance. For instance, the coefficient of variation, V, measuring the relative dispersion of events, is usually limited to 0.10 for the high-strength concrete. A premium has to be paid for the uniformity of material strength, and thus a high working stress can be utilized. For most road materials, the coefficient of variation ranges from 0.15 to 0.30. The quality of material is, therefore, widely dispersed. The reliability of statistical values is low and, consequently, a higher factor of safety is mandatory.

In the process of building a pavement, the variability of its performance is reflected by the variability of material, workmanship, environmental condition, and design concept. In the mathematical expression, the overall variability of the pavement performance is

$$V = (V_1^2 + V_2^2 + V_3^2 + \ldots)^{1/2} \tag{1}$$

If any one of the variables exceeds 0.30, such as the compaction of subgrade, the performance of a pavement as reflected by its surface deformation or stress intensity will deviate from the mean by a magnitude of ±10 percent on three out of four occasions. It can be seen that in the development of a pavement design system, a variation less than 10 percent from the average condition should be considered a perfect result. Consequently, some refined theories may not be required.

In Eq. 1, the variability of each contributing factor is considered to be equally important on the pavement performance. In actual construction, some contributing factors are more important than others. Therefore, a weighing factor should be applied to each contributing factor, such as

$$V = \left(\frac{V_1^2}{n_1} + \frac{V_2^2}{n_2} + \frac{V_3^2}{n_3} + \ldots\right)^{1/2} \tag{2}$$

By introducing a number of contributing factors, the random condition of each individual factor will be distributed by weight among all factors. This is similar to the standard error of sampling, σ_M, which decreases with increasing numbers of samples, N, such as

$$\sigma_M = t \cdot \sigma/(N - 1)^{1/2} \qquad (3)$$

in which t is the standard score computed for various degrees of certainty and σ is the standard deviation of a large sampling group.

In our present airport pavement design practice, the basic procedure consists of (a) determining the classification of the subgrade soil and drainage condition, (b) selecting the gross weight of the design aircraft, and (c) using a design chart. Without considering the merits or demerits of this procedure, the standard error according to Eq. 3 is 0.577 $t\sigma$. For modern pavement construction, a higher degree of reliability will be required. When construction is completed, most pavements will carry a very heavy traffic volume, making it extremely difficult to repair the pavement during its service.

For the system of pavement analysis proposed herein, the following factors will be included: vehicle response; crossing velocity; longitudinal profile; traffic volume; tire inflation pressure and contact area; transverse rutting; normal stress in subgrade; elastic as well as transient deformation; horizontal shear; bending stress; differential settlement; temperature difference; strength of pavement material; modulus of subgrade; crack propagation; and fatigue strength. If all design computations are as good as the use of a design chart or an empirical subgrade classification, the standard error of the new design approach according to Eq. 3 is 0.242 $t\sigma$, a great improvement over the present design procedure.

In any of the design theories, the determination of parameters requires a great deal of sound judgment. As any judgment involves human variables, the deviation from reality will affect the reliability of pavement design. Attempts should be made to correlate the test results with a set of theories that would be used in the final design. It is believed that, by using parameters directly derived from the test results, the design theories would be more meaningful in practical application.

Subgrade Reaction

Among all of the design parameters, the subgrade reaction is the most important governing factor, but it is also the most ambiguous subject in the present design method. There is nothing wrong in the use of CBR or K-values if the limitations of statistical correlations and the assumption of idealized material are precisely outlined in the pavement design. Oversimplifications in the design procedure and unwarranted extensions of its application will innocently result in a serious discrepancy in the pavement design. Attempts have been made to understand the stress-strain relation of the subgrade by use of parameters such as Poisson's ratio and Young's modulus. However, the first problem encountered in the analysis is the definition of modulus of deformation. There may be five definitions (Fig. 1), and the tangent modulus at a defined working stress level seems rather appropriate. If Boussinesq's theory is used in the determination of the E-value, the size of test bearing plate will be included in the computation.

There are many factors influencing the modulus of deformation. For a sandy subgrade, the loading history or the original consolidation pressure is not the primary governing factor. However, if the sand is confined, such as in the placement of a blanket of stone screenings, the modulus of deformation of the sand subgrade will increase considerably. The increase in load-deformation modulus due to the surcharge is rather deceptive if the basic mechanics of the subgrade deformation is carefully reviewed. In a confined condition, the deformation of the subgrade consists of the true nature of the sand under unconfined conditions and the counteraction of the confining pressure. Therefore, the deformation of a confined sand is always much smaller than the deformation in the unconfined condition. If the bearing test of the sand subgrade is conducted under a confined condition, the measured load-deformation coefficient, such as the CBR, K, or E-value, will be considerably higher than the actual soil property in its unconfined condition. An unconservative parameter is therefore innocently introduced into the pavement design. Attempts have been made to integrate the Boussinesq and Mindlin pattern of stress (3). A correction factor for the confining condition has been demonstrated (Fig. 2). The validity of the concept should be verified by future field observations. However, it

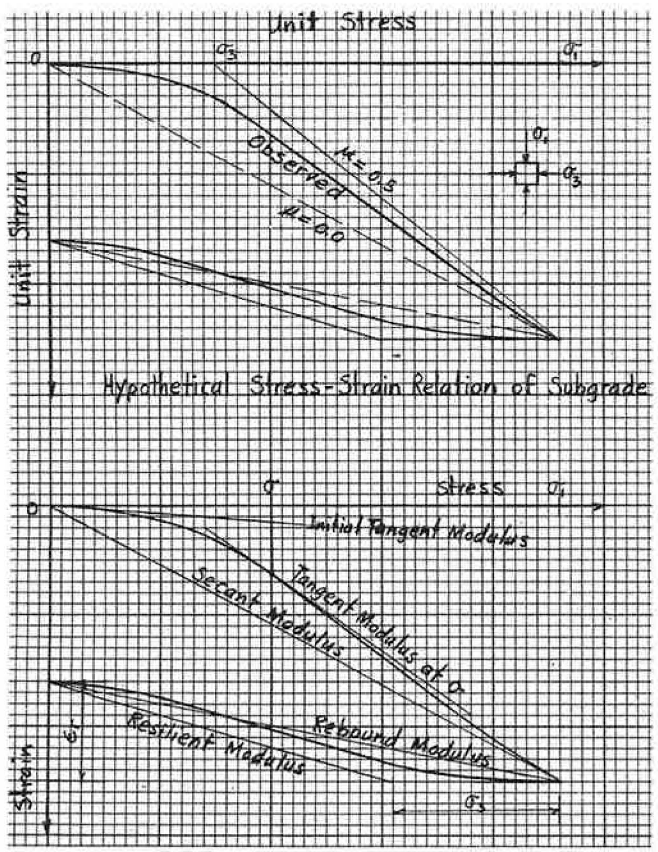

Figure 1. Definition of modulus of deformation.

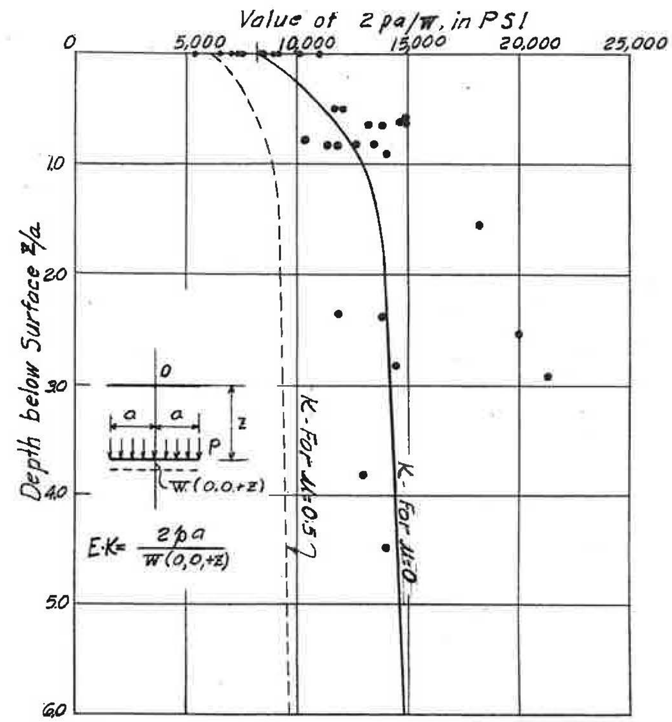

Figure 2. Value of $2pa/\overline{W}$ and Mindlin pattern of stress.

is a method attempting to correct the inaccuracies in our present concept of deformation modulus.

The increase of deformation modulus due to traffic coverages is also a very interesting subject. The subgrade does reach a higher degree of compaction under the influence of traffic coverages and so does its coefficient of variation. For the E-value at the Newark test, the coefficient of variation of the original subgrade is 0. 12 to 0. 15, while it is 0. 25 to 0. 30 after 3000 to 5000 traffic coverages. The change of coefficient of variation from 0. 15 to 0. 3 represents a 100 percent increase in standard error. For instance, if in one out of six tests on the original subgrade, the E-value will be lower than 85 percent of the mean, the score for the same percentage of mean value will be one out of three tests on subgrade subject to the traffic coverages. The increase of deformation modulus due to traffic coverages deserves consideration on its application in pavement design. However, without additional exploration on this subject, the reliance on the increase of the E-value should be reserved.

Mechanical Compaction

Various equipment, including vibratory or pneumatic-tired compactors, is available for improving the density of subgrade. Each piece of compaction equipment has its limitation, beyond which the density of the subgrade is practically independent of the effort of mechanical compaction. Since all compaction equipment, practically speaking, is developed for highway construction, the equipment is more critical for airport construction. For the largest pneumatic-tired compactor available to the construction industry, the maximum tire pressure can be as high as 150 psi and the imprint area is about 8 inches in diameter. For a modern aircraft, the tire pressure is 240 psi and the imprint area is about 19 inches in diameter. Additional compaction due to actual aircraft load is obvious and, consequently, so is the rutting of the pavement surface.

There are two methods to improve the bearing capacity of the subgrade beyond the limit of mechanical compaction. First, the density of the subgrade can be improved by the application of a surcharge load uniformly distributed over the pavement area. In practice, the cost of surcharge, up to 60 to 100 psi, will rule out the feasibility for such a method. The second method of improvement is essentially a procedure to change the physical properties of the subgrade. If the subgrade is basically deficient in cohesive bond, as in sandy soils, the subgrade can be stabilized, without considering their relative performance and economic aspects, by introducing fines such as clay slurry or flyash to improve the mechanical bond of the subgrade or by introducing portland cement, asphalt, lime, lime-flyash, and other chemical components to improve the physical properties of the subgrade. As modern vehicles become heavier and heavier, the need to improve the shearing strength in the base course is imminent. The use of a stabilized base course may offer some answers.

Stress-Strain Pattern of Pavement Components

In aggregate-based pavements, the stress distribution is in good agreement with the theoretical Boussinesq pattern (Fig. 3), and the total deflection of the pavement surface under a single application of a moving load is largely contributed by the transient deformation of the subgrade (Fig. 4). The stress distribution and elastic deformation can be related to the rule governing the stress-strain relationship in an elastic mass. Because the subgrade and aggregate base are not perfect elastic mediums, the strain, even under a transient load, is not completely recoverable. Thus, the rutting along the wheelpath is observed in every type of test section consisting of conventional aggregate base.

The local deflection, having a sharp curvature of bending, causes not only a higher stress level, but also a reverse stress level, thereby accelerating the fatigue failure of the surface layer. If the modern concept of pavement design emphasizes the smoothness of the pavement surface, it seems impossible to use a conventional aggregate base while trying to achieve a pavement without deep rutting. Disregarding construction cost, the pavement rutting will not be eliminated by simply increasing the thickness of aggregate base. The heavy aggregate base will improve that part of the rutting caused by subgrade deformation but will not eliminate the rutting produced in the aggregate base itself.

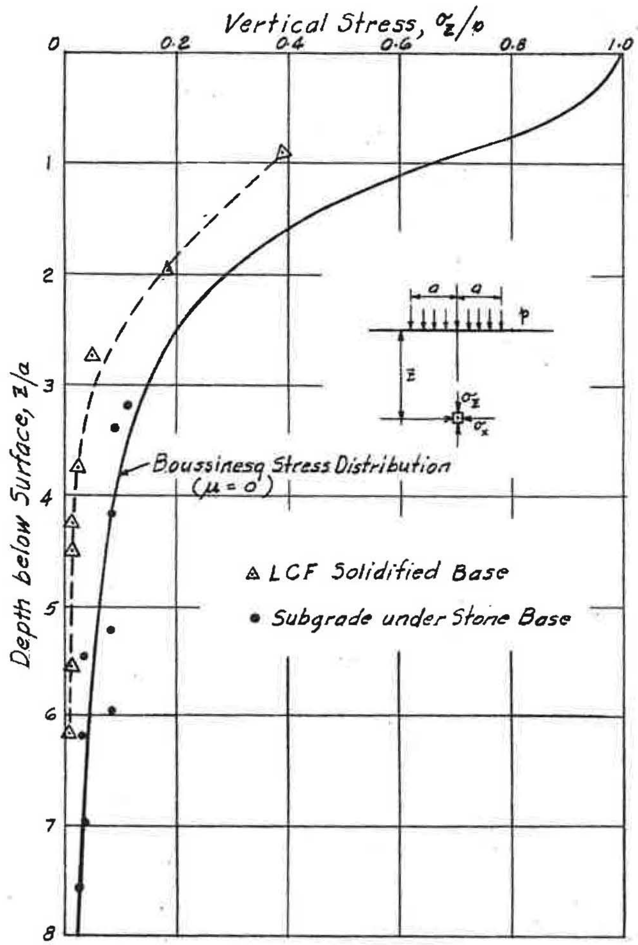

Figure 3. Calibrated stress record for gages at various depths.

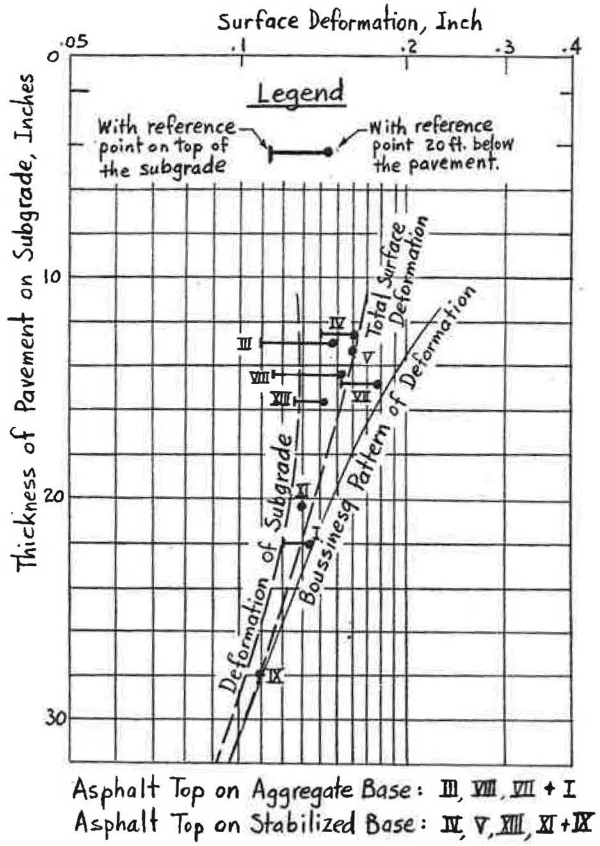

Figure 4. Transient deflection of test pavements.

The stress pattern in a stabilized base course, such as soil-cement or lime-cement flyash, is about half of that given by the Boussinesq theory. It is believed that the stiffness of the stabilized base has a significant effect in distributing the surface load over a much wider area. If the pavements are of identical thickness on identical subgrade, there seems no significant difference in total surface deflection between the stabilized or aggregate-based pavement (see actual measurements in Fig. 4). The total surface deflection is largely contributed by the deformation of the subgrade. However, the longer, smooth, deflection configuration of the stabilized base will produce a more durable and better performing pavement.

The presence of horizontal stress and its stress propagation for a great distance has revealed an important factor in the pavement study. While there is no conclusive observation, the indications are that:

1. On a resilient base material such as aggregate and asphalt stabilized base, the normal stress in the top course is relatively low. However, the lateral displacement of the resilient base creates sharp curvature of surface deformation in the top course. Surface cracks are encountered both transversely and longitudinally along the wheelpath.
2. On the lime-cement-flyash and soil-cement stabilized base, the normal stress in the top course is relatively high. The local concentration of wheel load will cause the consolidation of the asphalt top course. However, the wide stress distribution in the stabilized base will result in a long, flat deflection dish, and the bending stress is therefore distributed.
3. Outside the direct loading area, the normal stress in the top course changes from compression to tension as the phase of stress propagation changes. The reversal of stress level will greatly reduce the fatigue life of the pavement surface. It should be noted that a "hook" shape of cracked pattern has been observed in several airport pavements.
4. The wave propagation in the subgrade is in the range of 300 to 1500 fps. For modern aircraft, the speed at touchdown and takeoff is about 240 fps. Resonant vibration may be significant if the subgrade is in the lower range of wave propagation. It can be seen that the dynamic aspect of pavement response should be considered in the system analysis.

Failure Mechanism

The failure mechanism of pavement structure has been suggested by some academic researchers. However, from the viewpoint of a professional engineer, if the failure mechanism is thoroughly investigated, there is no indication that the design of a smooth pavement structure is always possible. The variability of testings, materials, construction, and even the method of interpretation will affect the correlation between the failure mechanism and the design of good serviceable pavement.

In the pavement test at Newark Airport, three types of failure mechanism have been observed:

1. The lean concrete base was placed with very low marginal safety, according to the formula developed by Meyerhof. When fatigue of the lean concrete was developed at 3,800 load coverages, the pavement was broken along the wheelpath. It is a typical bending failure and the equilibrium condition at failure was in the transition mode between the plastic state of equilibrium by Losberg-Meyerhof and the noncrack elastic condition by Westergaard. Prior to the pavement failure, the magnitude of rutting was very small. The rigid or stabilized base significantly contributes to reducing the longitudinal roughness and also the transverse rutting along the wheelpath.
2. The failure of the aggregate base is closely related to the stress level developed at the approaching of a wheel load. The aggregate base is more vulnerable in a horizontal direction than in vertical bearing. The aggregate base tends, therefore, to move laterally. Consequently, ruttings are encountered along the wheelpath. The progressive increase in rutting will result in the progressive increase in surface roughness, which, in turn, will increase the dynamic impact of the test vehicle. In this close cycle, pavement failure is greatly accelerated.

3. The failure of open-graded, large-size, asphalt-coated stone is very similar to the failure mechanism of an aggregate base. The excessive horizontal movement is largely responsible for the failure. Open-graded, large-size stone may have a superior resilience in supporting the light vehicle load. However, for a heavy aircraft load, the intensity of tire pressure and the size of footprint tend to increase the consolidation of the top course. An open void in the pavement may cause the rutting of the pavement surface.

Maintenance of Pavement Performance

When a smooth performance is the primary concern in pavement design, the stress-strain condition of the pavement components, including the supporting subgrade, should be constantly in the elastic state of equilibrium. Pavement tests at Newark Airport have demonstrated that any temptation to reduce the strength of the pavement, which in turn tends to increase the stress in the subgrade, is actually a false economy. The weakened pavement will not withstand a prolonged service load.

When the pavement structure is in the elastic state of equilibrium, the magnitude of permanent surface deformation will increase proportionately with an increasing number of load applications (Fig. 5). The upper boundary of the elastic state of equilibrium is represented by the yield condition where the permanent deformation increases rapidly and the pavement performance deteriorates excessively. In order to design a high-quality pavement, limiting its permanent surface deformation for a period of extended service life, the elastic theory should be employed in the design analysis. The strength of the pavement should always be stronger than the strength required by the yield condition.

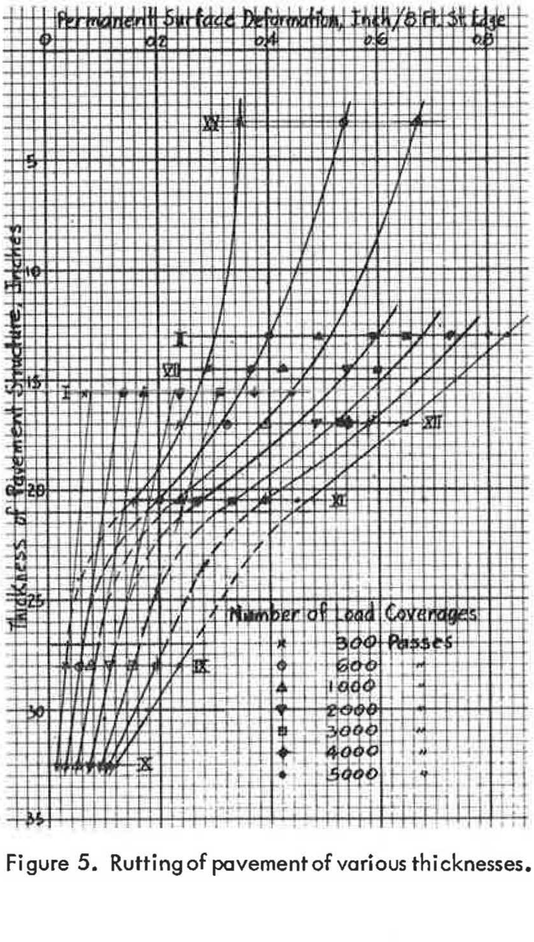

Figure 5. Rutting of pavement of various thicknesses.

SYSTEM OF PAVEMENT ANALYSIS

An analytical system is proposed for the design of new pavement based upon the foregoing discussions. The flow chart for this system is shown in Figure 6.

The basic concept involves: (a) the introduction of vehicle response as an important design parameter; (b) the integration of design governing "rigid" and "flexible" pavements; (c) the tolerance of surface deformation and stress intensity; and (d) the adoption of a modulus of deformation in defining stress-strain relation of the subgrade.

The system defies traditional design practice. All parameters used in the system analysis are either carefully evaluated by theoretical analysis or deducted from the pavement test. In the analysis of the test results, more emphasis is placed on the actual observed data than on the interpretation. The random nature of the test results suggests that the probability approach would be the best method to use to define the test model. If the parameters in an actual model are somewhat different from those in the test model, its correlation function is not applicable to the actual design analysis. Since this limitation exists when using probability analysis, all correlation functions developed for one pavement design should not

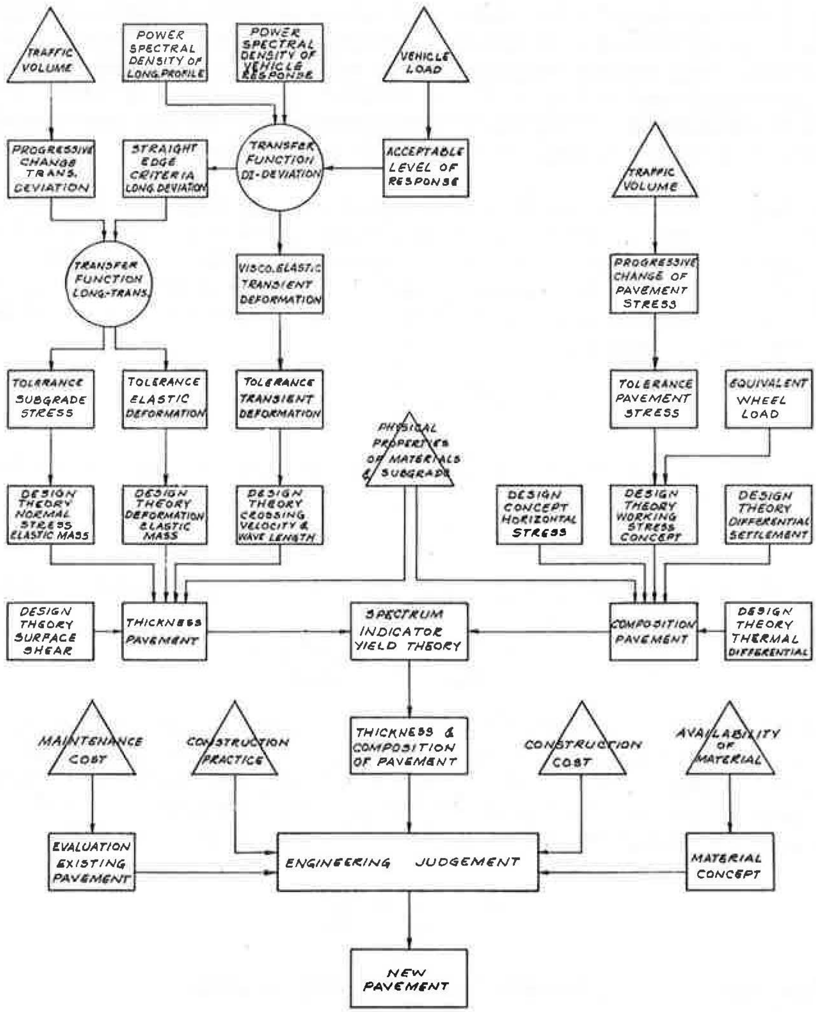

Figure 6. System of pavement analysis from test results of new pavement design.

be used for any other pavement design unless the new pavement conditions are in full agreement with the original ones.

CONCEPT OF LIMITING DYNAMIC RESPONSE OF VEHICLE

The first item in the analytical system is the determination of the response level of the vehicle while it is riding on the pavement surface. The most appropriate parameter for this measurement is the normal acceleration encountered at the center of gravity of the vehicle and the longitudinal riding profile of the pavement surface. From the viewpoint of dynamic response of a vehicle, there are three levels of forced vibration. First, the vehicle rolls on a smooth pavement surface. The vibration of a vehicle is the source of excitation and the pavement structure is responding. The second level of forced vibration is the excitation due to pavement roughness, as an input, and the vehicle is responding as an output. The dynamic increment in the vehicle causes the third level of forced vibration, that is, the pavement structure is responding again.

For a single degree of freedom system, the forced vibration with a harmonic excitation F is given by

$$X = F \cdot H \tag{4}$$

where H is known as the magnification factor or the response function at resonance. For a wide range of aircraft and highway vehicles, its natural frequency varies between 1.5 and 5.0 cps. The natural frequency of the suitable subgrade may range from 20 to 100 cps. The magnification factor, H, is therefore in the range of 0.002 to 0.02 when the system is not damped. Thus the maximum dynamic response, mentioned as the first level of forced vibration, is approximately equivalent to 2 percent of the static load of a vehicle.

For a vehicle riding on a rough pavement surface, the excitation is of a multi-frequency random vibration. The phase of the forcing function has little effect on the final outcome. The main concern is the average properties of random functions. The classical concept of the theory of probability deals with the study of random events. Mathematically, the variance of random function is expressed by the squares of the deviation from the mean value, such as

$$\overline{X}^2 = \frac{1}{T} \int_0^T X^2 \cdot dt \tag{5}$$

For a simple harmonic force, $F = F_0 \sin \omega t$, its mean square value of any number of forcing cycles is

$$\overline{F}^2 = \frac{F_0^2}{2} \tag{6}$$

In applying this to a multi-frequency function F(t) the integration of its Fourier series is

$$\overline{F}^2 = \sum \frac{F_n F_n^*}{2} = \sum \overline{F}_n^2 \tag{7}$$

where * is the conjugate of the complex number. Thus, the mean square value of the variance of a multi-frequency function is simply the sum of the mean square value of each frequency segment. Eq. 7 can be conveniently expressed by the distribution of the mean square value in each frequency interval, known as the power spectral density function $\varphi(\omega)$. For a discrete function, the mathematical expression is

$$\varphi(\omega) = \lim_{\Delta\omega \to 0} \frac{\Delta(\overline{F}^2)}{\Delta\omega} \tag{8}$$

For a continuous spectrum, the limit is replaced by derivatives

$$\overline{F}^2 = \int_0^\infty \varphi(\omega)\, d\omega \tag{9}$$

It can be seen in Eq. 9 that the area under the power spectral density curve is equal to the mean square value of the time function.

For the multi-frequency excitation, the mean square response of the vehicle is equal to

$$\overline{X}^2 = \sum \frac{F_n F_n^*}{2} H \cdot H^* \tag{10}$$

Substituting Eqs. 7 and 9 and integrating with respect to ω, Eq. 10 becomes

$$\overline{X}^2 = \varphi(\omega) \frac{\pi f}{4\beta} \tag{11}$$

in which f is the frequency of the vehicle and β is the damping factor of that system. It can be seen that the mean square response of a vehicle, $\overline{X}$, assumes a linear function with the power spectral density of pavement roughness.

There are several methods to compute the power spectral density function. For a

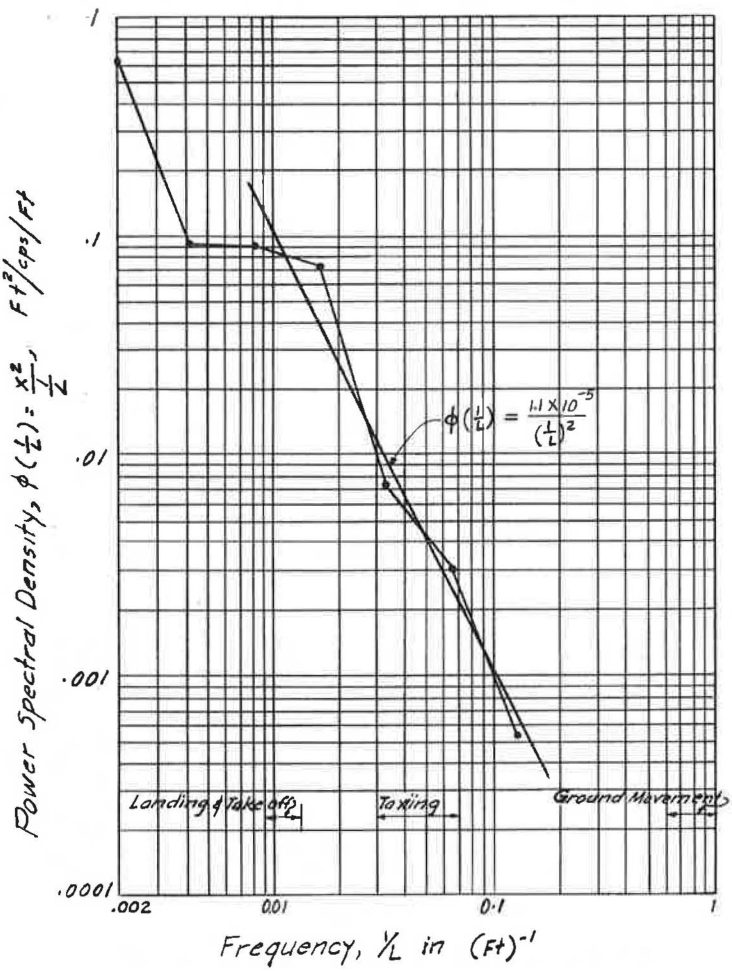

Figure 7. Power spectral density function of longitudinal profile, Newark test pavement—Sta. 10+18.75 to Sta. 19+75.00.

time function, having sufficient length of record and of a normal (Gaussian) distribution, the more accurate computation can be made by the use of autocorrelation function and, then, the power spectral density. For a limited record including some local disturbances, the power spectral density can be estimated by the folding frequency method, which yields a reasonable computation for the short wave vibrations (1, 4, 5, 6). Fortunately, they are in the practical range of pavement construction.

For the test pavement at Newark Airport, the power spectral density function of the longitudinal profile along the wheelpath has been condensed by the folding frequency method (Fig. 7). Within the significant range of wavelength, the power spectral density function is

$$\varphi\left(\frac{1}{L}\right) = \frac{1.1 \times 10^{-5}}{\left(\frac{1}{L}\right)^2} \tag{12}$$

For a discrete wavelength, the relation between the surface deviation Δ and the straightedge (wavelength) L is expressed by

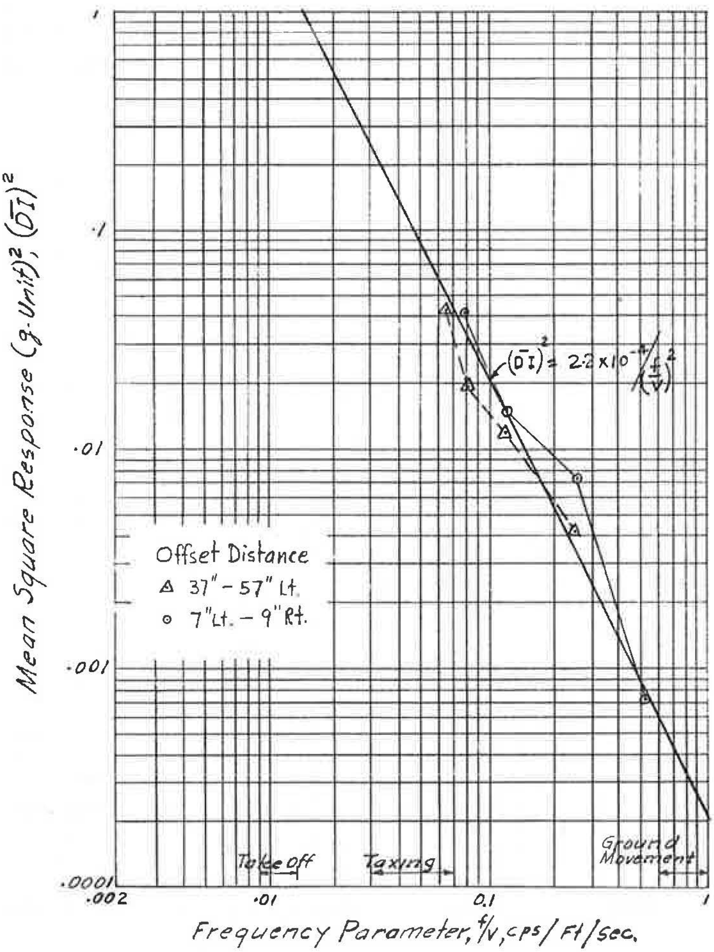

Figure 8. Mean square response of vehicle, Newark test.

$$\varphi\left(\frac{1}{L}\right) = \frac{\frac{1}{8}\Delta^2}{\left(\frac{1}{L}\right)} \tag{13}$$

The combination of Eqs. 12 and 13 yields the relation

$$\frac{106.5\Delta}{L^{1/2}} = 1 \tag{14}$$

The dynamic increment of vehicle response is measured by the output of strain gages and an accelerometer mounted on the vehicle. The continuous time function is processed by sampling the envelope of the peak dynamic response at 0.1-second intervals. Within the similar significant range of response frequency, the mean square response of the vehicle is (referring to Eq. 11 and Fig. 8)

$$\overline{DI}^2 = \frac{2.2 \times 10^{-4}}{\left(\frac{f}{v}\right)^2} \tag{15}$$

in which f and v are the natural frequency and velocity of the vehicle respectively. The average dynamic increment is, therefore,

$$\overline{DI} = \frac{.0148}{\left(\frac{f}{v}\right)} \tag{16}$$

The transfer function, according to the principle of random vibration, is equal to the ratio between the input and output power of the system, and is given by

$$\overline{DI} = \frac{1.58\Delta}{L^{1/2} \cdot \left(\frac{f}{v}\right)} \tag{17}$$

or in the form of straightedge criteria,

$$\Delta = .63\,\overline{DI}\left(\frac{f}{v}\right) \cdot L^{1/2} \tag{18}$$

In his study of NASA's roughness test, Houbolt suggested that the normal tolerance of mean dynamic increment is 0.12 g and that the upper limit of pavement roughness is likely to be the beginning of the development of a center of gravity peak response of 0.30 g. A similar range of dynamic response has been reported by other researchers. Leonard, of the British Road Research Laboratory, reported that the acceptable level of vehicle vibration is 0.1 g for normal traffic conditions. In the Newark pavement design, the dynamic increment is assumed to be 0.12 g and 0.30 g for pavements in the concentrated and infrequent traffic areas respectively. This is the best judgment possible, based on the present state of knowledge. There is a need for administrative agencies such as the FAA and BPR to coordinate the needs of airport users and road users and to conduct a more comprehensive research program.

In limiting the dynamic response of a vehicle, the roughness configuration of the pavement surface anticipated at the end of the service life shall meet the following straightedge criteria:

$$\Delta = K \cdot L^{1/2} \tag{19}$$

The significant range of velocity of aircraft operation is shown in the following table:

Operational Condition	Velocity, fps	Effect of Wing-Lift	Significant Wavelength, ft	K-Value in Eq. 19	
				DI = 0.12 g	DI = 0.3 g
Ground movement	10-15	0.00	3-7	0.0100	0.025
Taxiing	50-120	0.05	14-35	0.0036	0.009
Takeoff	170-240	0.50	50-70	0.0028	0.007

The service life of a pavement is measured by its structural integrity to withstand the traffic coverage and environmental changes. Insofar as traffic coverage is concerned, it is a parameter used in evaluating the fatigue strength and the progressive change of surface configuration.

At Kennedy International Airport, the average daily operation is 1,400 aircraft movements, of which 750 movements are jet traffic. In considering the number of runways and taxiways, the full-load aircraft operation is likely to be less than 120 movements

per day per runway. The probability of stress repetition in the pavement, defined as traffic or load coverages, would be less than 5,000 coverages per year; 100,000 such coverages should be anticipated during the useful life of the pavement. For new pavement at Newark Airport, the growth of air traffic as well as the weight of future airplanes should be considered in the evaluation of traffic coverage. It is assumed that the traffic growth is about 7 percent per year and new airplanes will weigh 700,000 pounds. The anticipated traffic coverage is estimated to be 1,000,000 coverages in the concentrated traffic area, 100,000 coverages in the normal traffic area, and 10,000 coverages in the infrequent traffic area.

Similar traffic evaluation can be applied to other types of pavement design. The number of traffic coverages, N, will be used in the evaluation of deflection tolerance.

CONCEPT OF LIMITING PAVEMENT DEFLECTION

According to the previous section, it is possible to evaluate the tolerance of longitudinal permanent deformation, Δ, and the number of traffic coverages, N, during the anticipated service life of a pavement. At the Newark test, a statistical relation exists between the longitudinal and transverse permanent deformation of the pavement surface at a common number of traffic coverages (Fig. 9):

$$D_N = 10\,(\Delta - .0012\sqrt{L}) \qquad \text{for stabilized base} \tag{20a}$$

$$D_N = 5.2\,\Delta \qquad \text{for aggregate base} \tag{20b}$$

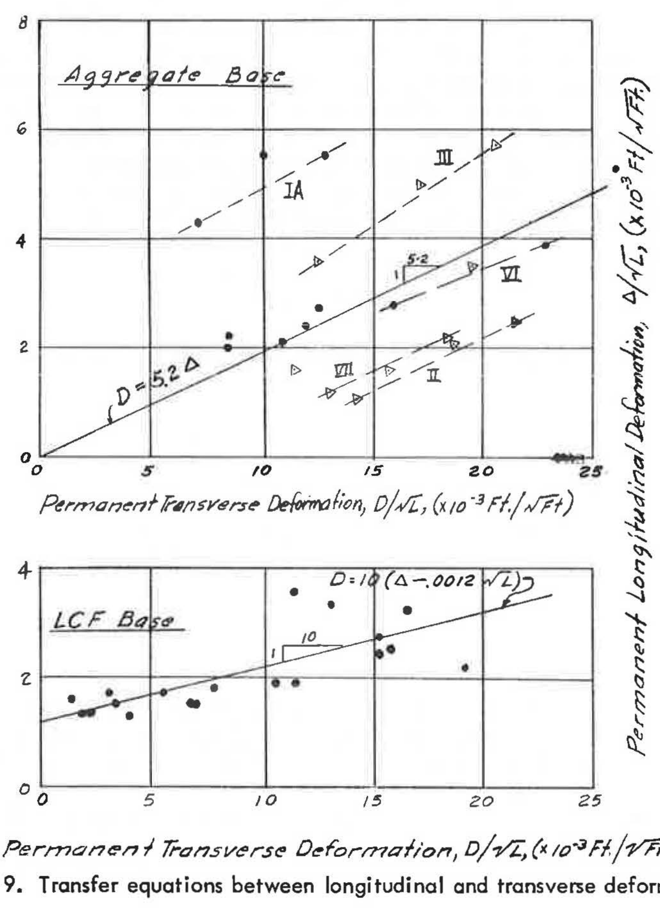

Figure 9. Transfer equations between longitudinal and transverse deformation.

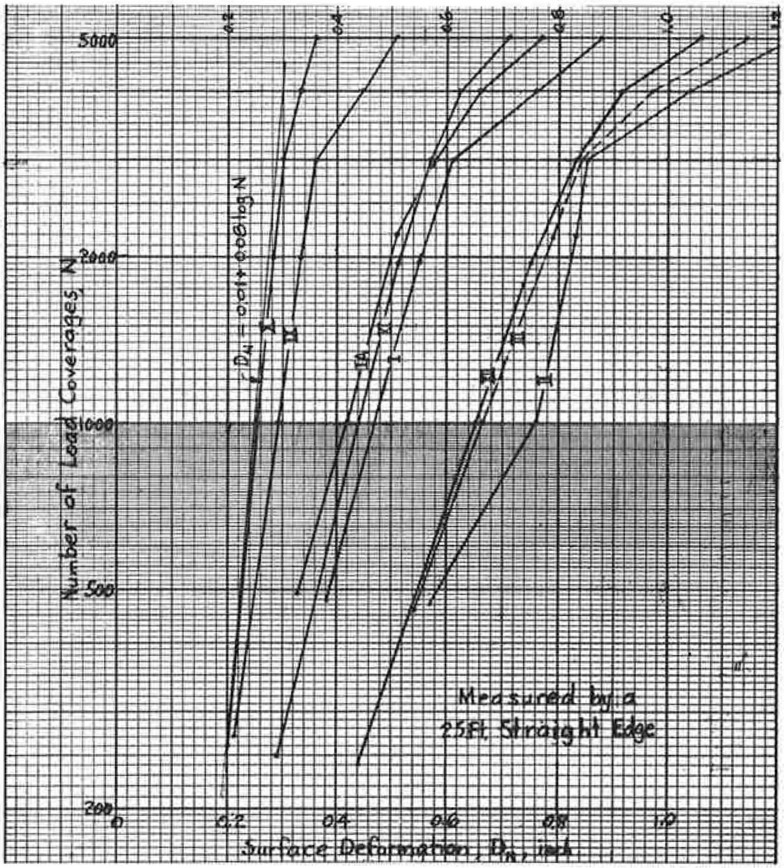

Figure 10. Surface deformation of various test sections.

During the test, another statistical relation is also deducted between the number of traffic coverages and the progressive change of transverse permanent deformation, such as (Fig. 10)

$$D_N = D_1 + D_0 \log N \tag{21}$$

in which D_N is the total transverse permanent deformation at the Nth traffic coverages, D_1 is a constant and D_0 is the rate of progressive transverse permanent deformation, expressed in feet per log cycle of traffic coverages. Equation 21 is very similar to the principle of evaluating the fatigue strength of materials.

The observed D_0-value is then correlated with the theoretical deformation by the Boussinesq equations. A statistical relation is determined, such as (Fig. 11)

$$\overline{W}_z = .16\,\overline{W}_0 + .43\,D_0 \qquad \text{for stabilized base} \tag{22a}$$

$$\overline{W}_z = .06\,\overline{W}_0 + .43\,D_0 \qquad \text{for aggregate base} \tag{22b}$$

in which $\overline{W}_0$ is the deflection on the surface and $\overline{W}_z$ is the deflection of the subgrade at a depth z below the surface. In the Newark test, it was observed that 90 to 95 percent of elastic deformation of the pavement was registered in the subgrade (Fig. 4). For the practical purpose of pavement design, the $\overline{W}_z$ value is assumed to be the deflection tolerance of the pavement surface. Equation 22a or 22b is a very important step in that it permits the use of an elastic theory in evaluating recoverable pavement deformation

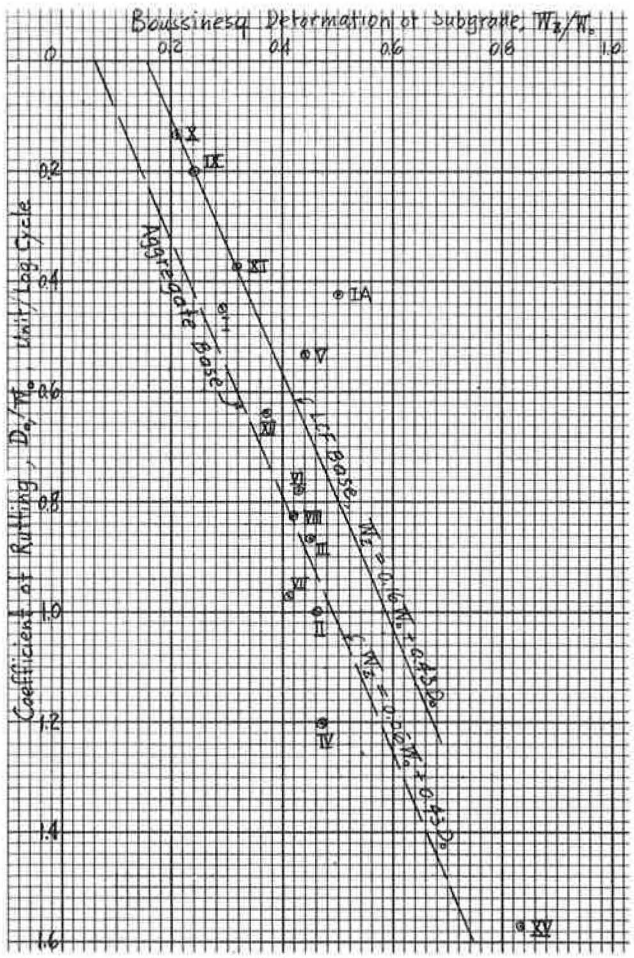

Figure 11. Transfer function — rutting and Boussinesq deformation.

for a specified dynamic response and the anticipated traffic coverages.

CONCEPT OF LIMITING STRESS LEVEL

There are two kinds of stress tolerance in pavement design. For the performance of the pavement surface, the limitation of stress level is applied to the subgrade below the pavement structure, where large permanent deformation occurs (Fig. 4). If the subgrade is subject to an excessive normal stress, the direct effect on the pavement's performance is excessive rutting (transverse permanent deformation) along the wheelpath. In the Newark test, the measured maximum normal stress, σ, in the subgrade has been correlated with the rate of change of transverse deformation D_0 and the theoretical surface deformation $\overline{W}_0$ by the Boussinesq equation. The statistical relation is plotted in Figure 12 and is given by

$$\sigma_z = 5.0 + 49.4\, D_0/\overline{W}_0 \qquad (23)$$

By using the deformation criteria developed above, the normal stress level in the subgrade should be limited to 8 psi for pavements under concentrated traffic and 11 psi for pavements under normal traffic loads.

For the integrity of the pavement structure to support the wheel loads, the stress tolerance in the pavement elements shall be divided into three groups: (a) normal stress, (b) horizontal stress, and (c) flexural bending stress. The normal stress and horizontal stress refer to the stress distribution in the elastic mass, subjected to vertical and horizontal forces. In the lime-cement-flyash stabilized base material, the distribution of normal stress σ_z is about half the intensity given by Boussinesq's formula (Fig. 13). Consequently, the normal stress in the subgrade is reduced by the same proportion:

$$\sigma_z' = \frac{1}{2}\sigma_z$$

in which σ_z' and σ_z are the actual and theoretical normal stress respectively.

In the Newark test, significant horizontal stress was encountered in the pavement. The influence of the test load was picked up by the pressure gages at a distance as far as 40 feet away. The effect of the horizontal stress on the performance of the pavement should be fully evaluated in the future study.

The rolling or braking resistance of a moving vehicle is governed by several factors: (a) surface smoothness of the pavement, (b) deformation of pavement under load,

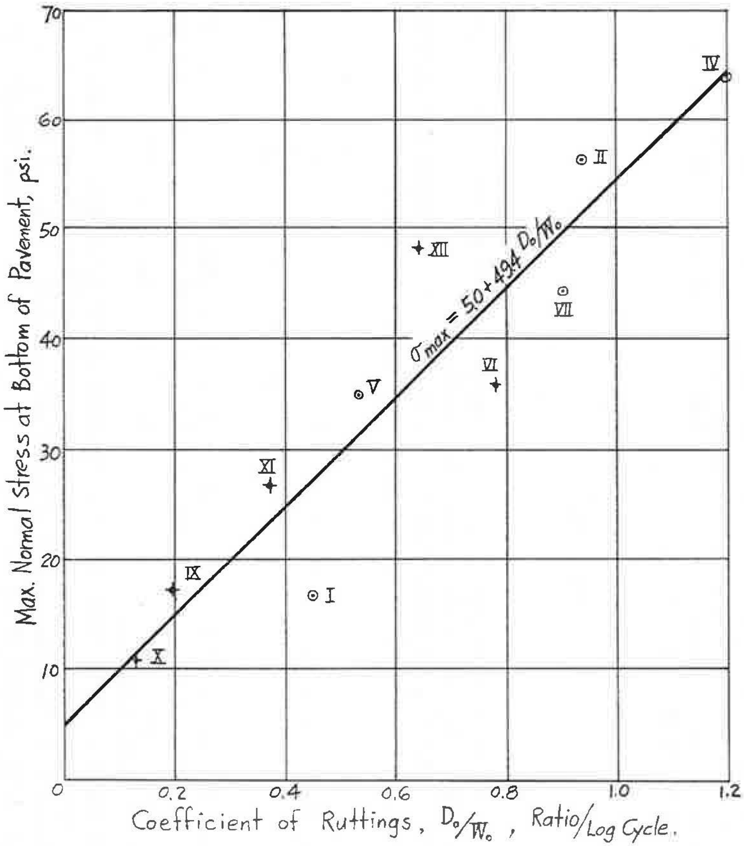

Figure 12. Transfer function — peak normal stress and ruttings.

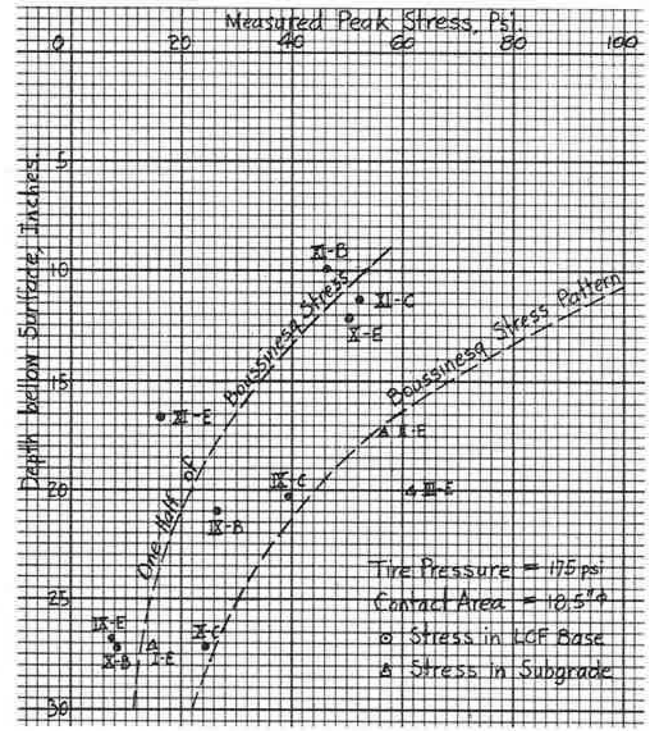

Figure 13. Calibrated peak stress reading in various pavements.

(c) flexibility of tire sidewall, (d) speed of vehicle, and (e) wheel bearing friction. Theoretically, the rolling resistance acts as a horizontal shearing force on the pavement surface. The relationship between the normal stress inside an elastic mass and the horizontal shearing force, Q, on the boundary surface of the elastic mass is expressed by (7)

$$\sigma_Z (x, z)_{y=0} = \frac{3Qx \cdot z^2}{2\pi (x^2 + z^2)^{5/2}} \tag{24}$$

The maximum value of σ_Z is encountered at $x = z/2$ and is equal to

$$\sigma_Z = \frac{-.136\,Q}{z^2} \tag{25}$$

in which σ_Z is the normal stress at depth z and x is the horizontal distance in the direction of vehicle movement, between the point of load application and the point of stress measurement.

The allowable bending stress in the pavement elements can be evaluated by its fatigue strength, as given by

$$\sigma_N = \sigma_b (1 - .092 \log N) \tag{26}$$

in which σ_N is the fatigue limit at N cycles of repetitive loading and σ_b is the flexural strength under static loading. A factor of safety, ranging from 1.25 to 2.0, shall be required in the pavement design (9).

Design Theory — Elastic Mass

The application of the Boussinesq theory in estimating the stress-strain of an elastic mass has been reviewed by many researchers (2). The equations are in simple algebraic form and are convenient for application by the engineer. For the stress distribution, the equation is of the form

$$\sigma_Z = p \left[1 - \frac{z^3}{(a^2 + z^2)^{3/2}} \right] \tag{27}$$

in which a is radius of load area, p is the intensity of loading, and σ_Z is the normal stress at a depth z below the surface of elastic mass.

The deformation $\overline{W}_Z$, from a depth z below the surface and along the vertical axis under the center of the surface load, can be obtained by integrating

$$\overline{W}_Z = \int_z^\infty \frac{1}{E} (\sigma_Z - 2\mu\sigma_X)\, dz = \frac{p}{E} (a^2 + z^2)^{1/2} \left[2 - \frac{z^2}{a^2 + z^2} - \frac{z}{(a^2 + z^2)^{1/2}} \right] \quad \text{for } \mu = 0 \tag{28}$$

When σ_Z and $\overline{W}_Z$ represent the tolerance of deformation and stress of the subgrade respectively, referring to Eqs. 22a, 22b, and 23, the depth z becomes the thickness of pavement for satisfying that level of tolerance. The design computation involves only the solution of cubic equations.

In actual design, the solution for the real root of the cubic equation can be determined with the use of design charts. For the solution of Eq. 27, the design chart is similar to the curve for Boussinesq stress distribution as shown in Figure 3. The design chart is represented by two dimensionless parameters, z/a and σ_Z/p. For the solution of Eq. 28, a similar chart can be plotted for the parameters z/a and $\overline{W}_Z E/p$.

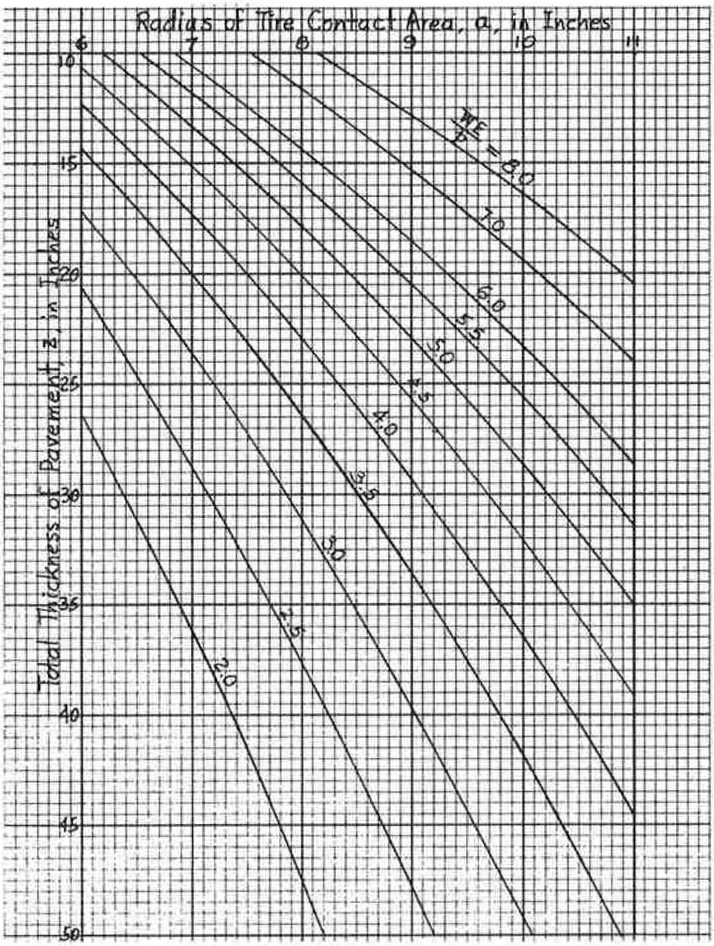

Figure 14. Design curves for Equation $\overline{W} = \frac{p}{E} (a^2 + z^2)^{1/2} \left[2 - \frac{z^2}{a^2 + z^2} - \frac{z}{(a^2 + z^2)^{1/2}} \right]$.

However, it is more convenient in practical design to use three parameters, such as a, z, and $\overline{W}_z E/p$. The graphical solution of Eq. 28 is shown in Figure 14.

Design Theory — Elastic Plate

The classical Westergaard theory was developed on the assumption that the pavement is treated as an elastic plate, supported by a uniform elastic medium. The ma imum tensile stress at the bottom of the pavement is expressed by

$$\sigma = \frac{P}{h^2} \cdot \frac{3 (1 + \mu)}{2 \pi} \left[\ln \frac{1}{\lambda a} + 0.616 \right] \tag{29}$$

in which

$$\lambda = \left[12 (1 - \mu^2) \frac{K}{Eh^3} \right]^{1/4}$$

and K is the constant modulus of the subgrade, a is the radius of tire contact area, and

P is the single wheel load. In the development of Westergaard's formula, the modulus of subgrade was assumed to be a constant over the entire pavement area and depth. Such a simplification is not consistent with the actual foundation behavior. The situation is made worse by the use of an arbitrary procedure that suggests the use of loading tests utilizing a 30-inch diameter steel plate. The original definition of the modulus of subgrade is expressed by the unit wheel load per unit length of deformation, i.e., $K = p/W$. By using Eq. 28, the relation between Westergaard's K-value and the elastic modulus of subgrade can be expressed by

$$K = \frac{E}{2a\,(1 - \mu^2)} \qquad \text{for } z = 0 \qquad (30)$$

Substituting this relation into the parameter of relative rigidity, Eq. 29 can be rewritten as

$$\sigma = 1.5\,(1 + \mu)\,p\left(\frac{a}{h}\right)^2\left(\frac{3}{4}\ln\frac{h}{a} + \frac{1}{4}\ln\frac{E_C}{E_S} + 0.168\right) \qquad (31)$$

For a thick plate, $a < 1.724h$, the a-value in Eq. 31 should be replaced by a value equal to $b = (1.6a^2 + h^2)^{1/2} - 0.675h$. The E_S and E_C value represent the elastic modulus of the subgrade and the pavement material respectively.

For the multi-wheel gear configuration, the effect of a cluster of wheels can be expressed by an equivalent single wheel load. Pickett and Ray used the stress distribution concept and developed a number of influence charts for deflections and moments of pavement slabs. It involved a tedious counting of total influence areas. When the surface deflection of an elastic mass is considered as the criterion in determining the effect of a multi-wheel gear, the influence factor of each wheel is given by

$$\text{Influence Factor} = \frac{2}{\pi}\,m^{-1/2}\left[E(m) - (1 - m)\,K(m)\right] \qquad (32)$$

in which $m = (a/x)^2$ and $E(m)$ and $K(m)$ are elliptic integrals for the modulus m. The results of Eq. 32 have been computed and are shown in the following table;

Distance From Reference Point	Influence Factor	Distance From Reference Point	Influence Factor
2.0a	0.2587	3.0a	0.1691
2.1	0.2456	3.2	0.1583
2.2	0.2337	3.4	0.1488
2.3	0.2229	3.6	0.1404
2.4	0.2132	3.8	0.1328
2.5	0.2043	4.0	0.1262
2.6	0.1961	4.5	0.1119
2.7	0.1886	5.0	0.1005
2.8	0.1816	6.0	0.0841
2.9	0.1751	7.0	0.0718
		10.0	0.5000

The equivalent single wheel load is basically a statical deflection conversion. While the vehicle is riding on a pavement surface, the dynamic response of the vehicle will produce additional load on the pavement, known as the dynamic increment, $\overline{DI}$. In the Newark test, pressure gages were installed to monitor the change of tire pressure due to the change of dynamic increment. Throughout the entire test, the pressure gages registered no deviation of the inflation pressure while there is a definite record of dynamic increment of the vehicle. The increase of dynamic load is, therefore, carried by the direct bearing of tire wall, and the tire contact area, πa^2, remains as a constant. In incorporating the dynamic increment, $\overline{DI}$, in the computation of pavement stress, Eq. 31 can be rewritten as

$$\sigma = 1.5\ (1 + \mu)\ (1 + \overline{DI})\ p \left(\frac{a}{h}\right)^2 \left(\frac{3}{4} \ln \frac{h}{a} + \frac{1}{4} \ln \frac{Ec}{Es} + 0.168\right) \tag{31a}$$

If the pavement is constructed on a land fill over a soft ground, regional subsidence should be anticipated. The application of surcharge load will definitely improve the situation and reduce the magnitude of total as well as differential settlement during the service life of the pavement. In designing the new pavement, the contour of differential settlement can be assumed to be a sine wave. The deflection coordinate is

$$y = \frac{1}{2} \Delta \cos \frac{2\pi x}{L} \tag{33}$$

The bending moment in the pavement is

$$M = EI \cdot \frac{d^2y}{dx^2} \tag{34}$$

The maximum bending moment at the bottom of settlement dish, $x = 0$, is

$$M_0 = 2\pi^2 EI \cdot \frac{\Delta}{L^2} \tag{35}$$

The Δ value is the total differential settlement in a wavelength of L. As differential settlement takes place over a long period, the E-value in Eq. 35 represents the creeping modulus of elasticity, which may be only one-third of the modulus of elasticity under short-term loadings. The bending stress in the pavement becomes a straightforward computation if the composite section modulus of the pavement structure is determined.

The volumetric change of pavement material has a significant effect on the structural integrity of the pavement. The change of temperature with depth will result in the warping of the pavement with resulting bending stresses in the pavement components. The radius of curvature, R, of the warping is a function of the coefficient of volumetric change, ϵ, and the thermal gradient, $\Delta t/\Delta z$, and

$$\frac{1}{R} = \epsilon \cdot \frac{\Delta t}{\Delta z}$$

The bending moment, M, in the pavement layer is given by

$$M = EI\,\epsilon \cdot \frac{\Delta t}{\Delta z} \tag{36}$$

The observed $\Delta t/\Delta z$ value is approximately 1.5 F per inch and the ϵ-value is in the range of $\times 10^{-6}$ in./in./deg F.

Spectrum Indicator — Yield Theory

Two distinctive families of deformation curves were observed during the pavement test at Newark Airport (Fig. 15). The deformation condition of a pavement thickness of 21 inches can be closely related to the equilibrium condition where center cracks are developed by Meyerhof's yield theory (13, 14). The deformation of a pavement thickness of 27 inches represents the yield condition when corner cracks, i.e., the first stress crack, might have been encountered in the pavement. The equilibrium of test pavements can be divided into three distinctive states: (a) the plastic state of equilibrium for pavements thinner than 21 inches; (b) the elastic state of equilibrium for pavements heavier than 27 inches; and (c) the transition state for those between 21 and 27 inches.

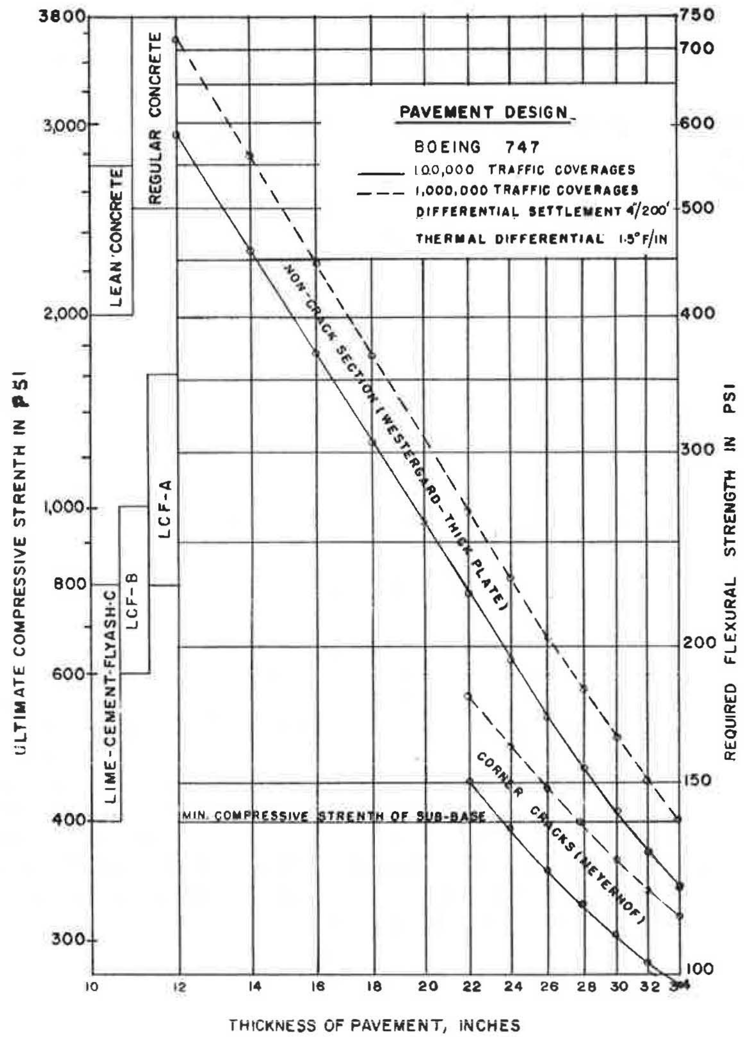

Figure 15. Pavement design by working stress concept.

When a smooth performance is the primary concern in pavement design, the stress-strain condition of the pavement components, including the supporting subgrade, should be constantly in the elastic state of equilibrium. To insure such a requirement, the corner crack condition of Meyerhof's yield theory can be used as a spectrum indicator to detect the state of equilibrium that a pavement will remain in at the passing of a wheel load. Moreover, the design theories governing "rigid pavements" and "flexible pavements" can be tied in together with the yield theory as an indicator.

Other Considerations

Other considerations include the factors governed by maintenance and construction practices, the availability of material, and the construction cost. These factors have a decisive influence on the final formulation of any pavement structure, and should be carefully evaluated at the early stages of pavement design and analysis.

Engineering Judgment

There is no substitute for good engineering judgment. In considering the variability of testings, construction, material, and other factors, there is no theory that can stand by itself. However, a thorough understanding of theories and the interaction of many parameters involved with the pavement design will result in a better, sounder, and more flexible engineering judgment.

Engineering judgment, as shown in Figure 6, represents the collective work of good theoreticians, practical engineers, material specialists, construction inspectors, and experienced maintenance crews. The most important section in the flow chart is the contribution of the pavement user who accepts the level of vehicle vibration and the one who pays the cost of construction. A sound engineering judgment can be established only by balancing the requirements of all contributors.

REFERENCES

1. Reports on Pavement Design and Tests — Redevelopment Program, Newark Airport. The Port of New York Authority, June 1967.
2. Vesic, Aleksandar S. Theoretical Analysis of Structural Behavior of Road Test Flexible Pavement. NCHRP Report No. 10, 1964.
3. Mindlin, R. D. Force at a Point in the Interior of a Semi-Infinite Solid. Physics, Vol. 7, May 1936.
4. Houbolt, J. C. Runway Roughness Studies in the Aeronautic Field. Trans. ASCE, Vol. 127, p. 427-447, 1962.
5. Morris, G. J. Response of a Turbojet and a Piston-Engine Transport Airplane to Runway Roughness. NASA TN-D-3161, National Aeronautics and Space Administration, December 1965.
6. Blackman, R. B., and Tukey, J. W. The Measurement of Power Spectra From the Point of View of Communications Engineer. Dover.
7. Harr, M. E. Influence of Vehicle Speed on Pavement Deflections. HRB Proc., Vol. 41, p. 77-82, 1962.
8. Harr, M. E. Foundation of Theoretical Soil Mechanics. McGraw-Hill Book Co., 1966.
9. Ahlberg, H. L., and Barenberg, E. J. Pozzolanic Pavements. Bull. 473, Engineering Experiment Station, Univ. of Illinois.
10. Hetenyi, M. Beams on Elastic Foundation. Univ. of Michigan Press, 1961, pp. 100-108.
11. Westergaard, H. M. Stresses in Concrete Pavements Computed by Theoretical Analysis. Public Roads, Vol. 7, No. 2, 1926.
12. Timoshenko, S. P., and Goodier, J. N. Theory of Elasticity. McGraw-Hill Book Co., 1959, p. 367.
13. Meyerhof, G. G. Load-Carrying Capacity of Concrete Pavements. Jour. Soil Mech. and Found. Div., ASCE, Vol. 88, SM3, June 1962, pp. 89-116.
14. Losberg, A. On Load-Carrying Capacity of Concrete Pavement. Discussion, Proc. ASCE, Vol. 89, No. SM2, March 1963, pp. 129-136.
15. Development of CBR Flexible Pavement Design Method for Airfields — A Symposium. Trans. ASCE, Vol. 115, 1950, Paper No. 2406, pp. 453-589.

Appendix

EXAMPLE OF PAVEMENT DESIGN

Part I — Load Distribution Concept

<u>Ground Load and Landing Impact</u>

Type of Airplane — Boeing 747
Main Gear Wheel Configuration — Twin-tandem 44 by 58 in.
Main Gear Coordinates — Four Trucks (6.25, 10.83 ft) (18.04, 0.46 ft), symmetrical
Size of Tires — 46 by 16 in. at normal inflation pressure (200 psi)
<u>Ground Load:</u> Taxiing Speed — 30-70 knots
Take-off Speed — 130-150 knots
Take-off Length — 5000-7000 ft at sea level, 90 F

1. Maximum Ramp Weight — 683,000 lb
2. Main Gear Load — 166,000 lb
3. Ground Turning (approx.) — 262,000 lb/gear
4. Rolling Friction (approx.) — 0.07 g (horiz.)
5. Brake Stop (approx.) — 0.3 g (horiz.)
6. Maximum Brake Force (approx.) — 0.8 g (horiz.)

<u>Landing Impact:</u> Approaching Speed — 130-150 knots
Landing Speed — 100-120 knots
Landing Length — 4500-5500 ft

7. Static Landing Load — 124,000 lb/gear
8. Normal Landing (approx.) — 62,000 lb/gear
9. Hard Landing (approx.) — 300,000 lb/gear
10. Ultimate Gear Load — 500,000 lb/gear
11. Ultimate Brake Force — 400,000 lb (vert.) and 200,000 lb (horiz.)

<u>Equivalent Single Wheel</u>

Tire Contact Radius $a = \left(\frac{166.000}{4 \times 200 \times \pi}\right)^{1/2} = 8.13$ in.

Distance From Reference Point	Influence Factor of a Single Tire
x/a = 0.000	1.000
5.41	.094
7.13	.070
8.95	.056
18.4	4 × .027
23.1	4 × .021
39.0	4 × .013
	1.464 Surface deflection of a single wheel

Equivalent Single Wheel Tire Pressure = 200 × 1.464 = 293 psi

<u>Modulus of Deformation of Subgrade, E_s</u>

Tangent Modulus at a stress range of 40 to 60 psi
Mean Value of 33 Bearing Plate Tests = 7,000 psi
Standard Deviation = 1,300 psi
Assumed Design Value = 5,700 psi
Reliability of Design Value:
15 percent of random tests will have an E-value < 5,700 psi

Limit of Dynamic Response of Airplane

Maximum Limit during the service life of the pavement:
Mean Response = 0.12 g in normal operational area
Mean Response = 0.30 g in infrequent traffic area
Traffic Coverages during the service life:

Anticipated Traffic Volume	7,000,000	Movements/Airport
	3,000,000	Movements/Terminal
	4,000,000	Movements/Runway
Full Load Aircraft	3,000,000	Movements/Airport

Deformation Parameter Eq. 28 for x = 0

$$\overline{W}_0 = \frac{2pa}{E_s} = \frac{2 \times 293 \times 8.13}{5.700} = 0.835 \text{ in.}$$

Significant Width of Transverse Deflection Dish

L = 2.3a + 2.0a + 2.3a = 53.7 in. = 4.5 ft
This L-value will be used in Eq. 19 to establish the transfer function between the longitudinal and transverse deflection.

Limiting Normal Stress in Subgrade

Area	Max. Stress in LCF Base (psi)	Max. Stress in Subgrade (psi)	$D_o/\overline{W}_o$	D_o (in.)
Gate position	6	12	0.14	0.117
Concentrated traffic area	8	16	0.22	0.184
Normal traffic area	11	22	0.34	0.284
Infrequent traffic area	20	40	0.70	0.584

Thickness of Pavement—Limiting Normal Stress in LCF Base (See Fig. 3)

Area	σ_z (psi)	σ_z/p	z/a	z (in.)
Gate position	6	0.0205	4.0	32.5
Concentrated traffic area	8	0.0273	3.7	30.1
Normal traffic area	11	0.0375	3.30	26.9
Infrequent traffic area	20	0.068	2.85	23.2

Thickness of Pavement—Limiting Normal Stress in Subgrade—Aggregate Base

Area	σ_z (psi)	σ_z/p	z/a	z (in.)
Gate position	6	0.0205	8.6	70
Concentrated traffic area	8	0.0273	7.4	60
Normal traffic area	11	0.0375	6.4	52
Infrequent traffic area	20	0.068	4.7	38

Surface Shear

Brake Stop: $Q = 0.3 \times \pi \times 293 \times 8.13^2 = 18,300$ lb
Normal Stress at a depth of 30 in.:
$\sigma_z = -0.136 \times 18.300/900 = -2.8$ psi

Part II — Working Stress Concept

Symbols:

h = thickness of pavement, in.
a = radius of tire contact area = 8.13 in.
E_s = tangent modulus of subgrade = 5.700 psi
f'_c = compressive strength of pavement components
σ_b = flexural strength of bottom layer of pavement
E_c = modulus of elasticity of subbase = 450,000 psi
E'_c = creeping modulus of elasticity = 150,000 psi
n = ratio of modulus of elasticity between the top and bottom fibers of pavement material

Bending Stress Due to Differential Settlement

Observed maximum differential settlement: 4 in. in 200 ft
Maximum bending moment: $M = 2\pi^2 EI \Delta/L^2$
Plastic equilibrium of pavement: $M_R = \sigma_b nh^2/2 (n+1)$
Bending stress, plastic state: $\sigma_b = 2(n+1) M/nh^2$
$\sigma_b = .52h$ (for $n = 2$)

Bending Stress Due to Thermal Differential

Maximum bending stress: $M = EI \cdot \epsilon \cdot \Delta t/\Delta z$
Thermal gradient, seasonal variation: $\Delta t/\Delta z = 1.5$ F/in.
maximum daily variation: $\Delta t/\Delta z = 0.5$ F/in.
Coefficient of volumetric change: $\epsilon = 5.8 \times 10^{-6}$ in./in./deg F
$\sigma_b = .33h$ (for $n = 2$)

Bending Stress Due to Wheel Load — Elastic Plate

Bending moment: $M = \frac{1}{4}(1+\mu)(1+\overline{DI})pa^2 \left[\frac{3}{4}\ln\frac{h}{b} + \frac{1}{4}\ln\frac{E_c}{E_s} + .168\right]$

Poisson's ratio: $\mu = 0.15$
Dynamic increment: $\overline{DI} = 0.12$ g
Elastic equilibrium of pavement: $M_R = \sigma_b nh^2/3 (n+1)$
Bending stress, elastic state: $\sigma_b = 3(n+1) M/nh^2$

$$\sigma_b = 21,000 \times \left[\ln\frac{h}{b} + 1.682\right]/h^2 \qquad \text{(for } n = 2\text{)}$$

Bending Stress Due to Wheel Load — Yield Line Method

Bending moment at yield state: $M = (1 - 2 \cdot \lambda a) P/4.6$

$$\lambda a = \left(\frac{6E_s}{E_c}\right)^{1/4} \cdot \left(\frac{a}{h}\right)^{3/4} = .524 \times 4.82/h^{0.75}$$

$\sigma_b = 3(n+1) M/nh^2 = 67.000 (1 - 5.04/h^{0.75})/h^2$ (for $n = 2$ and 22 in. $< h <$ 43 in.)

Fatigue Stress Due to Traffic Coverages

Normal working stress: $\sigma_N = \sigma_b (1 - .092 \log N)$
Equivalent bending stress:
$\sigma_b = 2.25\ \sigma_N$ for 10^6 traffic coverages
$\sigma_b = 1.85\ \sigma_N$ for 10^5 traffic coverages
$\sigma_b = 1.58\ \sigma_N$ for 10^4 traffic coverages
$\sigma_b = 1.38\ \sigma_N$ for 10^3 traffic coverages

Summary of Pavement Design—LCF Base

R/W = Runways
T/W = Taxiways
TA = Terminal Aprons
AP = Aircraft Parking

G = Gate Position
C = Concentrated Traffic Area
N = Normal Traffic Area
I = Infrequent Traffic Area

Factor	Symbol	R/W-C	R/W-N	T/W-C	T/W-N	TA-G	TA-N	AP-I
Traffic coverages		10^5	10^4	10^6	10^5	10^6	10^4	10^3
Limit of dynamic response	$\overline{DI}$	0.12 g	0.30 g	0.12 g	0.30 g	0.12 g	0.12 g	0.12 g
Longitudinal permanent deformation	k	0.0028	0.0070	0.0036	0.0090	0.010	0.010	0.010
$\Delta = k\sqrt{L}$	Δ	0.0059 ft	0.0147 ft	0.0076 ft	0.0181 ft	0.021 ft	0.021 ft	0.021 ft
Trans. permanent deformation		0.034 ft	0.122 ft	0.051 ft	0.164 ft	0.185 ft	0.185 ft	0.185 ft
$D_N = 10\ (\Delta - 0.0012\sqrt{L}$	D_N	0.412 in.	1.46 in.	0.61 in.	1.96 in.	2.22 in.	2.22 in.	2.22 in.
Progressive trans. permanent deformation $D_o = (D_N - 0.01)/\log N$	D_o	0.080 in.	0.362 in.	0.100 in.	0.390 in.	0.368 in.	0.552 in.	0.736 in.
Limiting stress in LCF base	σ_z	8 psi	11 psi	8 psi	11 psi	6 psi	11 psi	20 psi
$D_o = (2\sigma_z - 5)\overline{W}_o/49.4$	D_o	0.184 in.	0.284 in.	0.184 in.	0.284 in.	0.117 in.	0.284 in.	0.584 in.
Limiting elastic deformation		0.1335	0.1335	0.1335	0.1335	0.1335	0.1335	0.1335
$\overline{W}_z = 0.16\ \overline{W}_o + 0.43\ D_o$		0.0345	0.1220	0.0430	0.1220	0.0500	0.1220	0.2510
		0.168 in.	0.256 in.	0.176 in.	0.256 in.	0.184 in.	0.256 in.	0.385 in.
Parameter of $\overline{W}$ E/p $\overline{W}_z E_s/p\ (1 + \overline{DI})$		2.92	3.83	3.06	3.83	3.19	4.44	6.52
Thickness of pavement—limiting deformation, Fig. 14	z	33.4 in.	25.1 in.	31.8 in.	25.1 in.	30.4 in.	21.2 in.	13.8 in.
Thickness of pavement—limiting stress of LCF base	z	30.1 in.	26.9 in.	30.1 in.	26.9 in.	32.5 in.	26.9 in.	23.2 in.
Thickness of pavement—working stress concept (*yield condition)	z	30.5 in.	23.5 in.*	34.0 in.	26.7 in.*	34.0 in.	27.5 in.	25.4 in.
Proposed thickness		32 in.	26 in.	32 in.	26 in.	34 in.	28 in.	26 in.

Summary of Pavement Design—Aggregate Base

Factor	Symbol	R/W-C	R/W-N	T/W-C	T/W-N	TA-G	TA-N	AP-I
Traffic coverages		10^5	10^4	10^6	10^5	10^6	10^4	10^3
Limit of dynamic response	$\overline{DI}$	0.12 g	0.30 g	0.12 g	0.30 g	0.12 g	0.12 g	0.12 g
Long. permanent deformation	Δ	0.0059 ft	0.0147 ft	0.0076 ft	0.0181 ft	0.021 ft	0.021 ft	0.021 ft
Trans. permanent deformation		0.0307 ft	0.0764 ft	0.0395 ft	0.094 ft	0.110 ft	0.110 ft	0.110 ft
$D_N = 5.2\ \Delta$	D_N	0.368 in.	0.916 in.	0.474 in.	1.128 in.	1.32 in.	1.32 in.	1.32 in.
Progressive trans. permanent deformation	D_o	0.0716 in.	0.226 in.	0.0773 in.	0.223 in.	0.219 in.	0.328 in.	0.437 in.
Limiting stress in subgrade	σ_z	8 psi	11 psi	8 psi	11 psi	6 psi	11 psi	20 psi
$D_o = (\sigma_z - 5)\ \overline{W}_o/49.4$	D_o	0.05 in.	0.10 in.	0.05 in.	0.10 in.	0.017 in.	0.10 in.	0.25 in.
Limiting elastic deformation		0.050	0.050	0.050	0.050	0.050	0.050	0.050
$\overline{W}_z = 0.06\ \overline{W}_o + 0.43\ D_o$	$\overline{W}_z$	0.022	0.043	0.022	0.043	0.007	0.043	0.108
		0.072 in.	0.093 in.	0.072 in.	0.093 in.	0.057 in.	0.093 in.	0.158 in.
Parameter of $\overline{W}$E/p		1.25	1.39	1.25	1.39	0.99	1.62	2.75 in.
Thickness of pavement limiting deformation, Fig. 14	z	>50 in.	>50 in.	>50 in.	>50 in.	>50 in.	>50 in.	>35 in.
Thickness of pavement limiting stress in subgrade	z	60 in.	52 in.	60 in.	52 in.	70 in.	52 in.	38 in.

Discussion

G. Y. SEBASTYAN, Chief, Engineering Design Division, Airport Development, Construction Engineering, and Architectural Branch, Department of Transport, Canada — The author of the paper is to be complimented for his valuable contribution to the art of flexible pavement design and for focusing attention on the use of system analysis in this field. Because the work of the Canadian Department of Transport in designing, constructing, and maintaining Canadian airport facilities is directly related to Mr. Yang's study, we were extremely interested in the subject. Reviewing the paper in detail, we wish to make the following comments:

1. The rutting problem extensively discussed by the author is not evidenced to any major degree on Canadian airports unless design or specification requirements were not met. There could be three reasons for such a performance difference: (a) the difference in the quality of the surfacing and base materials used for airports under the jurisdiction of the New York Port Authority and the Canadian Department of Transport; (b) the difference in material and construction specification requirements and the compliance with these specifications for the density of the surfacing material, base, subbase, and subgrade; and (c) the difference in aircraft loading density and intensity.
2. Pavement structural design and the quality of the pavement components are indivisibly related. Any change in one has to be compensated by making an appropriate change in the other. It is our impression that the author did not take fully into account the effect of specification requirements as an integral part of design and the full enforcement of these specifications on the airport pavement performance.
3. The author assumed five possible definitions for modulus of deformation. There are many more alternative definitions as described in Ref. 16. In Ref. 16, a plea was also made for the standardization of the definition for modulus of deformation.
4. Vibratory rollers are used with success on Canadian airport projects to compact granular materials similar to those encountered in the New York City area.
5. Reference is made in the paper to the introduction of clay slurry into sand as a possible subgrade stabilization method. On the basis of our experience, we do not feel that this is a realistic or desirable approach.
6. The following statement is made in the paper: "If the pavements are of identical thickness on identical subgrade, there seems no significant difference in total surface deflection between the stabilized or aggregate-based pavement." We feel that this statement certainly should be clarified.

Reference

16. Sebastyan, G. Y. Flexible Airport Design and Performance. Second Internat. Conf. on Structural Design of Asphalt Pavements, Ann Arbor, Mich., 1967.

NAI C. YANG, Closure — The writer wishes to thank Mr. Sebastyan for his interesting discussion of the paper. There are a few details raised in the discussion which warrant clarification.

1. In The Port of New York area, no stabilized base has previously been used in airport pavement construction. The "bird bath" type of deformation is commonly observed on the surface of asphaltic pavement when heavy channelized traffic is encountered. In recent years, the aircraft loads and traffic volumes have increased so rapidly that the effect of surface deformation (such as rutting of the pavement) has been a big concern of airport operation.
2. The writer assumes that the paper deals only with the design and analysis of airport pavements. The preparation and enforcement of construction specifications are beyond the scope of this paper. In stating the basic engineering considerations, a coefficient of variation has been assigned for quality control and construction performance.

The design computation as given in the paper shows that the coefficient of variation is assumed to be 0. 2. The modulus of deformation of the subgrade and the compressive strength of the base material used in the design computation are equal to the mean value minus one standard deviation. In actual job construction, full enforcement of specification requirements has been constantly exercised. A coefficient of 0. 15 is normally observed.

3. A joint plea seems appropriate for standardization of the definition for the modulus of deformation of subgrade.

4. The vibratory compactor has been widely used in pavement construction at the area airports. The normal density reading is in the range of 95 to 97 percent of the modified Proctor test. At the Newark pavement test, an air-on-the-run pneumatic-tired roller was used. The density reading increased to 102 to 107 percent. Consequently, this type of compactor was selected for the new pavement construction at Newark Airport.

5. The use of clay slurry is another possible means for stabilizing the loose sand. No such practice has been exercised at the New York airports.

6. With regard to the magnitude of surface deflection, reference is suggested to the observed data shown in Figure 4. A meaningful interpretation may be derived by completing the quotation: "The total surface deflection is largely contributed by the deformation of the subgrade. However, the longer, smooth, deflection configuration of the stabilized base will produce a more durable and better performing pavement."

Design of Emulsified Asphalt Treated Bases

F. N. FINN and R. G. HICKS, Materials Research and Development, Inc.; and
W. J. KARI and L. D. COYNE, Chevron Asphalt Company

•ASPHALT pavements must be designed so that the thickness of the structure and the quality of the pavement components are sufficient to prevent not only plastic deformation (instability) but also fatigue cracking of the asphalt surfacing. To preclude both deformation and fatigue distress of pavements containing emulsified asphalt treated bases, it has been necessary to establish mix design requirements and thickness requirements that will satisfactorily prevent either type of distress. This report describes an investigation that combines current and established mix design and thickness design methods with layered system analysis for the design of emulsified asphalt treated bases.

Included as part of the investigation was a field survey of in-service projects constructed with asphalt emulsion treated bases. The purposes of this phase were (a) to obtain undisturbed samples of stabilized base for laboratory testing and (b) to observe the performance of pavements constructed with emulsion treated bases under a variety of environments.

It is the intent of this paper to:

1. Summarize the performance and properties of asphalt emulsion treated bases,
2. Illustrate how elastic theory is used to estimate changes in thickness requirements for pavement constructions,
3. Estimate the effect of curing rate of emulsified asphalt on the load-carrying potential, and
4. Present a method of mix design using asphalt emulsion as a binding agent.

PERFORMANCE OF IN-SERVICE PAVEMENTS

Condition surveys of in-service projects built with asphalt emulsion stabilized bases were made to establish the adequacy of performance of this type construction over a wide range of conditions. Pavement evaluations were conducted by use of a rating system adapted from those of the Highway Research Board (1) and the Washington State Department of Highways (2). Distortion (related to stability), cracking, and surface distress were considered in rating the pavements. The rated pavements were divided into five performance categories depending on the severity of the distress observed. At the time of the condition survey, core samples of the surface and base layers were taken to determine the ultimate or long-term elastic strength properties (resilient modulus) of bases stabilized with asphalt emulsions.

Projects were selected for survey on the basis of type of service and traffic volume, aggregate type used, and project location. Twenty-seven projects, located in seven states, were included in the survey program. Construction information was available on a number of projects to supplement the job performance ratings. A summary of the data is given in Tables 1, 2, and 3. Other case histories are available (3).

From these condition surveys, it was concluded that emulsion treated bases were performing satisfactorily. This was particularly true for those mixes designed in accordance with recognized criteria. Distress where noted was associated principally with local drainage conditions or construction problems. In some cases, although no distress was observed, cores could not be recovered, indicating that curing (drying) of the emulsion was still in progress. Cores obtained from the in situ base layers had low water contents, indicating the ability of emulsions to make these bases water-resistant.

Paper sponsored by Committee on Flexible Pavement Design and presented at the 47th Annual Meeting.

TABLE 1

JOB DESCRIPTION AND SUMMARY OF TEST RESULTS

Location	Brookings, Oregon	Aurora Casket Co. Airport	Big Bone Boone County Kentucky	Lake of the Woods Medford, Ore.	Collawash Oregon	Clackamas River Oregon
Emulsion Type	SM-K	SS-Kh	SS-Kh	SS-K	SS-K	SS-K
Mixing Method	Central Plant	Travel Plant	Travel Plant	Central Plant	Central Plant	Central Plant
Class of Traffic(1)	Light	Aircraft	Light	Heavy	Heavy	Heavy
Subgrade Classification	Good	Fair	Poor	Poor	Good	Good
Age When Cored	2 Years	4 Months	4 Years	1 Month	2 Months	1 Year
Core Gradation % Passing 3/4"	81	95	100	98	98	100
# 4	42	49	52	50	51	55
30	17	23	17	20	22	24
200	3	6	7	10	12	13
% Emulsion (Calc. From Extr. Asphalt)	10.8	7.2	9.8	6.4	8.0	7.3
Recovered Asphalt Penetration @ 77°F	24	47	38	41	46	58
Softening Point °F	143	128	138	130	130	123
Aggregate Sp. Gravity	2.69	2.71	2.72		2.60	2.77
Core Density, pcf	143.8	143.4	146.4	136.5	117.3-131.2	134.8-137.5
Core Moisture, %	1.1	0.4	1.5	1.1	1.7	1.9
Resilient Modulus, psi	176,000	132,000	210,000	27,200	96,100	60,600
Performance Rating	Fairly Good	Excellent	Excellent	Excellent	Poor to Excellent	Excellent

Location	Chula Vista Boat Ramp California	Jordan River National Fish Hatchery Core 1	Jordan River National Fish Hatchery Core 2	Jordan River National Fish Hatchery Core 3	Truck Haven Rd. Borrego Springs California	Fletcher Rd. Kalkaska Co. Michigan
Emulsion Type	SM-K		SS-Kh		DM-1h	SS-Kh
Mixing Method	In Place		In Place		In Place	Travel Plant (Duo-Stab.)
Class of Traffic(1)	Light		Light		Light	Light
Subgrade Classification	Fair		Very Good		Good	Good
Age When Cored	4 Years		2 Years		2 Years	2 Months
Core Gradation 3/4"		100	100	100	93	94
% Passing # 4	70	64	65	67	75	75
30	32	34	35	34	48	56
200	5	5	6	7	12	7
% Emulsion (Calc. From Extr. Asphalt)	9.5	10.0	10.4	9.8	3.7	10.2
Recovered Asphalt Penetration @ 77°F	31	51	33	34	9	29
Softening Point °F	133	127	135	133	151	134
Aggregate Sp. Gravity	2.68	2.64	2.63		2.61	
Core Density, pcf	128.8	138.6	138.0	138.3	131.7	134.5
Core Moisture, %	0.4					
Resilient Modulus, psi	500,000	401,000	218,000	500,000	526,000	340,000
Performance Rating	Excellent		Very Good		Very Good	Excellent

(1) The Asphalt Institute Thickness Design Manual (MS-1).

TABLE 2

JOB DESCRIPTION AND SUMMARY OF TEST RESULTS

Location	Sugar Island, Chippewa Co., Michigan: Core 1	Core 2	Core 3	(Lakeshore Drive) Mason County, Michigan: Core 1	Core 2	Core 3	Core 4
Emulsion Type		SS-Kh			SM-K		
Mixing Method		In Place			In Place		
Class of Traffic(1)		Light			Light		
Subgrade Classification		Poor			Good		
Age When Cored		2 Years			5 Years		
Core Gradation % Passing 3/4"	98	95	99	100	97	96	95
# 4	83	83	84	84	82	83	89
30	52	70	65	44	65	69	74
200	5	7	7	8	9	9	9
% Emulsion (Calc. From Extr. Asphalt)	13.3	11.7	9.8	5.3	4.9	5.5	6.7
Recovered Asphalt Penetration @ 77°F	36	34	48	22	43	29	9
Softening Point °F	134	133	128	148	140	140	159
Aggregate Sp.Gravity	2.62				2.62	2.66	
Core Density, pcf	130.2	129.3	130.4	136.5	141.3	140.7	135.4
Core Moisture, %		Nil					
Resilient Modulus, psi	164,500	268,000	386,000	325,700	783,000	750,000	961,000
Performance Rating	Fair	Fair	Fair		Excellent		

Location	Lola Pass Mt. Hood Oregon	NAS Alameda California	Tawas Park Rd. Michigan	Hilton Head Road 80 South Carolina		Cox Road Brevard Co. Florida	Perdido Bay Country Club Florida	
Emulsion Type	SS-Kh	DM-1h	SM-K	SM-K		SM-K	SM-K	
Mixing Method	Central Plant	In Place	Travel Plant (Duo-Stab.)	Travel Plant (Woods)		In Place	In Place	
Class of Traffic(1)	Light	Aircraft	Light	Medium		Light	Light	
Subgrade Classification	Very Good	Good	Good	Very Good		Good	Very Good	
Age When Cored	2 Months	16 Years	2 Years	1 Year	4 Years	4 Years	1 Year	3 Years
Core Gradation % Passing 3/4"	98		100					
# 4	88		92	99	100	99		
30	49	98	84	99	99	93	97	98
200	12	5	5	3	4	5	6	9
% Emulsion (Calc. From Extr. Asphalt)	10.3	4.5	8.7	13.0	8.4	3.4	8.3	9.1
Recovered Asphalt Penetration @ 77°F	37		62	27	31	16	28	25
Softening Point °F	130		123	149	144	157	144	143
Aggregate Sp. Gravity		2.66	2.55	2.67	2.65	2.61	2.63	2.62
Core Density, pcf	121.5	120.6	128.4		111.9	131.9	120.6	116.3
Core Moisture, %		7.6		3.3	6.5	9.1	10.1	3.8
Resilient Modulus, psi	95,000		49,800	137,000	83,500	497,000	91,200	177,500
Performance Rating	Excellent	Good	Good	Excellent		Excellent	Excellent	Very Good

(1) The Asphalt Institute Thickness Design Manual (MS-1).

TABLE 3

JOB DESCRIPTION AND SUMMARY OF TEST RESULTS

Location	Fort Rucker Mattison Range Alabama	Treasure Island California	Fort Rucker (Ech Field) Alabama	LaPalma Avenue Buena Park California	Rancho Santa Fe Los Arboles Road California		Pier "F" Long Beach California
Emulsion Type	SM-K	DM-1h	DM-1h	SM-K	SM-K		DM-2
Mixing Method	In Place	In Place	In Place	In Place	In Place (Seaman Mixer)		In Place
Class of Traffic(1)	Aircraft	Light	Aircraft	Heavy	Light		Very Heavy
Subgrade Classification	Fair	Very Good	Fair	Fair	Fair		Very Good
Age When Cored	3 Years	28 Years	11 Years	4 Years	6 Years		2 Years
Core Gradation 3/4"						100	
% Passing # 4		98		99	99	98	
30	89	90	87	89	65	80	99
200	10	12	14	15	16	13	18
% Emulsion (Calc. From Extr.Asphalt)	8.1	10.0	12.2	7.2	7.7	5.3	8.8
Recovered Asphalt							
Penetration @ 77°F	33		13	1	181	15	13
Softening Point °F	140		176	206	102	152	148
Aggregate Sp.Gravity	2.60		2.64		2.69	2.58	
Core Density, pcf	125.3	126.6	114.3	123.9	133.5	113.7	101.8
Core Moisture, %	1.7	7.9	1.0	1.1	1.3	1.4	0.3
Resilient Modulus, psi	398,000		290,000	415,000	86,800		142,000
Performance Rating	Good	Excellent	Very Good	Excellent	Very Good		Excellent

Location	182nd Avenue Torrance California	Avenue "O" 90 - 150th St. Palmdale, Calif.	Avenue "O" 105 - 140th St. Palmdale, Calif.	Santa Barbara Airport California	Acacia St. Cypress California	Northmont Tract, Oxnard California
Emulsion Type	SM-K	SM-K	SM-K	DM-2	SM-K	SM-K
Mixing Method	In Place	Travel Plant	Travel Plant (Woods)	Road Mix	In Place	In Place
Class of Traffic(1)	Heavy	Light	Light	Aircraft	Light	Light
Subgrade Classification	Poor	Poor	Fair	Poor	Poor	Poor
Age When Cored	5 Years	3 Years	2 Years	22 Years	4 Years	4 Years
Core Gradation 3/4"	100				100	100
% Passing # 4	99	99	100	100	88	98
30	96	92	94	99	75	90
200	19	20	28	24	33	35
% Emulsion (Calc. From Extr.Asphalt)	3.2	7.2	6.1	6.2	7.8	8.8
Recovered Asphalt						
Penetration @ 77°F	1	8	13	6	2	10
Softening Point °F	194	165	149	176	195	156
Aggregate Sp. Gravity			2.63	2.61	2.68	2.59
Core Density, pcf	123.1	114.7	113.3	111.6	126.5	121.4
Core Moisture, %	2.0	0.3	1.6	0.6	7.6	1.8
Resilient Modulus, psi	900,000	412,000	272,000	252,000	336,000	153,000
Performance Rating	Very Good	Very Good	Good	Good	Excellent	Excellent

(1) The Asphalt Institute Thickness Design Manual (MS-1).

USE OF LAYERED ELASTIC SYSTEM FOR BASE THICKNESS DESIGN

Background

Ever since Burmister (4) presented his paper for using the elastic theory to compute stresses and displacements in a layered system, engineers have been seeking ways to apply his analytical solutions to pavement design. For the most part, there has been some reluctance by engineers to use elastic theory to compute stresses and displacements in layered systems. The most probable reasons for this reluctance can be found in some or all of the following:

1. Assumption that a pavement construction can be modeled by an elastic, isotropic, homogeneous solid was generally unacceptable to most engineers.
2. Engineers were not convinced that the somewhat complicated layered system was any better than the simple Boussinesq equations for a single material.
3. Laboratory methods for measuring the elastic material properties were not well developed.
4. Analytical solutions were only available for two-layered systems and indirectly for three-layered systems, whereas asphalt pavements are frequently constructed with four or more layers.

Two significant technological advancements have been made that make it possible to pursue the layered system with more ease and confidence. First, in the field of soil mechanics, major improvements in test procedures have been achieved, including the ability to measure properties in dynamic loading and, second, the electronic computer is available as a fairly commonplace tool to solve complicated analytical problems rapidly.

Utilizing these tools, highway researchers have initiated extensive research programs to explore the potential of various theories to model pavement construction. Two theories have dominated the research; namely, linear elasticity and linear viscoelasticity (4, 5, 6, 7, 8, 9, 10).

In order to apply theory to pavement design, it is necessary to satisfy the following requirements:

1. Measure or estimate the physical properties required to characterize the pavement layer materials, e.g., modulus of elasticity (E) and Poisson's ratio (μ) for linear elasticity;
2. Combine these physical properties into a numerical analysis that will predict meaningful values of stress and strain in the various layers; and
3. Establish design criteria that can be related to the predicted stress and strain.

A discussion of the physical properties required to characterize pavements and techniques employed to measure these properties can be found in the references previously cited. The combination of these physical properties in numerical solutions of the layered elastic system has been described (10, 11, 12, 13). Very little comparable information is available for the viscoelastic system approach. Design criteria available in the literature also tend to favor the elastic approach (8, 10, 14, 15).

As a result of this work, many investigators now feel that as a first approximation the linear elastic layered system can be used to model asphalt pavement construction. It is pertinent to note that the use of the foregoing analytical procedures in pavement design requires careful and knowledgeable application of laboratory data to field conditions. For example, the generally accepted strength dependency of asphalt concrete or asphalt treated materials with rate of loading is accounted for by testing materials dynamically at frequencies compatible with vehicular traffic. The effect of temperature on the strength of asphalt treated materials is introduced by a similar technique, namely, testing materials in the range of temperatures anticipated for a particular environment.

Application of Theory to Design

The approach used to develop thickness requirements of the base as a function of its elastic properties was as follows:

1. Without regard for the precise type of base to be used, a series of hypothetical problems was solved by the five-layer elastic theory solution of Chevron Research Company (13). Each problem called for a prediction of stress, strain, and deflection as a function of the thickness and elastic properties of the layers.
2. An estimate was made of the thickness of base required, as a function of its elastic properties, to simultaneously satisfy the design criteria suggested in other studies (10, 15, 16).
3. The estimated thickness requirements were compared and reconciled with established design methods, specifically The Asphalt Institute and the California Thickness Design Methods.

Hypothetical Problems

Analytical solutions for a multilayered system were made using a range of strength values for the base and subgrade and a range of base thicknesses. The thickness and strength (resilient modulus) of the asphalt concrete were assumed to be constant for purposes of these solutions. The various problems included in the computer program are summarized in Table 4.

Two moduli of asphalt concrete were used, 150, 000 psi and 900, 000 psi. These are representative of values being measured and reported by a number of organizations, both in this country and abroad (10, 17, 18). The specific value is dependent on the temperature used for testing; the higher the temperature, the lower the modulus.

TABLE 4
PROBLEM STATEMENT FOR COMPUTING STREES-STRAIN AND DEFLECTION FOR LAYERED SYSTEMS

Thickness of A.C. Surfacing		3 Inches					
Elastic Modulus of Surface-psi		150, 000 psi			900, 000 psi		
Elastic Modulus of Subgrade-psi		3, 000	12, 000	21, 000	3, 000	12, 000	21, 000
Elastic Modulus of Base - psi	Thickness of Bases						
	6	x	x	x	x	x	x
	9	x	x	x	x	x	x
15, 000	15	x	x	x	x	x	x
	27	x	x	x	x	x	x
	33	x	x	x	x	x	x
	6	x	x	x	x	x	x
	9	x	x	x	x	x	x
40, 000	15	x	x	x	x	x	x
	27	x	x	x	x	x	x
	33	x	x	x	x	x	x
	6	x	x	x	x	x	x
	9	x	x	x	x	x	x
75, 000	15	x	x	x	x	x	x
	27	x	x	x	x	x	x
	33	x	x	x	x	x	x
	6	x	x	x	x	x	x
	9	x	x	x	x	x	x
250, 000	15	x	x	x	x	x	x
	27	x	x	x	x	x	x
	33	x	x	x	x	x	x
	6	x	x	x	x	x	x
	9	x	x	x	x	x	x
1, 000, 000	15	x	x	x	x	x	x
	27	x	x	x	x	x	x
	33	x	x	x	x	x	x

According to work reported previously (10), a modulus of 150, 000 psi for the asphalt concrete should correspond to a temperature of approximately 95 F. Such temperature readings are typical of those obtained in asphalt concrete wearing surfaces in many parts of the United States during the summer months. From an analysis of the computer output, it was shown that a greater responsibility must be assigned to the base layer for limiting the deflection and subgrade stress when the modulus of the wearing surface is 150, 000 psi. Hence, this value was used in further work dealing with base thickness requirements.

For the problems shown in Table 4, the base modulus at times exceeds the modulus of the asphalt concrete surface. Kallas (19) has shown that this is possible due to the lower temperatures below the pavement surface.

Three levels for the subgrade modulus were included, as shown in Table 4, to evaluate the effect of the subgrade strength and to bracket classes of subgrades ranging from poor to good.

Determination of Base Thickness to Satisfy Design Criteria

From an analysis of the computer output, it was found that the most critical design criteria were total deflection and vertical strain on the subgrade. The strain criteria on the underside of the asphalt concrete surface layer were invariably satisfied if these two responses were satisfied. As a result, only deflection and vertical strain criteria were considered.

Deflection Criteria

Recent publications of the California Division of Highways (16) have illustrated a relationship between limiting deflection and traffic. For instance, a 3-inch asphaltic concrete wearing surface is shown to have a tolerable deflection of 0. 040 inches for a traffic index of 5. 5.

Computer solutions for predicting deflection from base thickness and elastic properties are shown in Figure 1. For cases illustrated in Figure 1a, where the subgrade soil modulus is 3, 000 psi (poor) and the base modular values are 40, 000 psi and 250,000 psi, the respective thickness requirements of the base would be 18 inches and 7 inches, a ratio of 2. 6 to 1 for a traffic index of 5. 5.

Strain Criteria

Limiting values of compressive strain in the subgrade have been reported (10). The allowable strain on the subgrade decreases with traffic ranging from about 0. 06 inches for a thousand weighted load applications to 0.004 inches for 10 million load applications.

Computer solutions for predicting vertical strain at the surface of the subgrade soil for various subgrade moduli are shown in Figures 2a, 2b, and 2c. For Figure 2a, where the subgrade soil modulus is 3, 000 psi (poor) and the base modular values are 40, 000 psi and 250, 000 psi, the respective thickness requirements of the base would be 18 inches and 6½ inches, a ratio of 2. 75 to 1. For this case, it is assumed that deflection requirements would control.

Comparisons with Established Design Methods

As shown, initial attempts to obtain estimates of thickness requirements were made by finding the thickness of base necessary to simultaneously satisfy published criteria for surface deflection and vertical stress or strain on the subgrade (10, 16). While it was possible to do this arithmetically as a function of the level of traffic, the resulting thicknesses did not satisfy the test of reasonableness in that they were, at times, in substantial disagreement with design thicknesses obtained from empirical systems based on using untreated aggregate bases.

To reconcile these differences, it was decided to use an established empirical design system to set thickness requirements for the untreated aggregate base and to use theory as the basis for altering base thickness requirements as a function of strength in the

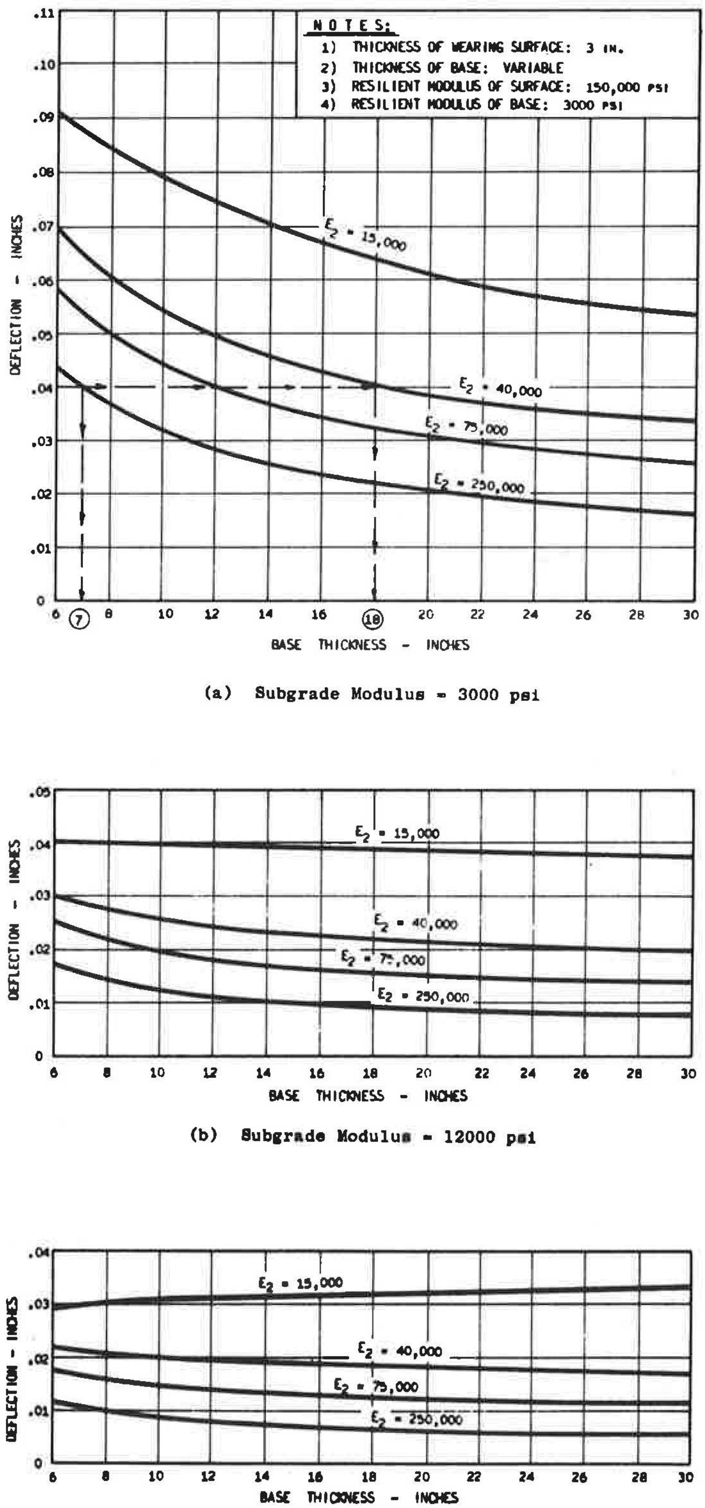

(a) Subgrade Modulus = 3000 psi

(b) Subgrade Modulus = 12000 psi

(c) Subgrade Modulus = 21000 psi

Figure 1. Surface deflection as a function of base thickness and base strength.

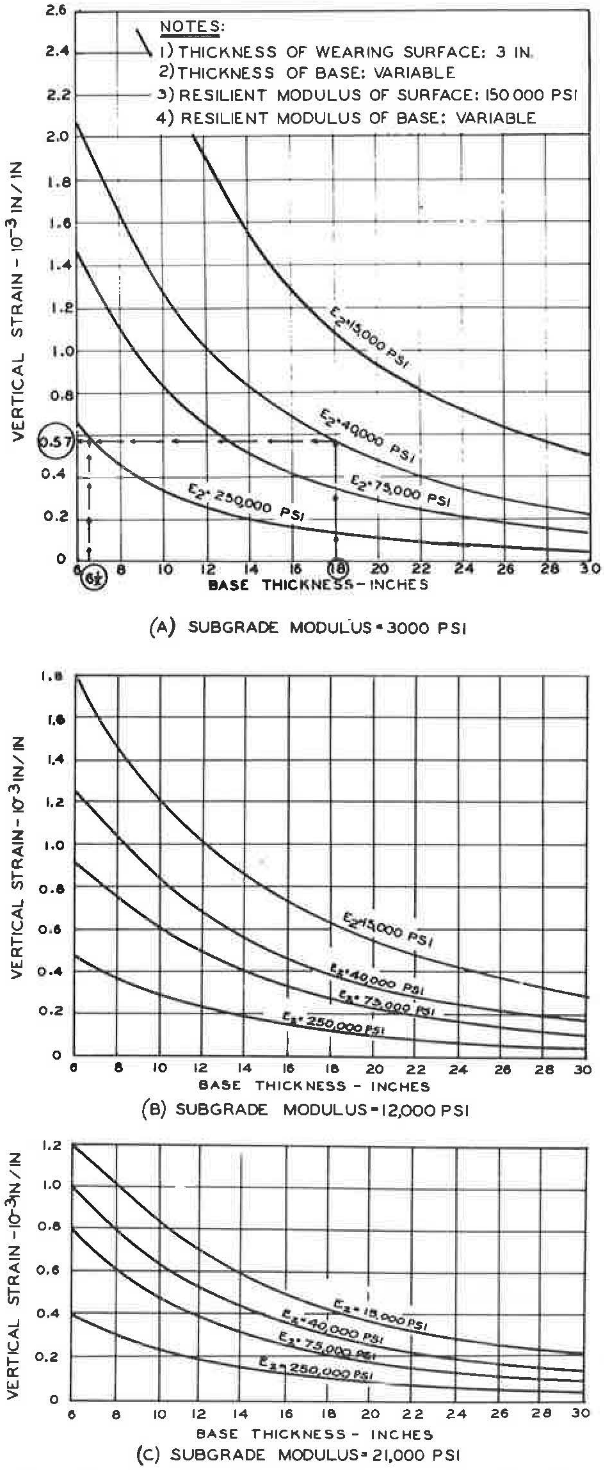

Figure 2. Vertical strain on the subgrade as a function of base thickness and base strength.

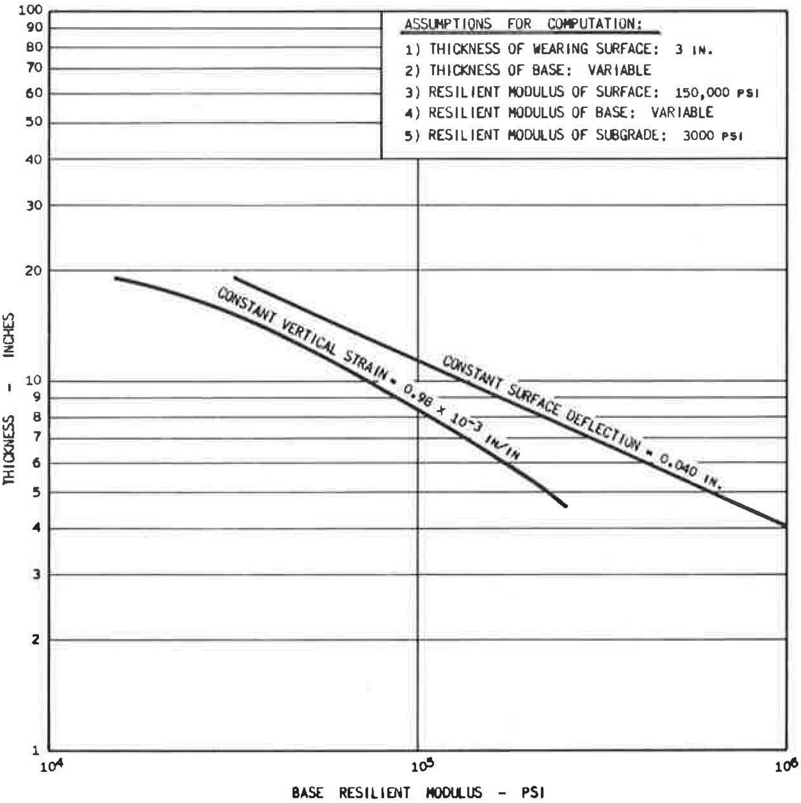

Figure 3. Illustration of linearity of base thickness to resilient modulus of base to maintain constant deflection and vertical strain.

base. The Asphalt Institute has developed thickness design procedures based on observations of performance from a very broad source of information including the AASHO (20) and WASHO (21) Road Tests. These procedures (22) include provision for the effect of traffic, subgrade strength, and relative strength of materials on the thickness of the pavement system. Specifically, it is possible to determine thickness requirements for either untreated aggregate base or asphalt concrete. No provision is currently made for base materials with strengths between these two materials.

Test results on cores obtained from existing pavements having asphalt emulsion treated bases indicate that these materials will have resilient modulus values ranging from 27,200 psi to over 900,000 psi at a test temperature of 77 F (see Tables 1-3). For the most part, these values fall between values reported for aggregate base and asphalt concrete.

In order to be able to use theory as a means of adjusting thickness as a function of base stiffness, it was hypothesized that any two pavement sections having identical thicknesses of wearing surface could be expected to provide the same performance if the surface (total) deflection and vertical stress or strain at the subgrade remain constant. From computations used to plot Figures 1 and 2, it is possible to replot the information for constant levels of deflection and strain as a function of base thickness and resilient modulus of the base as shown in Figure 3. This shows that for a constant deflection and vertical strain, the thickness will vary linearly on a log-log plot. The slope of this line indicates the rate of change of base thickness as a function of the base strength. Thus, theory has been used to show the nature of the change in thickness requirements for a range of resilient modulus values in the base layer.

In order to apply the information represented in Figure 3 to real base thickness requirements, it is necessary to fix the coordinates for aggregate base and asphalt concrete. For this purpose, it was assumed that the modulus of asphalt concrete base is 800, 000 psi when used as the base layer. This strength value is consistent with those reported in the literature for asphalt concrete at a temperature of 77 F. The strength values for aggregate base are more difficult to assess. Reported values of resilient modulus for this type of material range widely and tend to be affected by a variety of factors such as confining pressure, state of stress, water content, and density. Determinations of in-place elastic properties have been reported (18). These measurements indicate that the effective modulus of the aggregate base will exceed the modulus of the subgrade by a factor of from approximately 1.5 to 3. For the requirements of this study, the multiplier of 3.0 has been used. Thus, the base aggregate was assigned a modular value of 9,000, 18,000, and 36,000 psi, as a function of the subgrade strengths of 3,000, 6,000, and 12,000 psi respectively.

A typical example for estimating base thickness requirements is as follows:

1. Traffic—Assume a design traffic number (DTM) of 10.
2. Subgrade strength—Several strength tests can be used, e.g., R-value, CBR, and resilient modulus. Assume $R \approx 12$, $CBR \approx 2$, $M_R \approx 3,000$ psi.
3. Type and thickness of surfacing—Assume a thickness of 3 inches for asphalt concrete surfacing.
4. Thickness of asphalt concrete base—From the WASHO Road Test (21), the total thickness of asphalt concrete surfacing and base (T_A) is 9 inches. Thus, the thickness of asphalt concrete base is 6 inches.
5. Thickness of aggregate base—Convert the base thickness from asphalt concrete to aggregate by the most recent substitution ratio, in this case 1 to 2. Thus, the thickness of aggregate base would be 12 inches.
6. Effective modulus of aggregate base—This is determined by using the multiplier of 3.0 previously mentioned, i.e., 3.0 times subgrade modulus. The estimated modulus of the base is thus 9,000 psi.
7. Thickness of emulsion treated base—On a log-log graph, plot the thickness resilient modulus coordinates for each material.

The results of steps 1 through 7 are shown in Figure 4a. The line connecting the point for aggregate base and asphaltic concrete base can be used for estimating the thickness of materials of intermediate strength values (i.e., emulsion bases). It should be noted that the slope of the lines shown in Figure 4 are flatter than those shown in Figure 3 for constant deflection and vertical strain. Assuming that the thickness of aggregate base is properly fixed, then the flatter slopes shown are conservative, and greater reductions in thickness would be indicated as the strength or modular value of the base increases. Both the WASHO and AASHO Road Test results indicate the substitution ratio of 1 to 2 is conservative.

It is believed that the equivalency of designs indicated by the line connecting the end points established by procedures previously described are reasonable and conservative for the following reasons:

1. Thickness designs for aggregate bases have a longer history for evaluation and probably include a minimum factor of safety.
2. The equivalency used by The Asphalt Institute is considered conservative (low) in view of results from test roads.
3. The end-point thickness requirements have been established empirically; the strength of the stabilized base has been determined to be intermediate between the end points. For the interpolation provided, the layer equivalency can never exceed 2.0 as currently set for asphalt concrete.
4. The core samples of the treated base were tested with zero confining pressure, whereas the in situ pavement materials are subjected to some confinement.

Referring again to Figure 4, it is possible to draw a family of curves for each level of traffic and for each level of subgrade strength. It is apparent from these figures

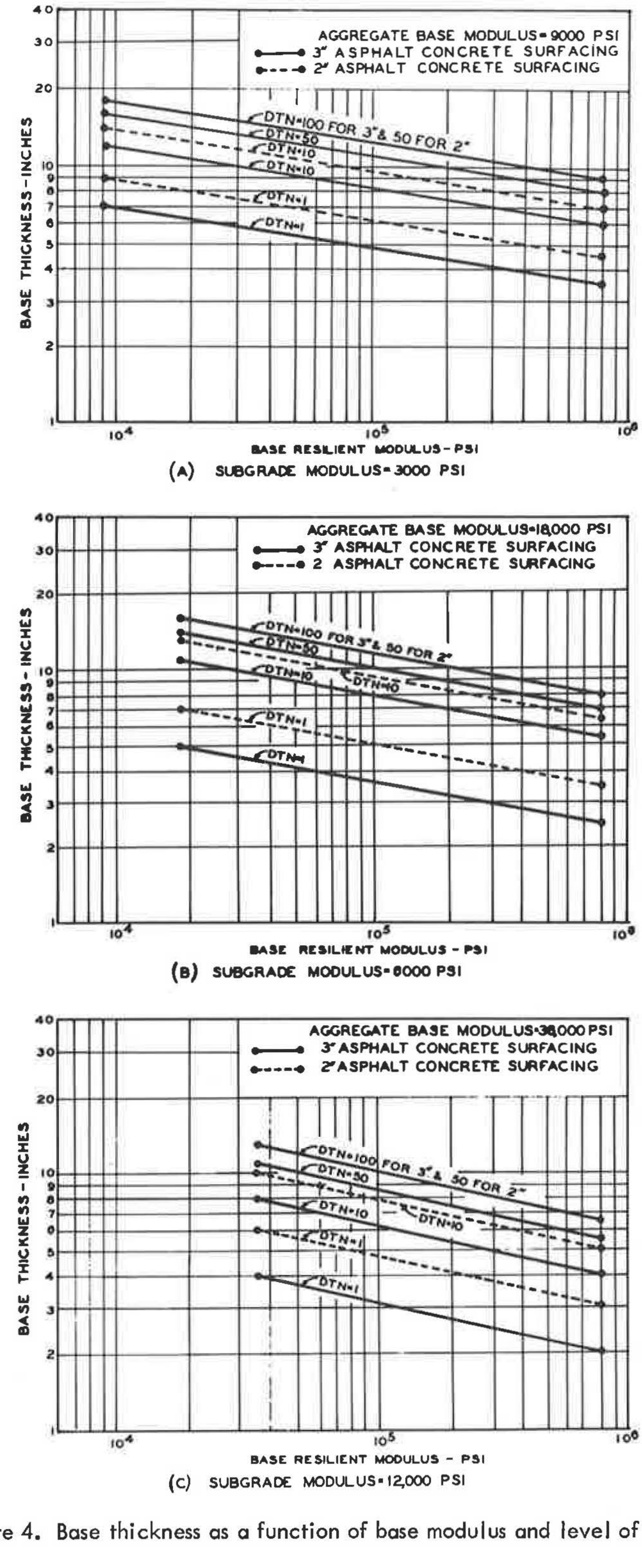

Figure 4. Base thickness as a function of base modulus and level of traffic.

TABLE 5

SUMMARY OF CORE DATA
(35 Cores)

Property	Average	Extremes	
		High	Low
Gradation: Sand fraction (No. 4-200)	71	100	18
Gradation: Filler fraction (-No. 200)	11	48	3
Gradation: Surface area, ft^2/lb	71	171	18
Core density, pcf	128.9	146.4	101.8
Percent emulsion (calculated from extracted asphalt)	7.9	13.3	3.2
Penetration of recovered asphalt at 77 F	33.2	181	1[a]
Resilient modulus, psi	318,000	961,000	27,200
Age of pavement	3½ years	22 years	1 month

[a]High fines, difficult to recover.

that precise measurements or estimates of the resilient modulus are not critical to this design procedure. The resilient modulus of treated base materials varies 30 to 40 fold. A two- to three-fold change in M_R will only change the base thickness requirement ½ to 1 inch.

RESULTS OF LABORATORY TESTS

Cores were obtained from in-service pavements to obtain the resilient modulus of the emulsion treated base layer. The laboratory determination of resilient modulus was made in accordance with procedures described elsewhere (23, 24, 25) except that strain gages were used to measure strain in lieu of differential transformers. The resilient modulus, M_R, is defined as the ratio of the applied stress (σ_1 - σ_3) to the recoverable strain. For this study, the cores were tested unconfined. This was considered to be a conservative estimate of M_R since confining stresses would tend to increase M_R. A number of cores could not be tested because the thickness of the base did not provide an adequate height-diameter ratio. The cores were tested at their in situ water content; no effort was made to saturate the specimens. In this regard, it was considered that the layers from which the cores had been obtained had been in service long enough to have achieved an equilibrium water content, and any effort to modify this condition would be unnecessarily conservative. The results of the resilient modulus tests are summarized in Table 5.

A laboratory testing program was initiated to establish procedures that could be used to duplicate the field cores in terms of density, moisture, and aged resilient modulus. This was reasonably accomplished with a dune sand from Tawas Park, Michigan, and a silty sand from Rancho Santa Fe, California. However, a specific method for preparing and curing treated specimens to simulate all field conditions could not be established. Because of this it was decided that an alternate approach was needed.

The alternate approach selected was to correlate physical properties of the emulsion treated base cores taken from each project with their measured resilient modulus. In this way, it was felt an expression could be developed to estimate the resilient modulus of emulsion treated base mixtures. The tests conducted on each core included (a) density, (b) gradation, (c) asphalt content, and (d) penetration of the recovered asphalt. All of this testing was done in accordance with regularly accepted procedures. The results of the laboratory tests are summarized in Table 5.

A regression analysis of data from the cores was used to develop an expression for estimating the ultimate aged resilient modulus for treated bases. The variables included in the analysis were

1. Gradation: (a) Sand fraction (No. 4 to 200 mesh), (b) Filler fraction (minus No. 200), and (c) Surface area.
2. Penetration of the recovered asphalt at 77 F.
3. Percent emulsion (calculated from extracted asphalt).

4. Age of pavement.
5. Core density, pounds per cubic foot.

Results of this analysis gave the following relationship:

$$\log_e M_R \text{ (Modulus} \times 10^{-3}) = -1.86 - 0.016 \text{ Penetration} + 0.047 \text{ (Density)} + 2.58 \text{ (Sand Fraction)}$$

The standard error was 0.680 with a correlation coefficient of 0.659. The fitting error in this equation may not be as precise as desired by some researchers; however, it is considered adequate for estimating purposes. Thus, it is possible to predict the stiffness of the treated base without actually conducting curing and resilient modulus tests.

The emulsion treated base moduli, as predicted in the above equation, were found to be dependent on

1. Density of the core—the higher the density, the higher the resilient modulus.
2. Sand fraction of the mix—for a given density, the resilient modulus will increase with an increasing amount of sand (i.e., percent passing No. 4 sieve and retained on the No. 200 sieve). Increasing the amount of sand excessively may result in a poorly graded material with a reduced density and, consequently, a lowered resilient modulus.
3. Stiffness of the asphalt binder—the penetration of the asphalt has a pronounced effect on the stiffness or resilient modulus of the mix.

The age of the in-service pavement has an important bearing on the strength properties. The resilient moduli of the older treated bases were higher than those found in new construction. This is due in part to the hardening of the asphalt binder in the mix. To ensure satisfactory performance during the early service life of the pavement (i.e., until the emulsion mix develops its full support capacities), quality requirements, such as shear strength and gradation, are superimposed on the mix. These requirements are described in a subsequent section of this paper.

To estimate the aged resilient modulus of an emulsion base, an average penetration of 35 was used in the equation. This penetration value is typical of those found from the analysis of aged emulsion base cores. The adjusted equation is shown graphically in Figure 5.

The test results indicate a relationship between the stiffness or resilient modulus of the base layer and its density and gradation. Mixes having a high density and/or high sand content generally have high M_R values. It is emphasized that it is necessary to have a well-graded aggregate in order to achieve high strength values. Optimizing the sand content to produce a mix of high density results in the highest resilient modulus.

Effect of Curing Time on Thickness Requirements

Emulsion treated bases require a curing period in order for the emulsion to fully develop the properties of the base asphalt. During this period, the resilient modulus of the treated base is likely to be less than the ultimate value used in design of the pavement thickness. The effect this temporary reduction in modulus will have on the service life has been investigated. The studies show that curing has no significant effect on thickness requirements if the base is properly constructed to reach its ultimate design strength in two years or less.

The following assumptions were made in this analysis:

1. That a given pavement has for its environment a unique load-carrying potential. Thus, most design procedures assume that each load application produces an increment of damage or reduces the pavement life expectancy. This hypothesis is compatible with the equivalent wheel load concepts developed in the AASHO Interim Guides for the Design of Pavement Structures and is supported by the AASHO Road Test results.
2. That there will be a traffic growth rate of 3 percent per year during the design period.
3. That the design period is 20 years.

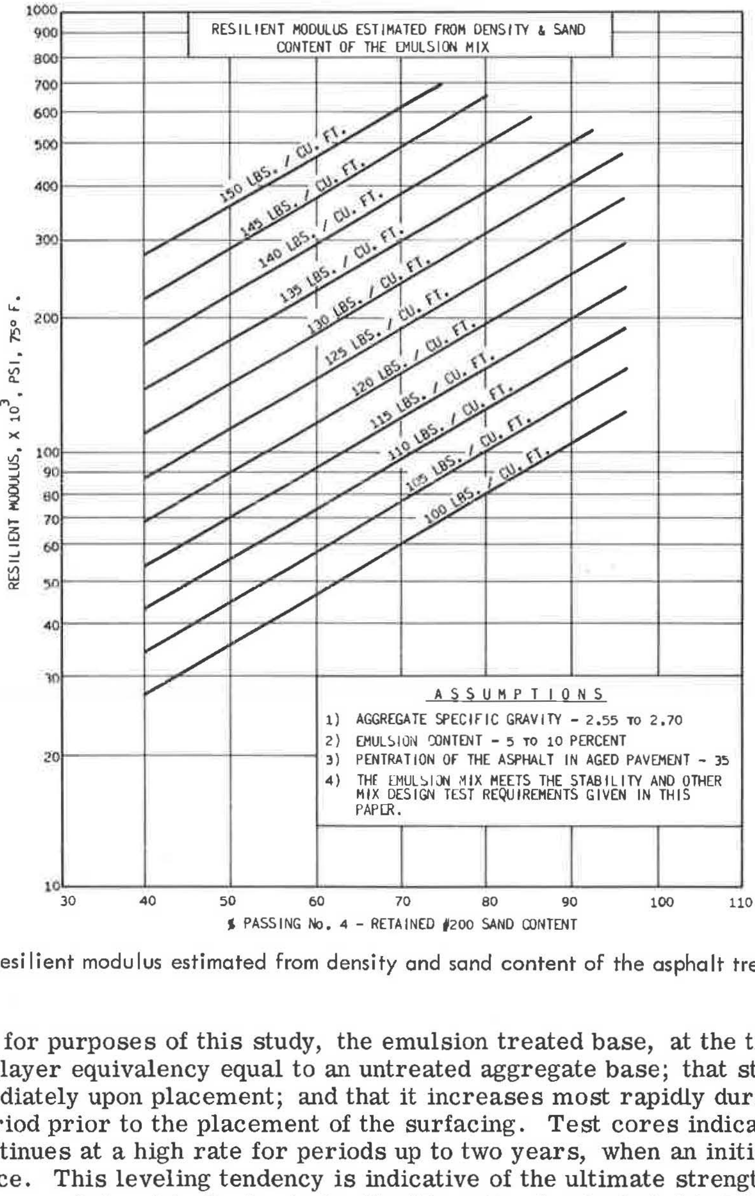

Figure 5. Resilient modulus estimated from density and sand content of the asphalt treated base.

4. That, for purposes of this study, the emulsion treated base, at the time of placement, has a layer equivalency equal to an untreated aggregate base; that strength develops immediately upon placement; and that it increases most rapidly during the construction period prior to the placement of the surfacing. Test cores indicate that this increase continues at a high rate for periods up to two years, when an initial leveling-off takes place. This leveling tendency is indicative of the ultimate strength associated with the curing period and is the basis for the M_R estimates included in Figure 5. Test results indicate that further increases in strength may extend over a period of ten years or more; however, for the present this increased strength is not programmed into the strength estimates and may be considered as another safety factor. The resilient moduli for in situ asphalt emulsion treated materials (exclusive of a poorly graded sand which would not qualify under the recommended design requirements) was approximately 50,000 psi or more after some six months of curing.

5. That 95 percent of the ultimate layer equivalency of the asphalt emulsion treated base is developed in two years or less. Laboratory and field studies indicate that the ultimate cured equivalency may be achieved, in many instances, at time intervals much shorter than one year. For example, on one project the resilient modulus increased from 50,000 to a modulus of over 200,000 in three months, well over the resilient modulus used in design. In general, the rate at which resilient modulus develops is related to the following factors: (a) class, type, and grade of emulsion; (b) type of aggregate

and gradation; (c) weather (temperature, wind velocity, and humidity); and (d) construction procedures and lift thickness.

6. That the subgrade strength will drop to its low equilibrium or design strength value immediately. This is conservative since the design value assumes saturation, which probably does not occur immediately.

The method used to evaluate the effect of curing time on the design thickness requirements makes use of The Asphalt Institute Manual (22) and a computer program. The increase in damage rate due to curing of the emulsion base is determined by a computer. Since the damage rate during the curing period is greater than that considered in design, a greater thickness of pavement will be required in order to obtain the desired 20-year design life. The magnitude of this increase was determined for a number of traffic and subgrade conditions and base strengths.

The method is illustrated by an example.

1. Assume that the anticipated traffic and the strength of the subgrade are as follows: (a) the design traffic number (DTN) is 50; (b) the strength of the subgrade is classified as good, i.e., E = 12, 000 (R-value about 35). A 3-inch asphalt concrete surface is to be used as the wearing surface. The analysis is to determine the difference in thickness due to the curing effect. It is assumed that the emulsion base will require one full year to achieve 95 percent of its design strength.

2. Determine the total thickness of asphalt concrete surface and base (T_A) in inches for the assumed DTN and subgrade strength from Figure IV-2 in The Asphalt Institute Manual Series MS-1 (22). For this example, the total thickness of asphaltic concrete surface and base (T_A) is 8.0 inches. If the thickness of asphalt concrete surface is 3.0 inches, then the thickness of asphaltic concrete base for this example is 8.0-3.0 or 5.0 inches.

3. Determine the ultimate layer equivalency for the emulsion treated base from the resilient modulus test result on the field core and Figure 4. In this example, the layer equivalency for a treated base with a modulus of 300, 000 psi is 1.6. The design thickness of the pavement is 3 inches of asphalt concrete and 6.3 inches of emulsion treated base ($2.0/1.6 \times 5.0 = 6.3$).

4. Assume that the layer equivalency of the treated base is 1.0 initially and increases exponentially to the ultimate value of 1.6 in one year. The increase in layer equivalency with time is a measure of the curing rate. The general expression for determining the layer equivalency as a function of time is

$$G_t = G - (G-1)/e^{bt}$$

where

G_t = actual layer equivalency at time t,
G = ultimate layer equivalency,
b = the curing rate, and
t = time in years.

The curing rate, b, is defined by the expression:

$$b = \log_e (1 - f_c)/t_c$$

where

f_c = the specified degree of curing, and
t_c = the specified time at which f_c occurs.

In this example, a value of f_c of 0.95 at a t_c of 1.0 year was used (i.e., 95 percent equivalency is achieved in one year). The values for layer equivalency as a function of time are shown in the column labeled Base Equivalency in Table 6 for each 0.1-year period.

5. From the design equations for Figures IV-1 and IV-2 of The Asphalt Institute Manual (22), the traffic capacity in DTN is determined for each 0.1-year interval for

TABLE 6

SAMPLE CALCULATION—EFFECT OF CURING RATE ON PAVEMENT THICKNESS

Design Data:

Daily traffic number (DTN) 20-year average	=	50, increasing at 3. 0 percent per year
Asphalt concrete thickness (surface)	=	3. 0 inches
Emulsion treated base thickness	=	6. 3 inches, with ultimate equivalency = 1. 60; 95 percent of this 1. 6 equivalency is achieved in one year
Subgrade R-value	=	35
Total equivalent asphalt thickness	=	8. 0

Damage History:

Years	Traffic (DTN)	Base Equivalency	Traffic Rating	Instantaneous Damage Rate	Cumulative Damage Total
0. 0	36. 491	1. 000	7. 370	0. 248	0. 0
1. 0	37. 602	1. 576	45. 921	0. 041	7. 4
2. 0	38. 748	1. 598	49. 788	0. 039	11. 3
3. 0	39. 928	1. 600	49. 989	0. 040	15. 2
4. 0	41. 144	1. 600	49. 999	0. 041	19. 3
5. 0	42. 397	1. 600	50. 000	0. 042	23. 5
6. 0	43. 688	1. 600	50. 000	0. 044	27. 8
7. 0	45. 018	1. 600	50. 000	0. 045	32. 2
8. 0	46. 389	1. 600	50. 000	0. 046	36. 8
9. 0	47. 862	1. 600	50. 000	0. 048	41. 5
10. 0	49. 258	1. 600	50. 000	0. 049	46. 3
11. 0	50. 758	1. 600	50. 000	0. 051	51. 3
12. 0	52. 304	1. 600	50. 000	0. 052	56. 5
13. 0	53. 897	1. 600	50. 000	0. 054	61. 8
14. 0	55. 538	1. 600	50. 000	0. 056	67. 3
15. 0	57. 229	1. 600	50. 000	0. 057	72. 9
16. 0	58. 972	1. 600	50. 000	0. 059	78. 7
17. 0	60. 768	1. 600	50. 000	0. 061	84. 7
18. 0	62. 619	1. 600	50. 000	0. 063	90. 9
19. 0	64. 526	1. 600	50. 000	0. 065	97. 2
20. 0	66. 491	1. 600	50. 000	0. 066	103. 8

Expected life at full base strength = 20. 00
Expected life from curing effects = 19. 43
Expected life lost life (years) = 0. 57

DTN required for full 20 year life = 51. 91
Total asphalt thickness (TA) required for full 20 year life = 8. 08
Asphalt concrete surface thickness required for full 20 year life = 3. 00
Emulsion treated base thickness required for full 20 year life = 6. 35

Difference in thickness due to curing effect = 0. 05 inches

the T_A determined in Step 2 and the subgrade support assumed previously. Example: The traffic rating is given in Table 6. The value for the traffic rating increases with time to the design DTN reflecting the increase in layer equivalency (curing) of the base.

6. The actual traffic in terms of DTN's for each 0.1-year period is determined at any time (t) using a simple exponential model:

$$T = Ke^{\alpha t}$$

where

T = traffic in DTN

$$K = \frac{(L^{\alpha})\ DTN}{e^{L\alpha} - 1}$$

α = the rate of increase in traffic per year.

In this example α is 3 percent per year and L is 20 years.

7. When the traffic capacity (DTN) is less than the actual traffic (DTN) for a 0.1-year period, damage occurs at an increased rate. An instantaneous damage rate is calculated. The instantaneous damage rate is expressed as 0.05 times the ratio of the actual traffic rate to the traffic rating at each point in time. (The 0.05 = 1/20 is simply a scale factor so that the integrated total damage will be 100 percent when the pavement is no longer serviceable.)

TABLE 7

DIFFERENCE IN DESIGN BASE THICKNESS REQUIRED TO COMPENSATE FOR CURING RATE

(Assume Two-Year Curing Time)

Design DTN	Subgrade Strength (R-Value)	Assumed Ultimate Emulsion Base Layer Equivalency	Thickness Difference (Inches)
1	12	1.6	0.06
		2.0	0.03
	35	1.6	0.06
		2.0	0.04
10	12	1.6	0.18
		2.0	0.19
	35	1.6	0.03
		2.0	0.09
50	12	1.6	0.16
		2.0	0.35
	35	1.6	0.10
		2.0	0.19

8. The total accumulated damage is obtained by numerically integrating the instantaneous damage rates at time intervals of 0.1 year, over the design life of 20 years. In the cases studied, the total damage reached 100 percent prior to the 20-year design life.

9. To ensure that the full 20-year design life is achieved, the base thickness is increased by an amount sufficient to obtain 100 percent total damage in exactly 20 years. This is done by adjusting the design DTN on an iterative basis until the 20-year total damage was 100 ± 0.001 percent. The thickness to account for the increased DTN is calculated. For this example, the new DTN required for emulsion treated base design = 51.91, increasing the base thickness to 6.35 inches or a difference from design thickness of 0.05 inches. The thickness increases for various subgrade strengths, base equivalencies, and traffic conditions are shown in Table 7. The maximum base thickness increase was only 0.35 inches for the cases studied. This difference in thickness is considered insignificant and well within the accuracy of the design procedures. It is, however, important to minimize the effects of curing, particularly in cases when designs are to be used in heavily trafficked roadways placed over weak subgrades. One such precaution would be to use mixing equipment that can achieve proper coatings with the minimum amount of added water. Continuous pugmills are considered ideal for this purpose.

DESIGN OF ASPHALT EMULSION TREATED BASES

It was noted at the outset of this report that the structural design must satisfy both fatigue and plastic deformation requirements. This section deals with criteria to prevent plastic deformation. Such criteria are predicated on established shear and tensile strength tests.

To guard against plastic deformation, a variation of the California Moisture-Vapor Susceptibility (MVS) Test, coupled with the Stabilometer Resistance (R) Value and the Cohesiometer (C-value) Test, is used (27). The MVS Test subjects the asphalt base to the damaging effect of moisture in the vapor state. This water vapor can cause swelling of improperly treated particles with a subsequent loss of stability. The R-value is used to provide an index of the shear strength of the mix after exposure to water vapor.

The moisture vapor can also cause a failure in the cohesion bond and at the aggregate-asphalt interface resulting in stripping and migration of the asphalt. To evaluate the extent of cohesion failure and stripping after exposure to water vapor, an index of the tensile strength is measured using the C-value Test.

Mix Design Criteria

In establishing the MVS R-value criteria for asphalt bases, the concepts developed by the State of California Materials and Research Laboratory were followed. In adapting the test procedures for asphalt treated bases, the following assumptions were made:

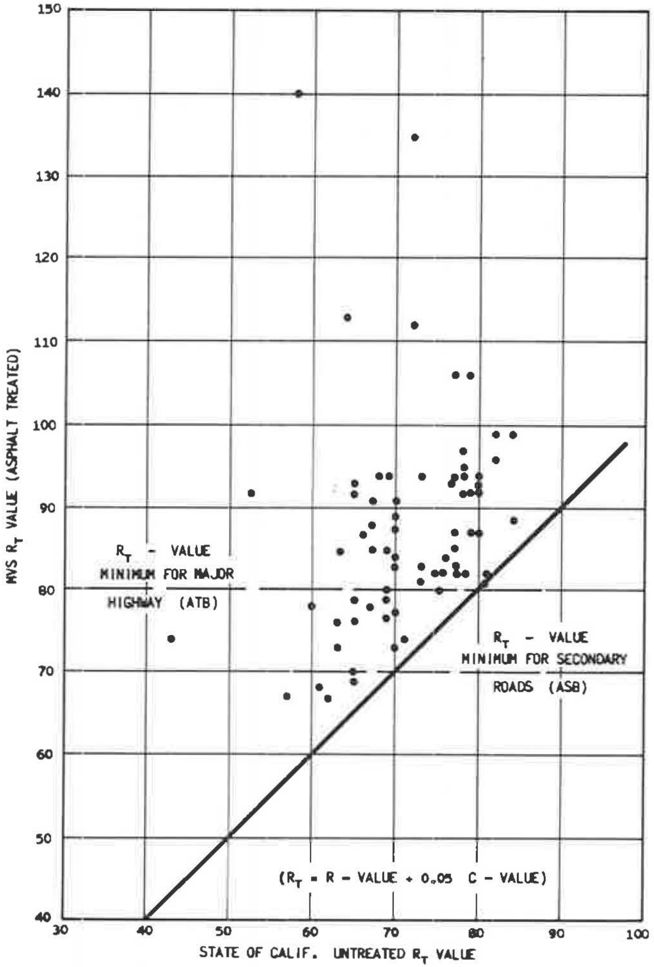

Figure 6. Increase in stability of asphalt treated bases.

TABLE 8

DESIGN CRITERIA FOR EMULSION TREATED BASES

1. Aggregate Requirements:

Category	Processed[a] Dense Graded Aggregates	Sands: Poorly Graded	Sands: Well Graded	Sands: Silty Sands	Semi-Processed Crusher, Pit, or Bank-Run Aggregates
Gradation and Passing	(ASTM C-136)				
1-½ in.	100				100
1 in.	90-100				80-100
¾ in.	65-90				
½ in.	—	100	100	100	—
No. 4	30-60	75-100	75-100	75-100	25-85
No. 16	30-60	—	35-75	—	—
No. 50	7-25	—	15-30	—	—
No. 100	5-18	—	—	15-65	—
No. 200	4-12	0-12	5-12	12-25	3-15

The combined aggregate shall also conform to the following requirements:

Test Property	Method of Test	Test Requirements
Sand equivalent, percent		30 Min.
Loss in Los Angeles Rattler[b] (after 500 revolutions)		Processed 50 Max. Semi-Processed 60 Max.

2. Mix Requirements:
The suitability of the resultant emulsion treated base mix is based on ease of mixing and curing, mix stability and cohesion, and resistance of the mix to the intrusion of moisture in the vapor state. Test criteria are:

Test Property	Method of Test	Test Requirements
Resistance R_I Value After MVS for light and medium traffic, DTN under 100[c];	Chevron Asphalt Company Method 67B-307	70 Min.
for heavy and very heavy traffic, DTN over 100[c]		78 Min.
Moisture pickup during MVS Test, 1 percent	Chevron Asphalt Company Method 67B-307	5.0 Max.

[a]Must have at least 25 percent crush count.
[b]Applies only to processed or semi-processed aggregates.
[c]The Asphalt Institute Thickness Design Manual (22).

1. The California untreated R-value test used in design of untreated aggregate bases is correlated to field performance. The conditions of the MVS design test method on untreated aggregate were set such that the R-value results after MVS were equal or near to the standard State of California R-value. It was assumed that this would provide a tie-in between the MVS R-value Test Method and field performance.

2. Since asphalt imparts cohesion, it was necessary to measure the tensile or breaking strength of the asphalt mix. The Cohesiometer Test was used to measure this tensile strength. The problem then centered on how much strength value to assign to the Cohesiometer result. A factor of 0.05 times the C-value was assigned as suggested by Hveem and Davis as being reasonable (28). This 0.05 C-value was added to the R-value and reported as the R_T-value. This assumption is not entirely correct since the influence of cohesion will vary, depending on load, temperature, thickness of the base, and possibly load repetitions. However, use of the C-value factor provides a means for comparison of the asphalt treated base with an untreated base. In this way, it is possible to obtain an indication of the improvement anticipated with asphalt treatment.

Asphalt Increases Strength

Evaluation of materials for emulsion treatment by the foregoing procedures shows significant increases in strength. Results of extensive testing of emulsion treated and untreated aggregates are shown in Figure 6. The average increase in the R_T-value as a result of emulsion treatment was approximately 14 points; however, the spread in R_T-value before and after treatment is considerable. A regression analysis of the data indicated that the R_T-value after treatment is most nearly related to the following factors: sand, filler, binder type, and content. The equation relating these variables is

$$R_T\text{-value} = 55.7 + 0.81\,(\text{percent sand}) - 0.0083\,(\text{percent sand})^2 - 0.017\,(\text{percent filler})^2 + 6.2\,(\text{percent binder}) - 0.39\,(\text{percent binder})^2$$

The constant in this equation should be modified by the following amount depending on the binder type selected: For SMK, subtract 5.6; for SSK-K, subtract 3.3. Insufficient data were available to evaluate correction constants for the other binder types used. A total of 393 data points was used in making the analysis.

Design Requirements

Emulsified asphalt treated bases must meet certain design requirements if they are to perform satisfactorily. Design criteria for untreated and treated aggregates are summarized in the following.

Aggregate Requirements—The mineral aggregate or aggregate blend shall be free from wood, roots, coal, ocher, mud balls, vegetable matter, and other deleterious substances. It shall conform to one of the gradation requirements listed in Table 8.

Asphalt Emulsion-Aggregate Combination—Five basic requirements must be met in order to impart the cementing and water-resisting qualities of asphalt emulsions to the aggregate mixture. These are:

1. Uniform dispersal of the asphalt throughout the mix,
2. Adequate coating of the aggregate by the emulsified asphalt,
3. Good adhesion of the asphalt to the aggregate so that action of water and traffic will not cause stripping and loss of mix tensile strength,
4. Resistance to shear deformation under load, and
5. High tensile strength within the asphalt film (i.e., high in-place cohesion).

The suitability of the resultant emulsion-aggregate mix is based on (a) ease of mixing and curing, (b) mix stability and cohesion, and (c) resistance of the mix to the intrusion of moisture in the vapor state. Design criteria for emulsion treated bases are given in Table 8.

SUMMARY

The stated objectives of this investigation were to (a) describe results of field condition surveys of pavements constructed with emulsion stabilized bases, (b) explore

possible uses of layered elastic theory for thickness design, (c) study the influence of curing time on performance, and (d) present a method for mix design adequate to resist deformation. The results of the condition survey show conclusively that emulsion stabilized bases are providing satisfactory performance under a variety of environments and loading conditions.

The analysis demonstrates the utility of using theory as a tool for design. However, the decision to satisfactorily meet suggested design criteria for deflection, strain in the asphalt concrete, and strain in the subgrade resulted in thicknesses substantially greater than commonly found adequate in the field. By combining theoretical concepts with the existing design methods of The Asphalt Institute a procedure was found that appears to provide a reasonable approach for the design of emulsion stabilized bases.

In order to provide some estimate of the properties to use for design, a nomograph is included which makes it possible to estimate the resilient modulus of the stabilized base without resorting to complicated laboratory tests involving time-consuming curing procedures.

Curing of emulsion bases was studied to determine the effects of time on strength with the specific objective of assuring adequate strength in the early stages of service life. Based on these studies, curing does not appear to be critical and only minor adjustments in thickness are necessary to compensate for such effects.

Mix design and material recommendations to prevent permanent deformation under load are presented. These procedures are based on well-established methods for evaluating the shear strength of mixes.

REFERENCES

1. A Method of Rating the Condition of Flexible Pavements. HRB Circular 476, Aug. 1962.
2. Unpublished report presented at Triaxial Institute, Klamath Falls, Oregon, 1967.
3. Bitumuls Base Treatment Manual. Chevron Asphalt Company, 1967.
4. Burmister, D. M. The General Theory of Stresses and Displacements in Layered Systems. Jour. Appl. Phys., No. 2, p. 89-96; No. 3, p. 126-127; No. 5, p. 296-302; 1945.
5. Pister, K. S., and Westman, R. A. Analysis of Viscoelastic Pavements. Proc. Internat. Conf. on Structural Design of Asphalt Pavements, Ann Arbor, Mich., 1962.
6. Monismith, C. L., and Secor, K. E. Viscoelastic Behavior of Asphalt Concrete Pavements. Proc. Internat. Conf. on Structural Design of Asphalt Pavements, Ann Arbor, Mich., 1962.
7. Papzian, H. S. The Response of Linear Viscoelastic Materials in the Frequency Domain with Emphasis on Asphalt Concrete. Proc. Internat. Conf. on Structural Design of Asphalt Pavements, Ann Arbor, Mich., 1962.
8. Peattie, K. R. A Fundamental Approach to the Design of Flexible Pavements. Proc. Internat. Conf. on Structural Design of Asphalt Pavements, Ann Arbor, Mich., 1962
9. Coffman, B. S., Kraft, D. C., and Tamayo, J. A Comparison of Calculated and Measured Deflections for the AASHO Road Test. Proc. AAPT, 1964.
10. Dormon, G. M., and Metcalf, C. T. Design Curves for Flexible Pavements Based on Layered System Theory. Highway Research Record 71, p. 69-84, 1965.
11. Peattie, K. R. Stress and Strain Factors for Three-Layer Elastic Systems. HRB Bull. 342, p. 215-253, 1962.
12. Jones, A. Tables of Stresses in Three-Layer Elastic Systems. HRB Bull. 342, p. 176-214, 1962.
13. Numerical Computations of Stresses and Strains in a Multiple-Layered Asphalt Pavement System. Computer Program No. 90 K191, Chevron Research Company (unpublished).
14. Skok, E. L., and Finn, F. N. Theoretical Concepts Applied to Asphalt Concrete Pavement Design. Proc. Internat. Conf. on Structural Design of Asphalt Pavements, Ann Arbor, Mich., 1962.

15. Hveem, F. N. Pavement Deflections and Fatigue Failures. HRB Bull. 114, p. 43-87, 1955.
16. Zube, E., and Forsyth, R. Flexible Pavement Maintenance Requirements as Determined by Deflection Measurement. Highway Research Record 129, p. 60-75, 1966.
17. Finn, F. N. Factors Involved in the Design of Asphaltic Pavement Surfaces. NCHRP Rept. 39, 1967.
18. Heukelom, W., and Klomp, A. J. G. Road Design and Dynamic Loading. Proc. AAPT, 1964.
19. Kallas, B. F. Asphalt Pavement Temperatures. Highway Research Record 150, p. 1-11, 1966.
20. Highway Research Board. The AASHO Road Test: Report 5—Pavement Research. HRB Spec. Rept. 61E, 1962.
21. Highway Research Board. The WASHO Road Test, Part 2: Test Data, Analyses, Findings. HRB Spec. Rept. 22, 1955.
22. Thickness Design—Asphalt Pavement Structures for Highways and Streets. Manual Series No. 1 (MX-1), The Asphalt Institute, 1963.
23. Seed, H. B., Chan, C. K., and Lee, C. E. Resilient Characteristics of Sub-Grade Soils and Their Relation to Fatigue Failures in Asphalt Pavements. Proc. Internat. Conf. on Structural Design of Asphalt Pavements, 1962.
24. Monismith, C. L., Seed, H. B., Mitry, F. G., and Chan, C. K. Prediction of Pavement Deflections From Laboratory Tests. Proc. Second Internat. Conf. on Structural Design of Asphalt Pavements, 1967.
25. Monismith, C. L., Terrel, R. L., and Chan, C. K. Load Transmission Characteristics of Asphalt Treated Base Courses. Proc. Second Internat. Conf. on Structural Design of Asphalt Pavements, 1967.
26. Von der Poel, C. Road Asphalt. In Building Materials, Their Elasticity and Inelasticity (M. Reiner, editor). Interscience Publishers, New York, 1954.
27. Bitumuls Emulsified Asphalt Base Treatment Methods Manual. Chevron Asphalt Company, 1967.
28. Hveem, F. N., and Davis, H. E. Some Concepts Concerning Triaxial Compression Testing of Asphaltic Paving Mixtures and Sub-Grade Materials. ASTM Spec. Tech. Publ. No. 106, 1950.

Design of Pavements Using Deflection Equations From AASHO Road Test Results

N. K. VASWANI, Highway Research Engineer, Virginia Highway Research Council

•THE OBJECT of this study is to investigate the structural performance of some satellite pavements in the Piedmont region of Virginia and to evaluate the thickness equivalency values (i.e., the ratio of the strength of material to the strength of asphaltic concrete) of the materials used on the basis of AASHO Road Test results. It is also proposed to recommend a tentative design procedure based on pavement rigidity.

The Benkelman beam rebound deflection method is a reliable and simple means of evaluating the structural performance of pavements and has been adopted in this investigation. The AASHO Road Test Committee has suggested model equations for designing pavements on the basis of pavement performance. These equations involve the following variables:

1. Thickness of each layer in the pavement,
2. Thickness equivalency of the material in each layer,
3. Subgrade strength,
4. Traffic,
5. Age, and
6. Climatic conditions.

The values of these variables were determined in the AASHO Road Tests but these values could not be applied to Virginia because of differences in (a) construction techniques, (b) type of materials used, (c) subgrade properties, (d) environmental conditions, (e) type and duration of traffic, and (f) age of pavement.

Twenty projects with varying pavement structures, all in the Piedmont region of Virginia, were chosen for this satellite study. All these projects are on primary or interstate roads. One is an experimental section on Route 360 with four different structural designs; another was an experimental project on Route 58 with four different designs. This last project was resurfaced in 1962 and only the data collected on it prior to 1962 have been evaluated. Thus a detailed study of 27 different sections—without any resurfacing or heavy maintenance—was undertaken. In addition, 16 other projects were considered.

The main purpose of this investigation was to conduct a pilot study for evaluating the thickness equivalency values of the different materials in the pavement system and to correlate these values with the pavement performance along with other variables such as soil support, traffic, and age. Since the study was within a limited geographic area, the climatic and regional factors were considered constant, and hence the unweighted traffic—i.e., actual traffic not corrected for climatic conditions—was considered in the analysis.

In order to introduce the soil support value in the correlation, a very preliminary study was proposed. After the study was initiated, additional details, such as tolerable rebound deflections and tentative designs for Virginia, were also investigated.

VARIABLES AND THEIR DETERMINATIONS

The variables required for this analysis are divided into two categories—dependent and independent. Only one dependent or performance variable has been considered in this investigation; as already explained, it is the Benkelman beam rebound deflection, d.

Paper sponsored by Committee on Flexible Pavement Design and presented at the 47th Annual Meeting.

The independent variables are the thickness of each layer in the pavement, h; the thickness equivalency value of the material in each layer of the pavement; subgrade strength; traffic; and age. As mentioned, the climatic conditions have been treated as a constant.

Determination of these variables could be divided into two parts: collection of data from the field or from past records, and evaluation of the data so collected. Thickness equivalency values, unlike other variables, are not directly determinable from the data, and their evaluation is discussed later.

Collection of Data

The type of data and the method of collection are described in the following.

Deflection—Benkelman beam rebound deflections for slow-moving vehicles were taken under 18-kip axle loads during the spring and fall of 1966 on the 20 satellite projects. The spring deflections were taken three times at the same place at 20-day intervals. The method of taking the deflections is given in Appendix A.

Layered Thickness—The thickness of each layer in the pavements was determined from construction records.

Subgrade Support—The Virginia design CBR values for the subgrade soil used by the Materials Division were adopted for this investigation. In order to correlate the subgrade support with AASHO Road Test results, Virginia CBR tests were carried out on the subgrade, subbase and base materials used for the AASHO Road Tests.

Subgrade soil samples were taken at the edges of the pavements because the moisture content at these locations would give some idea of the moisture content of the soil underneath the pavement; 142 soil samples were taken and their moisture contents determined, and 41 were tested for plastic limits.

Traffic—The data on the type and amount of each type of vehicle for each satellite project were available. Load surveys for sites with similar traffic were utilized to determine the 18-kip equivalents.

Age—The age of the pavement was calculated from the date of construction.

Evaluation of Data

The data collected and described in the foregoing were evaluated according to the following.

Deflection—In the past, Benkelman beam rebound deflections were generally taken anytime during the spring, i.e., between April 1 and June 30. It was therefore questionable whether these deflections could validly be considered as having been taken during the spring thaw period.

In this investigation, three deflection readings were taken on all satellite projects at about 20-day intervals commencing April 1. These results showed that the variations in the readings at the same place were not necessarily due to climatic conditions but may have been due to the testing conditions. In fact most of the projects showed very little difference between the three readings. Standard deviations were determined for each set of readings for each project, and the mean values of deflections as well as standard deviations are given in Appendix A. The method of evaluating curvature and the cross-sectional area of the deflection basin is also described in Appendix A. On the basis of these results, deflection data previously obtained on these projects and available on 16 additional projects from the Piedmont area were studied.

The spring deflection data showed that a straight-line relationship existed between (a) maximum deflection and curvature, and (b) maximum deflection and longitudinal cross-sectional area of the deflected basin. Deflection data taken in the Piedmont area prior to this investigation also showed the same kinship between deflection and curvature. This relationship is shown in Figure 1. The correlation coefficient is 0.97.

Since stresses are a function of curvature and since curvature has been shown to correlate well with the magnitude of maximum deflection, the stresses in asphaltic concrete pavements can be considered as being proportional to the magnitude of deflections, and the evaluation of relationships between the independent and dependent variables on

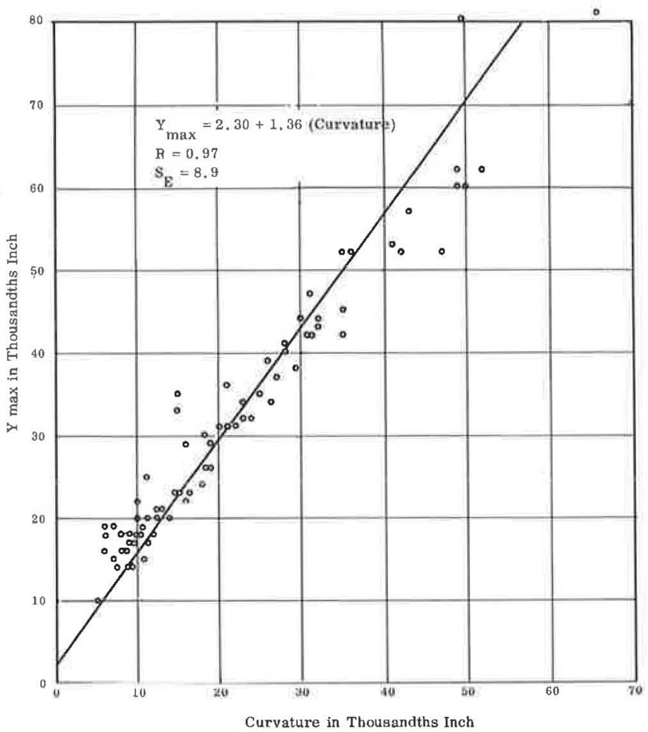

Figure 1. Correlation between maximum deflection and curvature.

the basis of maximum deflection will be as good as that made on the basis of curvature or the longitudinal cross-sectional area of the deflected basin.

Fall deflection data were also gathered and it was found that these data varied 60 to 80 percent from those obtained in the spring. Furthermore, there was no statistical relationship between the maximum deflection and the curvature using fall deflections. A curvilinear relationship did exist between the maximum deflection and the longitudinal cross-sectional area of the deflected basin.

Since a poor relationship existed between spring and fall deflections, and since spring deflections show higher deflections and hence the worst condition of pavements, the analysis of deflection in this investigation is based on spring deflection data only.

Subgrade Support—The subgrade support value depends on two important factors: (a) resistance to a single applied load, and (b) rebound due to soil resiliency. The value of the resistance due to a single applied load is determined by various methods—in Virginia the CBR method is used. Resiliency is the property that causes material to rebound after the load has been removed. Due to rebound, fatigue often results in failure of the pavement. The subgrade soils in the Piedmont area are silty, contain mica and are generally highly resilient. Resiliency is not presently considered quantitatively in the design of pavements; however, in such soils, soil-stabilized subgrades are usually provided to reduce deflections and hence the detrimental effect of resiliency combined with high deflections.

In this investigation, three methods of determining the subgrade support value were tried: (a) CBR test method, as adopted in Virginia, (b) design CBR-resiliency method, and (c) design CBR-physiographic method.

Subgrade Support Value Based on CBR Test—The AASHO Design Chart for flexible pavements (1) is based on subgrade support values. Many states are trying to correlate their CBR or other soil strength values (obtained by the method adopted by them) with these subgrade support values. Their correlation is based primarily on the soil strength tests carried out by them on AASHO Road Test materials.

The Virginia CBR values determined on AASHO Road Test materials were reported in 1961 by Shook and Fang (2). These values showed that the CBR of the subbase material was higher than that of the base material, the values being 95 and 53, respectively. To verify these illogical results, more AASHO Road Test materials were tested. This second test did indeed verify that the CBR of subbase material was higher than that of the base material; the values were about 140 and 40, respectively. No reason for the reverse order of these values is known. The highlights of the Virginia CBR method are given by Shook and Fang (2).

It was therefore not possible to correlate Virginia CBR values with the subgrade support values given in the AASHO Design Chart.

Subgrade Support Value Based on Design CBR-Resiliency—From prior knowledge, resiliency was thought to be a very significant factor in determining subgrade support. It was therefore thought that resiliency combined with the CBR value might give a better evaluation of the soil-subgrade support. During this preliminary stage of investigation, the property of resiliency was divided into three classifications—low, medium, and high—and these were assigned values of 1.5, 1.0, and 0.5, respectively. Thus a soil with low resiliency with a design CBR of 4 (i.e., CBR-resiliency value = $1.5 \times 4 = 6$) is considered to have the same subgrade support value as a soil with high resiliency with a design CBR of 12 (i.e., CBR-resiliency value = $0.5 \times 12 = 6$).

Subgrade Support Value Based on Design CBR-Physiographic Regional Factor—Virginia has been divided into 12 physiographic regions based on pavement performance (3). These regions have been classified according to the support properties of the subgrade materials found. In this investigation, these properties were divided into five categories, with 1.5 being the best quality soil and 0.5 the poorest. Subgrade soil support values based on this method were obtained by multiplying the design CBR by the physiographic regional factor in a manner similar to that mentioned earlier for CBR-resiliency.

A stepwise regression analysis was carried out to correlate the variables and evaluate the thickness equivalency values, as explained later. In this analysis the subgrade support values obtained by each of the two methods described were introduced separately to determine which of the values gave the better correlation. It was found that the subgrade support values obtained by either method gave better correlation between variables than without them. However, values based on design CBR-resiliency gave better correlation than the values based on design CBR-physiographic regional factor. The former values have, therefore, been used for further analysis.

Moisture Content of the Subgrade Soil—The study of the moisture content of the subgrade soils of the satellite projects showed that in most cases the moisture content was higher than that of the soaked CBR samples during the time of construction.

As mentioned, 41 of the soil samples were tested for plastic limits. About 40 percent of these soils were non-plastic and most of the rest had field moisture contents less than 20 percent of their plastic limits. In the case of pavements with cement-treated subgrade, when the subgrade moisture content was within 10 percent of the plastic limit (two cases only), no increase in pavement deflection from the usual pattern was noted. In the case of one pavement (no cement-treated subgrade) with the subgrade moisture content near the plastic limit, a slight increase in pavement deflection from the usual pattern was noted. From the above it seems possible that in cases of pavements with soil-stabilized subgrade, the increase in subgrade moisture content does not affect the deflection values, while with an increase in subgrade moisture content with non-stabilized subgrades there is a slight increase in deflections when the moisture content approaches the plastic limit of the soil.

EVALUATION OF THICKNESS EQUIVALENCY VALUES

In the previous paragraphs the methods and the determination of all the variables have been discussed with the exception of thickness equivalency values. In this section, the method and the determination of thickness equivalency values are presented. Further, a new conception of tolerable rebound deflection based on pavement rigidity is presented.

To determine the thickness equivalency values, it is essential to have a basic idea of the behavior of pavements, particularly with respect to the region for which they are to be designed. This is discussed in the following paragraphs.

Behavior of Pavements

In the past, pavements were designed against plastic and shear failure. An example of this is shown in Figure 2 for the experimental project on Route 58. This figure shows that the deflections increased during the third to the fifth year. This indicates that the pavements were poor in design, and that after failure the deflections increased until

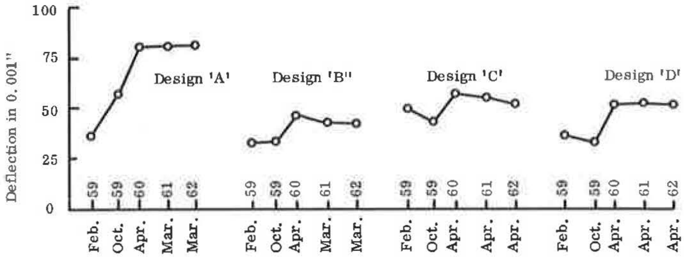

Figure 2. Examples of pavement deflections when failure is by shear (experimental project on Route 58—cement-treated subgrade).

the pavements achieved stability, and then the deflections again became uniform. During the period of increased deflections the pavement became cracked and rutted.

Study of the rebound deflection data of the satellite projects shows that for a certain period immediately after construction the rebound deflections decrease with an increase in the total traffic, indicating a consolidation phase. The duration of this consolidation phase varies with the pavement rigidity from 3 to 18 months; the more rigid the pavement, the shorter the duration of this phase. A typical example of this phase is shown in Figure 3 for four designs on Route 360. On this project, designs B and C are provided with soil-stabilized base and hence are more rigid than designs A and D. In designs A and D the consolidation phase is clearly indicated by the falling rate of deflection from December 1962 to March 1963, while in designs B and C the consolidation phase is absent.

A recent survey (4) of flexible pavements in Virginia has shown that the distress of pavements due to rutting is generally uncommon. This study showed that the deterioration is mostly due to other causes, such as extensive longitudinal and pattern cracking in the wheelpath. These cracks are usually seen after a period of about 5 to 8 years and it is felt that they are the result of fatigue failure of an elastic pavement.

Thus the pavements could be considered to pass through three different phases—the consolidation phase, the elastic phase, and failure due to fatigue. During the consolidation phase, the materials in the layered system of the pavements and the subgrade soil consolidate and become more dense and, as this process continues, the pavement deflections decrease. During the elastic phase the consolidation is almost negligible and the materials, including the subgrade, behave more or less elastically unless the axle weight increases, in which case further consolidation occurs. During this phase, the pavement does not seem to crack, and the deflections remain more or less constant. In Virginia this phase lasts for a period of about 5 years.

The elastic phase slowly creeps into the third phase, i.e., fatigue. Thin longitudinal cracks develop and later widen and are then followed by pattern cracks, all of which usually take place in the wheelpaths. The pavements are resurfaced after the third phase.

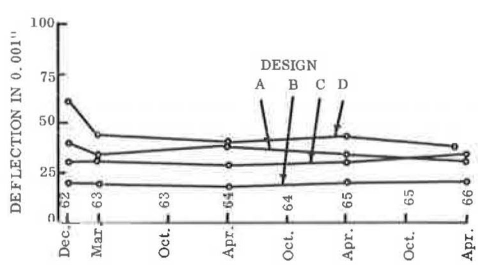

Figure 3. Examples of pavement deflection during elastic phase (experimental project on Route 360—cement-treated subgrade).

Method Recommended for Design

In view of the general behavior of pavements, the pavements could be designed on the basis of elastic theory. The AASHO Committee (5) has recommended a model equation of the form, $\log d = a_1h_1 + a_2h_2 + a_3h_3 + \ldots$ where a_1, a_2, a_3, etc., are the strength coefficients of the materials in the layers having thickness equal to h_1, h_2, h_3, etc., respectively.

Burmister's elastic theory (6) shows that the deflection of a pavement is not merely a summation of the strength of the individual

layers, but a ratio of the strengths of adjoining layers. Thus deflection is not merely a function of a_1h_1 (as indicated in the model equation given by AASHO) but also of

$$\frac{a_1h_1}{a_2h_2 + a_3h_3 + \ldots}$$

Thus, for elastic design, if the ratio of the strengths of adjoining layers remains more or less constant, the AASHO Committee's model equation would be applicable. It was, therefore, necessary to determine whether the pavements in Virginia satisfy this criterion. The layered system and the range of values for the pavements studied are given below.

The asphalt concrete mat is about 5 to 10 in. thick, consisting of about 3 to 7½ in. of asphalt base (Marshall stability less than 300 lb), overlaid by about 2 to 2½ in. of bituminous binder and surface course (Marshall stability of about 700 to 900 lb). This asphalt mat is underlaid by a stone base of about 6 to 9 in., which may or may not be cement-treated. A cement-treated subgrade or select material, if provided, is sandwiched between stone base and subgrade soil. The thickness of the cement-treated subgrade is about 6 to 8 in.

The description of the pavement structure in Virginia shows that the ratios of the strengths of the adjoining layers, though variable, remain more or less constant to satisfy Burmister's elastic theory requirements. It is therefore believed that the AASHO Committee's method of design might hold good. The thickness equivalency values determined from the study of such pavements will be applicable only to pavements with layered systems and with materials of the type used and placed in the order described.

Method Adopted for Determining Thickness Equivalency Values

As already mentioned, the thickness equivalency of a material is the ratio of the strength coefficient of the material to the strength coefficient of asphaltic concrete. The strength coefficients of the materials in each layer have been taken as follows:

- a_1 = strength coefficient of asphalt mat; the asphalt mat may consist of surface, binder, and base layers of asphaltic concrete.
- a_2 = strength coefficient of stone base.
- a_{21} = coefficient for additional strength due to cement stabilization of stone base; thus, cement-stabilized stone base has a strength coefficient equal to $(a_2 + a_{21})$.
- a_{22} = coefficient for additional strength due to bitumen-stabilized stone base; thus, bitumen-stabilized stone base has a strength coefficient equal to $(a_2 + a_{22})$.
- a_3 = strength coefficient of select material.
- a_4 = strength coefficient of soil-stabilized layer in the subgrade.
- a_r = strength coefficient of subgrade when graded according to design CBR-resiliency factor.

A stepwise regression analysis was carried out with a computer to determine the thickness equivalency values of the materials by means of the equation

$$\log d = a_0 + a_1\left(h_1 + \frac{a_2}{a_1}h_2 + \frac{a_3}{a_1}h_3 + \ldots + \frac{a_s}{a_1}G_s\right)$$

where $\frac{a_s}{a_1}$ = thickness equivalency value of the subgrade and G_s the equivalency grading of the subgrade soil support. The object of this analysis was to determine the thickness equivalency values of the materials and the effect of each variable on these values.

About 70 combinations of different variables have been tried; the different groups used are given in Appendix B.

TABLE 1
THICKNESS EQUIVALENCY VALUES OF MATERIALS

Material	Thickness Equivalency As Determined	Thickness Equivalency As Given by AASHO
Asphalt	1.0	1.0
Stone base	0.35	0.31
Cement-treated stone in base	1.1	0.52
Asphalt-treated stone in base (lean-mix)	0.75	0.77
Select material in subbase	0.0	0.25
Cement-stabilized subgrade	0.5	not given

The same equation was tried with log curvature and log ($d + 2\sigma$) instead of log d on the left-hand side. The results showed almost the same trend as with deflections and hence are not reproduced here.

The stepwise regression analysis clearly pointed out two broad aspects of design:

1. Within each group, a change in the number of variables did not greatly affect the thickness equivalency values. However, with a change in groups, the thickness equivalency values of any given layer changed, sometimes to a great extent. This, therefore, shows that with the change in the arrangement and thickness of the layers, resulting in a change in ratio of the strengths of adjoining layers, these values will change.
2. The increase in the number of independent variables within each group gave higher values of the correlation coefficients and lower values of the standard error of estimate. This, therefore, shows that with an increase in the number of independent variables the analysis improves.

The thickness equivalency values obtained by regression analysis of the satellite projects are given in Table 1. The values given by the AASHO Committee are also given in this table for comparison. These obtained values apply only to those designs which are similar to those of the satellite pavements, and should be considered tentative. These values are discussed in the following paragraphs.

Thickness Equivalency Value of Asphaltic Concrete, $\frac{a_1}{a_1}$ —The thickness equivalency value of this material is usually higher than that of any other material, and is taken as 1.

Thickness Equivalency Value for Stone Base, $\frac{a_2}{a_1}$ —The value of the thickness equivalency of this material varies from 0.35 to 0.40 for all satellite projects. The Asphalt Institute (7) and the CGRA (8) have recommended a value of 0.31. On the basis of this investigation a thickness equivalency value of 0.35 appears appropriate.

Thickness Equivalency Value of Cement-Treated Stone Base, $\frac{a_2 + a_{21}}{a_1}$ —The additional thickness equivalency value of stone base due to stabilization with cement was found to vary from 0.5 to 1.25. If we assume the thickness equivalency of stone base as equal to 0.35, the thickness equivalency of cement-stabilized base would vary from 0.85 to 1.55. A tentative value of 1.10 is assumed. It may be mentioned that only two of the 27 projects had cement-treated bases.

Thickness Equivalency Value of Asphalt-Treated Stone Base, $\frac{a_2 + a_{22}}{a_1}$ —None of the 27 projects in the satellite study had asphalt-treated (lean mix) stone base. Of the 43 projects in the Piedmont area only two had this base. Analysis of these projects gave additional thickness equivalency values varying from 0.25 to 0.50. If we assume the thickness equivalency of stone base as 0.35, the thickness equivalency of asphalt-stabilized stone base would vary from 0.60 to 0.85. A tentative value of 0.75 is recommended.

Thickness Equivalency Value for Select Material, $\frac{a_3}{a_1}$ —Analysis of all groups of projects, except the group with no stabilized subgrade, showed that the value of a_3 was negative and tended almost toward zero. The negative sign was probably due to an interaction in the regression analysis. In the case of the group with no stabilized subgrade the value of a_3, though positive, was very small. It could therefore be concluded that the select materials do not contribute appreciably to reducing deflections and the thickness equivalency value of this material could therefore be taken as zero.

This is no reason for not providing a subbase. It is felt that a subbase may be necessary for improving drainage and preventing the penetration of subgrade material into the base course, etc.; however for better structural performance of the pavements the subbase material, if provided, should be nonresilient.

Thickness Equivalency Value of Soil-Stabilized Subgrade, $\frac{a_4}{a_1}$ —The value of the thickness equivalency of this material varies from 0.42 to 0.49 for the satellite projects. This value varied greatly from group to group. For satellite and other projects, but including the experimental project on Route 360, this value was found to be above 1.0. The reason probably is the variation in strength of the cement-stabilized material. A value of 0.5 is considered suitable for design. The AASHO Road Test has not recommended any value for stabilized soil subgrade.

Thickness Equivalency Value of Subgrade Strength, $\frac{a_S}{a_1}$ —As already explained, the soil support value was evaluated in terms of design CBR-resiliency factor and design CBR-physiographic factor. As mentioned previously, regression analysis showed that the correlation was better with the variable using the CBR-resiliency value than with the CBR-physiographic value. Thus it shows that the design based on CBR-resiliency method would give better results than design based on CBR-physiographic method. In the 70 combinations of different variables tried the value of $\frac{a_S}{a_1} G_S$ was found to be 0.13.

Deflection as a Function of Thickness Index

The thickness equivalency values discussed in the preceding paragraphs were obtained from the equation

$$\log d = a_0 + a_1\left(h_1 + \frac{a_2}{a_1} h_2 + \frac{a_3}{a_1} h_3 + \ldots + \frac{a_S}{a_1} G_S\right)$$

The expression in parentheses on the right-hand side of this equation without considering $\frac{a_S}{a_1} G_S$ —the subgrade support value—when multiplied by a_1 is known as the thickness index, D, and represents the strength of the pavement without considering the support value of the subgrade. With the thickness equivalency values tentatively recommended above, the correlation given in Table 2 was obtained for different groups of projects between thickness index, D, and log d, where d is deflection in thousandths of an inch.

In Table 2, the group of 19 satellite projects shows a better correlation. These projects have shown consistently good performance. Their ages vary from 5 to 12 years and none of them have been resurfaced. A design based on the results of these projects may, therefore, be acceptable for pavements similar to those studied. In this investigation, a new concept of design, as explained in the following section, is proposed.

THE CONCEPT OF TOLERABLE DEFLECTION AS A FUNCTION OF PAVEMENT RIGIDITY

Rigidity of Layers

When a load is applied, stresses are created in a pavement. These stresses will cause only bending in a perfectly rigid layer and only compression in a perfectly flexible layer. A semiflexible layer will partly bend and partly compress under the applied load. Further, the amount of bending will decrease as the rigidity (or modulus of elasticity) and thickness of the layer increase. Compression will increase as the rigidity (i.e., modulus of elasticity) decreases and thickness increases. In a pavement these properties of the layers could be evaluated by determining the deflections at the top and the bottom of each layer under a given applied load. If the deflections at the top and bottom of any layer are almost the same, the layers could be considered as rigid. A good example of this is a concrete slab.

TABLE 2

CORRELATION BETWEEN THICKNESS INDEX AND log d

Group of Projects	Standard Error Of Estimate = S_E	Correlation Coefficient = R	Equation
1. Satellite study projects, excluding the two experimental projects (number of projects = 19)	.087	-0.86	$\log d = 2.06 - 0.068 D$
2. Satellite and other projects including the two experimental projects (number of projects = 43)	.110	-0.70	$\log d = 2.81 - 0.130 D$

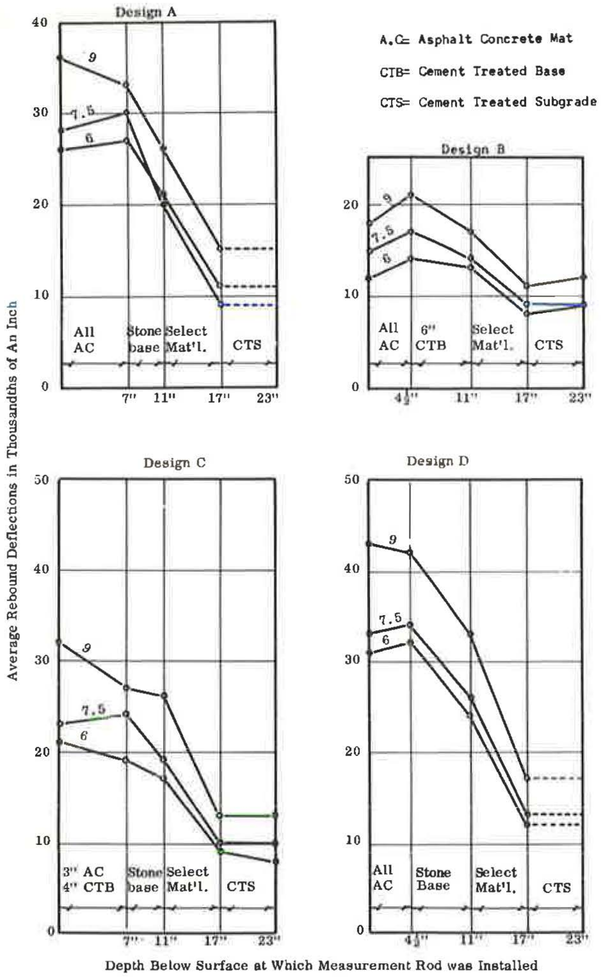

Figure 4. Average rebound deflections at surface and at various depths below surface corresponding to layer interfaces produced by indicated single wheel loads.

In the case of a perfectly flexible layer, the deflection at the bottom of a layer is zero with a certain amount of deflection at its top. A good example of this is the subgrade soil, which because of its infinite thickness absorbs all the deflection by compression.

A graphical interpretation of this hypothesis is shown in Figure 4, which gives the measured values of deflection of different layers of pavement on the Route 360 experimental project. In order to get some specific results from these four figures we have ignored the shortcomings of the deflection measuring tool; e.g., in some cases the deflection is more beneath the asphaltic concrete layer than on top of it.

These figures show that the moduli of elasticity and thicknesses of the asphaltic-concrete layer and cement-treated subgrade are such as to cause bending and very little compression in these layers. This is because the deflection of the top of the layer is almost equal to that at the bottom of the layer. It could therefore be assumed that layers with such materials are rigid, and hence the deflection is due to bending only. These figures also show that the stone base and select material layers have higher values of deflection at the top than at the bottom, indicating they both are under bending and compression. Thus, in design A, under a 9-kip load the deflection of the stone base is 0.033 in. at the top and 0.026 in. at the bottom, indicating that the deflection of 0.026 is due to bending and (0.033 - 0.026) = 0.007 is due to compression.

Since the pavements are being considered as elastic, the failure of the pavement would be by fatigue due to repetition of bending only. Thus the best approach to pavement design would also be on the basis of bending only, a function of rigidity. However, this is impracticable because it is not possible to separate the increase (or change) in deflection due to the presence of the flexible (compressible) layer from that due to bending. Hence in this preliminary investigation, the total deflection has been used for analysis.

Design Based on Tolerable Deflection vs Rigidity

Many investigators have recommended certain values of tolerable deflections for flexible pavements with and without soil-stabilized subgrades. Some recommended tolerable deflections are as follows: WASHO Committee (9)—0.030 in.; Nichols (10)—0.036 in.; Ruiz (11)—0.035 in.; Hveem (12) has qualitatively recommended lower maximum values of deflection with increases in the thickness of asphaltic-concrete or cement-stabilized base.

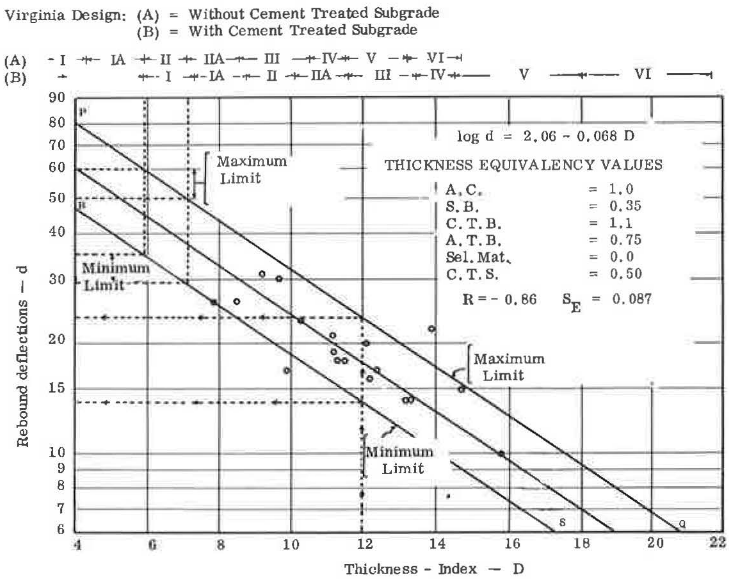

Figure 5. Minimum permissible and tolerable deflection limits.

Previously it has been shown that the pavement deflection is a straight-line function of the thickness index and in the case of 19 projects it could be represented by

$$\log d = 2.06 - 0.068\ D = 2.06 - 0.068\ a_1 \left(h_1 + \frac{a_2}{a_1} h_2 + \frac{a_3}{a_1} + \ldots \right)$$

having a correlation coefficient R = 0.86 and a standard error of estimate S_E = 0.087 on the log scale. This equation is based on the values of thickness equivalency of asphaltic concrete, stone base, cement-treated base, asphalt-treated base, select material, and soil-stabilized subgrade of 1.0, 0.35, 1.1, 0.75, 0.00, 0.50 respectively.

This relationship is shown in Figure 5. In this figure line PQ has been drawn for log d + 1.5 S_E (which includes 43 percent of the area under the normal curve) to indicate the maximum permissible limits—comparable to a tolerable deflection—of deflection for a given value of thickness index. If the deflection of a pavement exceeds this limit, the pavement is considered to be under-designed. The line RS in the figure has been drawn for log d - 1.5 S_E (which includes an additional 43 percent of the area under the normal curve) to indicate the minimum permissible limit of deflection for design. Thus a pavement is considered to have been over-designed if the deflection is much less than this limit.

To make this relationship adaptable for the pavement design categories based on traffic in Virginia, an additional scale based on traffic categories adopted in Virginia is also shown in Figure 5, in parts A and B. The design categories and the thickness indices with and without stabilized subgrade are given in Appendix C.

To illustrate the design based on these limits, let us assume a traffic category of II and a nonresilient subgrade soil with a high design CBR value that does not need a cement treatment. Figure 5 shows that under these conditions the maximum limit of deflection would be 0.050 to 0.060 in. and the minimum about 0.030 to 0.035 in. A design based on the average of these two values, i.e., 0.040 to 0.047 in., would be appropriate. Figure 5 shows that for these design deflections the pavement should have a thickness index of between 5.9 and 7.1. This is also shown in Appendix C. The pavement should therefore be designed for an average thickness index of 6.5 so that the

deflections should lie between the maximum and minimum permissible limits. Various choices in the structural cross section could be made:

	Choice A	Choice B	Choice C
Asphalt mat	5 in.	4.5 in.	4 in.
Stone base	4 in.	6 in.	8 in.
D =	6.4	6.5	6.8

The flexible pavement design chart (Appendix C) recommends 4 to 8 in. of subbase, 3 in. of asphalt base (Marshall stability less than 300 lb, say), and 1½ in. of surface course (Marshall stability of about 700 to 900 lb). Thus we find that design of new pavements on the basis of rigidity—with the help of Figure 5 or Appendix C—may help in choosing a more economical structural cross section. It is likely that in providing the structural section as in choice A above, the deflections would be less, i.e., be nearer to line RS, than would be the case with choice C. In case of choice C the deflections would be nearer to line PQ. The reason for this would be that asphalt mat is more rigid and less compressible while the stone base is not. Hence with an increase in thickness of the asphalt mat and a reduction in the thickness of stone base, the deflections for the same thickness index would decrease. A proper selection of design on the basis of rigidity of layers is therefore essential.

Since in Virginia the pavements have been considered to behave elastically after a short consolidation phase, increased rigidity of a layer would result in decreased deflections. Increased rigidity is also due to increased values of the thickness index caused by increased rigidity or thickness of rigid layers such as asphaltic-concrete or cement-stabilized base. This shows that permissible or tolerable deflection of the pavement is a misnomer, unless the rigidity of the pavement is known. Thus a pavement with high rigidity will completely fail at a value of deflection which may be well within the permissible value of deflection for a pavement with low rigidity.

In support of these conclusions, reference could be made to the work by Nijboer and Van de Poel (13), who have shown that deflection and stiffness could be correlated as follows:

$$\log d = a_0 - \log(\text{stiffness})$$

or

$$= a_0 - \text{rigidity}$$

or

$$= 2.06 - 0.068\,D \text{ in this investigation.}$$

Deflection is therefore a function of the thickness index of the pavement or a function of thickness equivalency values and vice versa. Since rigidity indicates resistance to deflection only, the thickness equivalency values would therefore represent the same.

Thus, given two layers of different materials but of the same thickness, the one with the higher value of thickness equivalency or rigidity will have a lower tolerable deflection under bending than the one with the lower value of thickness equivalency or rigidity. Furthermore, with two layers of different thickness but of the same materials, the one with the higher thickness will have a lower tolerable deflection under bending than the one with the lower thickness.

Further, when designing flexible pavements with flexible layers sandwiched between rigid layers, the increased deflection due to the flexible layers should be kept within permissible limits so as not to overstress the overlying rigid layers. This was clearly evident on the experimental projects on Route 360, which have higher deflections as compared to other projects with cement-treated subgrade and no select material. The reason for this is the introduction of a select material layer as shown in Figure 4. This figure shows that if select material was not provided the total deflection might have been less.

TENTATIVE DESIGN METHOD FOR VIRGINIA

The design recommended below is based entirely on the present design method used in Virginia. This method has resulted from experience and research in the state. It is based on the principle that when the subgrade support value—based on the CBR value—is low, soil stabilization is to be provided. In the method recommended for design, the soil support value is obtained from the CBR-resiliency method as discussed earlier.

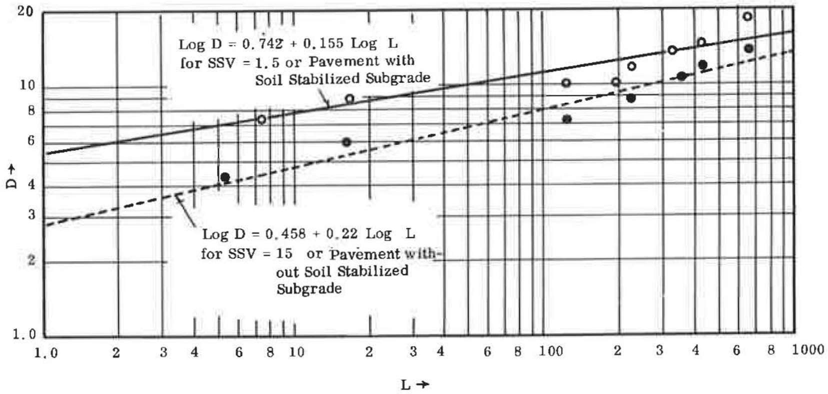

Figure 6. Correlation between thickness index and total traffic for pavements with and without soil-stabilized subgrades.

Thickness Index of Different Design Categories

Pavement design in Virginia is divided into eight categories, which are given in Appendix C. The thickness indices for each category based on the tentative thickness equivalency values determined in this investigation are also given in Appendix C. These thickness index values have been calculated for two classes of pavement, i.e., with and without soil-stabilized subgrades. For soils having low subgrade support values (i.e., say CBR-resiliency = 1.5) it is assumed that the soil-stabilized subgrade will be provided and hence the thickness index value for the design with a stabilized subgrade will be suitable. For soils with a high subgrade support value (i.e., CBR-resiliency = 15) it is assumed that a soil-stabilized subgrade will not be necessary and hence the thickness index value for the design without stabilized subgrade will be suitable.

A regression analysis between daily 18-kip equivalent loads and thickness index was carried out and the relationships obtained are as follows (L = equivalent daily 18-kip single axle loads):

1. For SSV = 1.5, or pavements with soil-stabilized subgrades,

$$\log D = 0.742 + 0.155 \log L$$

having $R = 0.95$ and $S_E = 0.12$.

2. For SSV = 15, or pavements without soil-stabilized subgrades,

$$\log D = 0.458 + 0.22 \log L$$

having $R = 0.98$ and $S_E = 0.047$.

The graph for these equations is shown in Figure 6. A nomograph based on these values is shown in Figure 7. Thus, in Figure 7 the range of soil support values varies from 0 to 15, with an approximate value of 1.5 for highly resilient soils in the Piedmont area of Virginia.

The SSV scale on this nomogram has been divided into three categories from the point of view of soil treatment. The author feels that the soils with an SSV value of less than 6 should be stabilized and the soils with SSV values more than 12 do not require stabilization. The soils with SSV values between 6 and 12 are left to the option of the designer. However, as a guide it is felt that in cases of highly resilient soils with design CBR-resiliency values = 0.5 the soil should be stabilized; in cases of a medium-resilient soil with design CBR-resiliency values = 1.0 the soil should be modified; and with a CBR-resiliency value of 1.5 no soil treatment should be provided.

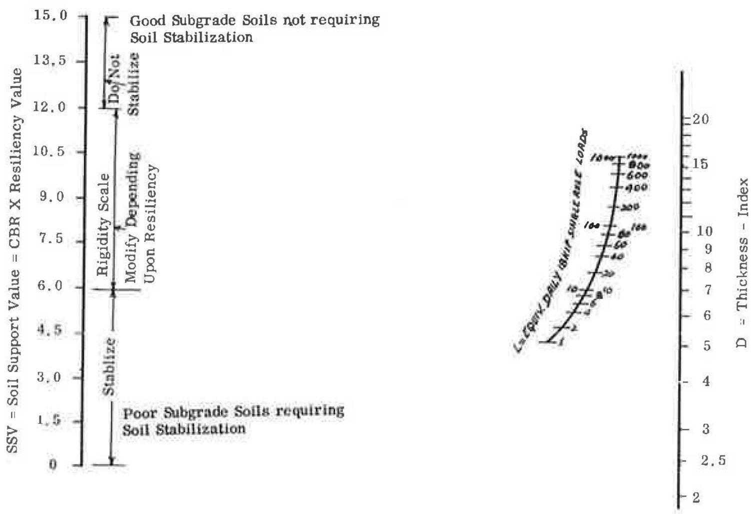

Figure 7. Nomograph for determining thickness index.

This nomograph can be utilized for determining the thickness index required for the design of new pavements, based on the subgrade soil properties and traffic in terms of daily 18-kip equivalents, or can be used for maintenance by evaluating the modified thickness for the revised traffic in terms of daily 18-kip equivalents. For example, for projects on Route 220 and Route 360, the load survey study in 1963 showed that the design daily 18-kip equivalents (average of 20 years) on these projects are 326 and 622 respectively. The pavement on Route 220 has a stabilized-soil subgrade and the pavement on Route 360 has no stabilized-soil subgrade. Assuming their SSV to be 1.5 and 15 respectively, the thickness indices (from Fig. 7) required are 14.5 and 13 respectively. Thickness indices provided are 14.1 and 11.1. Thus it is seen that the project on Route 220, built in 1962, does not need additional strength on the basis of 1963 traffic data while the project on Route 360, built in 1959, needs 2 inches of asphaltic concrete on the basis of 1963 data.

If a new pavement was proposed on Route 360, with the same amount of traffic (18-kip equivalent = 622) but with SSV = 1.5, the thickness index required with a soil-stabilized subgrade would be 17.2. The choices of the structural cross section could be very many; for example:

	Choice A	Choice B	Choice C	Choice D
Asphalt mat	7 in.	8 in.	9 in.	10 in.
Stone base	6 in.	6 in.	5 in.	8 in.
Cement-treated base	5 in.	5 in.	4 in.	—
Cement-treated subgrade	6 in.	4 in.	4 in.	8 in.
D =	17.6	17.6	17.2	16.8

Thus, with the help of this nomograph, pavement design can be simplified to facilitate the most economical design compatible with engineering judgment. While designing on the basis of this chart, it is recommended that, in addition to the basic fundamental requirements of better service and durability, the following requirements must be met. These requirements are recommended on the basis of the author's engineering judgment.

1. Flexibility or rigidity is a function of strength and the thickness of material in each layer. Too much flexibility might overstress the asphaltic concrete.

2. A minimum thickness of 1½ in. of asphaltic concrete is necessary for low-traffic roads such as designs I and IA. With an increase in traffic the thickness must also be increased to keep the deflection category low. Thus, for medium traffic it should not

be less than 4 to 6 in. and for daily 18-kip equivalents of 660, the thickness of asphaltic concrete might be 10 in.

3. The stone aggregate base course thickness may vary from 4 to 8 in. Since pavement flexibility increases with the increase in thickness of the base course, an approximate rule of one inch of stone base for every inch of asphaltic concrete may be a good one.

4. Select material has a thickness equivalency value of zero. It may therefore be provided for improving drainage only.

CONCLUSIONS

The following conclusions drawn from this investigation are applicable mostly to the Piedmont area of Virginia from which the satellite study projects were chosen. Some are tentative pending further investigation.

1. The structural performance of the pavements can be evaluated from rebound deflection or curvature, or longitudinal cross-sectional area of the deflected basin, obtained from the Benkelman beam data.

2. Subgrade soil strength, when determined by the Virginia CBR method, cannot be correlated with subgrade soil support values given by the AASHO Committee.

3. Assuming the thickness equivalency value of asphaltic concrete as equal to 1.0, the following thickness equivalency values could be considered for design in Virginia with the layers placed in the order described. In the base course, either a cement-treated or asphalt-treated base layer is to be provided if desired. Below the base, either select material or cement-treated subgrade is to be provided, if desired. Any layer, excluding the asphaltic-concrete layer, could be omitted but not interchanged.

a. Material in surface course = Asphaltic concrete = 1.0
b. Materials in base course = Stone base = 0.35, cement-treated base = 1.1, asphalt-treated base = 0.75
c. Materials in subbase for non-stabilized subgrade = Select material = 0.0
d. Subgrade = Cement-treated soil = 0.50

4. The tolerable deflection of a pavement is a function of its rigidity; the higher the rigidity the lower the tolerable deflection.

5. The method presently used in Virginia is suitable for design but could be made more flexible by using a system as shown in Figure 7 and a design based on thickness equivalency values.

ACKNOWLEDGMENTS

It is a pleasure to acknowledge the help received from C. S. Hughes and the staff of the Pavement Section. Mr. Hughes was at all times available for free and open discussions and guided the study so that it would serve the best interests of the Virginia Department of Highways. He also offered helpful criticism of the paper.

The author is also grateful for the encouragement and support given by Dr. Tilton E. Shelburne, State Highway Research Engineer.

This investigation was conducted in cooperation with the Bureau of Public Roads.

REFERENCES

1. Interim Guide for Design of Flexible Pavement Structures. AASHO Committee on Design, Oct. 1962.
2. Shook, J. F., and Fang, H. Y. Cooperative Materials Testing Program at the AASHO Road Test. HRB Spec. Rept. 66, pp. 59-102, 1961.
3. Stevens, J. C., Maner, A. W., and Shelburne, T. E. Pavement Performance Correlated With Soil Areas. HRB Proc., Vol. 29, pp. 445-466, 1949.
4. Hughes, C. S. Reconnaissance of Pavements on Virginia's Interstate System. Virginia Highway Research Council, Charlottesville, 1967 (unpublished).
5. The AASHO Road Test—Report 5, Pavement Research. HRB Spec. Rept. 61E, 1962.

6. Burmister, D. M. Theory of Stresses and Displacements in Layered Systems and Applications to the Design of Airport Runways. HRB Proc., Vol. 23, pp. 126-154, 1943.
7. Thickness Design—Asphalt Pavement Structures for Highways and Streets, 7th Ed. The Asphalt Institute, Sept. 1963, and March 1964.
8. A Guide to the Structural Design of Flexbile and Rigid Pavements in Canada. Canadian Good Roads Association, Sept. 1965.
9. WASHO Road Test—Part 2: Test Data, Analyses, Findings. HRB Spec. Rept. 22, 1955.
10. Nichols, F. P. Deflections as an Indicator of Flexible Pavement Performance. Highway Research Record 13, pp. 46-65, 1963.
11. Ruiz, C. L. Sobre el calculo de Espesores para Refuerzo de Pavimentos. Quinto Reuniao Anual da Associacao Brasileira de Pavimentacao, 1964.
12. Hveem, F. N. Pavement Deflections and Fatigue Failures. HRB Bull. 114, pp. 43-87, 1955.
13. Nijboer, L. W., and Van de Poel, C. A Study of Vibration Phenomena in Asphaltic Road Constructions. Proc. AAPT, Vol. 22, 1953.
14. Pavement Evaluation Studies in Canada. Special Committee on Pavement Design and Evaluation, Canadian Good Roads Association. Proc. Internat. Conf. on Structural Design of Asphalt Pavements, pp. 137-218, 1962.

Appendix A

DETERMINATION OF DEFLECTION, CURVATURE AND LONGITUDINAL-SECTIONAL AREA OF BASIN

Method of Measuring Deflections

In Virginia, Benkelman beam deflections are determined under a very slowly moving tandem wheel. The tandem wheel has a tire pressure of 60 to 80 psi and a load of 9,000 lb. The procedure used is to begin the test with the truck wheels 2 ft behind the tip of the beam. An initial reading at -2 ft is taken while the truck is stationary at this position. The truck then is moved forward and the maximum dial reading is recorded as the 0-ft reading. The truck is then stopped briefly at a point 2 ft in front of the tip of the beam, and this reading recorded as +2 ft. Simiarly, the readings at +4, +9 and +50 ft are recorded. The deflection at 0-ft reading is therefore equal to 2 (0-ft reading -50-ft reading).

In case the 9-ft dial reading differs from the 50-ft dial reading, the front leg of the beam is assumed to have been in the deflection basin. The Canadian Good Roads Association (14) recommends a formula for correcting this situation. This formula is based on the difference between the 9-ft and 50-ft readings. The standard deviation of the repetitive Benkelman readings in this investigation was found to be 0.0019 in. compared to a value 0.0016 in. which had been obtained previously. As indicated by the standard deviation of 0.0019, the standard deviation of the dial reading (which is one-half the deflection value) would be approximately 0.001 in. Therefore, because of the imprecision of the dial reading, no correction has been made in this investigation for a difference of 0.001 in. This procedure agrees with the procedure used in the Canadian Good Roads Association method, in which no corrections are made unless the 9- and 50-ft readings differ by more than 0.001 in. A difference larger than 0.001 in. was very seldom found in this investigation and hence no correction was applied.

The average deflection readings $\overline{X}$, their standard deviations σ, and the values of $\overline{X} + 2\sigma$ are given in Table A-1.

Method of Measuring Curvature

The curvature was measured by deducting the average of the initial reading at -2 ft and the 2-ft reading from the maximum dial reading recorded at the 0-ft reading.

TABLE A-1

BENKELMAN BEAM DEFLECTION DATA
(Average Standard Deviations and Average Plus 2 σ)

Serial Nos.	Project No.	Project	Average Deflection Readings at 20 Day Intervals			Standard Deviations of Col. 4, 5, and 6			$\bar{X}$ = Mean of Col. 4, 5 and 6	σ = Mean of Col. 7, 8 and 9	$\bar{X}$ x 2σ = Col. 10 + 2 Col. 11
			I	II	III	I	II	III			
1	2	3	4	5	6	7	8	9	10	11	12
1	5	Exp. Proj. Rte. 360 (Design A) (6 Groups)	32	29	35	4.18	4.28	4.27	32.0	4.24	40.48
2	6	Exp. Proj. Rte. 360 (Design B) (6 Groups)	22	18	21	4.69	5.03	6.28	20.0	5.33	30.66
3	7	Exp. Proj. Rte. 360 (Design C) (6 Groups)	35	31	36	13.96	11.27	14.82	34.0	13.35	60.70
4	8	Exp. Proj. Rte. 360 (Design D) (6 Groups)	40	35	39	5.56	4.19	2.19	38.0	3.98	45.96
5	10	7220-033-032	20	20	-	3.59	3.13	-	20.0	3.36	26.72
6	11	220-044-030 (10 Groups)	20	21	25	6.66	3.74	4.74	22.0	5.05	32.10
7	12	220-044-019-C501	20	16	18	3.79	6.45	5.04	18.0	5.09	28.18
8	13	058-071-020	23	22	25	4.27	3.80	5.23	23.33	4.43	32.19
9	14	501-041-102-C501	26	24	27	8.67	8.46	13.47	25.67	10.20	46.07
10	15	304-041-002-C501	16	14	17	1.23	1.52	2.51	15.67	1.75	19.17
11	16	015-019-101, C-2 (Light Design) (8 Groups)	15	17	20	4.83	4.94	6.44	17.33	5.40	28.13
12	17	015-019-101, C-2, (Heavy Design) (6 Groups)	18	15	17	5.04	4.26	6.83	16.67	5.38	27.43
13	18	017-030-008-C	16	13	14	2.66	2.73	3.37	14.33	2.92	20.17
14	19	066-030-001-PI	9	7	13	1.79	2.04	6.01	9.67	3.28	16.23
15	20	066-076-101-PI	15	14	16	2.81	3.21	3.17	15.0	3.06	21.12
16	21	0236-029-007-008	16	12	14	3.89	3.28	3.19	14.0	3.45	20.90
17	33	Exp. Proj. Rte. 58 (Design A) 1962	81 in 1962				24.6		81.0	24.6	130.2
18	34	Exp. Proj. Rte. 58 (Design B) 1962	42 in 1962				3.5		42.0	3.5	49.0
19	35	Exp. Proj. Rte. 58 (Design C) 1962	52 in 1962				12.9		52.0	12.9	77.8
20	36	Exp. Proj. Rte. 58 (Design D) 1962	52 in 1962				16.4		52.0	16.4	84.8
21	37	460-009-019	33	29	29	9.33	8.71	9.28	30.33	9.11	48.55
22	38	460-009-017	27	36	30	12.73	9.38	14.6	31.0	12.23	55.46
23	39	501-041-102-C502	36	37	39	10.16	9.71	11.66	37.33	10.51	58.35
24	40	015-014-101, C-502	25	24	29	5.80	6.58	7.27	26.0	6.55	39.10
25	41	0360-020-031-GI	21	17	16	1.84	1.88	1.94	18.00	1.89	21.78
26	42	0360-020-032-028	19	20	19	6.64	6.38	6.36	19.33	6.46	32.25
27	43	0360-020-019-027	19	22	23	5.41	7.06	6.89	21.33	6.45	34.23

Method of Measuring Cross-Sectional Area of Basin

The longitudinal area of the deflected basin was calculated by assuming the shape of the basins either as a sin curve of the equation $Y = a \sin\left(\frac{\pi}{2} - c\right)$ or a triangular deflection of the equation $Y = b - a\,x$ or a sin curve within a 2-ft radius of applied load, followed by a straight-line slope. In these equations, Y = maximum deflection, a = a constant, and $c = \pi \div$ horizontal distance of the deflected basin.

Appendix B

GROUPS OF THE COMBINATIONS FOR REGRESSION ANALYSIS ON B5500 COMPUTER

1. Satellite projects without stabilized subgrades (7 projects).
2. Satellite projects with stabilized subgrades only (12 projects).
3. All satellite and other projects but excluding experimental project on Route 360 (39 projects).
4. Satellite projects without stabilized subgrades, experimental project on Route 58 and other projects without stabilized subgrades (22 projects).
5. Satellite projects with stabilized subgrades and experimental project on Route 360 (16 projects). The Route 360 project has select material between the soil-stabilized layer and the stone base.
6. Satellite projects with stabilized subgrades, experimental project on Route 360 and five other stabilized subgrade projects in the Piedmont area (21 projects).
7. All satellite projects excluding experimental projects (19 projects).
8. All satellite projects including the two experimental projects and other projects in Piedmont area (43 projects).

Appendix C

FLEXIBLE PAVEMENT DESIGN CHART — PRIMARY AND INTERSTATE SYSTEM — REVISED APRIL, 1967

Traffic Category	Daily Equivalent 18 kip Axle Loads	*Stabilized Subgrade	*Subbase	Base	Binder Course	Surface Course	Thickness Index: with subgrade stabilization	Thickness Index: with no subgrade stabilization
1	2	3	4	5	6	7	8	9
I	0 - 7	6"	None	4" - 6" (a)	None	P & DS (b)	5.9 to 7.3	2.9 to 4.3
IA	8 - 16	6"	None	6" - 8" (a)	None	P & DS (c)	7.3 to 8.8	4.3 to 5.9
II	17-124	6"	4" - 8"	3" B-3 (345#)	None	165# S-4 or S-5	8.8 to 10.1	5.9 to 7.1
IIA	125-224	6"	4" - 8"	4" B-3 (460#)	None	165# S-4 or S-5	10.1 to 11.6	7.1 to 8.6
III	225-329	6"	4" - 8"	6" B-3 (690#)	None	165# S-5	11.6 to 13.5	8.6 to 10.5
IV	330-429	6"	6" - 10"	6" B-3 (690#)	165# I-2 (1.5")	100# S-5 (1.0")	13.5 to 14.5	10.5 to 11.5
V	430-659	6" - 12"	6" - 10"	8" B-3 (920#)	None	165# S-5 (1.5")	14.5 to 18.0	11.5 to 13.2
VI	660 and Over	6" - 12"	8" - 12"	8" B-3 (920#)	165# I-2 (1.5")	100# S-5 (1.0")	18.0 to 20.7	13.2 to 14.7

(a) Stone-base.

(b) Prime and Double Seal on Contract I. — 165# Plant Mix on Contract II when warranted.

(c) Prime and Double Seal on Contract I. — Up to 300# Plant Mix on Contract II.

*Minimum depth of subgrade stabilization and subbase will depend on soil conditions and design CBR value.

Discussion

W. H. CAMPEN and L. G. ERICKSON, Omaha Testing Laboratories, Inc.—We wish to ask two questions and make some comments.

Question and Comment No. 1: You classify the resilience of subgrades in terms of low, medium, and high, and assign values of 1.5, 1.0 and 0.5 respectively. However, these values appear to be arbitrary without coordination with some field test which can give a numerical range for the three categories. We are wondering what these ranges might be in terms of plate load tests or Benkelman beam measurements.

Question and Comment No. 2: We question the implication of your definition of a flexible layer. You say that a flexible layer shows compression on loading and rebound when the load is removed. This is not necessarily so. You, yourself, have come to the conclusion that asphaltic concrete layers are practically incompressible. It can be proven also that base and subbase layers for flexible pavements can be so designed and compacted as to render them incompressible. The elasticity or rebound in such cases is due entirely to the subgrade resilience.

Since we question your implication, it seems up to us to attempt to define a flexible pavement. We will admit that although we have used the term "flexible pavement" for 30 years, we have not read or heard a definition for it. However, engineers seem to have a common understanding concerning its composition, mechanical properties, and load-distributive characteristics.

As far as composition is concerned, a flexible pavement contains a bituminous paving mat as a wearing surface and layers of base and subbase. The bituminous layer may range from sheet asphalt to coarse asphaltic concrete. The base and subbase layers may consist of compacted soil-aggregate or crushed-aggregate mixtures, or mixtures of the two. These mixtures may be coated with bituminous material and designated as bituminous-treated bases. The layer components must be stable enough to resist displacement (plastic flow) under traffic. Generally, these mixtures possess very little cohesion.

As far as the principal mechanical property of each layer is concerned, it must be able to distribute load to the layer beneath. The layered system as a whole must be able to distribute load over the subgrade. For a given load and a given subgrade, the total thickness of the layered system must be such as to limit the elastic deformation or rebound at the top of the system to prevent cracking and eventual destruction.

This describes the composition and mechanical property of a flexible pavement. In giving a definition for such a pavement, reference must be made to a rigid pavement. The distinction between the two types is based on manner in which they distribute load. A rigid pavement layer distributes load by beam action, whereas a flexible pavement layer distributes load by some angle of distribution such as described by the Boussinesq equation.

N. K. VASWANI, Closure—In reply to Question No. 1 by Messrs Campen and Erickson, the resiliency of subgrade soils has been classified in terms of low, medium and high and arbitrarily assigned values of 1.5, 1.0, and 0.5. These resiliency values are based on the soil classification reports of the satellite projects in the Piedmont area of Virginia and the general knowledge of the types of the soils prevalent; e.g., micaceous silts could be considered to be highly resilient. These values are therefore not recommended for adoption in other soil areas.

In the Piedmont area of Virginia, the Benkelman beam rebound deflections of the pavement are high and the values mentioned were multiplied by the CBR values to provide the effect of resiliency in reducing the soil support value.

The answer to Question No. 2 has been divided into 3 parts: (a) the implication of the definition of a flexible layer; (b) rebound of a flexible layer; and (c) design of a pavement with incompressible layers of asphaltic concrete, base, and subbase.

Implication of the Definition of a Flexible Layer

The term "flexible pavement" was probably used when portland cement concrete rigid pavements came into use. The flexible pavement was considered to consist of materials whose ingredients were not well bonded together and hence had no bridging effect like the materials in the rigid or concrete pavements.

Sophisticated design methods and construction techniques, e.g., improved bituminous mix designs and better compaction techniques, provide a high modulus of elasticity of the materials in the pavement layers. The flexible pavements built presently are of a

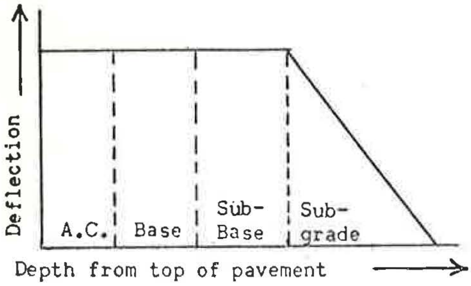

Figure 8.

more rigid type than those built in past years. The old understanding of the term "flexible layer" or "flexible pavement," therefore, needs modification. The modification is necessary to express the concept of present design techniques. This was the object of the definition provided here.

The discussants agree that a "rigid layer" or "rigid pavement" is one which exhibits the bridging effect, which, in terms of design concept, indicates a high modulus of elasticity in bending. Road materials which satisfy this requirement also have a high modulus of elasticity in compression, and since the modulus of elasticity = stress/strain, it follows that the compression produced in such a pavement or layer is very low for a given amount of stress or load.

Thus a perfectly rigid pavement has been defined in the paper as one which does not compress but only bends due to the applied load. A portland cement concrete pavement is, for all practical purposes, considered a perfectly rigid pavement and hence is designed on the basis of the theory of bending only.

The question now arises as to what the other extreme case would be that only compresses and does not bend due to the applied load. We should be able to supply a term for this extreme case. The discussants admit that they have not read or heard a definition of a "flexible pavement," though this word is commonly used. Why then hesitate to define this extreme case by the terms "flexible pavement" or "flexible layer" as the case may be? These terms would retain the same meaning as they have in the past and also would pinpoint the properties of this case.

In the paper these two terms have been defined under the heading "rigidity." The time is coming when the term flexible pavement will be forgotten and the pavements will be designed on the basis of the "degree of rigidity." Design on this basis has been given in the paper for the Piedmont area of Virginia.

Rebound of a Flexible Layer

In the paper, the author states only that a flexible layer shows compression on loading, and not that it is a flexible layer because it rebounds.

Design of a Pavement With Incompressible Layers of Asphaltic Concrete, Base, and Subbase

If these layers are stable enough to resist displacement—due to plastic flow—under traffic, the deflection of the layers could be represented by the graph shown in Figure 8. In such case the pavement should preferably be designed on the basis of the theory of bending as given by Westergaard for design of portland cement concrete slabs, rather than on Boussinesq's equation for homogenous isotropic plastic materials.

Theoretical Asphaltic Concrete Equivalences

BONNER S. COFFMAN, GEORGE ILVES, and WILLIAM EDWARDS
Respectively, Associate Professor of Civil Engineering and Research Associates, Ohio State University

Theoretical asphaltic concrete equivalences were calculated on a continuous hourly or fourth-hourly basis for a 245-day period. For these calculations equivalence was defined as that thickness of base necessary to replace one inch of surfacing for equal deflection. Deflections were calculated using the layer elastic theory and the results of static and dynamic lab tests of the pavement materials in the frequency domain. The materials investigated were two asphaltic concrete surfacings and three asphaltic concrete bases. The effect of testing specimens with H/D ratios of less than two was investigated. The subgrade was that determined from the 1960 trenchings at the AASHO Road Test and the continuous hourly temperature data were those reported by the Asphalt Institute. Continuous 19-kip single-axle loadings moving at 50 mph were assumed for the principal calculations. The effects of different loadings were examined as functions of weight, speed, time, and contact area together with the effects of different subgrades and layer thicknesses. It was concluded that there is no unique equivalence and that the inclusion of a failure term is necessary to the theoretical calculation of equivalence for given materials, environment and loadings.

•THE objective of this study was the investigation of a theoretical approach, using laboratory test results, for determining the relative structural equivalences of asphaltic concrete surfacings to base materials in highway pavements. This problem is significant because of the possible geometries and diversities of materials available for use in pavements, the traditional approach to pavement design, and the relative insensitivity, as well as the time and money costs, of on-the-road performance-type tests. Similar studies of this problem in the past have been based on various criteria using average conditions, performance, etc., and the equivalences so determined can show a rather large range (1, 2, 3). In this study the criterion used to determine equivalence involves finding the increased thickness of a material that compensates for the deflection resulting from a unit thickness decrease in another material. The importance of deflection as a criterion was shown by the AASHO Road Test, in which deflection correlated as well with performance as did loadings and structural design (4).

The prediction of pavement deflections using the results of laboratory tests and the elastic layer theory has been of major interest in past work here. The results of comparisons of predicted and measured deflections have been reported (5, 6) and form the base for this study. The initial development of an approach to determining material equivalences using deflections was accomplished in work performed under a grant by the Asphalt Institute (7). That work showed the importance of variations in pavement-material properties with time-associated changes in temperatures, moisture contents,

Paper sponsored by Committee on Flexible Pavement Design.

and densities. Based on that work it was concluded that there was no unique equivalence and that the theoretical determination of average equivalences must be based on climatic conditions as they actually vary with time.

Changes in pavement material properties with time, excluding the effects of aging, will vary with the pavement, its geographical location, and the time under consideration. Such changes are easily recognized in the rapidly changing temperatures in the asphaltic concretes and in the relatively slowly changing moisture contents and densities in the underlying layers. These changes are interrelated to some degree and in any study that considers the effect of such changes, it is necessary that the various data be compatible. Unfortunately no complete source of such compatible data is known and to investigate theoretically the equivalences of various asphaltic concretes for this study, it was necessary to devise a hybrid pavement-climate history. The resulting artificial conditions were composed of the hourly 12-in. asphaltic concrete temperature data reported by Kallas for 1964-5 in College Park, Maryland, and the subgrade conditions reported for the 1960 trenching studies of the AASHO Road Test (8, 9). For these conditions the equivalences of two asphaltic concrete surface and three asphaltic concrete base materials were investigated for those months in which the Road Test subgrade was not frozen.

Samples of the investigated materials have been tested in the laboratory and, using these test results, calculations of deflection under a 19-kip single-axle load moving at 50 mph were made using the three-layer elastic theory (10). These calculations were made for consecutive hours for 12-in. thick pavements composed of 3- and 9-in. thicknesses of surface and base materials. For each of these times 1 in. of the surface material was removed, in theory, and the amount of base necessary to bring the calculated deflection back to the original value was found by successive approximations.

While this study was restricted to asphaltic concretes in two constant layers, the methods used are believed applicable to such pavements in any number of layers. In that connection the greatest significance of this work may well be in the theoretical simulation of pavement response to moving loads with continuous time.

MATERIALS

The asphaltic concrete materials investigated in this study were the AASHO Road Test surfacing and base together with Ohio's T-35 surfacing and B-21 and B-35 bases. Complete laboratory test results for the Road Test surfacing, subgrade and base materials have been reported (5, 7) as have similar results for Ohio's T-35 and B-21 asphaltic concretes (6). As constructed for pavement service, the AASHO and the T-35 surfacings were composed of wearing and leveling courses. The preparation of laboratory test specimens of each of these materials involved the creation of a simulated mix in which the gradation of the aggregate was the average for the two courses. In addition, for the T-35 surfacing, data were available from tests on pavement cores in which the strain gages bisected the two courses. Samples of the Ohio B-35 base were tested as a part of this study.

Specimens of the B-35 base were taken from an in-service pavement using diamond core drills. This pavement, Hamilton Rd., was constructed during the fall of 1964 and the core specimens were taken on May 31, 1966. Figure 1 shows the average aggregate gradation of the B-35 base from extraction tests made during construction of the pavement. These tests gave an average asphalt content of 4.9 percent (of total mix) of a 70-85 penetration asphalt. Also shown for comparison in Figure 1 are the gradation curves of the other asphaltic concretes as well as average data from similar tests on the lab specimens.

The average core diameter from the Hamilton Rd. pavement was 3.75 in. and the average height was 7.5 in., of which some 3.5 in. were of the B-35 base and the remainder was of the surfacing. The surfacing layer was removed from the core specimens by sawing with a diamond saw, as was a thin layer representing the irregular bottom of the asphaltic concrete. This gave rather short test specimens 3.75 in. in diameter and 3.0 in. high or an H/D ratio of about 0.8.

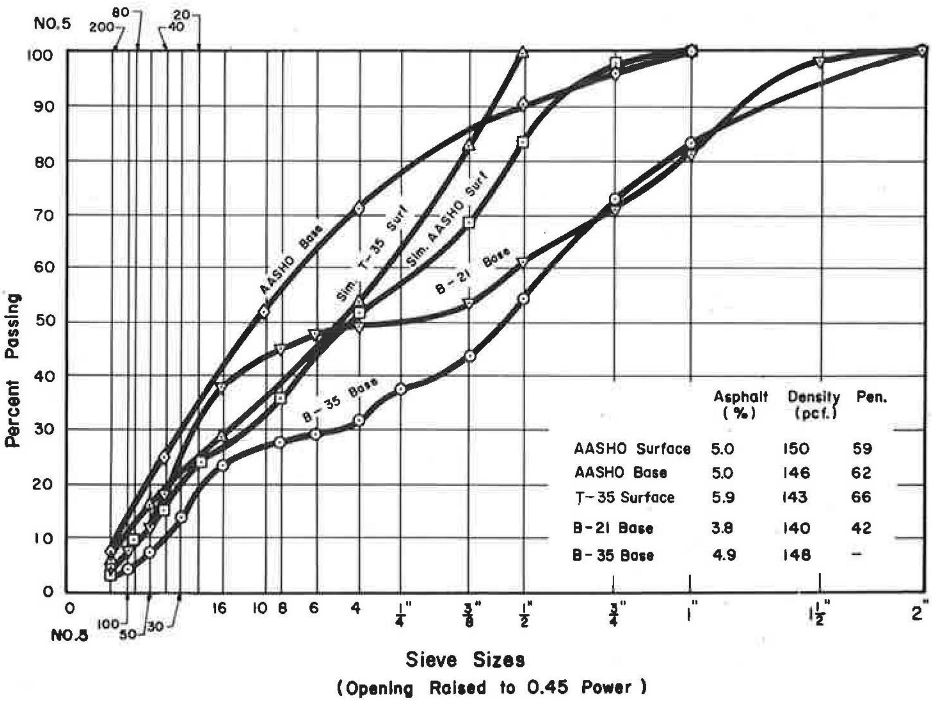

Figure 1. Aggregate gradations.

The B-35 core specimens were tested under dynamic loading to determine the variation in complex modulus $|E^*|$ and phase shift ϕ with changes in specimen temperature and in loading frequency. In these tests the asphaltic concrete specimens were subjected to simple axial compressive loading in the form of a sine wave and the resulting strain was measured with SR-4 gages mounted at specimen mid-height. These test procedures, involving relatively small loads and strains, and the analysis of the resulting data have been given in some detail previously (9). In brief, for unconfined dynamic compressive tests where steady-state sinusoidal loading is of the form $\sigma_v = \sigma_o \sin \omega t$ and the resulting strain is of the form $\epsilon_v = \epsilon_o \sin (\omega t - \phi)$, by definition:

$$|E^*| = \frac{\sigma_o}{\epsilon_o} \text{ and } \phi = \frac{t_1}{t_p} (360°)$$

where

$|E^*|$ = complex modulus,
ϕ = phase shift,
σ_o = amplitude of stress wave,
ϵ_o = amplitude of strain wave,
t_1 = time between homologous points on the two curves, and
t_p = period.

Before this study no tests of specimens with an H/D ratio of appreciably less than 2 had been performed here. Because of the relatively thin layer of the B-35 base in the Hamilton Rd. pavement it was necessary to investigate the feasibility of testing specimens with H/D ratios on the order of one.

End Effects

The effect of end conditions can be marked in test specimens with plane and parallel ends and H/D ratios of appreciably less than 2. This is a historic problem in elasticity,

as shown by the theoretical work of Filon in 1902 (11). There are two practical difficulties associated with testing short specimens. These involve the problem of achieving plane ends perpendicular to the axis of the specimen and the problem of eliminating the end restraint (or vice versa) that results when end platens are of different E and μ than the specimen. Past efforts to solve the latter problem have involved the use of segmented end platens, oiled membranes, low-friction membranes, combinations of these, etc. (12, 13, 14). For the purposes of this study a limited experimental investigation into these problems was undertaken.

To investigate the effect of specimen treatment and end conditions, a group of 16 asphaltic concrete test specimens was prepared that represented the range in materials that had been used in past studies. These capped specimens were 4 in. in diameter by 8 in. high and were mounted with $^{13}/_{16}$-in. active length SR-4 strain gages at sample mid-height. The specimens were repetitively tested over a period of several days to provide datum values of individual and average $|E^*|$ to which the effects from subsequent variables could be referenced. As a side variable in this test series, the effect of end irregularities (introduced by inserting feeler gages up to 0.050 in. in thickness) was investigated as well as the effect of using different end materials, such as $^1/_4$-in.-thick gasket-cork layers, 10-mil sheet Teflon, triaxial rubber membranes, etc. As would be expected there was no effect on average test values from the introduction of any of these conditions or materials at the ends of the capped specimens.

Eight of the 16 specimens were then used to investigate the effect of "freezing" (0 F) followed by annealing (1 hour at 150 F) on capped specimens. This question was of interest because it was expected that sawing would be better accomplished with frozen specimens. The results of these tests showed no effect on average $|E^*|$ as a result of freezing; subsequent experience with sawing indicated that it was as easy to saw unfrozen as frozen specimens and that the effects from sawing were similar.

Following these tests, the caps (only) of eight of the datum series were removed by diamond sawing. These specimens were then annealed at 150 F for 1 hour and repetitively tested at 88 F and 10.8 rad/sec over a period of several days. They were tested with steel end platens, with steel platens and feeler gages 0.004, 0.008 and 0.015 in. thick inserted (between sample and platen) directly over a strain gage as well as with the feeler gage at 90° from over the strain gages. There was no effect on average $|E^*|$ with steel end platens. There was no effect of end irregularity introduced by feeler gage below the 0.015-in. level. At that level there was a trend, barely significant, of slightly lower average $|E^*|$ with the feeler gage directly above the strain gage, and slightly higher average $|E^*|$ with the feeler gage away from the strain gages. There was no effect with cork alone nor was there any effect of feeler gage when used with cork. Other capping materials gave results similar to those with cork.

These specimens were then shortened by sawing to a height of $5^1/_4$ in., after which they were annealed and retested. At this point an effect from sawing was first observed in that first tests gave higher strains than did all subsequent tests. The latter gave values that were stable under repetitive testing performed daily for several days. Apparently some disturbance was caused by the sawing that was corrected in subsequent handling. At this time tests with cork showed no change from datum in average $|E^*|$ while tests with steel platens (only) gave individually erratic results that were somewhat higher in average $|E^*|$. Deviations of the ends of these samples from planes were estimated to be on the order of 0.002 in. from measurements made with an Ames dial by sliding the sample across plate glass. The difference in height across the specimens was on the order of 0.030-0.060 in. Tests with stacked triaxial membranes as well as those with stacked Teflon layers gave results intermediate between steel and cork, whether the layers were oiled or not.

After these tests the specimens were shortened by sawing to a height of 3 in. after which they were annealed and re-tested. The effect of sawing was again noted in first tests. Individual test results with steel platens were wildly erratic. Subsequent test results with two layers of $^1/_{16}$-in.-thick lab gasket rubber and with cork were consistent and were significantly lower than the datum test values; cork was somewhat better than rubber. In this later test series there was no effect of specimen rotation with respect to cork or rubber end materials. The results of tests using polyurethane foam caps

were similar to those with cork and rubber except that the average $|E^*|$ determined with foam showed no significant difference from the original datum tests.

From the results of these tests it was believed that both the foam and the cork showed promise as capping materials and that these two materials should be investigated at other test temperatures and frequencies with a larger number of test specimens. These tests were performed with results that, in brief, showed that the effects of these capping materials were variable under the different conditions of temperature and frequency. It was concluded that they could not be generally used as cappings for short asphalt concrete test specimens to eliminate end effects, even at the relatively low strain levels used in these tests. These results indicated that perhaps the only hope of solving the "like E and μ" problem with short specimens was to use caps of the same materials as the test specimens.

Following these findings the test datum specimens were ground at a local steel supplier with a Blanchard grinder. This equipment is rated to give ends out of parallel or of plane of less than 0.002 in. and the resulting surfaces were well within these tolerances. Check tests on these specimens, using the capping materials previously investigated, revealed the test-sequence effect first noted with sawing—the lower first-test value was again followed by recovery to the pregrinding value. Tests were performed using two of the datum specimens as caps while a third specimen, placed between the two capping specimens, was tested. The results showed that at the higher temperatures the resulting average $|E^*|$ were at datum values but that there was some effect of rotation of the caps with respect to the middle test specimen. It was suspected that the rotation effect was dependent on relatively small end-surface irregularities.

The ends of the capping and test specimens were carefully hand ground, using decreasing grit size down to No. 180, and retested at high and low temperatures. The results of these tests showed that the effect of rotation was more pronounced at the lower temperatures. Analysis of these data suggested that the rotation effect was strain-dependent; i. e., in tests at the higher temperatures and higher strains there was enough strain to overcome the effect of small end irregularities. This thesis was checked by performing tests at high temperatures at both low and high strains and the rotation effect that had been observed at low strains and temperatures was replicated. In these check tests the strain levels were about 30 and 120 microinches per inch—values that were comparable to those at which the effect was first noted. In check tests at the 40 F level it was not possible to achieve the higher strain level with the loading equipment available although lower strains could be attained. These tests did show, however, the same trend of decreasing dispersion in test values with increase in strain level. In these tests the strain levels were some 15 and 30 microinches per inch.

Based on analysis of all data it was concluded that hand-grinding to the No. 180 grit level brought the $|E^*|$ values to within ranges that were acceptable for the purposes of this study. One of the findings in this test series was that specimen ends, once prepared by grinding, must be maintained by keeping the specimen capped with plane surfaces. Asphaltic concretes are viscoelastic and surfaces ground plane will change with time and handling technique. In this study plate glass was used for this purpose and the insertion of 1- or 2-mil Teflon between the glass and specimen prevented bonding of the two.

This study was not exhaustive, by any means, and further research on the problem of testing short asphaltic concrete specimens at low strain levels is needed. Where specimens with fairly smooth ends and with H/D ratios on the order of 2 are available, or can be made, there is no particular problem as would be expected and as was experimentally confirmed in this study. If it is desired to test samples from in-service pavements, however, layer thicknesses and aggregate sizes will control the size of the specimens that can be used for such tests. For many pavements, such as the Hamilton Rd. pavement in this study, it will be necessary to test specimens with low H/D ratios. In these cases it will be necessary to use extraordinary techniques to minimize the end-effect problem.

For the tests of the Hamilton Rd. base specimens in this study the ends were ground through the No. 180 grit size as discussed previously. After each specimen was hand-ground it was stacked to give composite specimens composed of two central and active

specimens capped on the ends with inactive or capping specimens. First tests of these composite specimens were at 110 F and 10.8 rad/sec at which point the specimens, which had a tendency to bond, could not be easily separated. Following these tests the B-35 specimens were tested at other temperatures and frequencies and at the end of testing bonding was complete to the point that the composite specimens could be lifted by the top without separation. The average results of these tests are given graphically in Figure 2. Check tests for linearity of response (to increases in compressive stress) are not shown but gave results on the order of those of the other asphaltic concretes in this study.

Asphaltic Concretes

The study was concerned with the response of the different asphaltic concretes to a truck moving at 50 mph. With the truck loading represented by a cycle length of 6 feet, as used in past studies (5, 6), this is equivalent to a lab sinusoidal loading frequency of 77 rad/sec. The moduli response of the five asphaltic concrete materials to temperature change at this frequency is given in Figure 3. These data represent an interpolation for frequency and an extrapolation for temperatures higher than 110 F and lower

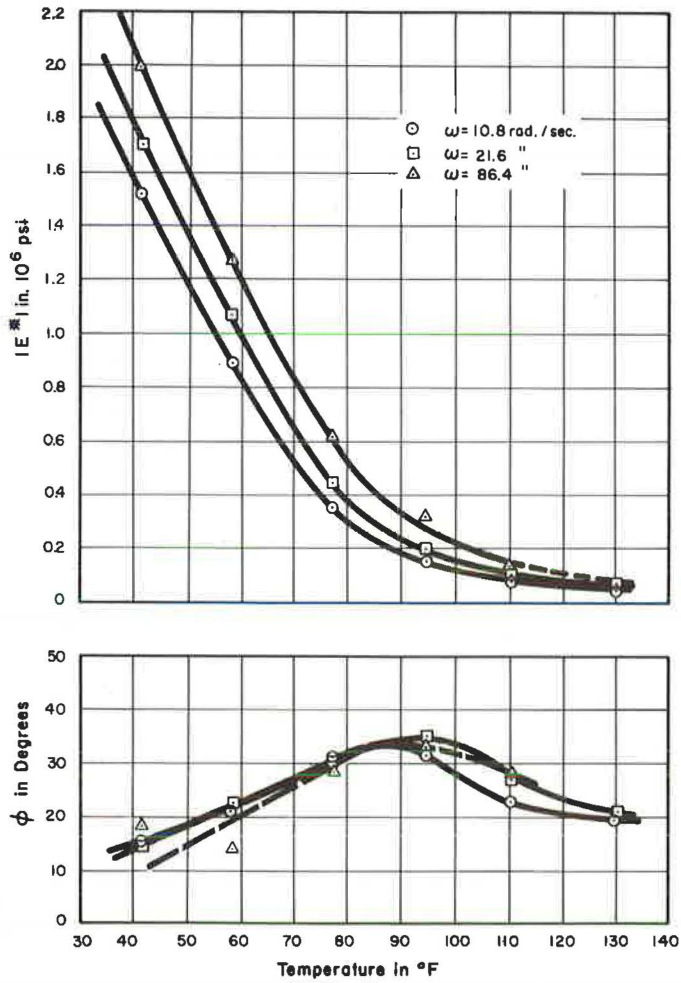

Figure 2. B-35 base results.

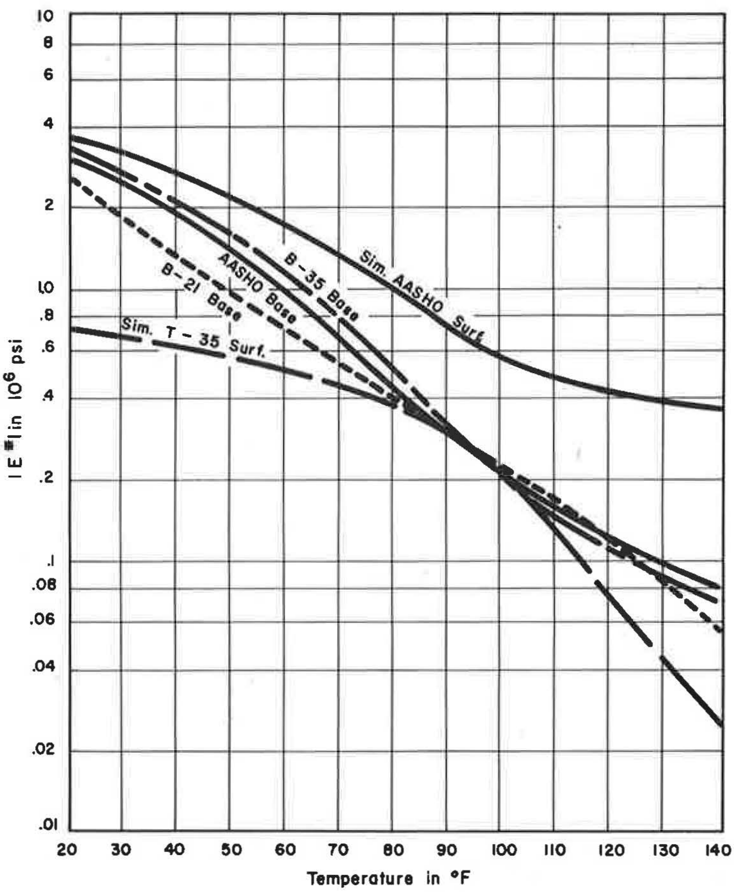

Figure 3. Complex moduli at 77 rad/sec.

than 40 F, except for the AASHO surfacing which was tested at temperatures between 120 and -20 F and the B-35 base which was tested up to 130 F. The data for each of these curves were fitted with polynomials for machine processing, so that each material was represented by two fourth- or fifth-order polynomial equations representing the laboratory test relation between $|E^*|$ and temperature at ω = 77 rad/sec.

Subgrade

The response of the subgrade to changes in saturation represents a similar interpolation for frequency and for the range in saturations involved in this study. This range was based on the results of the 1960 Road Test spring and fall trenching studies; the variation of saturation with calendar time was estimated. For convenience in processing, the data were reduced to an equation expressing the relation between subgrade modulus and AASHO Day for ω = 77 rad/sec:

$$|E^*| = 5.2587058 + 2.062026\,(10)^{-2}D - 1.8678979\,(10)^{-4}D^2 + 1.1368754\,(10)^{-6}D^3 - 4.0310894\,(10)^{-9}D^4 + 5.6703537\,(10)^{-12}D^5$$

where D = AASHO Day - 1370 (between 1370 and 1615), Day 1370 = April 1, Day 1615 = December 2, and $|E^*|$ is in $(10)^3$ psi. The range expressed in this equation is from about 5,300 to 6,400 psi.

Temperature Data

The source of the temperature data used in this study was that reported by Kallas for a 12-in.-thick asphaltic concrete pavement section at College Park, Maryland (8). The data consisted of hourly temperature measurements at the surface and at each 2-in. depth to the bottom of the pavement for a continuous 12-month period from June 1, 1964, to May 31, 1965. That portion of the data that included the calendar days represented by AASHO Days 1370 to 1615 was entered on punched cards for machine processing. Within this time period a relatively small amount of data was missing. The missing times were filled by inserting hourly temperatures from days with similar precedent temperatures. Interestingly, at the junction of the 1964 and 1965 temperatures (hour 2400 on May 31, 1965, and 0100 on June 1, 1964) there was no break in the trend of temperatures with time and no adjustments at this junction were necessary.

CALCULATIONS

For this study, equivalence was defined as that thickness of base that would compensate for the effect on deflection of decreasing the surface layer thickness by 1 in. The pavement section used consisted of 3 in. of asphaltic concrete surfacing and 9 in. of asphaltic concrete base. This structure was underlain by the subgrade represented in the data from the AASHO Road Test and was theoretically subjected to the temperature represented in the Asphalt Institute temperature data. Loading was a 9.5-kip wheel load moving at 50 mph for which the equivalent loaded area was 137 sq in. (R = 6.6 in.) and the equivalent laboratory test frequency was 77 rad/sec. Deflections were calculated using the "n" elastic layer solution developed by the Chevron Asphalt Co. This computer programmed solution was used as three layers with $\mu = 0.35$ and the respective layer moduli, $E_i = |E_i^*|$ for $\omega = 77$ rad/sec.

Equivalence

To calculate the equivalence of layer 1 to layer 2 (surface to base) for a given day and hour, the deflection under the center of the loaded area is calculated for that time. In this calculation E_1 is determined by the average temperature of the upper 3 in. (h_1) of the 12-in. pavement section, E_2 is determined by the average temperature of the lower 9 in. (h_2) and E_3 is determined by the AASHO Day. With this deflection known and E_3 constant, calculations are then made with $h_1' = 2$ in. and with variable base thickness, h_2', to find that thickness at which the deflection is the original value. In these calculations E_1' is determined by the average temperature of the upper 2 in. and E_2' is determined by the average temperature within the thickness under consideration. This procedure can be visualized as a graphical plot of deflection vs h_2' calculated with a surfacing thickness of 2 in. The intersection of the resulting curve with the original deflection (calculated with $h_1 = 3$ in. and $h_2 = 9$ in.) determines the equivalence which, for this pavement section, is the h_2' intercept minus 9. To determine the equivalence at the next succeeding hour this procedure is repeated using the different temperature gradient that normally exists in the asphaltic concrete at the different time. When h_2' is greater than 10 in., the temperature data are linearly extrapolated using the measured temperatures at the 10- and 12-in. depths.

With the data available in this study it was possible to determine the equivalences of two asphaltic concrete surfacings to three asphaltic concrete bases under the hybrid climatic conditions created for each hour of a 245-day period. For one set of materials (one surface and one base) this entails some 5,880 calculations of equivalence. To this end a computer program was developed that would calculate continuous hourly equivalences for the 245-day period.

In programming the calculation of equivalence, an iteration process was used to converge on the value of h_2' at which the deflection was the original value. To start this process a $\Delta h_2'$ of 1 in. is used, i.e., $h_2' = 10$ in. (in calculations for successive hours the first $\Delta h_2'$ tried is the equivalence for the previous hour). The deflection calculated with the first $\Delta h_2'$ is compared with the original value and if the deflections differ

by more than 0.00002 in., a new $\Delta h_2'$ is found using the empirically derived relation

$$\Delta h_2' = h_2' - 9 - \frac{\Delta W}{0.156}$$

where ΔW is the difference in the two calculated deflections. In successive iterations $\Delta h_2'$ is found by linear interpolation using the results of the last two calculations. The iteration process is discontinued at any point when the new $\Delta h_2'$ is less than 0.009 in. This process was relatively efficient and converged on the equivalence in an estimated average of 2½ trials in successive hourly calculations and in 3 trials in calculations for every fourth hour. No significant differences were found between computer solutions and relatively large-scale graphical solutions.

Because of the number of calculations involved in continuous hourly calculations it was desirable to investigate sampling plans that would reduce the total number of calculations without significantly affecting average equivalences while giving fairly

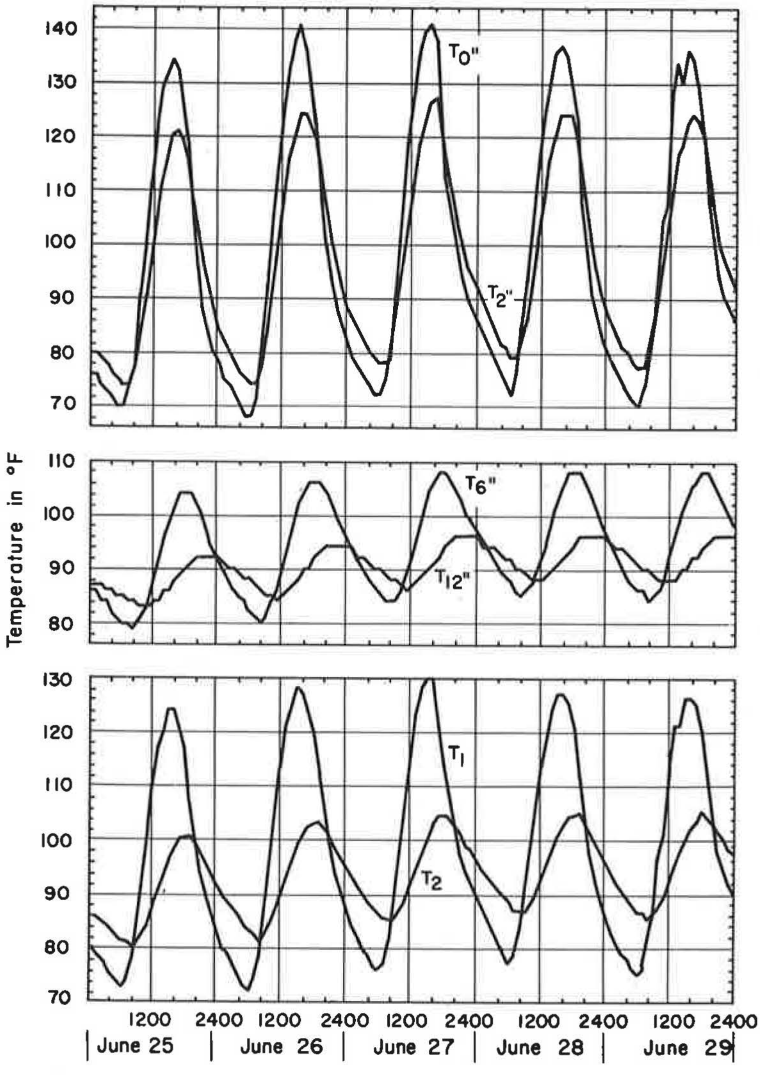

Figure 4. Hourly temperatures in June.

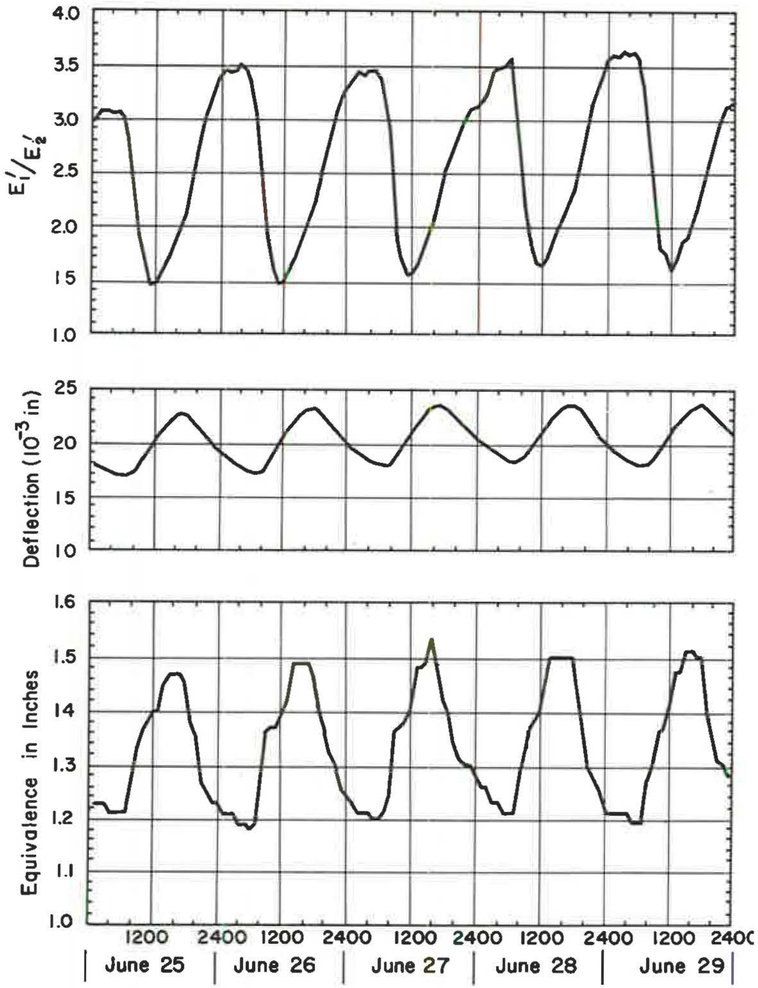

Figure 5. AASHO surface and base in June.

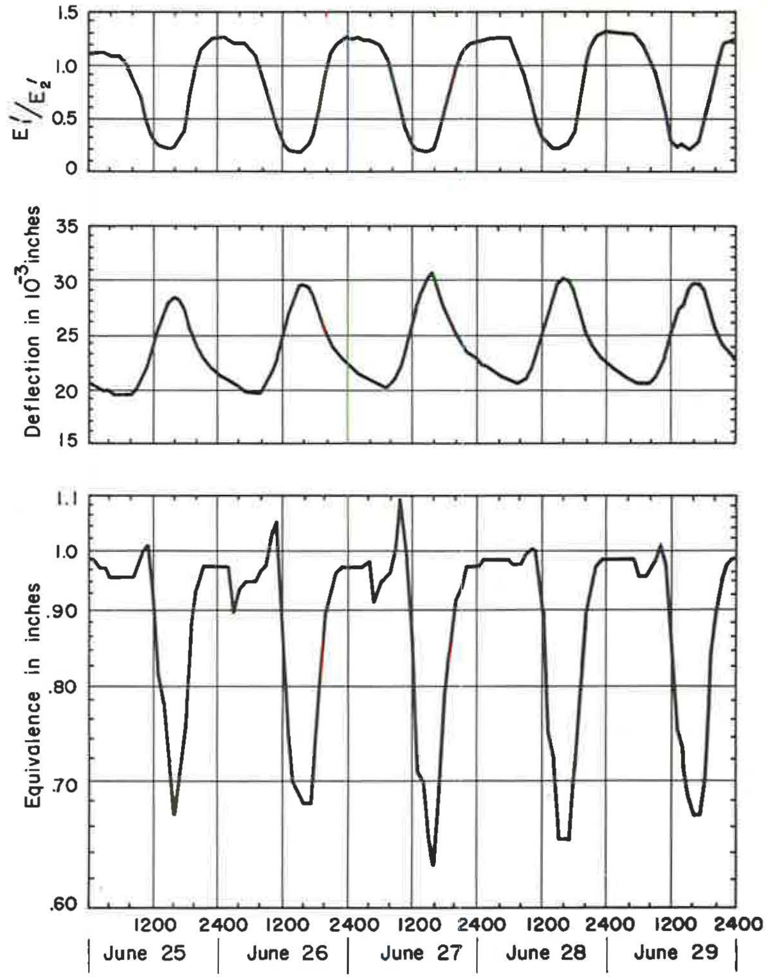

Figure 6. T-35 surface and B-21 base in June.

representative ranges in the resulting data. For this purpose seven 5-day blocks were selected that represented a 14 percent sample of the 245-day data. This selection was based on study (for all of the 5, 880 hours) of the trends with time of E_1, E_2 and E_1/E_2 using the Ohio T-35 surfacing and B-21 base lab test data. These trends were in the form of machine-plotted graphs, some 25 ft in length, in which 24 hours of data were plotted over a length of 1. 2 in.

The sampling plans investigated were based on sampling starting on any hour at frequencies of up to every sixth hour. The results of this study indicated that calculations made every fourth hour, starting on the fourth hour, were best. This plan gave a maximum positive variation in average equivalence in all 5-day blocks of 0. 003 in. and a maximum negative variation of 0. 001 in. Differences of this magnitude have no practical significance. Similar variations in high and low hourly equivalences (at any hour) were a positive 0. 00 in. and a negative 0. 11 in. for all 5-day blocks.

Variations in high and low equivalences with sampling plan reflect the success of the plan in proportionally sampling at the hours of critical temperature conditions relative to the two asphaltic concrete layers. For these data these hours vary in different 5-day blocks and no general statement can be made as to just when these times will occur. For any one 5-day block the critical hours would be expected to vary with the thicknesses of the layers under consideration and the respective moduli response to temperature changes in the two layers. In addition, for temperature data from other

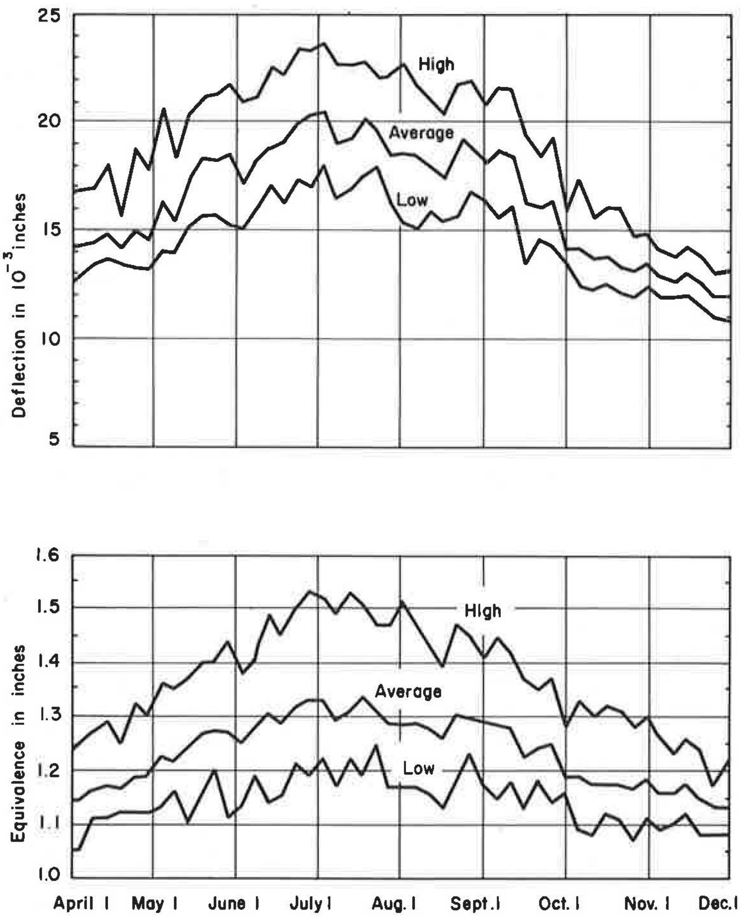

Figure 7. Five-day equivalences, AASHO surface and base.

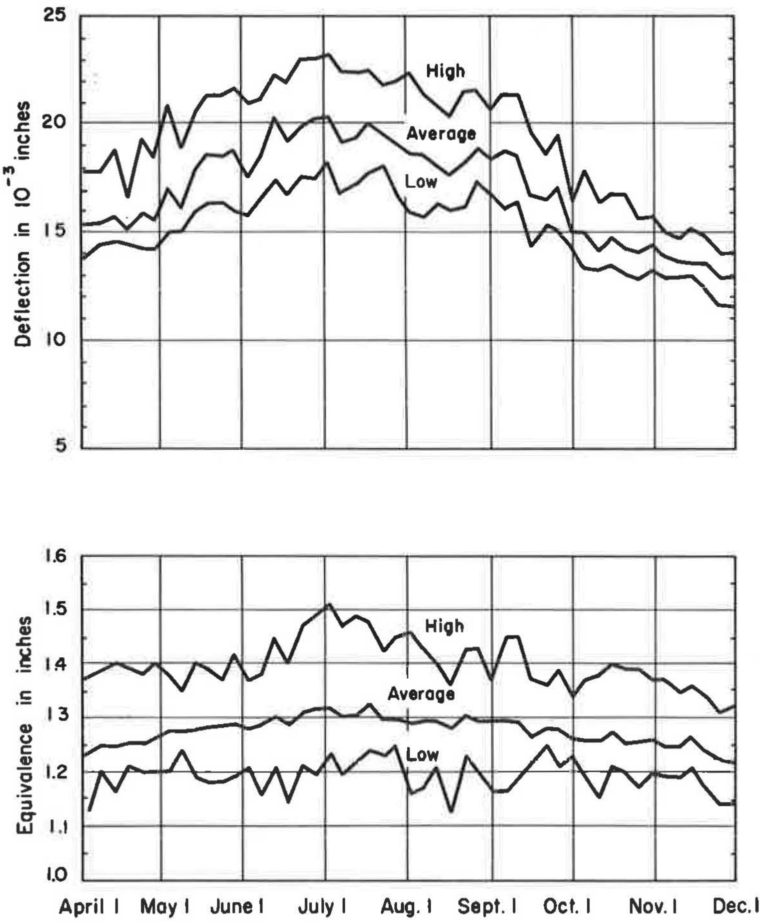

Figure 8. Five-day equivalences, AASHO surface and B-21 base.

sources at similar latitude, these times would be expected to be a function of the longitude in reference to the local time convention followed at the temperature recording sation, i. e., standard or daylight.

Typical Data

Figure 4 shows hourly temperatures at four pavement depths for a 5-day block beginning at 1:00 a. m. on June 25. Also shown in the figure are the corresponding hourly average temperatures for the upper 3 in. of pavement (T_1) and the lower 9 in. (T_2).

For the same time block Figure 5 shows the hourly deflections with the AASHO surfacing and base materials. Also shown are the moduli ratios of layer 1 to layer 2 at the thicknesses giving equivalence. The lower part of the figure gives the calculated hourly equivalences in which the 1 representing the surfacing in the ratio, 1: equivalence, is understood.

Figure 6 shows similar data for the same 5-day block with the T-35 surfacing and B-21 base. Equivalences below 1 in this figure are plotted to inverted scale; this results in a graphical presentation that is comparable to plotting equivalences greater than 1 to an arithmetic scale.

Average Equivalences

Figures 4 through 6 presented data for continuous hourly calculations over one 5-day block. To calculate equivalences for the full 245-day period, similar calculations were made for every fourth hour starting on the fourth hour in April 1; the effect of this sampling procedure on average and extreme equivalence was discussed earlier.

The data from the fourth-hourly calculations were treated in consecutive 5-day blocks. The results of this treatment are given in Figures 7 through 11 for all materials investigated. These figures show the 5-day average equivalences and deflections, plotted at the midpoints of consecutive 5-day blocks, for the different material combinations. For example, the average of all equivalences in Figure 5 is shown as the point, just before July 1, on the "average" curve of Figure 7. Shown in addition are the respective highs and lows within the successive 5-day blocks.

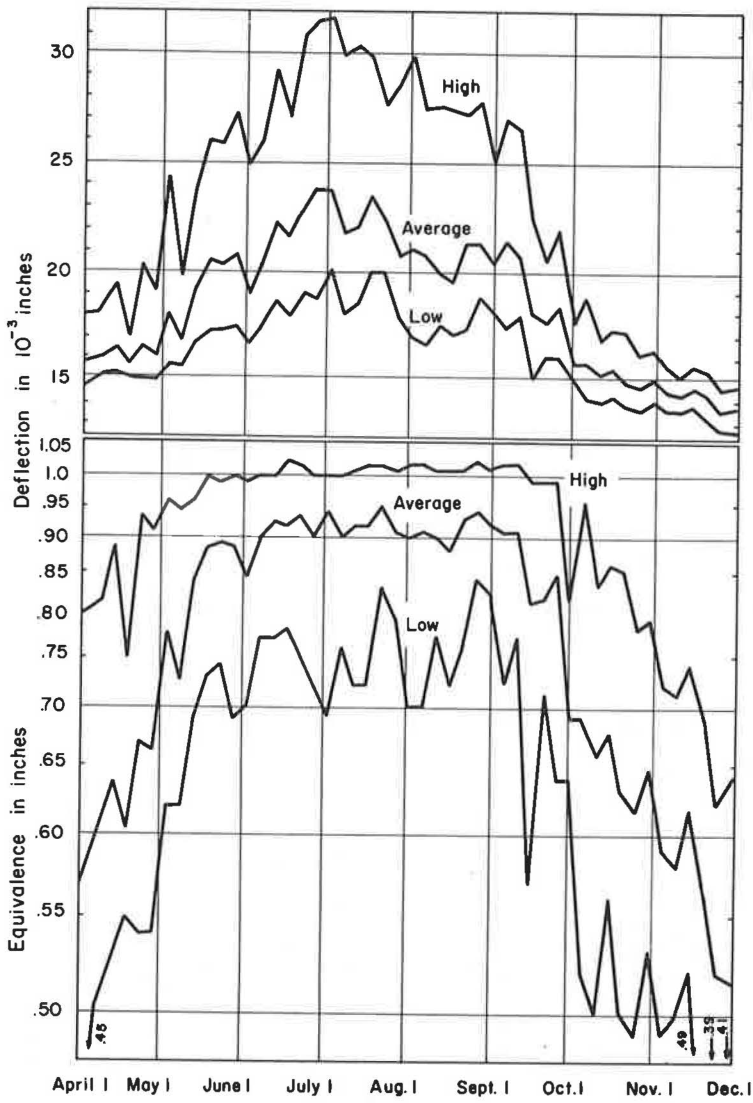

Figure 9. Five-day equivalences, T-35 surface and B-35 base.

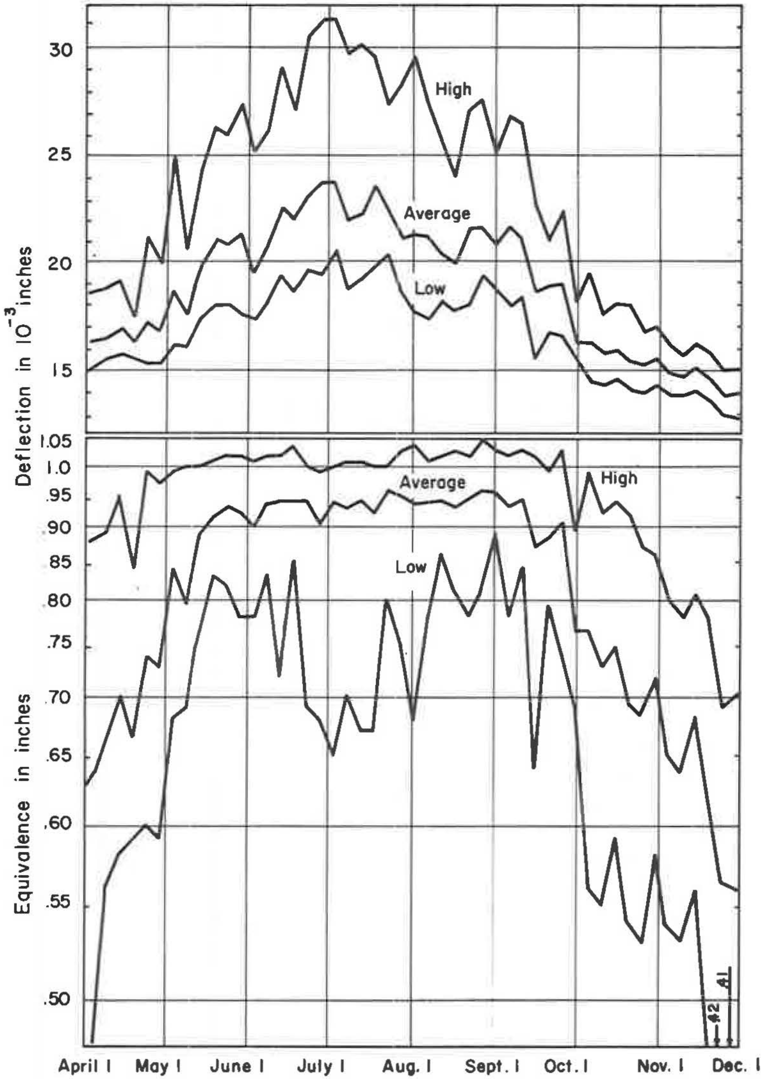

Figure 10. Five-day equivalences, T-35 surface and AASHO base.

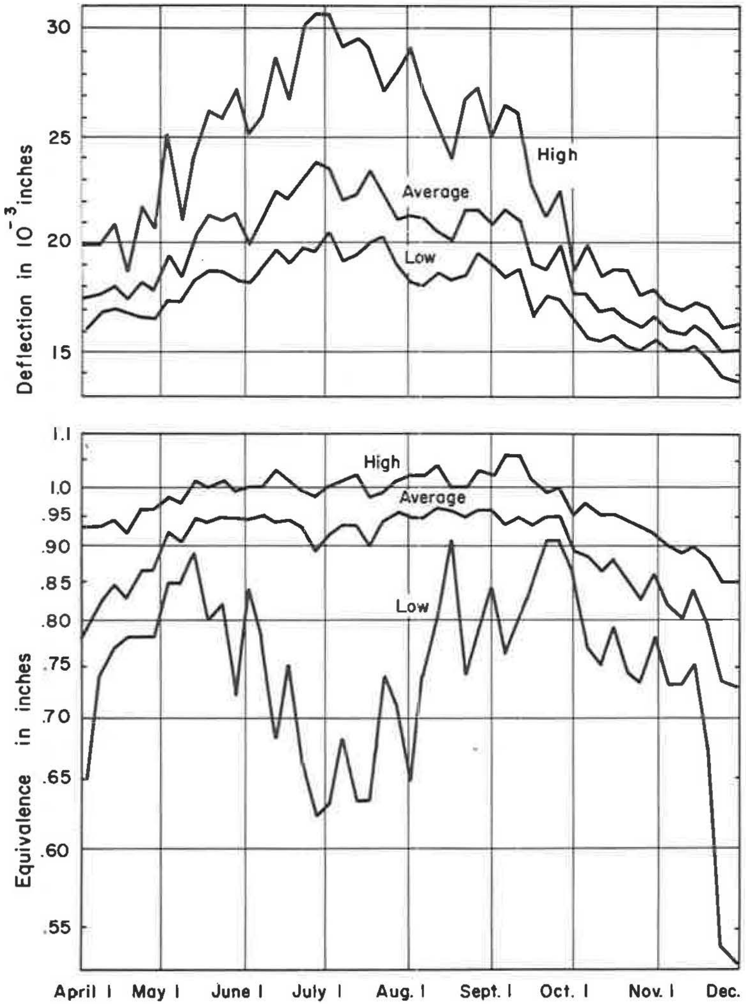

Figure 11. Five-day equivalences, T-35 surface and B-21 base.

TABLE 1

245-DAY DATA

Category	AASHO Surf. / AASHO Base	AASHO Surf. / B-21 Base	T-35 Surf. / B-35 Base	T-35 Surf. / AASHO Base	T-35 Surf. / B-21 Base
			Equivalence (in.)		
Average	1.24	1.28	0.78	0.83	0.90
High (4th hour)	1.53	1.51	1.03	1.05	1.06
Low (4th hour)	1.05	1.12	0.39	0.41	0.53
			Deflection (10^{-3} in.)		
Average	16.5	16.9	18.5	18.9	19.5
High (4th hour)	23.7	23.2	31.7	31.3	30.7
Low (4th hour)	10.9	11.6	12.5	12.7	13.6

The data may be further reduced to the average equivalence for the 245-day period. The results of this reduction are given in Table 1.

Costs

Equivalence calculations were made using the IBM 7094 computer with the hourly temperature data on magnetic tape and with moduli data in the form of equations as discussed. The average cost of fourth-hourly calculations for a 245-day period was about $1700 and required some 290 minutes of machine time when done in 25-day blocks. For the combinations of materials used a ± 10 percent variation was experienced. Had calculations for continuous hourly equivalences been made for all material combinations it is estimated that these would have cost some $5, 800 for the 245-day period on an average basis.

DISCUSSION

In these calculations combinations of two surfacings and three bases of asphaltic concrete were theoretically subjected to the same loading and "environmental" conditions of a 245-day period. Of the six possible combinations of these materials, five were investigated at constant thicknesses. With these combinations it is possible to directly compare the relative effect of the two surfacings with two of the bases. It is also possible to directly compare the relative effect of two of the bases with the two surfacings and of all three bases with respect to one surfacing.

245-Day Data

For pavements of the type studied, the trends of the 5-day average data (Figs. 7-11) indicate that equivalence varies seasonally, like deflection, with hot summertime conditions giving the highest values. For deflection this is different from asphaltic concrete pavements constructed largely of crushed stone; for these pavements springtime conditions normally give the highest deflections. Within these trends the data indicate that the three bases were substantially alike and that the largest differences were in the two surfacings. This is in qualitative agreement with the temperature-moduli curves of Figure 3. It is similarly in agreement with the trends of the 245-day average deflections and equivalences in Table 1. In the latter it is interesting that, with constant surfacing, higher deflections give higher equivalences and that the inverse is true for the inverse case, i. e., with base constant, higher deflections give lower equivalences. From the AASHO Road Test factorial sections (4, p. 137) it was concluded that:

> ...The performance of the flexible pavements was predicted with essentially the same precision from load-deflection data as from load-design information. Deflections taken during the spring when the subsurface conditions were adverse gave a better prediction of pavement life than those taken in the fall.

An extrapolation of that statement to an evaluation across the materials of this study is most attractive; however, it should be recognized that a number of factors must be considered before making such an extrapolation. These will be discussed in some detail in subsequent sections. Within this broad context, however, the data in Table 1 show that base equivalence is a function of the surfacing and suggest that the Road Test surfacing was substantially better than the T-35 surfacing. Within the bases, which were essentially alike, the averages suggest that the B-35 was slightly better than the Road Test base, which would be similarly rated with respect to the B-21 base. If deflections are ignored the apparent difference in average equivalence in the three bases has little meaning in a practical sense. If it is hypothesized that to compare equivalences

for the three bases, with common surfacing, it is necessary to set the three deflections equal, then it is possible to evaluate qualitatively this effect. Each of the three bases was used with the T-35 surfacing and the average deflections and equivalences increase in the same order. To reduce the deflections to that of the lowest, it is necessary to increase the other base thicknesses which, in turn, will increase the comparable equivalences with the net effect of making the differences in average equivalence greater than shown in Table 1. The validity of this hypothesis will be discussed subsequently.

The calculated equivalences of the AASHO Road Test surfacing to base materials can be compared with those estimated on the basis of performance at the Road Test. The Road Test staff did not make a mathematical (statistical) analysis of the performance of the base-experiment sections; however, on the basis of graphical analyses it was noted that for an 18-kip single-axle load at 10^6 applications to p = 2.5 (with 3 in. of surfacing and 4 in. of subbase), that 6 and 13 in. of the bituminous-treated and crushed-stone bases were needed, respectively (4, pp. 46, 58). Using these thicknesses and the Road Test equation for thickness index, $D = .44D_1 + .14D_2 + .11D_3$, this would indicate an equivalence ratio of 1: 1.45 (A. C. surface to A. C. base), or, as expressed in the convention of this study, an equivalence of 1.45. The 6 in. of bituminous base noted above is appreciably higher than that shown in the graphical data of Report 5 (4) and in a subsequent publication by Benkelman, et al (15), and it appears that the thicknesses were adjusted. In the graphical data and for equal performance at lower applications of this load, a range in comparable equivalences of from about 1.16 at 200,000 applications to perhaps 1.31 at 400,000 applications is indicated; at 1,000,000 applications an equivalence of about 1.26 appears more reasonable, based on the same data. At loads greater than 18-kip, similar ranges of 1.23 to 1.46 can be noted at 22.4-kip and of 1.34 to 1.67 at 30-kip. At 12-kip the equivalences are lower ranging from about 0.83 to 0.95. The 245-day average calculated equivalence of this study (1.24) compares favorably with these ranges as it does with the 1.29 advanced, indirectly, by the AASHO Design Committee (16).

It should be noted that the equivalence ranges cited here, both with varying load and within constant loadings, are anomalous with the thickness index equation in which equivalences are constant.

Representative Conditions

It is of some interest to examine the effect of shortening the calculations of this study by the use of a "representative" time or condition. Beginning with the hourly calculations, it is obvious that the time of day makes a significant difference in calculated equivalence and that, while there is at least one time that is representative of the average effect of all hours for that day, there is no obvious rationale that can be followed in its determination. In this connection it should be noted that this "representative" time will seldom correspond with an hourly observation. It follows that this finding can be expanded to include longer time periods without loss in net effect and that the concept of an "average" time, which can be taken as being representative of all times, has little if any real meaning. This is perhaps more easily visualized by examining "average" conditions. If, for example, average temperatures are calculated with depth for the data in Figure 4 (T_1 = 97.8 and T_2 = 93.5 F), and the 5-day average E_3 is determined, the use of these data does not predict the average equivalence for that time block. As a matter of fact those average temperatures never existed simultaneously in the trends of the recorded temperature data.

Biased Traffic

The hourly calculations of this study theoretically simulate a constant stream of trucks at all hours. If the traffic were actually biased as might happen, for example, with loaded mine trucks that operated only in the daylight hours, or with, perhaps, steel mill trucks leaving in the nighttime hours, the equivalences and deflections determined using only those hours would be expected to vary from those in Table 1. Some concept of the effect of time-of-loading variations is apparent in the continuous hourly data of Figures 5 and 6. The effect of similar but seasonal variations (June to November) are

TABLE 2
EFFECT OF LOWER SUBGRADE MODULI

Category	Deflection (in.)		Equivalence (in.)	
	E_3	$E_3/2$	E_3	$E_3/2$
Average	0.024	0.037	0.89	0.90
High	0.031	0.047	1.09	1.10
Low	0.020	0.031	0.63	0.69

far more dramatic but cannot be shown because of space limitations. Comparisons of this type are illustrative of some of the risks that may be involved in comparing the performances of in-service pavements at different locations. In this regard it is interesting that on the AASHO Road Test the daily 5-hour non-traffic period was shifted every two weeks but was always in the local time range of about 5 a.m. to 9 p.m.

Effect of Changed Subgrade

Equivalence could also be expected to vary with changed subgrade moduli. Such changes might result from different climatic conditions or with different subgrade soils. To investigate this effect, on a short time basis, the 5-day time block and conditions of Figure 6 were used (June, T-35 surface with B-21 base) except that the subgrade moduli, E_3, were fixed at one-half of those used in the calculations for that figure (6170 to 6190 psi). The resulting deflections were different as would be expected. The equivalences were closely the same, however, and a graph of the hourly calculations would show essentially no difference from the equivalences plotted in Figure 6 at the scale used. Table 2 gives the average and extreme data from these calculations and the corresponding data from Figure 6. These data indicate that calculated equivalences will not be affected by significant reductions in subgrade moduli even though total deflections are appreciably changed. If, however, subgrade moduli are increased by very large factors, interesting effects can be achieved. For this calculation the conditions at the hour of the low equivalences in Table 2 (hour 1600) were used. At that time $E_1 = 0.043$, $E_2 = 0.199$, $E_3 = 0.006$ or 0.003, all in 10^6 psi, and the equivalences were 0.63 and 0.69 in. for the two subgrade moduli respectively. If equivalence is calculated under the same conditions but with the subgrade modulus increased by a factor of ten ($E_3 = 0.006 \times 10^7$ psi), the equivalence becomes negative (about -0.35 in.) consistent with decreased deflection with decreased surface thickness. On the other hand, if the same conditions are used but with the subgrade modulus decreased by a factor of ten ($E_3 = 0.006 \times 10^5$ psi), the equivalence is 0.76 in., which is comparable with the 0.63 in. of Table 2.

Effect of Vehicle Speed

Equivalence would also be expected to vary with vehicle speed. The previous calculations represented a truck moving at 50 mph. The data in Figure 12 represent calculations for the same truck moving at 5 mph (a lab test frequency of 7.7 rad/sec). These hourly data are for the T-35 surfacing and B-21 base for a 5-day block in June and are directly comparable with the data in Figure 6 for the same time and materials. The 5-day average equivalence with the truck moving at 50 mph (Fig. 6) was 0.89 in. and at 5 mph (Fig. 12) was 1.03 in. Average deflections were 0.024 and 0.032 in., respectively. The larger deflections for the slower moving vehicle reflect the lower moduli that exist in all layers at the lower test frequencies. The lower vehicle speed resulted in a 20 percent decrease in E_3 while E_1 and E_2 were decreased by roughly 20 and 40 percent, respectively. It is interesting that the range of fluctuations in hourly equivalence is higher for the higher speed. Neither these nor the changes in average equivalence can be explained by changes in E_3 (a decrease of 20 percent vs the 50 percent of the "changed subgrade" calculations). The difference in average equivalences is, however, consistent with the nonproportional relative moduli shifts of the two upper layers (20 and 40 percent), i.e., the base layer was proportionally "weaker" and more thickness would be required. For in-service pavements this indicates that vehicle speed can affect equivalences and that the effect may be quite significant.

Effect of Thinner Base

Equivalence would also be expected to vary with changed base-layer thickness. The June 5-day time block of Figure 4 was used to investigate this effect on a short time

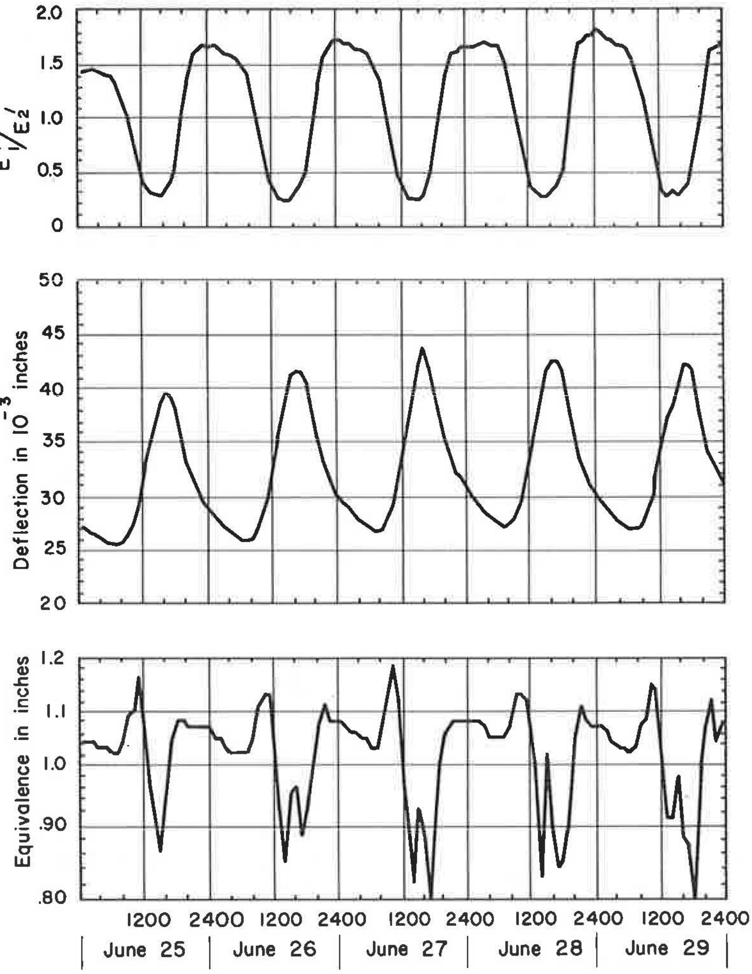

Figure 12. T-35 surface and B-21 base in June (5 mph).

basis. Materials were the AASHO surface and B-21 base, vehicle speed was 50 mph, layer 1 was 3 in. thick and the base layer thickness was fixed at 3 in. instead of 9 in. as used in all previous calculations. Figure 13 shows the average hourly temperatures of the 3-in. base layer and, for comparison, the same temperatures when the base was 9 in. thick. In both cases the surfacing was 3 in. thick. Also shown in Figure 13 are the resulting calculated hourly deflections, equivalences and moduli ratios at equivalence. Table 3 is a comparison of the average and extreme effects of the changed base thickness; in the table the 3-in. base thickness data are from Figure 13 and the 9-in. base data are from Figure 8.

TABLE 3
EFFECT OF THINNER BASE

Category	Deflection (in.)		Equivalence (in.)	
	3 in. Base	9 in. Base	3 in. Base	9 in. Base
Average	0.037	0.020	1.16	1.32
High	0.043	0.023	1.31	1.49
Low	0.031	0.017	1.06	1.19

For this time period, decreasing the base thickness by two-thirds roughly doubled the deflections while the effect on average equivalence was relatively slight. Two changes were effected in reducing the base thickness—the geometry change and the effect of this change on average temperatures and corresponding base moduli. If it were possible to effect only a thickness change with no change in base temperature and moduli (more con-

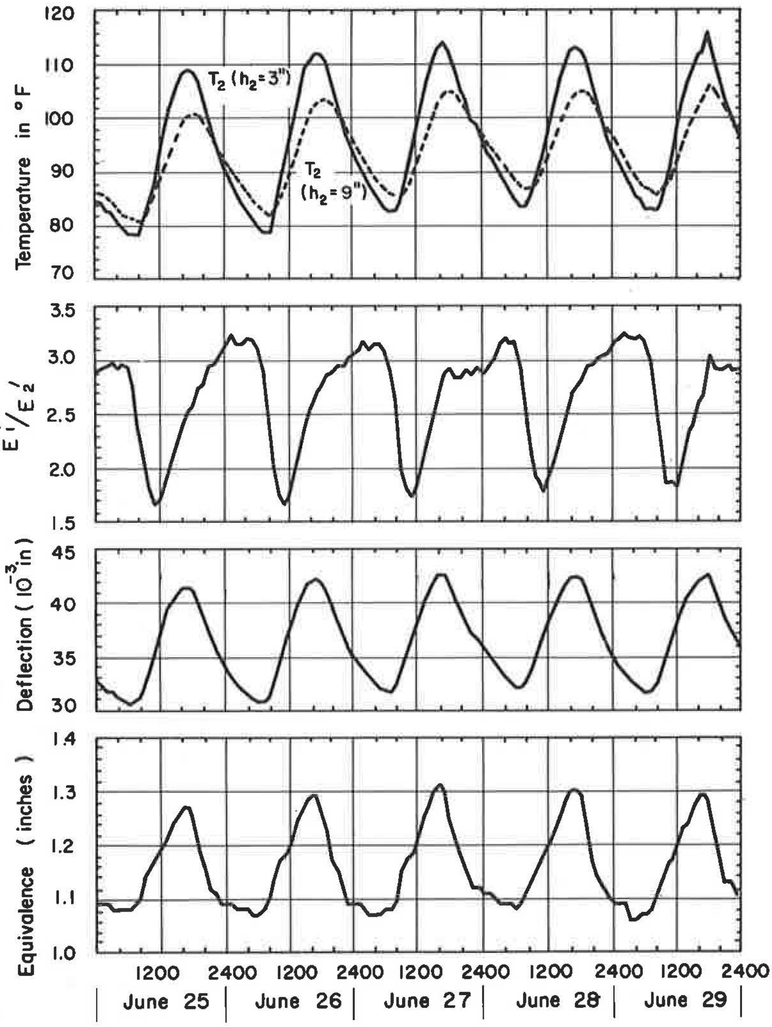

Figure 13. AASHO surface and B-21 base in June (h_2 = 3 in.).

sistent with a crushed-stone base), the effect of a thinner base layer would be a lower equivalence; i.e., the thicker the base layer the less efficient it is in replacing the surfacing as determined by deflection. Decreasing the base thickness in the data, however, changed the average base temperature and, on the average, this change resulted in a higher temperature in the thinner base as is shown by the hourly temperatures in Figure 13. This higher temperature in the thinner base results in lower moduli in the base which, all other things being equal, will require more base in the replacement of surfacing; i.e., a higher temperature causes a lower modulus which will result in a higher equivalence. For this 5-day block the effects of the geometry and temperature changes on average equivalence were in opposition with the thinner base tending to decrease equivalence and the changed temperatures tending to increase equivalence. The geometry effect was dominant and the net effect was a slightly lower equivalence than with the 9-in. base. While not investigated, the relative effect of a thinner base for other 5-day blocks would be expected to be different as a function of the relative temperature changes; however, this effect would be expected to be small.

To illustrate the geometry effect, equivalence was calculated for one point in time at which moduli were held constant while base thickness was changed from 7.9 to 11.1,

TABLE 4
EFFECT OF CHANGING LOAD AND RADIUS

Category	Deflection (in.)		Equivalence (in.)	
	L	L/2	L	L/2
Average	0.020	0.011	1.32	1.48
High	0.023	0.012	1.49	1.64
Low	0.017	0.009	1.19	1.34

then to 14.4 in. For this calculation: R = 7.04 in., p = 72 psi, h_1 = 3 in., $E_1 = .67(10)^6$, $E_2 = .31(10)^6$ and $E_3 = 4.08(10)^3$ psi and the resulting deflections were 0.033, 0.025 and 0.020 in. At these three thicknesses the equivalences were 1.22 in. at h_2 = 7.9 in.; 1.32 in. at h_2 = 11.1 in.; and 1.39 in. at h_2 = 14.4 in. These data indicate that with all other conditions constant, calculated equivalence increases at decreasing rate as base thickness increases.

Effect of Reduced Load and Contact Area

The effect of thickness changes with unchanged temperature can be secured by reducing the radius of the equivalent loaded area while holding contact pressure constant. To investigate this effect for a short time period, the June 5-day time block of Figure 4

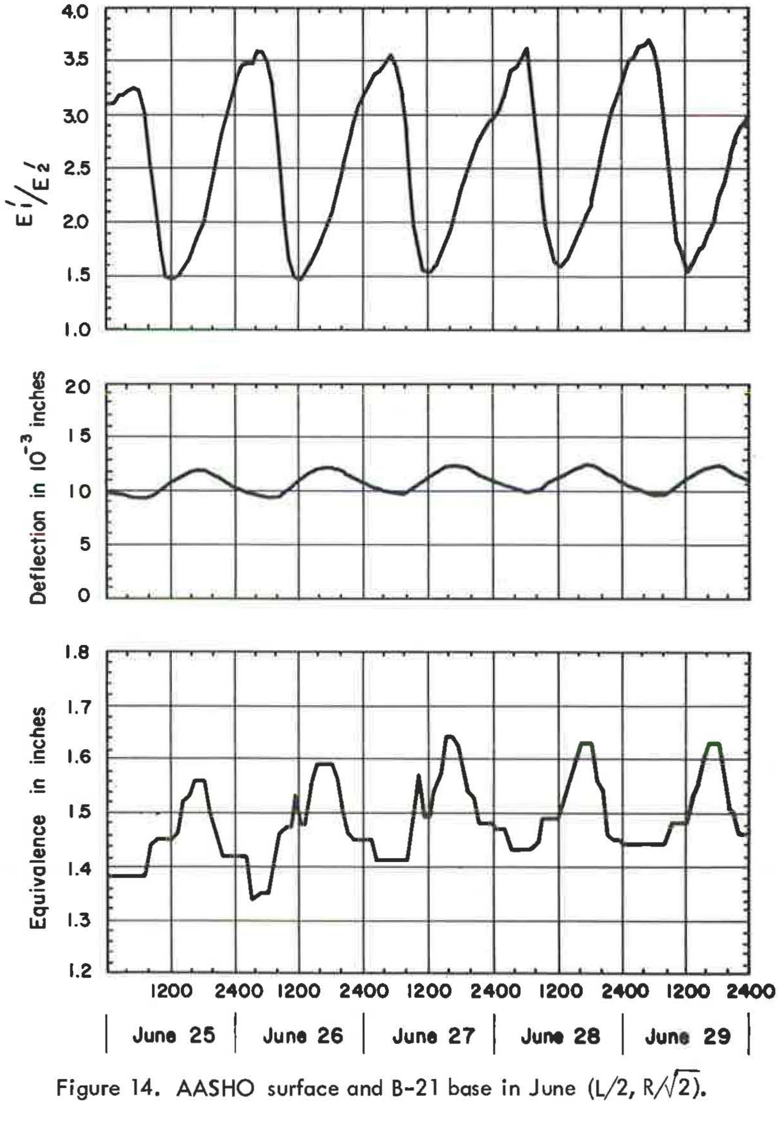

Figure 14. AASHO surface and B-21 base in June (L/2, R/$\sqrt{2}$).

TABLE 5
CHANGES AFFECTING DEFLECTION AND EQUIVALENCE

Change In:	Gives Change In:			
	Deflection (from changed)		Equivalence (from changed)	
Hour of determination	yes	(moduli)	yes	(moduli ratio)
No. of hrs. used for avg.	yes	(moduli)	yes	(moduli ratio)
Vehicle speed	yes	(moduli)	yes	(moduli ratio)
Load (constant cont. press.)	yes	(load and geom.)	yes	(geom.)
Load (constant cont. area)	yes	(load)	no	-
Surface material	yes	(modulus)	yes	(moduli ratio)
Base material	yes	(modulus)	yes	(moduli ratio)
Subgrade material	yes	(modulus)	no[a]	-
Surface material thickness	yes	(moduli and geom.)	yes	(mod. ratio and geom.)
Base material thickness	yes	(moduli and geom.)	yes	(mod. ratio and geom.)

[a]Not significant, in avg. equiv., for relatively large changes in moduli; can be significant in hourly equiv.

was used with 3- and 9-in. thicknesses of the AASHO surfacing and B-21 base, respectively. Vehicle speed was 50 mph and the only change from the conditions of Figure 8 was the reduction of total load by one-half and the effect of this reduction on radius at constant contact pressure ($1/\sqrt{2}$). The results of hourly calculations for these conditions are shown in Figure 14. The average and extreme equivalences and deflections are given in Table 4 together with the same results from the full-load case. The effect on deflection of decreasing the load by one-half was a decrease of about the same order as would be expected at constant pressure. Similarly, the effect on equivalence was an increase; this is consistent with the concept that the relative geometry change attained was qualitatively equivalent to proportional increases in the thicknesses of the layers with constant load, contact pressure and moduli. Had only the load been changed—i. e., a change in pressure with no change in contact area—no effect on equivalence would be expected even though deflections would show a change proportional to the change in load. Points such as these have interesting implications in considering material equivalences and pavement failure.

Equivalence and Failure

It was noted near the beginning of this discussion that for single-axle loadings at constant serviceability level, equivalences from the AASHO Road Test factorial sections were reduced to constants while those from the special base sections appear to vary with applications. To gain some insight into possible explanations of this apparent anomaly, Table 5 has been prepared to show those changes that affect equivalence and deflection in the theoretical work of this study. This table shows that any one of the listed changes will affect deflection and that the same is true for equivalence with the exceptions of load changes made without changing contact area and of, perhaps, changes in subgrade moduli. Considering the conditions at the Road Test and excluding the first three listed changes for purposes of discussion, it is of some interest to examine the loads, pressures and contact areas for the vehicles at the Road Test. These data, for the single-axle loadings, are shown in Table 6 (17). Contact pressures for the tandem axle loadings were very similar.

The data in Table 6 indicate that, at the Road Test, changes in load were accompanied by changes in equivalent radius and that, excluding Loop 2 (not in the special base experiments), these load changes were not accompanied by appreciable changes in calculated average contact pressure. Table 5 shows that these changes (load and radius at constant contact pressure) would be expected to affect deflection but that only the changed radii would be expected to change equivalence with constant materials at constant thicknesses. As noted, this effect would be expected to be relatively small. It should be reiterated, however, that for either of these conditions there would be a change in deflection. If deflection is a predictor of performance, the changed deflection would result in changed applications to failure for the two different loads. For a constant pavement design, an increase in load with no change in contact pressure would increase deflection, decrease the applications to failure and decrease the theoretical equivalence as a result of the geometry change.

TABLE 6
ROAD TEST TIRE DATA

Loop	Test Tire Load (lb)	Stnd. Load (lb)	Inflation[a] (psi)	Meas. Contact Area (sq. in.)[a]	Avg. Contact Press. (psi)[a]
2	1,000	1,065	24	36.6	29.1
2	1,500	1,580	45	37.4	42.3
3	3,000	2,980	75	45.4	65.7
4	4,500	4,580	75	67.8	67.5
5	5,600	5,150	75	77.7	66.4
6	7,500	6,780	80	97.3	69.7

[a]At standard load.

TABLE 7

ROAD TEST EQUIVALENCE DATA[a]

Category	Loop 2	3	4	5	6
Within loop regression coefficients					
D_1	.83	.44	.44	.47	.33
D_2	.25	.16	.14	.14	.11
D_3	.09	.11	.11	.11	.11
Within loop equivalences					
D_1	1	1	1	1	1
D_2	3.32	2.75	3.14	3.36	3
D_3	9.23	4.00	4.00	4.27	3
No. of test sections used	12	26	40	60	60
Avg. design h (in.)					
Surf.	2.5	3	4	4	5
Base	4.5	4.5	4.5	6	6
S. Base	4	6	8	8	12

[a]From Tables 2 and 10 of Reference 4.

For the same conditions, an increase in load with no change in contact area would have the same effects except that no change in equivalence would be expected. Obversely, at constant load, contact area and failure level, increased applications to failure will accompany increased base thicknesses and equivalences would be expected to increase as a result of the geometry change. If applications to some failure level are constant, it would be expected that increased loads at constant contact pressure, tending to give lower equivalence, would require increased base thickness, tending to give higher equivalence. Since these trends are in opposition the net effect of both geometry changes on equivalence could be rather small. No similarly general statements are possible for the changed load, area, and contact pressure conditions because both deflections and equivalences would be a function of the initial geometries (radius, h_1 and h_2) as well as of the moduli ratios, for constant materials.

The preceding relations were based on the assumption of constant materials with varying base thicknesses or applications. If only surfacing thickness is varied with applications, the given effects of the relative geometry changes on equivalence are reversed when E_1 is greater than E_2. With this addition it is possible to examine the Road Test main factorial equivalence data for some insight into the expected effect of the theoretical relations discussed.

The Road Test data for the main factorial sections are summarized in Table 7. If the regression coefficients for each loop in these data are multiplied by the number of sections used and these are summed and divided by the total number of sections, the results are the coefficients of D_1, D_2, and D_3 in the thickness index equation. On the basis of the data combined in Tables 6 and 7 it is apparent that the load changes at constant pressure across Loops 3-6 were accompanied by average layer thickness changes. The previous discussion suggests that the gross effect of these changes (radius and thickness) on equivalence would be in opposition on a qualitative basis and that roughly comparable equivalence ratios might be expected as is indicated in the data for these four loops. For Loop 2 the load and thickness changes were in the same qualitative direction but the contact areas were not changed as they were in the other loops. This could help to explain the difference in regression coefficients for this loop and the unusually high equivalence for the subbase material. These statements assume that the effect of changes in the Lane 2 tandem axle loadings across the loops were proportional, which appears reasonable in the absence of more data.

Within any one loop at the Road Test there were a large number of thickness changes; however, there are no readily available data with which to evaluate qualitatively, in a similar manner, the relation between the field data and the effects that would be theoretically expected. If it is assumed that in the analyses of the Road Test data the geometry effects were considered as a part of the spread or scatter in the data, then the measure of this scatter is an indication of the possible (but not at all probable) limits of these effects. Saying this another way, in developing the thickness index equation, it is not clear how the Road Test analyses may have considered geometry effects such as those discussed—whether these may have been included as a part of the load or of similar across-lane and loop parameters, or if such effects are perhaps implicit in the statistics. In any event, the scatter in individual data points was evaluated as a part of that analysis. This was given as ± 14 percent of D and includes effects from all causes, among which could be those resulting from geometry changes. If it could be assumed that all of this scatter was a result of the geometry effects, and this is taken in the base or D_2 coefficient, then for an 18-kip single-axle loading with $p = 2.5$ at 10^6 applications and D_1 and $D_3 = 3$ and 6 in. respectively, the coefficient of D_2 could vary from 0.10 to 0.18 about a ± 29 percent range. Similarly, except that $D_3 = 16$ in., the D_2 coefficient could vary from 0.05 t0 0.23, about a ± 64 percent range. For the Road

Test, geometry effects would be theoretically expected with changes in load, or surface thickness or in base and/or subbase thicknesses. On the basis of these calculations it is clear that the inclusive "scatter term" of the thickness index equation provides space for rather large individual effects among which may be the geometry effects that would be expected on a theoretical basis.

If materials are varied, the number of applications to some failure level will vary as is shown in the special base studies of the Road Test. In the Road Test analyses the concept that deflections predict performance was based on the main factorial sections, in which materials were constant, and was most nearly true for springtime conditions. Presumably this concept would hold for other materials so long as the materials are constant; however, it is not clear that this concept can be extrapolated across materials, i. e., equal deflections with different materials should not be expected to give equal performance, a priori. In this connection the Road Test findings noted that deflections in sections with gravel were somewhat lower than those with crushed-stone base even though the performance of the crushed stone was considerably better than that of the gravel base sections (4, p. 85). This is a subtle point: Had equal structural thicknesses given equal deflections under equal loadings, theoretical deflection-based equivalences would also have been equal, in the absence of failure criteria. Lower deflections for the gravel would indicate lower equivalence, on the same basis, and it would follow that equal thicknesses and loadings would give higher applications to failure for the gravel. This was not the case, however, and on this basis it seems clear that failure criteria are necessary to a theoretical evaluation of the equivalences of different materials. Summarizing this discussion of equivalence and failure, equivalence—as defined in this discussion—is a function of load and contact area, of the layer thicknesses, of the materials and environment, and of the number of applications to failure.

SUMMARY AND CONCLUSIONS

The 245-day theoretical data for the Road Test asphaltic concrete surfacing and base materials, the only such materials for which field performance data were available, gave a remarkably close estimate of the field results. Points of similarity in the theoretical simulation include the use of essentially the same materials, the use of only one load, close to the average, at comparable contact pressure and the use of common vehicle speeds insofar as the effect of the 35- to 50-mph vehicle speed shift affects moduli ratios. The main points of dissimilarity are the temperature regime used and, as a part of that, the representativeness of the length of time over which theoretical average equivalence was calculated. In regard to the first difference, there are no data with which to base an estimate of the differences between temperatures in the 12-in. asphaltic concrete pavements at Ottawa, Ill., in 1958-60 and those measured at College Park, Md., in 1964-65. It can be rationalized, however, that over the length of time used, the cumulative differences were probably not significant. A similar rationalization can be advanced for the representativeness of the length of time used in the calculations. The trend of five-day averages of Figure 7 indicates that a 365-day average equivalence would be lower. Had calculations been made for this longer time span it can be speculated that the total average equivalence would not have dropped below one and would most likely be higher. This would not represent a large change in consideration of the apparent spread in the field data cited for the special base studies.

For the remaining materials of this study the calculations show that the equivalence of a base is a function of the surfacing, and vice versa. Unfortunately there are no comparable sources of field performance data for these materials. Because of this it was necessary to seek other data relating deflection and performance for different materials. The AASHO Road Test data demonstrate that deflection-based equivalences have no causal relation to the number of applications to some failure level with different materials. This suggests that it is entirely possible to simulate theoretically two pavement designs of different materials that will give the same average calculated equivalence for the same loading and time history. For this, however, it would be expected that the number of applications to failure of the two would be different. On the other hand, the term equivalence implicitly assumes equal performance or applications to

failure and this, in turn, indicates that the theoretical determination of equivalences for different materials requires the inclusion of failure criteria. On this basis equivalence can be defined in the terms of this study by the following generalized equation:

$$\text{Equiv.} = f(L, V, T, A, H, E, C, N)$$

where

L = the loadings,
V = their velocities,
T = the times of their applications,
A = the contact areas,
H = the layer thicknesses,
E = the materials,
C = the climate or environment, and
N = the number of applications to failure.

This is an interesting equation. With the inclusion of the failure term to the concept of average equivalence, as anticipated in this study, it is clear that exactly those considerations that would be expected in a rational design formula are collected in the equation. With the exception of N, it is also clear that the tools and techniques necessary to such an approach are available and indeed have been used in this study, to some approximation. This points to the pressing need for research that will fill the blanks represented in the failure term. When these blanks are completely filled the need for equivalences will presumably have vanished.

ACKNOWLEDGMENT

This study was sponsored by the Ohio Department of Highways in cooperation with the U. S. Bureau of Public Roads and grateful acknowledgment is made of the continued interest and cooperation of representatives of those orgnizations. Particular recognition is due Willis B. Gibboney, Flexible Pavement Engineer of the Department, whose many thoughtful suggestions and enthusiastic cooperation made this study possible. Similar recognition is due Carroll J. Notestine, Programmer, OSU Computational Center, for the development and optimization of the computational procedures used, and to Miss Joanne Roth for her patient assistance in typing the formidable tables.

REFERENCES

1. Shook, J. F. Development of Asphalt Institute Thickness Design Relationships. Proc. AAPT, Vol. 33, 1964, pp. 187-220.
2. Skok, E. L., Jr., and Finn, F. L. Theoretical Concepts Applied to Asphalt Concrete Pavement Design. Internat. Conf. on the Structural Design of Asphalt Pavements, Univ. of Mich., Preprint Vol., 1962, pp. 575-604.
3. Burmister, D. M. Applications of Layered System Concepts and Principles to Interpretations and Evaluations of Asphalt Pavement Performances and to Design and Construction. Internat. Conf. on the Structural Design of Asphalt Pavements, Univ. of Mich., Preprint Vol., 1962, pp. 218-233.
4. The AASHO Road Test: Report 51—Pavement Research. HRB Spec. Rept. 61-E, 1962.
5. Coffman, B. S., Kraft, D. C., and Tamayo, J. A Comparison of Calculated and Measured Deflections for the AASHO Test Road. Proc. AAPT, Vol. 33, 1964, pp. 54-92.
6. Coffman, B. S. Pavement Deflections from Laboratory Tests and Layer Theory. Second Internat. Conf. on the Structural Design of Asphalt Pavements, Preprint Vol., Jan. 1967, pp. 664-708.
7. Coffman, B. S. A Method for Determining the Equivalences of Asphalt Concretes in Pavements. Unpublished report to the Asphalt Institute, Nov. 1965.
8. Kallas, B. F. Asphalt Pavement Temperatures. Highway Research Record 150, pp. 1-11, 1966.

9. Data System 4180. Trench Study, Main Loops, Flexible Pavement, Spring-Summer 1960. AASHO Road Test, Highway Research Board.
10. Burmister, D. M. The General Theory of Stresses and Displacements in Layered Systems. Jour. Applied Physics, Vol. 16, 1945.
11. Filon, L. N. G. On the Elastic Equilibrium of Circular Cylinders Under Certain Practical Systems of Load. Phil. Trans. Royal Soc. of London, Vol. 198, Ser. A May 1902.
12. Rowe, P. W., and Barden, L. Importance of Free Ends in Triaxial Testing. Proc. ASCE, Jour. S.M. & F. Div., Vol. 90, No. SM1, Jan. 1964.
13. Barden, L., and McDermott, J. W. Use of Free Ends in Triaxial Testing of Clays. Proc. ASCE, Jour. S.M & F. Div., Vol. 91, No. SM6, Nov. 1965.
14. Blight, G. E. Shear Stress and Pore Pressure in Triaxial Testing. Proc. ASCE, Jour. S.M. & F. Div., Vol. 91, No. SM6, Nov. 1965.
15. Benkelman, A. C., Kingham, R. I., and Schmitt, H. M. Performance of Treated and Untreated Aggregate Bases. Internat. Conf. on the Structural Design of Asphalt Pavements, Univ. of Mich., Preprint Vol., 1962, p. 129.
16. Langsner, G., Huff, T. S., and Liddle, W. J. Use of Road Test Findings by AASHO Design Committee. HRB Spec. Rept. 73, p. 411 (Appendix D), 1962.
17. The AASHO Road Test: Report 31—Traffic Operations and Pavement Maintenance. HRB Spec. Rept. 61C, Table 5, p. 16, 1962.

Michigan Investigation of Soil-Aggregate Cushions and Reinforced Asphaltic Concrete for Preventing or Reducing Reflection Cracking of Resurfaced Pavements

F. COPPLE, Supervisor of Pavement Evaluation and Field Tests, and
L. T. OEHLER, Director, Research Laboratory Division, Michigan Department of State Highways

In an effort to reduce reflection cracking of bituminous resurfacing over rigid pavement, the Michigan Department of State Highways has investigated the use of both soil-aggregate cushions and continuous reinforcement in the bituminous-concrete resurfacing layer. Because of high traffic volumes, it is often important that any interruption of vehicle flow during resurfacing operations be for short durations.

During the past five years, Michigan has observed the performance of an old, distressed highway, resurfaced with soil-aggregate cushions of various materials as an insulator between the old portland cement concrete and the new bituminous-concrete mat. For comparison, some lengths of the project were resurfaced in the conventional manner, with the bituminous mat constructed directly on the old rigid pavement. Additional resurfacing projects incorporating soil-aggregate cushions have been constructed throughout the State during the past five years. No great construction problems were encountered and soil-aggregate cushions carried traffic well in the interim before bituminous-concrete mats were placed. Soil-aggregate cushions have proved effective in reducing reflection cracking, but additional research is suggested to determine the best cushion materials.

In 1955, the Department resurfaced a rigid pavement by placing wire-mesh fabric on the old surface and then applied the bituminous-concrete resurfacing. Control areas were also constructed, using bituminous-concrete resurfacing without reinforcement. After about six-years service, it was concluded that this method of reinforcement was unsatisfactory because (a) reflection cracking was not significantly reduced, (b) potholes occurred in reinforced areas but not in conventional areas, and (c) extensive corrosion of reinforcing steel occurred even in apparently sound areas of the pavement.

•AS THE mileage of bituminous resurfacing of rigid pavement has increased, reflection cracking has become an increasingly important problem in highway maintenance. The riding quality of the road is directly affected by the cracks, and foreign matter easily penetrates crack openings causing further damage to the pavement. Reflection cracks are apparently caused by horizontal and vertical movement of the resurfaced rigid pavement. The rigid slabs deflect and rock under heavy traffic and are subject to thermal expansion and contraction. Two methods investigated in Michigan for preventing or reducing reflection cracks are (a) the use of a soil-aggregate cushion between

Paper sponsored by Committee on Composite Pavement Design and presented at the 47th Annual Meeting.

the old pavement and the new surface, and (b) the use of continuous reinforcement in the bituminous-concrete resurfacing layer. Michigan experience with these two methods is described in this report.

SOIL-AGGREGATE CUSHION

Soil-aggregate cushions placed between rigid pavement and the bituminous surface had been tried in several states, with varying degrees of success, on the assumption that the cushion would absorb most slab movement without transmitting detrimental effects to the resurfacing.

In August 1962, with the approval of the Bureau of Public Roads, the Research Laboratory Section established a research project with the following specific objectives:

1. To determine whether a soil-aggregate cushion would significantly reduce or eliminate reflection cracking when bituminous concrete is used to resurface rigid pavements.
2. To determine whether a soil-aggregate cushion would provide sufficient thermal insulation to prevent blow-ups in the original rigid pavement.
3. To investigate the relative effectiveness of various aggregates as cushion material.
4. To determine whether a soil-aggregate cushion may be stabilized economically by admixture or mechanical means, in order to carry traffic loads prior to the construction of the bituminous-concrete surface. This is a very important consideration in areas where traffic cannot conveniently be detoured during the construction period.

Description of the Test Area

A 3-mile section of rigid pavement on M 60, northeast of Leonidas in St. Joseph County, apparently constructed over an old gravel road which lay directly on soil classed pedologically as the B-horizon or zone of accumulation, was selected for the investigation. In areas of considerable frost heave, the old base material had been replaced with granular soil and surfaced with new concrete over the rebuilt areas. The pavement was in generally poor condition, showing a mean average of about 10 transverse cracks per 100-ft slab length, and had a history of blow-ups (Fig. 1). The old pavement was condition-surveyed and roughness measurements were taken using the Michigan Roughometer.

Figure 1. Original rigid pavement. Note transverse patch replacing blow-up.

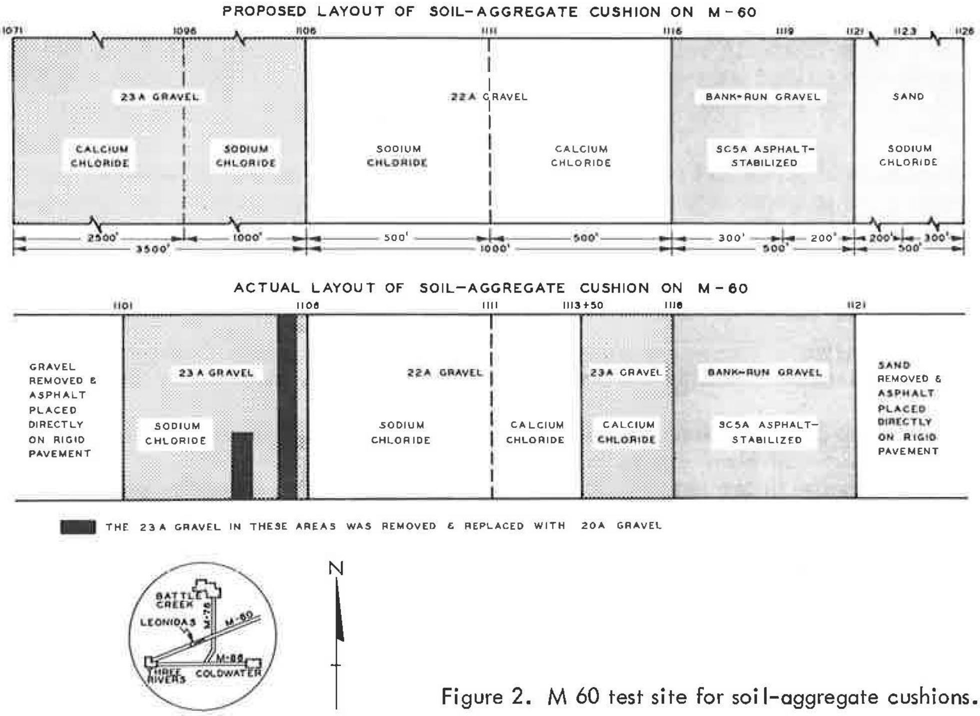

Figure 2. M 60 test site for soil-aggregate cushions.

Soil-aggregate cushions were placed over the rigid pavement for 5500 ft of its total length. The remaining length of pavement, used as a standard of comparison, was resurfaced conventionally by placing bituminous concrete directly on the rigid pavement. The entire 3-mile length of rigid pavement including the soil-aggregate cushion was covered with 250 lb per sq yd of bituminous concrete. All sections of soil-aggregate cushion were constructed to a uniform compacted depth of 4 in.

Construction procedures were in accordance with 1960 Michigan Department of State Highways Standard Specifications for Road and Bridge Construction. Six different materials were used for the cushion: 22A and 23A gravel with calcium chloride admixture, 22A and 23A gravel with sodium chloride admixture, "bank-run" gravel with SC-5A asphalt admixture, and sodium chloride-treated "bank-run" sand (Fig. 2). Michigan Department of State Highways grain-size specifications (1960) for 22A and 23A soil aggregates are given in Table 1. The bank-run gravel used in the M60 soil-aggregate cushion has a grain-size distribution according to the AASHO classification as follows: gravel, 28.4 percent; coarse sand 32.8 percent; fine sand 27.8 percent; silt 6.2 percent; and clay 4.8 percent. The grain-size distribution indicates that this bank-run gravel would be unstable if no admixture were used.

TABLE 1

TOTAL PERCENT PASSING STANDARD SIEVE SIZES

Class	1 In.	¾ In.	⅜ In.	No. 10	No. 40	Loss by Washing Through No. 200 sieve
22A	100	90-100	65-85	30-45		3-7
23A	100		60-85	25-50		7-15
20A*		100	60-80	40-50	15-30	0-7

*Used for replacing distressed cushion material.

All the 22A and 23A processed gravel had been mixed with 6 lb of Type 1 calcium chloride per ton of gravel in the stockpiles. Because it was believed that some of the admixture had leached out, an additional 4 lb of Type 1 calcium chloride were added to each ton of gravel.

Construction of the Cushion

1. Calcium chloride-treated 23A gravel. Some trouble was experienced in eliminating moist spongy areas in the cushion. Traffic was easily maintained during construction, and on completion of the cushion the roadway appeared smooth and stable.

2. Calcium chloride-treated 22A gravel. The material was compacted easily and traffic was maintained over the cushion without difficulty. No spongy areas developed.

3. Sodium chloride-treated 23A gravel. Approximately 4 lb of sodium chloride were added to each ton of gravel as it was hauled to the job site. Density was readily obtained with a rubber-tired roller. Traffic was easily maintained over the cushion during construction.

4. Sodium chloride-treated 22A gravel. Approximately 6 lb of sodium chloride were added to each ton of gravel as it was hauled to the site. The material was compacted very readily with a rubber-tired roller and traffic was easily maintained over the cushion.

5. Asphalt-treated bank-run gravel. The asphalt and gravel were combined at an asphalt mixing plant and hauled about 20 miles to the construction area. The bitumen content of the mixture was 4 percent by weight, the temperature of the mix was 250 F. The material was easily compacted with a steel-wheeled roller. About six hours after compaction traffic was permitted to travel over the cushion. The cushion held up very well under traffic, especially in view of the heavy trucks traveling over it after the short curing period. The compacted cushion appeared to be somewhat "rich" in bituminous material and even better results might possibly be obtained by a slight reduction of the bitumen content of the gravel. The unit cost of this asphalt-stabilized gravel was about four times that of the 22A gravel.

6. Sodium chloride-treated bank-run sand. This material was produced specifically for use in this section and contained about 8 percent silt, which was ineffective as a binder material. Each ton received about 8 lb of sodium chloride. Despite the addition of water and considerable rolling, the sand could not be stabilized and would not carry traffic. As a result, the sand was taken away to be used elsewhere and the bituminous concrete placed directly on the old rigid pavement.

Porous aggregate shoulders were placed to a compacted depth of 4 in., constructed to provide adequate drainage for the cushions. Because of the impermeable appearance of the cushion, it was decided to omit the prime coat under the leveling course. A leveling course of 130 lb of bituminous concrete per sq yd of area was placed over the entire 3 miles of test pavement, followed by a 120 lb per sq yd bituminous-concrete wearing course.

PERIODIC PERFORMANCE REPORTS

Early Performance of the Test Sections

After carrying traffic for about one day, signs of failure began to appear in the bituminous leveling surface over the 23A gravel cushion. Two types of early failure were noted, both influenced by high moisture content. With the first type of failure the asphalt surface was spotted with moisture, giving the appearance of water migrating up from the base, and areas of map cracking or longitudinal cracks appeared. The second type appeared to be a shear failure resulting in rutting of the cushion and asphalt mat. Then the asphalt appeared to disintegrate with damage spreading into large broken areas (Figs. 3 and 4). However, these failures were confined to areas where asphalt had been placed over the 23A gravel and did not appear to be as frequent or as serious in those areas in which the 23A gravel contained sodium chloride admixture. There was considerable rainy weather during placement of the 23A gravel cushion on the west end of the project where calcium chloride admixture was used. Since both calcium chloride and sodium chloride are hygroscopic, the use of these admixtures probably made the problem worse. Attempts were made to patch the distressed areas but the

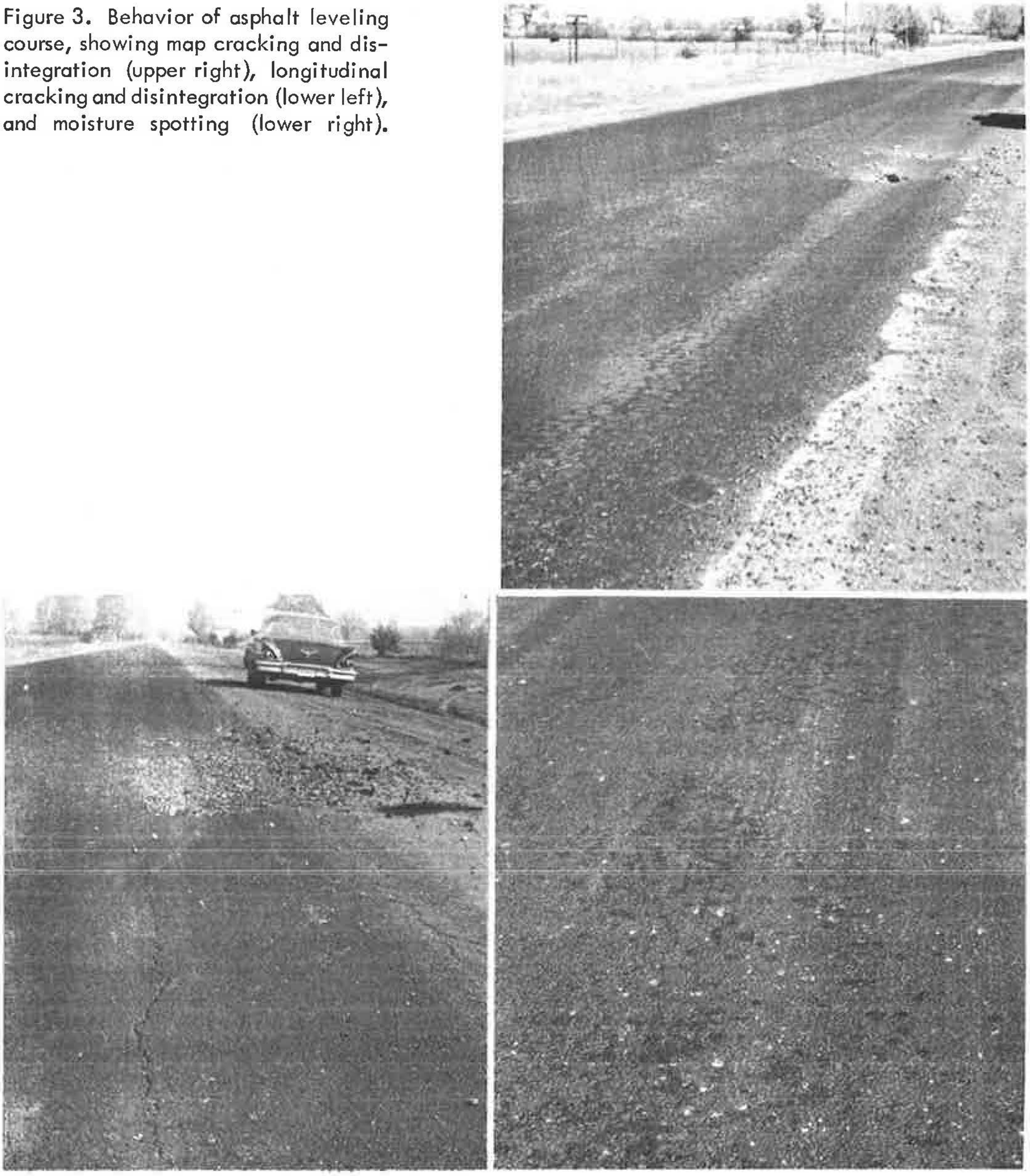

Figure 3. Behavior of asphalt leveling course, showing map cracking and disintegration (upper right), longitudinal cracking and disintegration (lower left), and moisture spotting (lower right).

failure became so widespread that it was necessary to remove large areas. These were replaced by asphalt applied directly on the rigid pavement surface.

Inspection of the distressed areas revealed that no bond existed between the asphalt and the 23A gravel. A thin film of moisture existed between the asphalt and gravel which appeared to act as a lubricant. Tests indicated a moisture content of 10 to 12 percent in the top $\frac{1}{2}$ in. of cushion but only 4 to 5 percent below this.

After a month, severe map cracking was noted in wearing surface areas which covered the remaining 23A gravel. Again, the 23A gravel which contained sodium chloride admixture exhibited fewer distressed areas than the 23A gravel which contained only calcium chloride. In retrospect, it appears that the surface failures just discussed might have been prevented by reducing the hygroscopic soil admixture quantities.

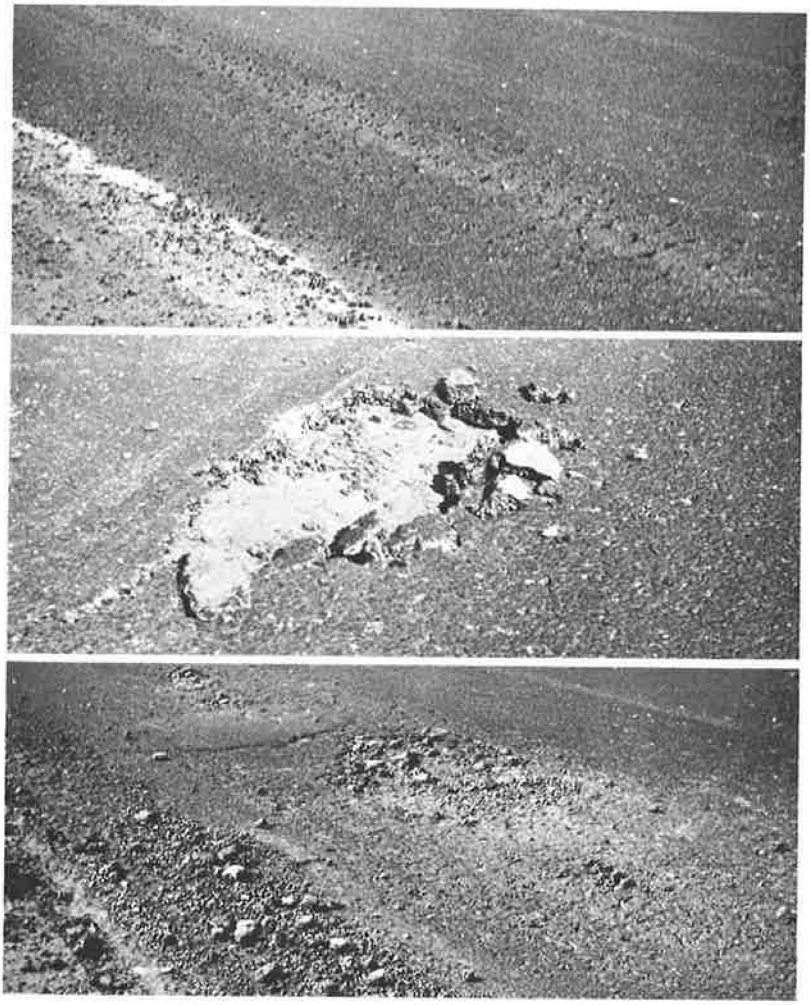

Figure 4. Behavior of asphalt leveling course, showing severe alligator cracking (top) and localized distress (center and bottom).

Performance of the Test Section After Five Years

Five annual surveys of the project have been made and progress reports surveying the condition of the pavement were published by the Department after two and four years of service. Because only slight differences appeared between pavements over the two gradations of processed gravel and since the test sections involved are so short, no significant difference could be proven, and the four 22A-23A cushions will be considered as a single unit in comparisons with the asphalt-stabilized bank-run gravel and sections where resurfacing was applied directly over old pavement.

Figure 5 shows how transverse reflection cracking increases as a function of time. After five winters, about 54 percent of the transverse cracks had reflected through the bituminous surface where no cushion was used, about 26 percent through the 22A-23A gravel cushion area, and about 20 percent in the asphalt-stabilized bank-run gravel cushion area. It is interesting to note that most transverse reflection cracking occurred during the first year of service.

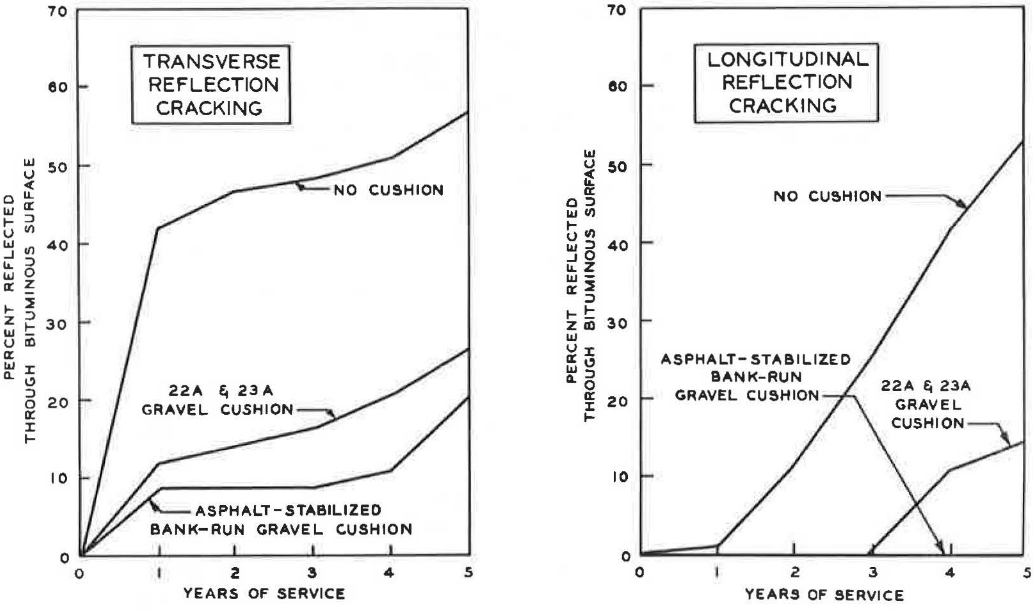

Figure 5. Transverse and longitudinal reflection cracking as influenced by aggregate cushion.

Figure 5 also shows how longitudinal reflection cracking increases as a function of time. In areas where the asphalt-stabilized cushion was used, no longitudinal reflection cracking was present. No longitudinal cracking had been noted in the 22A-23A gravel cushion for the first three winters, but after the fourth about 10 percent of the length of widening strip had reflected through the pavement. Statistical tests of the data indicate that the effect of the gravel cushions in reducing longitudinal reflection cracks was highly significant. Further, the test indicated the asphalt-stabilized cushion to be significantly better than the 22A-23A in reducing longitudinal reflection cracks.

Although a few joint blow-ups were observed in areas of conventional resurfacing, none were apparent in any of the cushioned areas. Map cracking extended about 8 in. in from the edge of the pavement in the 22A-23A gravel cushion areas. None was observed in the asphalt-stabilized gravel cushion area.

SUMMARY OF M 60 INVESTIGATION

After nearly five years of service, the soil-aggregate cushions used in these tests have been of significant value in reducing reflection cracking of the bituminous overlay. Of the cushion materials, asphalt-stabilized soil aggregate appears to be more effective in reducing reflection cracking and in preventing map cracking at the edge of the pavement than the 22A-23A gravel.

All cushion materials except the sand proved satisfactory for carrying traffic in the interim before the bituminous overlay was constructed.

Bank-run sand, similar in gradation to that used in this test, should not be used as a soil-aggregate cushion where traffic must be maintained unless an acceptable means of stabilizing it can be found.

Slow-curing (SC-5A) asphalt-stabilized bank-run gravel costs more initially and must be allowed to cure for about six hours before traffic can be permitted to travel over it.

A reason for the effectiveness of the asphalt-stabilized cushion may be that the relatively unstable bank-run gravel particles are able to shift and absorb movements of the underlying rigid pavement.

DETROIT INDUSTRIAL EXPRESSWAY (I-94) PROJECT

Subsequent to the M 60 experimental project, Michigan resurfaced a number of rigid pavements with asphaltic concrete underlain with soil-aggregate cushions. The most important soil-aggregate cushion project is being constructed over a length of about 14 miles on I-94, the Detroit Industrial Expressway (DIE), located west of Detroit. Much of the DIE was constructed of portland cement concrete during World War II and contained no load transfer dowels or reinforcing steel. Although the original divided four-lane rigid pavement had been resurfaced with a 3-in. thickness of asphaltic concrete, the surface, a two-lane roadway for each direction, had deteriorated and riding quality was poor. Further, because of the high average daily traffic volume of 45,000 vehicles, about 17.5 percent of which were commercial, it was determined that both the existing two-lane roadways were of insufficient capacity. After considering relocation of the highway, it was decided to widen each two-lane pavement with an additional 12-ft width of portland cement concrete, 9 in. thick, and to construct an asphalt-stabilized 22A soil-aggregate cushion approximately 8 in. in depth over all three lanes of each roadway. The highway would then be resurfaced with a 3-in. thickness of asphaltic concrete.

The full length of the project has not been completed. After two years of service, however, the first section to be completed (a three-lane pavement about one mile in length) showed no transverse cracks and about 277 linear feet of longitudinal cracking per lane-mile. Longitudinal cracking occurred at joints between lanes where the bituminous mats were joined and therefore the cracking may not have been due to reflection. A lane-mile is defined as a one-mile length of pavement 12 ft or one lane in width. Areas of the project approaching bridges where no soil-aggregate cushion was used showed about 232 transverse cracks per lane-mile and 2538 linear feet of longitudinal cracking per lane-mile. Thus, at this stage the soil-aggregate cushion has been very effective in reducing reflection cracking.

M 15 PROJECT, NORTH AND SOUTH OF MILLINGTON

Route M 15 north of Millington in Tuscola County (Mich. Proj. No. F679031C, C4) is another area where an asphalt-stabilized soil-aggregate cushion was used. Also an adjacent area of M 15 south of Millington (Mich. Proj. No. Fb79031C, C3) was resurfaced at about the same time without a soil-aggregate cushion. Both projects are two-lane roadways which were resurfaced with asphaltic concrete about 1½ in. in depth. The cushioned project north of Millington was about 3½ miles long, with a 4-in. thick asphalt-stabilized 22A soil-aggregate cushion. After 3-years service, this area showed 70 transverse cracks per lane-mile and 36 ft of longitudinal cracking per lane-mile. The project south of Millington, where the asphaltic concrete overlay was placed directly on the old pavement, was 3.6 miles in length and showed 94 transverse cracks per lane-mile and 2614 ft of longitudinal cracking per lane-mile. Longitudinal cracking occurred over both the old pavement centerline joint and concrete widening strip joints.

Other Michigan resurfacing projects were constructed over a length of about 24 miles of US 23 north of Tawas and on a 30-mile length of M 53 south of Port Austin. With these latter two jobs, there were no conventional resurfacing projects in the area to use as standards of comparison.

CONTINUOUSLY REINFORCED BITUMINOUS RESURFACING

Another method of preventing reflection cracking was tried in Michigan in 1955 where two sections of continuously reinforced bituminous-concrete resurfacing were placed over widened portland cement concrete on a 1½-mile length of Detroit Industrial Expressway west of Ypsilanti (now I-94). Control sections of non-reinforced resurfacing of similar lengths (totaling 1¼ miles) were placed at the same time. The portland cement concrete pavement to be resurfaced was constructed in 1943 under wartime specifications, where load transfer and reinforcing steel were omitted. Expansion joints were spaced at 120 ft with weakened plane contraction joints at 20-ft intervals.

The project carried heavy commercial and passenger traffic continuously since completion. By 1955 this pavement had severe transverse cracking and faulting of joints and cracks. Prior to resurfacing, the old pavement was widened from 22 to 24 ft. This 2-ft concrete base course widening was added to the outer edge of the traffic lane, reinforced longitudinally with deformed bars but not tied to the old pavement. The widening and the old pavement was 9-in. uniform thickness.

The Wire Reinforcing Institute advised the Department of various aspects of design and construction. At about the same time, crack control in bituminous resurfacing by means of reinforcement was attempted in research-oriented projects in California, Minnesota, Ohio, Texas, Indiana, New Jersey, Illinois, District of Columbia and in England. Welded wire-mesh fabric (3 × 6-10/10) was installed as continuous reinforcement. The cleaned pavement surface was sprayed with a bond coat of asphalt emulsion without elaborate patching or resealing of deteriorated joints, cracks, or rough slab surfaces. The reinforcement was then laid directly on the pavement followed by a binder course of 190 lb per sq yd (about 2 in. thick) and a surface course of 130 lb per sq yd (slightly over 1 in. thick). The mesh was supplied in 7.5 by 15-ft flat sheets which were lapped one transverse wire spacing (6 in.) at the leading edge. Hog rings were used to tie the lapped sheets. A "hold-down sled device" was used beneath the paver to ride along and depress the wire-mesh wires under the spreader. The "hold-down sled" was only partially effective and problems arose with buckling of the wire-mesh sheets ahead of and behind the paver. Some replacement of entire sheets was necessary but in other cases, where smaller areas were involved, the buckled reinforcement was cut out and not replaced.

The performance of reinforced and non-reinforced sections was observed for six years. During this period, the average daily traffic increased from 10,600 with 19

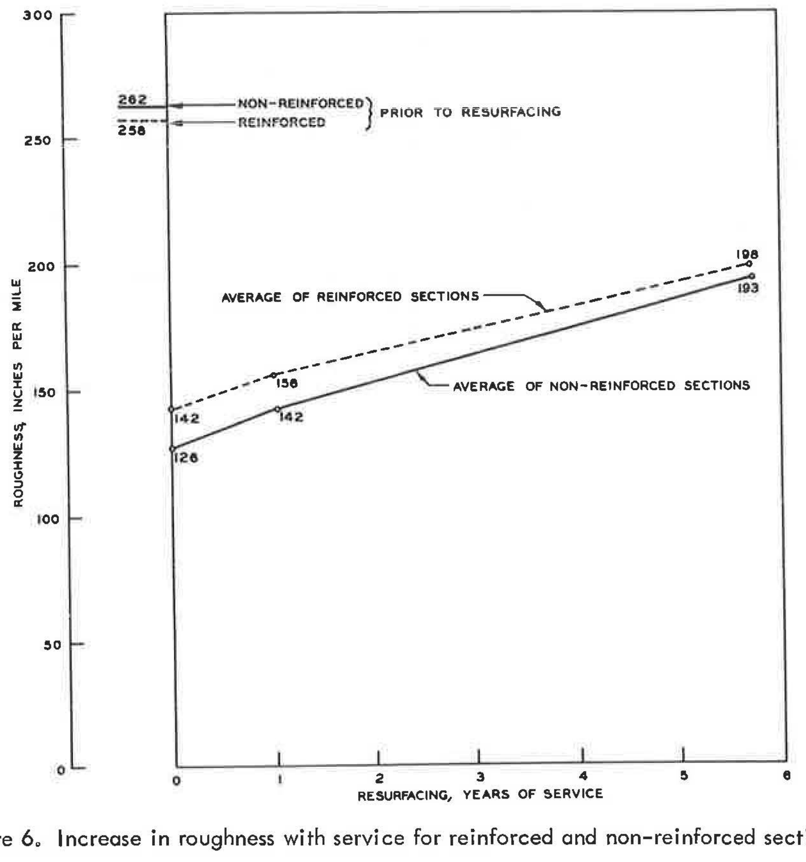

Figure 6. Increase in roughness with service for reinforced and non-reinforced sections.

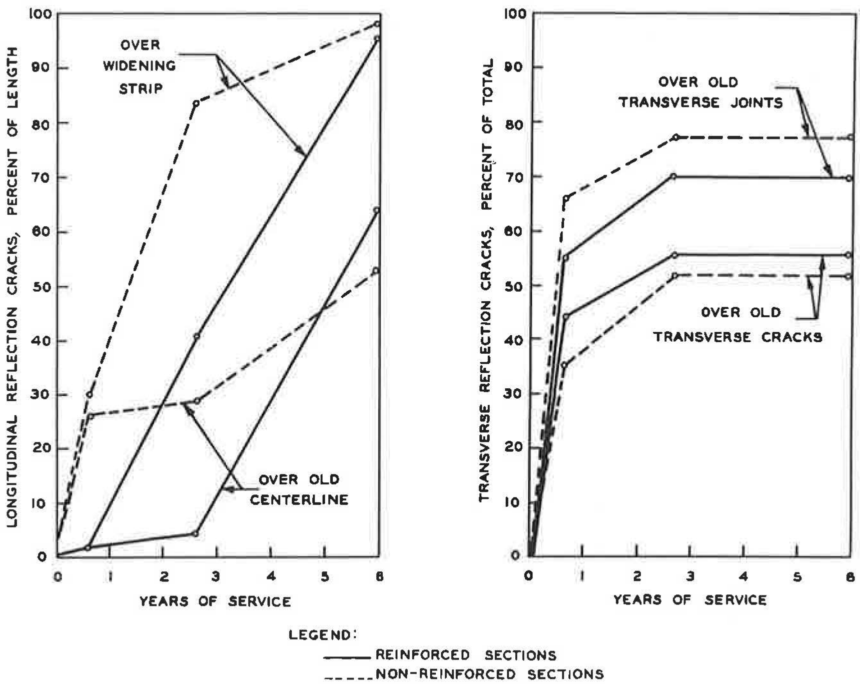

Figure 7. Average reflection cracking for reinforced and non-reinforced sections.

percent commercial, to 19,750 with 22.5 percent commercial. The difference in roughness with service was insignificant for reinforced and non-reinforced sections (Fig. 6). However, the first reinforced section was initially rougher than the other sections, probably due to construction problems incident to buckling and deforming of wire-mesh mats which was most prevalent in the first two days of constructing the first reinforced section.

During the first eight months of service, transverse and longitudinal cracks developed both in reinforced and non-reinforced sections (Fig. 7). Survey procedures included specific detailed mapping of the entire project length.

The reinforcement seems to have controlled longitudinal cracks over the centerline and the widening strip quite effectively for a while but showed reduced effectiveness by $2\frac{1}{2}$ years and was completely ineffective by the end of 6 years.

The ineffectiveness of reinforcement in crack control over transverse joints and cracks even for a short time can be seen in Figure 7. No significant reduction of transverse reflection cracking was noted. In addition, transverse reflection cracks also developed over lapped mat edges on the reinforced sections with 13 percent reflected through the resurfacing by the end of 8 months and 17 percent by the end of 32 months.

The reinforced sections were also prone to an additional problem which did not occur in the non-reinforced sections. At the intersection of transverse and longitudinal reflection cracks over the widening strip, the reinforced sections developed alligator cracking which produced potholes requiring patching in 15 cases for a total of 127 sq ft (Fig. 8).

During final inspections, bituminous concrete was removed from potholes at other locations to expose the reinforcement. The wires were fractured and severely rusted in potholes over intersections of transverse and longitudinal joints in the old pavement, indicating extensive infiltration of moisture to the steel. However, steel exposed at other locations, where no surface deterioration had occurred, suggested that the reinforcement after 6 years had been reduced throughout the overlay to disconnected networks of broken and corroded wire fragments (Fig. 9).

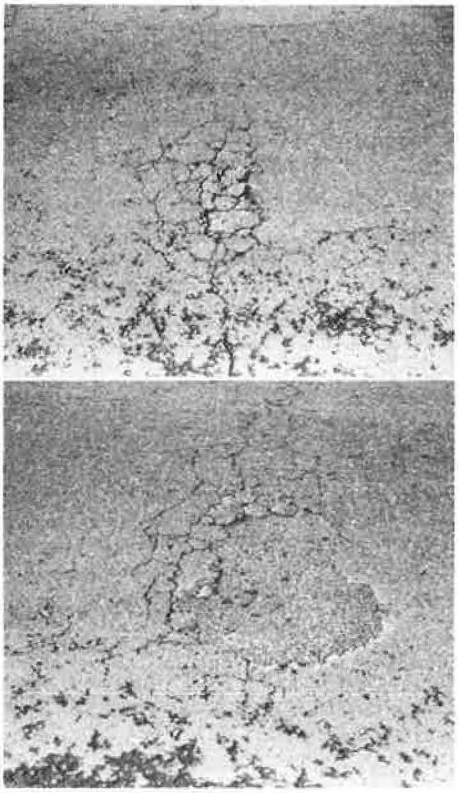

Figure 8. Alligator cracking leading to pothole patching of resurfacing in reinforced sections.

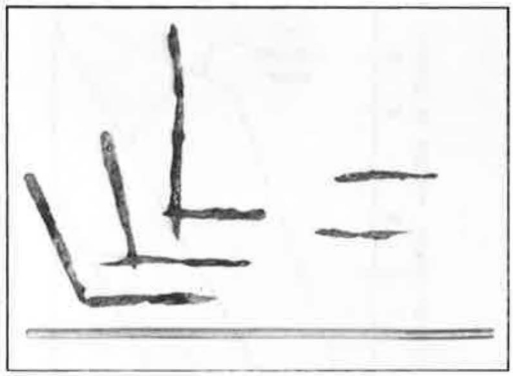

Figure 9. Reinforcement specimens removed from sound and unsound resurfacing areas. Sample of new No. 10 gage wire at bottom.

Of all the steel examined, the best preserved after 6 years was a lightly rusted short length of wire that had never been covered during resurfacing, but had been left exposed to the weather at the pavement edge. This exposed wire was in better condition than parts of the same sheet that had been covered with bituminous concrete (Fig. 10). It would seem that any bituminous-concrete reinforcement lacking specific treatment for corrosion prevention would be liable to rust and

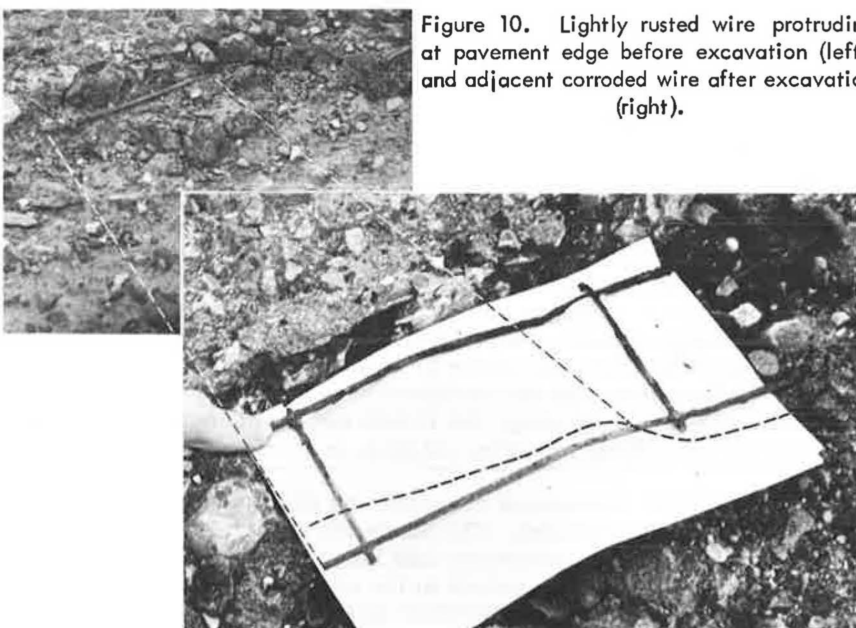

Figure 10. Lightly rusted wire protruding at pavement edge before excavation (left), and adjacent corroded wire after excavation (right).

fracture after about 5 years, wherever winter maintenance chemicals were used extensively.

SUMMARY

Soil-Aggregate Cushion

Wherever comparisons between resurfaced projects with and without soil-aggregate cushions could be made, soil-aggregate cushions proved capable of reducing reflection cracking. However, with the 4 to 8-in. thicknesses used in Michigan, soil-aggregate cushions have not completely eliminated reflection cracking. The Detroit Industrial Expressway, I-94, project has indicated that heavily traveled highways can be rehabilitated without reflection crack problems by using a soil-aggregate cushion. The cushions have proved satisfactory for carrying traffic during construction periods, and thus time can be minimized when a project is closed to vehicles.

In conclusion, it appears that soil-aggregate cushions significantly reduce reflection cracking. However, the preceding discussion shows the performance of cushions is variable and further research is required to minimize variability and maximize efficiency.

Reinforced Asphaltic Concrete

The Michigan experiment with welded wire-mesh continuous reinforcement placed directly on a widened portland cement concrete base and then covered with two-course bituminous-concrete resurfacing indicates:

1. Reinforcement offers no significant advantage in control of transverse or longitudinal reflection cracking or in preserving a smooth riding resurfacing.
2. Alligator cracking at intersections of transverse and longitudinal joints leading to potholes requiring patching was a performance problem unique with only the reinforced resurfacing sections.
3. Extensive corrosion and fragmentation of reinforcing steel, a performance factor not mentioned in the literature, was encountered even where the overlay surface was in good condition.

On the basis of other experimental studies, the Wire Reinforcing Institute and state agencies active in this research area now advise against installation of reinforcement directly on the base pavement. Notably successful experiments have been reported in other states by placing a leveling or binder course over the concrete base, then laying reinforcement, and completing the resurfacing with a wearing course, for a "sandwiched" type cross section. In some cases, the sandwiched reinforcement is placed over a leveling course or binder course and then covered with a separate binder and surfacing courses for a three-layer cross section.

Experimental Composite Pavement in New Jersey

JOHN L. HALLER, Assistant Supervising Engineer, Bureau of Structures and Materials, Division of Research and Evaluation, New Jersey Department of Transportation

An experimental composite pavement design was constructed in New Jersey in 1963. The terrain involved is essentially marshland. This route is one of New Jersey's most heavily traveled; presently carrying approximately 80,000 vehicles daily, of which 17 percent are in the heavy truck category.

A composite design was chosen as that which would most likely satisfy the requirements of a highway in this area. That is, a pavement that would provide inherent stability to carry the exceptionally heavy traffic, as well as surface continuity, for a relatively long period of time with a minimum of maintenance.

Over the 42-month period of operation thus far observed, the composite pavement has performed in accordance with design objectives. There has been an average total settlement of 0.06 ft in this period, most of which occurred within the first 18 months of service. Maintenance has been negligible thus far.

•THIS paper concerns a composite pavement design constructed on Route 3 in New Jersey. The subject pavement was designed in the latter part of 1961 and construction was completed in the middle of 1963. Because of the unique pavement design proposed for this project, the Bureau of Public Roads requested the New Jersey Department of Transportation to consider it as an experimental project. It was agreed that the State would study the behavior of the composite pavement design and report annually on the observations and collected data. The completed project has been reported on at periodic intervals of $1\frac{1}{2}$, $2\frac{1}{2}$, and $3\frac{1}{2}$ years since construction.

The basic reporting methodology agreed on consists of: (a) traffic data including loadings, (b) determination of the serviceability index, (c) deflection measurements, (d) settlement determinations, (e) concrete base performance, and (f) bituminous concrete surface performance.

The composite pavement design was used on a portion of the projects in New Jersey involving the Route 3 and New Jersey Turnpike approach complex to the Lincoln Tunnel, connecting New Jersey with New York. Several factors influenced the use of a composite design rather than a conventional design in the approach section of the Route 3 crossing of the Hackensack River. The terrain over which this portion of the highway was constructed is meadowland; the subsoils consisted of thin varved layers of silt, clay, and sand. Approximately 12 feet of organic peat and muck overlaid the underlying soils.

Because of the urgency of the need for improvements to the overall approach complex, the following factors were involved in the design of the pavement section:

1. In 1961, Route 3 over the Hackensack River was carrying approximately 80,000 vehicles daily, and about 17 percent of these vehicles were in the heavy truck category. Therefore, it was imperative that the pavement section be of an unusually sturdy construction so that it remain virtually trouble-free and require an absolute minimum of maintenance over a relatively long period of time.

Paper sponsored by Committee on Composite Pavement Design and presented at the 47th Annual Meeting.

2. A decrease in construction time was desirable and could be accomplished by removal and replacement of the organic peat and muck with Zone 2 material (open-graded quarried or bank-run material, 0 to 8 percent passing No. 200 mesh), placing a normal earth embankment and constructing a pavement thereon. However, this type of construction would not permit preconsolidation of the underlying compressible materials.

3. Serious doubts existed as to the advisability of employing New Jersey's standard design of reinforced concrete pavement (78 ft 2 in. slab length) because of the compressible nature of the underlying soil and the possibility of appreciable differential settlements causing serious cracking.

4. Investigations and studies, available at that time, of the performance of flexible pavements on major trucking routes in New Jersey, on the AASHO Road Test, and on sections of the New Jersey Turnpike in the area of this project, led to uncertainty as to the adequacy of any conventional flexible pavement under the extreme traffic conditions of this project.

5. Bituminous surfacing materials are apparently capable of satisfactorily carrying heavy truck traffic and remaining crack free, provided they are on a very stable foundation. This was borne out by the outstanding performance of the pavements on two rehabilitation projects which involved thick overlays placed on existing concrete pavement. In both instances, the existing pavement was badly cracked, depressed, and undergoing pumping. An overlay consisting of a 3-in. FA-BC-2 surfacing on 8 in. of macadam base, on 3 in. of essentially stone screenings, was constructed on US 22 between Somerville and Chimney Rock in 1952, and is still in satisfactory condition. In the northbound roadway of US 130, in the vicinity of Deans, an overlay was constructed in 1949 consisting of a 2-in. FA-BC-1 surfacing on 3 in. of penetration macadam, on 6 in. of macadam base, on 5 in. of bank-run gravel. This overlay, under considerable heavy truck traffic, is also still in satisfactory condition, whereas, a then-considered relatively high-type flexible section constructed in the northbound roadway is now very badly cracked, appreciably rutted, and exhibits numerous areas of localized settlement.

The particular design objectives for use of a composite pavement on this project were as follows:

1. To maintain the structural integrity of surface despite an anticipated differential settlement resulting from the deep fill and the compressible nature of the underlying soil.

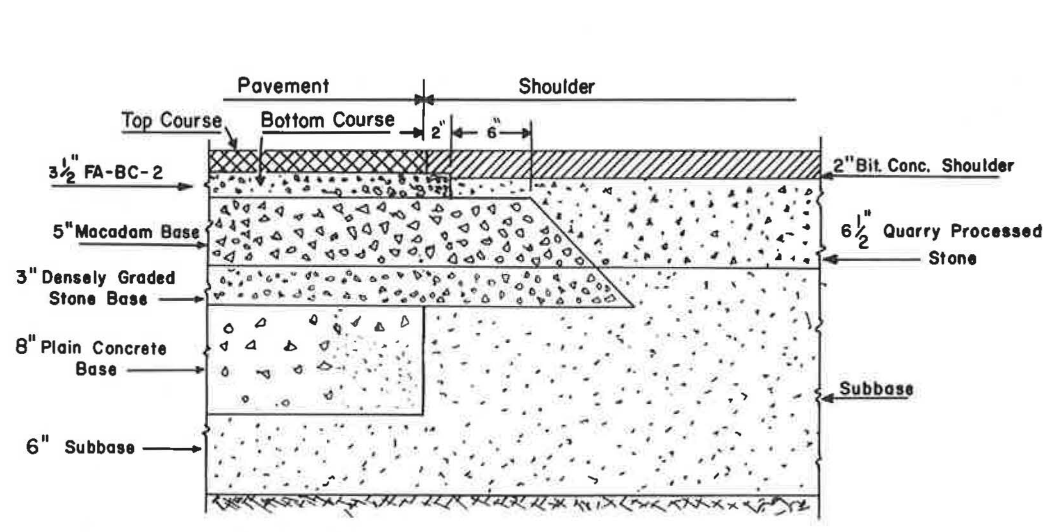

Figure 1. Experimental composite pavement section.

2. To achieve the high load-carrying capacity of a rigid pavement necessitated by the large volume of heavy truck traffic.
3. To achieve the continuity of surface of a flexible pavement.

The section of the mainline composite pavement and shoulder, designed on these principles, is shown in Figure 1.

Contraction joints, providing aggregate interlock load transfer, were constructed in the concrete base at intervals of 15 ft. A 3-in. base of densely graded stone was applied between the concrete base and the 5-in. macadam base. This was to act as a buffer to prevent the reflecting of cracks from the concrete base up into the 3 ½ in. of FA-BC-2 surface pavement.

Several construction contracts were associated with the approach complex to the Lincoln Tunnel. Reporting is limited to the Route 3 westbound roadway on the east side of the Hackensack River. The available initial data on the west side of the river and the eastbound roadway are not sufficient for analysis.

Construction cost of the pavement for the initial contract amounted to $12. 39 per square yard. This cost, much higher than originally anticipated, was attributed to the inexperience of the contractor with this type of pavement. In subsequent contracts, the cost was reduced to $9. 85 per square yard. A high-type bituminous concrete pavement or a reinforced portland cement concrete in New Jersey averages approximately $6. 00 to $9. 00 per square yard.

The two-way AADT experienced on this portion of Route 3 for the indicated periods were 1963—80, 400 vehicles; 1964—83, 890 vehicles; 1965—84, 730 vehicles; and 1966—83, 460 vehicles.

The truck percentage for westbound Route 3 was 19. 0 percent (approximately constant for the 1964-1966 period) with an approximate lane distribution of: lane 4 (inside left)—6. 0 percent, lane 3—32. 0 percent, lane 2—43. 0 percent, and lane 1 (outside right)—19. 0 percent.

Route 3 westbound was constructed on new alignment and completed in mid-1963. While existing Route 3 was being rehabilitated to accommodate eastbound traffic, from July 2, 1963, to May 27, 1964, the completed Route 3 westbound was divided into five lanes, each 10 ft wide, and was utilized for both eastbound and westbound traffic. During this period, it was subjected to approximately 3, 505, 056 eighteen-kip equivalent axle repetitions. Since May 28, 1964, the roadway has been used exclusively as four lanes for westbound traffic. The accumulated by-lane 18-kip equivalent axle repetitions since May 28, 1964, up to November 29, 1966, the date of the latest surveys, are lane 4 (inside left)—276, 059, lane 3—1, 472, 311, lane 2—1, 979, 230, and lane 1 (outside right)—874, 188—making a total of 4, 601, 788 eighteen-kip equivalent axle repetitions.

The relatively high traffic-load condition for the initial period up to May 1964 is due to the fact that the route carried traffic in both directions.

Roughometer surveys were conducted periodically on all lanes of the approach section of the Route 3 crossing of the Hackensack River from July 1963 (prior to opening to traffic) to November 1966 (latest survey). The first three surveys were conducted by personnel of the Structural Research Division of the Bureau of Public Roads. The latest survey was conducted with the assistance of the Port of New York Authority. Although no acceptable roughness levels have been established for New Jersey using a BPR-type roughometer, limited roughness data are available for both the reinforced portland cement concrete and bituminous concrete pavement types. The measured values obtained for the subject composite pavement are within the limits of the available data. Virtually no change was found in the pavement roughness and the serviceability index since construction.

TABLE 1

AVERAGE PERIODIC DEFLECTION MEASUREMENTS

Date	Deflections (thousandths of an inch)	
	Joints	Midpoints
Dec. 1963*	5	5
May 1965*	8	7
Oct. 1965	7	7
June 1966	7	7
Nov. 1966	7	6

*7,500-lb wheel load.

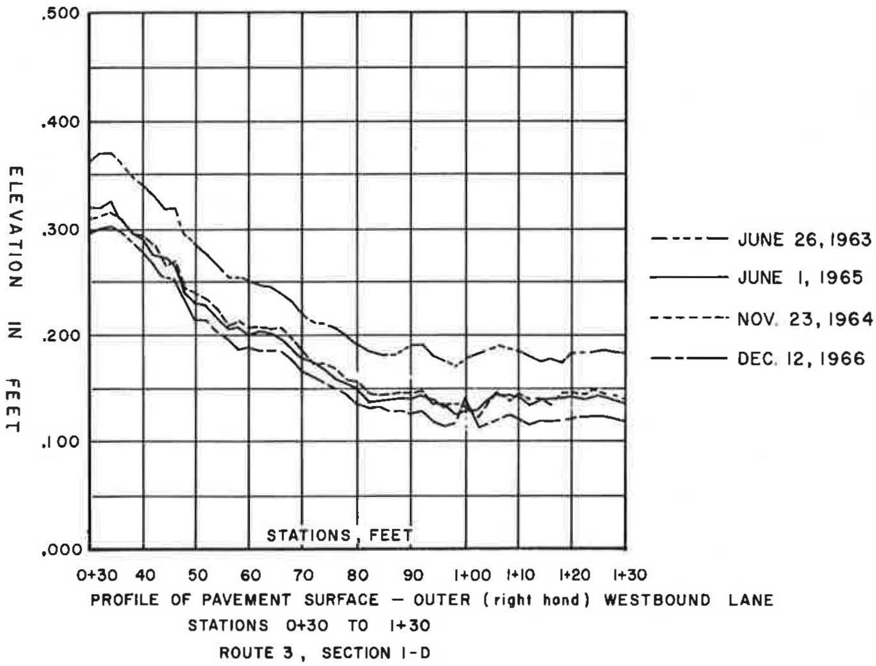

Figure 2.

Periodic Benkelman beam surveys have been made on the outside (right) and inside (left) lanes of the Route 3 westbound roadway east of the Hackensack River since the inception of the study. Initially, a 7,500-lb wheel load was employed. The more recent surveys were made with a 9,000-lb wheel load. Deflections were obtained in the right wheelpath of the outside (right) lanes at contraction joints (aggregate interlock load transfer), construction joints (no load transfer), and midpoints of the concrete base slabs. Table 1 gives the average periodic deflection measurements.

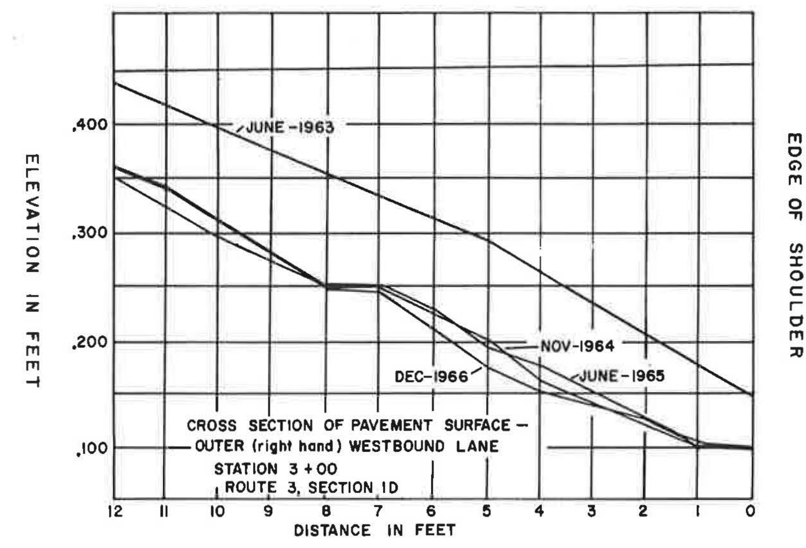

Figure 3.

Available limited data for other New Jersey pavements indicate deflection ranges of 0. 01 to 0. 03 in. and 0. 006 to 0. 010 in. for bituminous concrete and portland cement concrete pavements, respectively. The deflections observed thus far on Route 3 indicate they are well within acceptable limits.

Periodic close interval profile and cross-section readings have been taken on Route 3, Section 1 D—the section to which this report pertains. Figure 2 shows a portion of a typical profile as of June 1963 (as constructed), November 1964, June 1965, and December 1966. Figure 3 indicates a portion of a typical cross section taken on the above dates.

The settlement observed thus far has been approximately 0. 06 ft. Most of this settlement took place during the first 18 months.

Visual inspections of Route 3, Section 1 D were made in November 1963, January 1966, and March 1967. These inspections revealed no significant defects in the composite pavement. Several very minor longitudinal cracks were observed. They are not considered as being detrimental to the overall performance of the composite pavement. No transverse cracking of the pavement has been observed, except immediately adjacent to the structure. This absence of transverse cracking in the surface indicates the buffer layers of densely graded stone and macadam are preventing the contraction joints of the concrete base from being reflected into the surface. Maintenance thus far has been negligible. Some minor patchwork was accomplished at the structure because of pavement settlement.

Profile surveys and visual inspections have shown no unusual conditions in the performance of the composite pavement. Therefore, no intimate study of the concrete base has been undertaken. All joint locations have been marked, however, and if necessary, excavations can be made to determine the condition of the joints and the performance of the base.

Over the 42-month period of operation thus far observed, the composite pavement has performed in accordance with the original design objectives, namely:

1. To maintain the structural integrity of surface despite an anticipated differential settlement resulting from the deep fill and the compressible nature of the underlying soil.
2. To achieve the high load-carrying capacity of a rigid pavement necessitated by the large volume of heavy truck traffic.
3. To achieve the continuity of surface of a flexible pavement.

ACKNOWLEDGMENTS

The author wishes to express his sincere thanks to those members of the current and past staff of the Bureau of Structures and Materials who were involved in the preparation of previous interim reports on which this paper was based—particularly, John J. Quinn and John M. Salt, Jr., who were primarily responsible for the collection, analysis, summarization and reporting of data. A special note of thanks is extended to William VanBreemen (retired December 1963) who conceived this composite design and was involved in establishing the basic methodology for reporting.

Field Study of Performance and Cost of a Composite Pavement Consisting of Prestressed Concrete Panels Interconnected and Covered With Asphaltic Concrete

EMIL R. HARGETT, Associate Professor of Civil Engineering, South Dakota State University

This report describes the design, construction, and field testing of a new concept in highway pavement design—a composite of favorable features of both rigid and flexible pavements consisting of prefabricated prestressed concrete structural components covered with a leveling course of asphaltic concrete. The prestressed structural panels are placed on the prepared roadbed and interconnected with special steel connectors and grout keys. The panels produce the structural effects of a spread footing, yet possess a high degree of flexibility and resistance to permanent cracking. The asphalt leveling course furnishes a flexible and waterproof surface with excellent riding characteristics. Design details, construction costs, and field tests for an evaluation of structural performance are included and discussed in view of the short period of the field performance study.

•AFTER receiving favorable structural performance from the laboratory investigation of composite pavement, the South Dakota Department of Highways approved a small-scale field study of this type of pavement. The field study was designed to furnish additional information regarding costs, construction problems, and structural performance of the composite pavement under field conditions. The primary factors investigated in the study of structural performance were load-carrying capacity and expansion-contraction characteristics.

LOCATION AND DESIGN OF FIELD TEST SECTION

The location of a field study of this new type of pavement on a mainline highway was not recommended because it was in its early stages of development. The site selected was the driveway to the South Dakota Highway Maintenance building east of Brookings, where it was possible to subject the composite pavement to actual traffic and typical weathering conditions for the area.

The longitudinal panel arrangement was selected for this investigation in view of its promising riding characteristics. The length of the test section was limited to 96 ft by the high construction costs anticipated for this new concept in pavement construction. Figure 1 shows a plan and elevation view of the composite pavement as designed for the field study. The individual panels were designed with the following dimensions: 6 ft wide, 24 ft long, and $4\frac{1}{2}$ in. thick. The panels were interconnected with grout keys and tongue-and-fork connectors developed during the latter part of the laboratory in-

Paper sponsored by Committee on Composite Pavement Design.

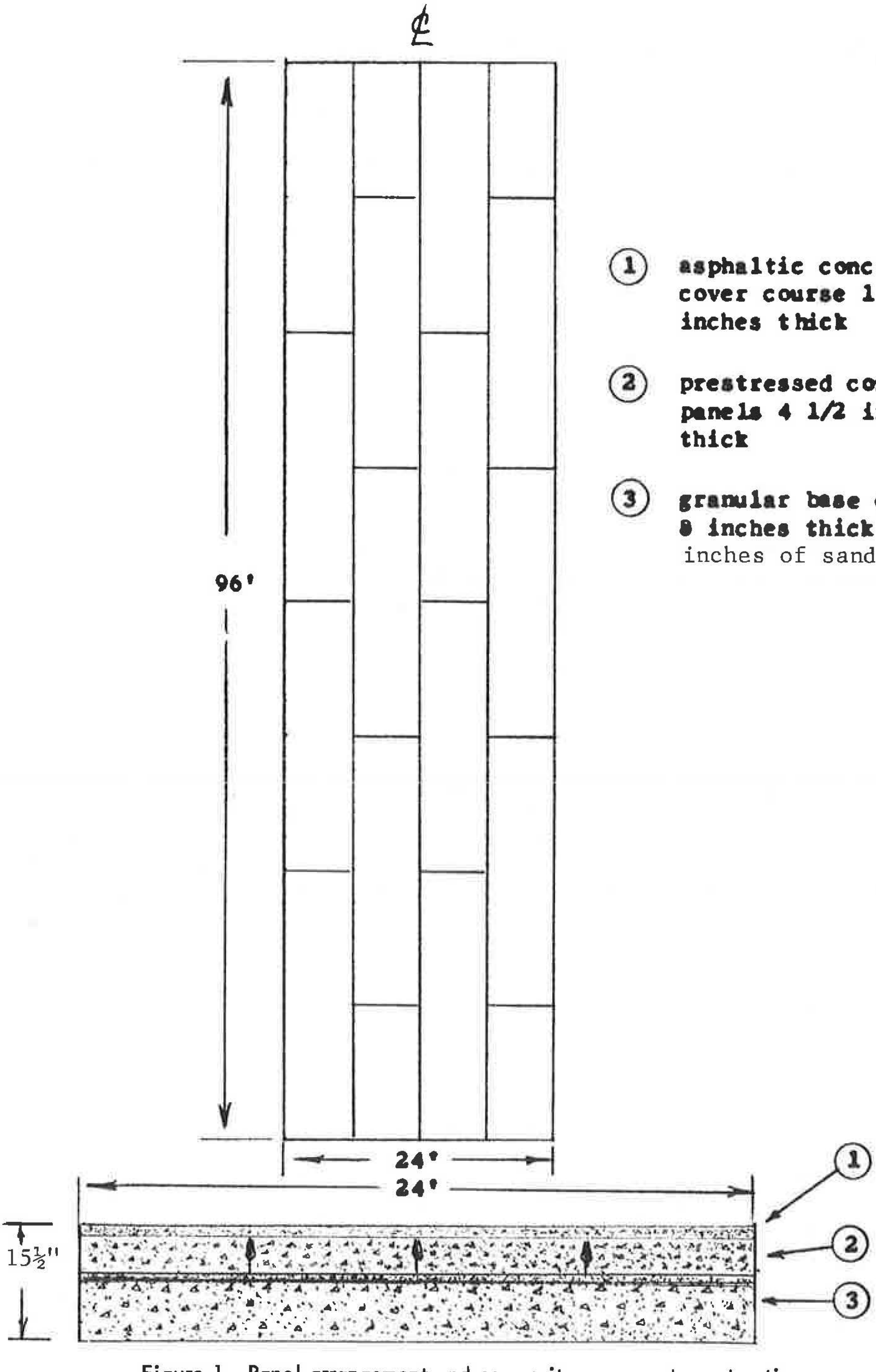

1 asphaltic concrete cover course 1 1/2 inches thick

2 prestressed concrete panels 4 1/2 inches thick

3 granular base course 8 inches thick + 1½ inches of sand bedding

Figure 1. Panel arrangement and composite pavement construction.

vestigation. Figure 2 shows a half section of an interior panel with connectors and grout keys. Figure 3 shows the details for the tongue-and-fork connectors. The panels were designed for a longitudinal prestress of 350 psi. Nine 7-strand tendons of $\frac{3}{8}$-in. diameter were used to develop the 350-psi uniform prestress in the longitudinal direction.

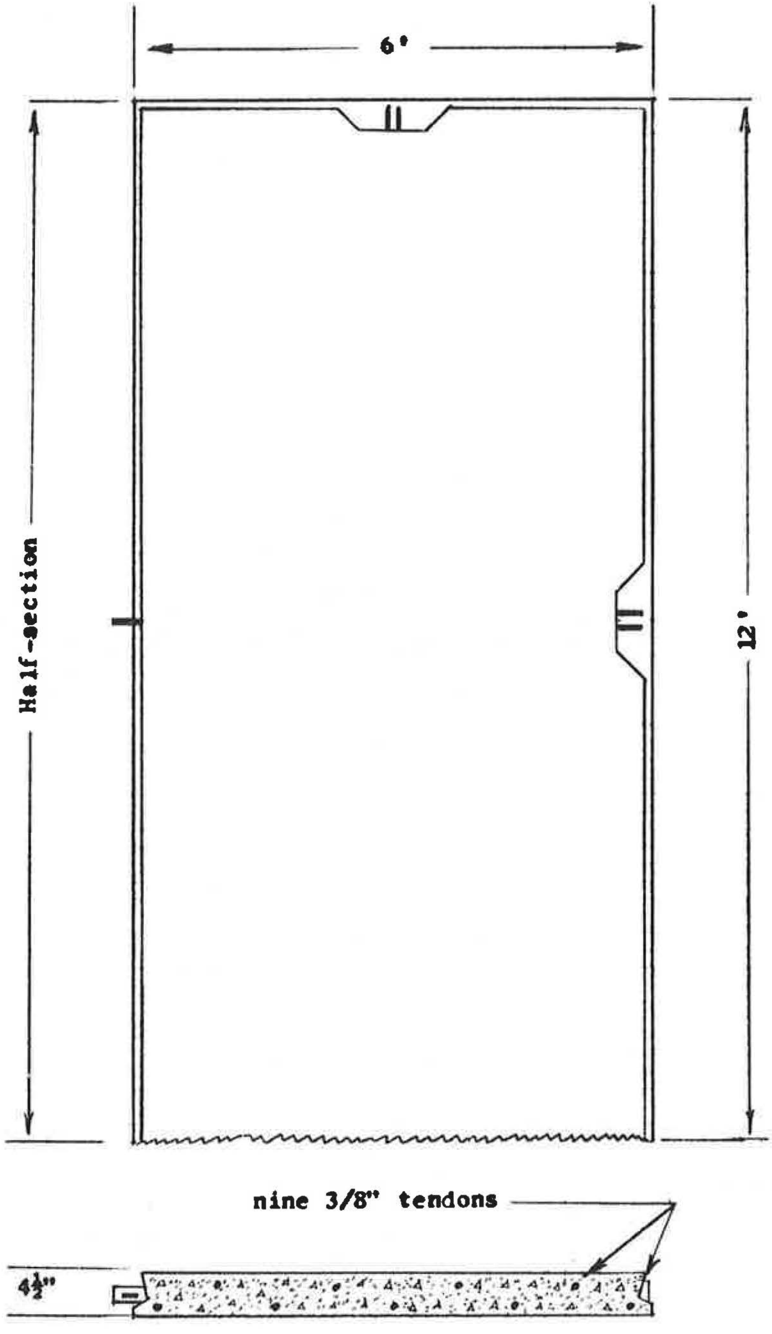

Figure 2. Half-section of an interior panel with connectors.

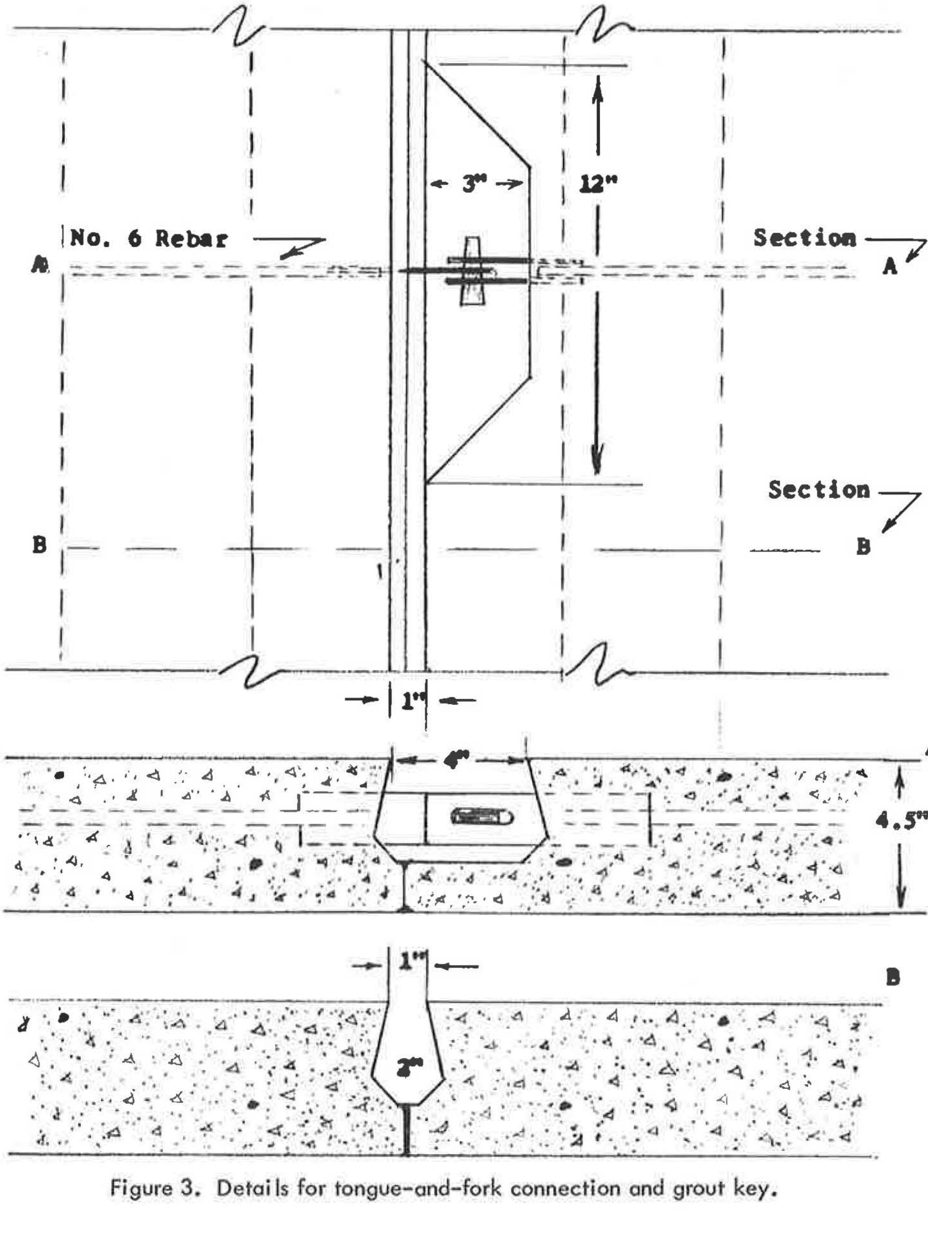

Figure 3. Details for tongue-and-fork connection and grout key.

CONSTRUCTION AND CONSTRUCTION COSTS

The test section was prepared for placement of the panels by the South Dakota Department of Highways. The work items consisted of shaping and compacting the subgrade, constructing an 8-in. granular base course, and placing the sand bedding course. The subgrade material consisted of silty clay and black topsoil with a maximum dry density of 112.0 pcf. Compaction of 99 percent of standard Proctor was obtained from one field density test. The base course material was predominately fine grained; 74 percent passed the No. 4 sieve and 3 percent passed the No. 200 sieve. A vibratory compactor was used to compact the base course. The sand used for the bedding course met ASTM specification C 33-63 for fine aggregate for portland cement concrete. In order to exercise strict control over the grading of the sand, it was necessary to fine-grade

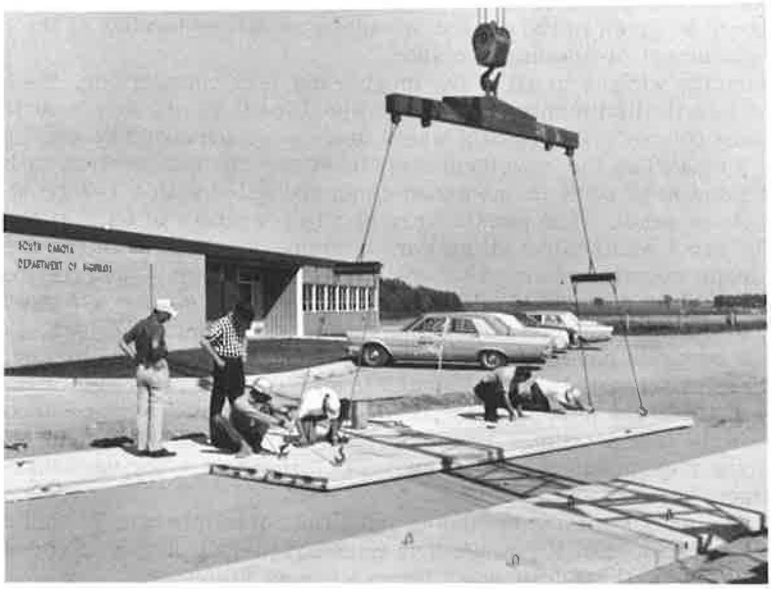

Figure 4. Field placement of prestressed panels.

the sand bedding course by hand with the use of screed strips and "blue tops." The sand bedding course was prepared the same day that the panels were laid.

The prestressed panels were produced and laid by Gage Brothers Concrete Products Co. of Sioux Falls. Figure 4 shows the placement of the prestressed panels during September 1966. No major difficulty was encountered during the laying operation. The construction tolerances in the panel dimensions did not affect the positioning of the panels in this 96-ft test section. Observations were made regarding the need for further simplification of the tongue-and-fork connection. The limited tolerance in the vertical alignment of the slots in the tongue-and-fork connections made it difficult to insert the wedge, as shown in Figure 5. The tolerance was further restricted by the section of concrete below the fork. In a few cases, this section of concrete served as

Figure 5. Inserting the wedge in a tongue-and-fork connection.

a bearing area for the tongue from the adjacent panel. It was decided that further consideration should be given to the design of panel connectors in view of the high material cost and the placement problems described.

After driving the wedges in all of the tongue-and-fork connections, the test section was subjected to a limited number of impact wheel loads in order to seat the panels in the sand bedding course. The impact wheel loads were produced by placing timbers (2 by 4's and 4 by 4's) on the pavement and traversing the test section with a front-end loader. The grout keys were then washed clean and filled with a 1-2 grout (1 part of cement, 2 parts of sand). The panels were at a temperature of 68 F at the time of grouting. The grout was sealed with a curing compound about 2 hours after placement. The pick-up loops were then burned off with an electric welder, and the test section was closed to traffic for a period of 7 days to let the grout cure. A 7-day (field-cured) test cylinder of the grout developed a compressive strength of 4775 psi.

The asphalt concrete cover course was applied to the surface by blading and rolling about 2 weeks after the panels were grouted together. The reference markers (bolts) were then installed in the pavement for the measurement of expansion and contraction of the panels in the test section. A temperature well was installed near the edge of the pavement for the measurement of differences in temperature for various depths in the pavement structure.

Unit construction costs were computed from the actual charges submitted by the South Dakota Department of Highways and Gage Brothers Concrete Products Company. Construction costs for the major work items were as follows:

Item	Unit Cost	Total Cost
Compacted 8-in. granular base course	\$ 0.39/S.Y.	\$ 101
Sand bedding course 1½-in. thick	\$ 0.30/S.Y.	78
Prestressed concrete panels	\$11.33/S.Y.	2900
Transportation of panels and panel placement	L.S.	350
Grouting panels	\$ 0.13/lin. ft.	50
Bituminous cover course 1½-in. thick	\$ 0.86/S.Y.	220
Total	\$14.45/S.Y.	\$3699

STUDY OF STRUCTURAL PERFORMANCE

The field study of the structural performance of the composite pavement consisted of the following measurements and observations:

1. Measurements of contraction and expansion of the panels due to changes in temperature.
2. Benkelman beam measurements of pavement deflections under dynamic wheel loads.
3. Measurement of plate load vs pavement deflection according to ASTM Standard Test D1196-64.
4. Visual observation of pavement performance under traffic and actual weathering conditions.

Measurements of Temperature Contractions and Expansions

Permanent reference markers were set in the pavement for the measurement of contraction and expansion resulting from changes in temperature. The reference markers were established by grouting bolts in holes drilled into the prestressed panels. The bolt heads were drilled and tapped for ¼-in. Allen screws. When measurements

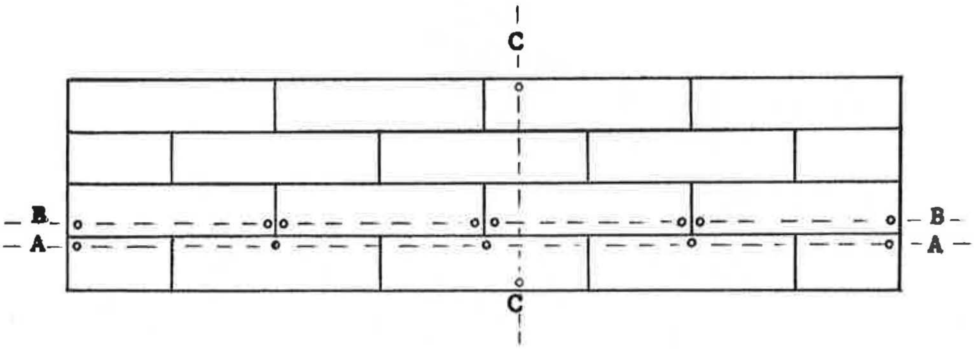

Figure 6. Location of reference markers in the test section.

were made, the Allen screws were removed and replaced with short studs for reference "stops." Figure 6 shows the arrangement of permanent reference markers in the test section. Measurements were made of the contractions and expansions in the entire length of the test section, as well as the contractions and expansions reflected at transverse panel joints.

The changes in the length and width of the test section were measured with a 100-ft steel tape equipped with one sliding stop and one fixed stop. The tape was used to measure changes in the lengths of lines A, B, and C in Figure 6. Table 1 shows the lengths of these three lines for various changes in air temperature.

These measurements show an average contraction of 0.019 ft in the length of the test section due to a 78-deg change in temperature. However, the transverse contraction obtained from measurements along line C was found to be 0.010 ft for the same change in temperature. These data indicate that the transverse panel joints accommodated approximately 50 percent of the longitudinal contraction.

The contractions at transverse panel joints were measured with an extensometer (Fig. 7). When the air temperature was decreased 78 deg, a contraction of 0.005 in. was measured at the transverse panel joint at the center of the test section. Measurements indicate that the two transverse panel joints 24 ft from the end of the test section accommodated contractions of 0.003 in. and 0.004 in. The primary forces resisting contraction consist of the resistance offered by the panel connector, friction along the joint, and subgrade friction. The accumulation of stress resulting from expansion will be dictated in a large measure by the level of end restraint developed between individual panels.

The maximum changes in length of a 24-ft panel are as follows: expansion = 0.086 in. for a 60 deg change in temperature, contraction = 0.144 in. for a 100 deg change. The joints between 24-ft panels may be designed to accommodate expansion (0.086 in.). Therefore, the composite pavement could be constructed as a continuous pavement as far as expansion is concerned. However, the magnitude of contraction precludes construction as a continuous pavement. The distance between contraction joints is

TABLE 1

PAVEMENT DIMENSIONS VS CHANGES IN TEMPERATURE

Change in Air Temp. (deg F)	Line A (ft)	Line B (ft)	Line C (ft)
0	94.940	94.925	23.150
-22	94.941	94.925	23.149
-13	94.941	94.922	23.149
-42	94.934	94.923	23.148
-49	94.930	94.910	23.143
-29	94.926	94.904	23.145
-20	94.938	94.919	23.147
-78	94.922	94.905	23.140
-49	94.925	94.910	23.144
-46	94.924	94.911	23.143
-53	94.924	94.907	23.142
-19	94.937	94.919	23.146
- 8	94.936	94.921	23.149
+ 1	94.936	94.921	23.149

Figure 7. Extensometer used to measure contractions and expansions at panel joints.

dictated by subgrade friction and the tensile strength in the critical cross-sectional area in pavement. In the following expression the tensile force in the pavement is equal to the force of subgrade friction developed in one-half of the distance between joints:

(Area of concrete) (prestress + tensile stress) = (Normal force) (Coefficient of friction)

The area of concrete, A_c, is critical at one-half the distance between contraction joints (L/2). The critical area consists of the two panels adjacent to the two transverse panel joints. The level of prestress, f_p, in the panels was equal to 350 psi. The tensile strength, f_t, in the concrete is assumed to be about 500 psi. A coefficient of subgrade friction of 0.5 is used since the smooth face of the panel is laid on the ground. A weight of 156 pcf is used for the weight of the pavement, W_c, ($4\frac{1}{2}$ in. prestressed concrete + $1\frac{1}{2}$ in. of asphalt). These data are used to determine the length between contraction joints according to the following formula:

$$
\begin{aligned}
A_c\ (f_p + f_t) &= W_c\ (C_f)\ (L/2) \\
2 \times 6 \times 12 \times 4.5\ (350 + 500) &= 6/12 \times 24 \times 156 \times 0.5 \times L/2 \\
648\ (850) &= 468\ L \\
L &= 1175 \text{ ft}
\end{aligned}
$$

It may be possible to increase this length, L, after analyzing the effects of reversed contraction forces in adjacent longitudinal panels (longitudinal panel arrangement).

Relative elevations of the 15 reference markers (bolts) were determined during the fall and spring with an engineer's level. These elevations failed to reveal any significant changes in the vertical alignment of the panel assembly.

Benkelman Beam Deflections

Benkelman beam equipment was used for the study of load-deflection characteristics of the composite pavement. The pavement was loaded with a 9000-lb wheel load and 85-psi tire pressure. Measurements of pavement deflection were obtained during the fall of 1966 and the spring of 1967. Pavement deflections were measured at panel joints and panel interiors along the two wheelpaths. Locations of the Benkelman beam test stations are shown in Figure 8. Pavement deflections measured at these stations

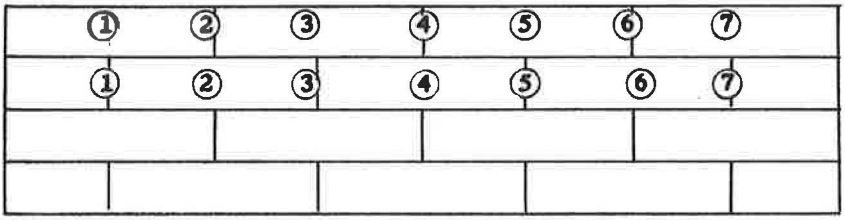

Figure 8. Location of Benkelman beam test stations.

TABLE 2

BENKELMAN BEAM DEFLECTIONS
(Thousandths of an inch)

Test Station No.	Beam Deflections—Fall 1966		Beam Deflections—Spring 1967	
	Panel Interior	Panel Joint	Panel Interior	Panel Joint
1	24	40	24	22
2	26	38	16	28
3	32	48	20	26
4	32	52	18	26
5	28	38	24	30
6	26	38	18	30
7	32	22	20	26

Figure 9. Field equipment for Benkelman beam deflections.

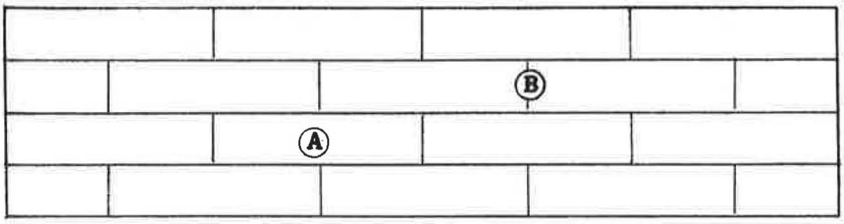

Figure 10. Location of plate bearing tests.

are given in Table 2. Figure 9 shows the equipment used to measure pavement deflections.

The test data show an increase in pavement firmness during the winter months (October 1966-April 1967). Part of this increase in pavement firmness is attributed to the densification of the sand bedding course under traffic.

Plate Bearing Tests

A further study of the load-deflection characteristics of the pavement was made from plate bearing tests. The Physical Research Division of the Department of Highways made the tests according to ASTM Standard Method D 1196-64. The plate bearing tests were made at two locations during the fall of 1966 and spring of 1967 (Fig. 10). The center of one of the prestressed panels was selected for one of the test locations (A) and the other was located at a transverse panel joint (B). These two locations were tested with 15- and 18-in. plates. Figure 11 shows the equipment used for the plate bearing tests. Table 3 gives the plate load test data obtained.

Measurements were made during the spring to determine the radius of influence for the 18-in. plate load. The following deflections were obtained from a 46, 000-lb plate load: 0.038 in., 4 ft from the plate; 0.012 in., 8 ft from the plate; and 0.003 in., 10 ft from the plate. These deflections indicate that the 46,000-lb plate load was distributed over an area approximately 24 ft in diameter. This deflection pattern reflects favorable structural performance.

Figure 11. Field equipment for plate bearing tests.

TABLE 3

PLATE LOAD TEST DATA

Location	15-in. Plate		18-in. Plate	
	Plate Pressure (psi)	Deflection (in.)	Plate Pressure (psi)	Deflection (in.)
	October 1966			
A	93	0.053	70	0.049
	158	0.103	118	0.090
	196	0.143	162	0.135
	239	0.187	194	0.180
	0	0.073	0	0.041
B	109	0.064	43	0.048
	141	0.096	80	0.098
	182	0.151	116	0.145
	229	0.205	154	0.200
	0	0.074	0	0.039
	April 1967			
A	76	0.048	47	0.038
	149	0.092	94	0.080
	218	0.140	137	0.127
	280	0.202	181	0.183
	0	0.027	0	0.028
B	44	0.037	25	0.040
	90	0.083	55	0.083
	137	0.122	84	0.128
	155	0.165	125	0.192
	194	0.214	0	0.038
	0	0.050		

The plate bearing data in Table 3 show that the pavement deflections measured at the panel joint during the spring were larger than the corresponding deflections measured during the fall. However, at the panel interior the deflections obtained from the 15-in. plate test were larger in the fall than the corresponding deflections measured during the spring. It is believed that the deflections measured at the panel joint during the fall reflected the effects of bonding between the grout key and the panels. This bonding effect was unquestionably destroyed by the first series of plate load tests. The increase in pavement firmness at the panel interior may be attributed to a densification of the base material.

VISUAL OBSERVATIONS OF PAVEMENT PERFORMANCE

The limited visual observations of pavement performance are considered significant even though the field test conditions were not severe. The test conditions were established by collecting traffic and weather control data.

A traffic counter was used during the fall of 1966 for a measure of the traffic carried by the test section. The average daily traffic was 25 vehicles per day for the period surveyed. A major part of the traffic consisted of vehicles weighing less than 4000 lb. However, the South Dakota Department of Highways hauled approximately 120 truckloads of cold mix across the test section during the last two weeks in November. The truck loads ranged between 22,000 and 26,000 lb (gross weight).

The weather control data consist of maximum and minimum temperatures and averages of the maximums and minimums for the period from September 1966 through April 1967. These temperatures are shown in Table 4.

The composite pavement demonstrated favorable structural performance during the observation period. There were no indications of joint failure or changes in the vertical alignment in the test section. Reflection cracks corresponding to panel joints did appear in the asphalt surface about one month after the surface was applied. These cracks were attributed to the "hinge action" of the pavement at the panel joints. Very small cracks developed along the transverse grout keys due to contraction of the panels at lower temperatures. These cracks provide contraction joints for the pavement with-

TABLE 4

TEMPERATURE CONTROL DATA FOR BROOKINGS[a]

Period	Minimum	Maximum	Average Minimum	Average Maximum
Sept. 1966	30	86	46	71
Oct. 1966	17	84	32	60
Nov. 1966	-11	58	15	40
Dec. 1966	-24	43	6	26
Jan. 1967	-21	46	4	26
Feb. 1967	-23	48	-4	20
March 1967	-10	20	20	44
April 1967	19	78	32	54

[a]U.S. Weather Bureau figures.

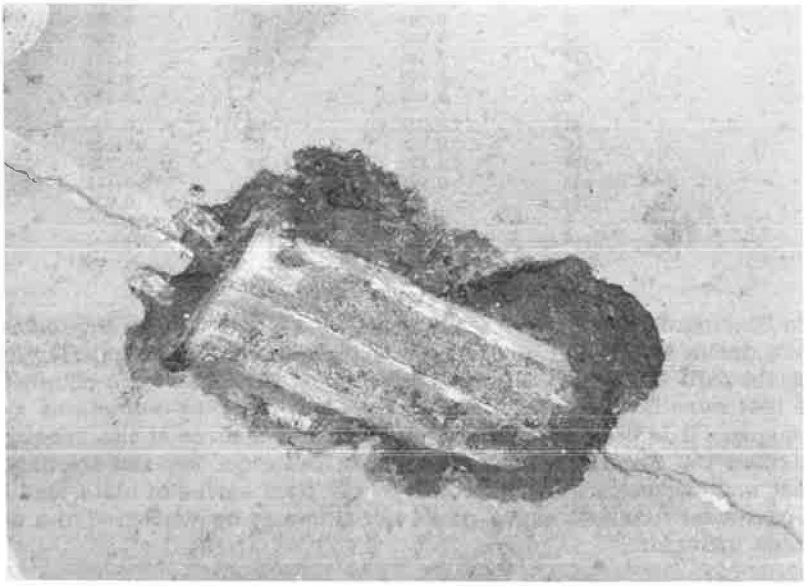

Figure 12. Tension cracks in the grout key and reflection cracks in the asphalt surface.

out affecting the riding characteristics of the asphalt surface. Figure 12 shows a crack along the grout key and the reflection crack in the asphalt surface. There was evidence of the grout spalling along the contraction crack. This was attributed to the hinge action between the panels.

There was some indication of pavement pumping during the time the pavement was subjected to heavy truckloads. This evidence appeared at the lower end of the test section. Some of the sand was pumped through the crack that developed at the end of the test section. It is believed that this condition was caused primarily by impact wheel loads applied to the ends of the resilient panels.

DISCUSSION

Field placement of 4-ton prestressed concrete panels for highway construction did not reveal any significant placement or construction problems. The placement and fine grading of the sand bedding course by hand was a time-consuming operation. This problem may be eliminated with the use of mechanical equipment normally available

for a large-scale operation. The bedding course should consist of material that is not susceptible to pumping action.

Field measurements indicate that the longitudinal panel arrangement facilitates a distribution of the pavement contraction throughout the pavement. The staggered pattern of 6-ft transverse joints coupled with longitudinal friction joints precludes a significant build-up of contraction stresses. Calculations indicate the feasibility of constructing sections of this type of pavement 1175 ft long without any special provisions for contraction. However, due consideration should be given to the maximum and minimum field temperatures anticipated and the temperature of the panels at the time of placement in order to provide panel spacings that are balanced for contraction and expansion.

An increase in pavement firmness was observed after the first winter. Part of this increase was attributed to a densification of the base material and sand bedding course under traffic. There was no indication of a significant change in the supporting capacity of the pavement due to pumping.

The primary purpose of the measurement of plate loadings and corresponding deflections was to evaluate the wheel load distributions. Test data show that the wheel load was distributed over the width of the 24-ft pavement. The flexible but spread footing effect, developed through the use of prestressed concrete panels, is recognized as one of the favorable characteristics of this type of pavement.

The observations of the structural performance of this type of pavement during the first year of service were favorable. The interconnected panels demonstrated a continuous slab effect. The reflection cracking of the asphalt at the transverse panel joints is not considered a serious problem.

This type of pavement holds definite promise for the increasing demand for a construction method that may be used under unfavorable weather conditions and without causing a major disruption in the normal flow of traffic. It offers even greater promise for airports in view of the increasing demand for methods that may be used to reinforce existing airport pavements, taxiways, and aprons without disrupting the normal airport operation.

ACKNOWLEDGMENTS

Acknowledgments are extended to the South Dakota Department of Highways in cooperation with the U.S. Bureau of Public Roads for the financial support and the excellent cooperation that made this investigation possible. An acknowledgment is extended to Gage Brothers Concrete Products Co. for an outstanding spirit of cooperation in this program for the development of prestressed panels, and the construction of a test section of composite pavement.

A Statewide Deflection Study of Continuously Reinforced Concrete Pavement in Texas

B. F. McCULLOUGH and HARVEY J. TREYBIG
Highway Design Division, Texas Highway Department

This report summarizes a performance study of continuously reinforced concrete pavement in terms of load-deflection studies. In this study the following factors affecting pavement performance were considered: subgrade support, subbase type, concrete modulus of elasticity, concrete modulus of rupture, pavement thickness, season of the year, and soil moisture condition. The effect of each of the factors on the deflection and stress or curvature is discussed.

The variables that significantly affect deflection and radius of curvature are correlated into model equations. The constants in the equations were determined from the data using multiple regression techniques. This study validates some initial assumptions made in the design and development of continuously reinforced concrete pavement for Texas conditions.

•THIS report is a part of a continuing study by the Texas Highway Department pertaining to the development and design of continuously reinforced concrete pavement (CRCP) in Texas. The Texas Highway Department pioneered the use of CRCP in the Southwest with the construction of an experimental pavement in Fort Worth during 1951. Recent reports issued by the Concrete Reinforcing Steel Institute indicate that Texas now has more mileage of CRCP than any other state (1).

During the initial design development stages of CRCP in Texas, several assumptions were made, which the authors wish to reiterate at this point. Among the initial assumptions were the following:

1. To prevent pavement deterioration, the transverse cracks in the pavement must be of small enough magnitude to permit the retention of granular interlock and prevent the entrance of water. If sufficient granular interlock is maintained, then 100 percent load transfer will be experienced across the crack and thus the pavement continuity will be maintained (2).

2. The Westergaard interior loading condition was used for determining the pavement thickness, with additional steel being used at the edge to compensate for the difference in required thickness between an edge and interior loading condition. This approach results in a 1- to 2-in. thinner pavement than would be obtained with normal procedures used in designing jointed concrete pavements (3, 4).

Although the AASHO Road Test provided valuable information for use in the design and construction of rigid pavements, numerous areas remain to be investigated, especially in the field of CRCP, since this pavement type was not covered at the Road Test (5). The deflection data obtained at the AASHO Road Test are difficult to extrapolate to a formula for the design of continuous pavement in Texas because (a) they are not directly applicable to this pavement type, (b) only one natural soil type and strength was considered, (c) only one concrete modulus of elasticity was used, and (d) lime stabilization was not included.

To establish the effect of these parameters and verify the original design assumptions, the Texas Highway Department in 1963 initiated a large research project to

Paper sponsored by Committee on Rigid Pavement Design and presented at the 47th Annual Meeting.

investigate the performance of continuously reinforced concrete pavement. This is the fifth report in connection with this study and the third relating to pavement deflection. The earlier reports pertain to equipment and technique development (6), deflection study on an experimental pavement section (7), and a 24-hour deflection study on several new untrafficked pavements (8).

Since 1963, in excess of 15,000 individual measurements of deflection, radius of curvature, crack width, and temperature have been taken on numerous continuous pavements located throughout the state. The schedule of field observations is given in Table 1. Many of the procedures and techniques used are those developed at the AASHO Road Test or modifications thereof (5, 6). Much work has been done by the Texas Highway Department in developing experimental techniques for studying CRCP.

TABLE 1

SCHEDULE OF FIELD OBSERVATIONS

Run No.	Season	Date Ran
1	Fall	Oct.-Dec. 1963
2	Winter	Jan.-Mar. 1964
3	Summer	June-July 1964
4	Spring	Mar.-Apr. 1965

The overall objective of this investigation is to determine the effects of design variables on pavement deflection and radius of curvature. After establishing the parameters considered to be variables, a statistical expression will be derived that can be used for calculating the deflection and radius of curvature produced by a wheel load on continuous pavement. In addition, the assumptions used in the original design analysis of CRCP will be investigated to determine their validity.

DESCRIPTION OF EXPERIMENT

Factorial Design

The entire experiment was functional through a factorial design that encompassed the variables involved in pavement design. The chart representing the factorial

X = 8" CRCP Y = 6" CRCP

Subgrade Support	Subbase Type	Subbase Material	Modulus of Elasticity: 3,500,000 psi; Concrete Flexural Strength: Low 580 psi(-)	3,500,000 psi; Medium 580-690 psi	3,500,000 psi; High 690 psi(+)	5,500,000 psi; Low 580 psi(-)	5,500,000 psi; Medium 580-690 psi	5,500,000 psi; High 690 psi(+)	Line
Poor 5.5+	Non-Stabilized	Fine Grain		XY			XX		1
		Crushed Stone		XX			X	X	2
	Stabilized	Cement		X	X		XXY	XY	3
		Asphalt		XY	X		X		4
		Lime	X	X					5
Fair 5.0-5.5	Non-Stabilized	Fine Grain		X			X		6
		Crushed Stone		X	X				7
	Stabilized	Cement					XX		8
		Asphalt		X			X		9
		Lime		X					10
Good 4.0-5.0	Non-Stabilized	Fine Grain		X			XXX		11
		Crushed Stone		X			X	X	12
	Stabilized	Cement		X			XXXY	XY	13
		Asphalt		X					14
		Lime		XY			X		15
Column			1	2	3	4	5	6	

Figure 1. Experiment design for continuously reinforced concrete pavement.

J8 = 8" Slab J9 = 9" Slab J10 = 10" Slab

Subgrade Support	Subbase Type	Subbase Material	Modulus of Elasticity 3,500,000 psi — Concrete Flexural Strength Low 580 psi (-)	3,500,000 psi — Medium 580-690 psi	3,500,000 psi — High 690 psi (+)	5,500,000 psi — Low 580 psi (-)	5,500,000 psi — Medium 580-690 psi	5,500,000 psi — High 690 psi (+)	Line
Poor 5.5 +	Non-Stabilized	Fine Grain		J10					1
		Crushed Stone		J9, J10			J8, J9, J10		2
	Stabilized	Cement							3
		Asphalt							4
		Lime		J9, J10					5
Fair 5.0 - 5.5	Non-Stabilized	Fine Grain					J8		6
		Crushed Stone		J10			J8, J9, J10		7
	Stabilized	Cement							8
		Asphalt							9
		Lime		J10					10
Good 4.0 - 5.0	Non-Stabilized	Fine Grain		J10			J9		11
		Crushed Stone		J9, J10			J8, J9		12
	Stabilized	Cement					J9, J10		13
		Asphalt							14
		Lime							15
Column			1	2	3	4	5	6	

Figure 2. Experiment design for jointed concrete pavement.

experiment design in shown in Figure 1. In order to represent each entry in the factorial design for one pavement thickness, 90 different test sections would be required. Figure 1 shows the entries in the factorial table that were filled. Each symbol represents a test section; therefore, small degree of replication was provided for. It was quite impossible to fully complete the table due to the closely standardized design criteria. In this report the test sections will sometimes be referred to by number; e.g., 1-6 means line 1, column 6 on the factorial.

The variables represented in the factorial are the controlled variables—the subgrade support, subbase type, concrete modulus of elasticity, and concrete modulus of rupture. Similar charts were prepared for pavement thickness. Figure 2 shows the jointed pavement test sections in factorial arrangement.

Controlled Variables

In this experiment each level of the subgrade support variable was grouped in accordance with the Texas Triaxial Classification Chart (9, 10). For this factorial, the subgrades were classified as poor, fair, and good. Only the strength parameter was used for classifying the subgrade support variable, with no attempt to further subdivide with index properties such as sand, clay, grading, plasticity, etc. For each of these classifications, the triaxial class range was as follows:

Poor:	Class	5.5	and	above
Fair:	Class	5.0	through	5.4
Good:	Class	4.0	through	4.9

(In the Texas Triaxial Classification Chart, the numbers range from Class 1.0 to Class 6.0(+). The larger the number the weaker the material.)

The subbase was categorized in two general divisions, stabilized or unstabilized. Unstabilized subbases were subdivided into two basic categories, those with fine-grain materials (natural sands) and granular material. The stabilized subbases were either lime-, cement-, or asphalt-treated base material. As was the case with subgrade support, further subdivision in accordance with index properties was not considered. Therefore, a cement-stabilized material may be an iron gravel, crushed limestone, a sand shell, etc. The subbases were generally constructed in accordance with the Standard Specifications of the Texas Highway Department (11).

The modulus of elasticity (tangent modulus of elasticity) of the concrete pavement was based on the type of coarse aggregate used. In Texas, experience indicates that concretes with siliceous river gravel coarse aggregate exhibit a modulus of elasticity of about 5.5 million psi, whereas concretes with crushed limestone aggregate have a lower modulus of about 3.5 million psi. Thus it was on this basis of coarse aggregate source within the state that the modulus of elasticity of each pavement section was selected.

The modulus of rupture was divided into three categories—low, medium and high—representing concrete flexural strength ranges of less than 580, 580 to 690, and above 690 psi respectively (modulus of rupture obtained with mid-point loading). Each of the modulus of elasticity levels was subdivided into these three levels of modulus of rupture. Most of the pavement sections entered in the factorial were in the medium range, which is considered the optimum strength for CRCP.

Pavement thickness, also a controlled variable, could not be investigated to the extent desired because most of the CRCP in Texas is 8 in. thick. There has been some 6-in. CRCP built, but in a limited number of designs. Thus, it has been quite difficult to truly examine pavements with a lesser thickness than 8 in. Two different symbols are used in Figure 1 to represent the two pavement thicknesses considered.

Figure 2 shows the jointed pavement test sections. The three thicknesses are represented by symbols indicating the slab thickness. The sections represented in column 2 of Figure 2 are plain concrete and the sections in column 5 are reinforced. The load transfer at the transverse joints was by mechanical devices. This made it possible to make direct comparisons between jointed and continuous pavement. Everything was held constant in the factorial comparison except the pavement type.

Semi-Controlled Variables

Two other variables that were given due consideration but are not shown on the factorial in Figure 1 are the season of the year and the general soil moisture condition. The field data were taken in such a manner that all pavement test sections were studied in each of the four seasons of the year. The second semi-controlled variable was the general moisture condition of the soil, which is somewhat a function of the season. Data taken in winter and spring were in general taken under wet conditions, the spring being more so. The data taken in summer and fall were taken under generally dry conditions.

Another parameter considered to be constant was the subbase thickness, which was generally 6 in. ± 2 in. Studies at the AASHO Road Test found that subbase thickness has very little effect on pavement deflection in the range of 3 to 9 in. (5). Therefore, the assumption of equal thickness is reasonable for the range of thickness considered, i.e., 4 to 8 in. The cement factor for the concrete pavement is generally $4\frac{1}{2}$ sacks per cubic yard. The longitudinal reinforcement for the pavement was approximately 0.5 percent in all cases.

Pavement Test Sections

The pavement sections used for test sections were essentially made up of three parts: the test section, the transition area, and the replicate test section. The test section and the replicate test section are both 1200 ft long and separated by a 100-ft transition area (Fig. 3). Jointed concrete pavement test sections were laid out the same as the CRCP.

West of the Balcones Fault Zone through central Texas, generally all pavements are flexible due to a combination of traffic density and availability of high-grade flexible

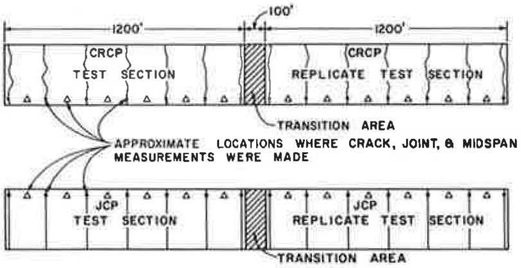

Figure 3. Layout of test pavements.

base construction materials. Consequently, the pavement test sections for this experiment were scattered throughout the eastern half of the state. Some of the criteria used in choosing the test sections were as follows:

1. The entire test section should be in a 2500-ft long tangent section with no grade in excess of 1 percent.
2. Longitudinal reinforcement should be approximately 0.5 percent steel.
3. The general soil conditions should be relatively constant as far as could be ascertained by engineering judgment and inspection.
4. The entire length, 2500 ft, when in cut or fill sections should be entirely therein to attain uniformity.
5. The structural components of the pavement must classify it into one of the 90 entries in the chart in Figure 1.
6. In no case were side-hill sections chosen for test sections.
7. The subbase must extend the entire crown-width of the roadway; trench-type sections were not considered.

Table 2 gives a brief description of materials components, location, traffic applications, etc., of the pavement test sections studied in this experiment.

METHOD OF ANALYSIS AND ACCURACY

The voluminous amount of data taken in this experiment required a careful and detailed analysis to obtain the desired end product. The 1604-A Control Data Computer was used to facilitate the analysis of the data to the greatest extent possible.

The computer program for the data reduction was written in such a fashion that all the pertinent data gathered would be presented for analysis. All data taken in the field were recorded on a data sheet, from which the data were key-punched, then processed, stored permanently on magnetic tape, and printed out. The print-out included the following: the pavement depth, identification of the test section, average crack spacing, general moisture condition of the soil, deflection data, crack width data, radius of curvature data, temperature data, and a statistical analysis of the temperature, deflection, radius of curvature, and crack width data. Also included on the computer print-out were the average deflections corrected to a zero degree temperature differential (6).

It should be emphasized here that each data point used in the following discussions and analysis represents the average of numerous readings. For each type of data point, the magnitude used to represent a test section was derived from an average of at least 14 data points.

Method of Analysis

The data were analyzed by investigating one variable at a time, i.e., holding all others constant. By using this method, it was possible to determine if the variable being studied was truly a variable or not. This method of having all but one variable constant in a comparison was made possible by the factorial design (Fig. 2). For example, in comparing subgrade support, any factorial entry under "poor" could be compared with a corresponding entry under "fair" or "good." This comparison would be clean, i.e., the subgrade support would be the only variable. This same procedure was used to investigate each variable under consideration in this study. Analysis of variance techniques were used on several of the parameters; however, not enough entries were filled in the factorial to validate the analysis of variance results, even though some trends were shown.

TABLE 2

DESCRIPTIVE INFORMATION RELATIVE TO SUBBASE AND SUBGRADE FOR THE TEST SECTIONS

Fractorial Number Line-Column	Test Section Number	County	Highway	Subbase				Subgrade			Remarks[a]
				Type	Tri-axial Class	Unconfined Compres-sive Strength[b]	Stabilization	Type	Triaxial Classifi-cation[c]	Stabili-zation	
1-2	8-13-1	Tarrant	IH 820	Dark brown sand	1.0	117	6% Lime	Black clay	5.5	5% Lime	6-in. CRCP
1-2	8-13-2	Tarrant	IH 820	Dark brown sand	1.0	117	6% Lime	Shaley clay	5.5	5% Lime	
1-5	675-7-1	Walker	IH 45	Crushed sandstone	2.2	16.1	None	Sandy clay	5.5 (1.0)	3% Lime	
1-5	675-7-2	Walker	IH 45	Crushed sandstone	2.2	16.1	None	Sandy clay	5.5 (1.0)	3% Lime	
2-2	95-4-1	Kaufman	IH 20	Crushed limestone	1.0	50	None	Taylor marl	5.5 (1.0)	4% Lime	
2-2	94-7-1	Dallas	SH 183	River gravel	3.5	15.0	None	Del borrow	5.5	None	
2-5	739-2-4	Jefferson	IH 10	6 in. Sand-shell	2.0	65	None	Clay	6.0 (1.0)	4% Lime	
2-6	15-2-1	McLennan	IH 35	4 in. Bosque gravel	3.4	20.9	None	Silty clay	5.5 (1.0)	6% Lime	
3-2	739-2-7	Jefferson	IH 10	6 in. Sand-shell	1.0	600	7.1% Cement	Clay	6.0 (1.0)	4% Lime	
3-3	156-7-1	Wichita	US 277	4 in. Sandstone	1.0	270	3.0% Cement	Clay	5.5	None	
3-5	739-2-2	Jefferson	IH 10	6 in. Sand-shell	1.0	600	7.1% Cement	Clay	5.9 (1.0)	4% Lime	
3-5	500-3-3	Harris	IH 45	6 in. Sand-shell	1.0	1100	7.0% Cement	Silty clay	5.8	None	
3-6	27-13-1	Harris	US 59	6 in. Sand-shell	1.0	1100	7.0% Cement	Silty clay	5.6	None	
4-2	675-6-1	Walker	IH 45	4 in. Bituminous concrete (crushed sandstone)	1.0	226	5% OA-90 Asphalt	Sandy clay	5.5 (1.0)	3% Lime	
4-3	156-7-2	Wichita	US 277	Sandstone	2.7	28	Asphalt	Clay	5.5	None	
4-5	495-10-1	Harrison	IH 20	6 in. Sandy clay		30	Asphalt	Silty clay	5.5	None	
5-1	14-16-2	Tarrant	IH 35	6 in. Clay	1.0	100	5% Lime	Clay	5.5	None	
5-2	8-13-3	Tarrant	IH 820	6 in. Lime-treated subgrade	1.0	115	None	Dark brown clay	5.5	None	
6-2	14-16-1	Tarrant	IH 35W	Red sand-gravel	3.5	–	None	Black clay	5.7	None	
6-5	495-4-2	Smith	IH 20	Natural soil	4.0	6.5	None	Sandy clay	5.0	None	
7-2	17-10-1	Bexar	IH 35	Crushed limestone	1.0	41.0	None	Clay	5.5	3.5% Lime	
7-3	16-5-1	Comal	IH 35	Crushed limestone	1.0	–	5% Lime	Clay	5.6	None	
8-5	500-3-2	Harris	IH 45	6 in. Sand-shell	1.0	1100	7% Cement	Silty clay	5.2	None	
8-5	739-2-1	Jefferson	IH 10	6 in. Sand-shell	1.0	600	7.1% Cement	Clay	5.2 (1.0)	4% Lime	
9-2	675-6-2	Walker	IH 45	4 in. Bituminous concrete	1.0	226	5% OA-90 Asphalt	Sandy clay	5.2 (1.0)	3% Lime	
9-5	495-10-2	Harrison	IH 20	6 in. Sandy clay		30	Asphalt	Sandy clay	4.5	None	
10-2	442-2-1	Dallas	US 67	River gravel	2.0	15.0	3% Lime	Del borrow	5.2	None	
11-2	495-4-3	Smith	IH 20	Foundation course	3.5	16.9	None	Sandy clay	4.0	None	
11-5	495-4-1	Smith	IH 20	Foundation course	4.0	6.5	None	Sandy clay	4.0	None	
11-5	675-7-3	Walker	IH 45	Crushed stone	2.2	16.1	None	Sandy clay	4.6 (1.0)	3% Lime	
12-2	9-11-1	Dallas	IH 20	River gravel	3.5	15	None		4.0	None	
12-5	739-2-5	Jefferson	IH 10	6 in. Sand-shell	2.0	65	None	Clay	4.5 (1.0)	4% Lime	
12-6	15-2-2	McLennan	IH 35	Austin chalk	3.4	20.9	None	Silty clay	4.5 (1.0)	6% Lime	
13-2	739-2-6	Jefferson	IH 10	6 in. Sand-shell	1.0	600	7.1% Cement	Clay	4.5 (1.0)	4% Lime	
13-5	271-14-3	Harris	IH 610	6 in. Sand-shell	1.0	1100	7.0% Cement	Sandy clay	4.8	None	
13-5	535-8-1	Colorado	IH 10	Sand	1.0	492	4% Cement	Silty clay	4.6	None	
13-5	610-7-2	Bowie	IH 30	8 in. Sandy clay	1.0	315	Cement	Sandy clay	4.5	None	
13-6	271-14-1	Harris	IH 610	6 in. Sand-shell	1.0	1100	7.0% Cement	Sandy clay	4.8	None	
14-2	675-6-3	Walker	IH 45	4 in. Bituminous concrete	1.0	226	5% OA-90 Asphalt	Sandy clay	4.5 (1.0)	3% Lime	
15-2	8-13-4	Tarrant	IH 820	Shaley clay	1.0	100	5% Lime	Shaley clay	4.5	None	
15-5	610-7-1	Bowie	IH 30	6 in. Clay gravel	1.0	175	Lime	Sandy clay	4.5	None	
12-2	9-11-2	Dallas	IH 20	River gravel	1.0	114	3% Lime		4.0	None	
15-2	581-1-1	Dallas	Loop 12	River gravel	1.0	70	3% Lime	Houston clay	4.5 (1.0)	4% Lime	6-in. CRCP
2-2	14-16-3	Tarrant	IH 35N	6 in. Flexible base	3.5	–	None	Clay, rocky	5.5	Mechanical	
2-2	1068-1-1	Tarrant	IH 20	6 in. Flexible base	3.0	–	None	Clay, rocky	5.5	Mechanical	
11-5	675-7-4	Walker	IH 45	Crushed sandstone	2.2	16.1	None	Sandy clay	4.6 (1.0)	3% Lime	

[a]Unless specified otherwise in the "Remarks" column all pavements are 8-in. CRCP.

[b]Unconfined compressive strength at an age of 7 days tested in accordance with THD procedures.

[c]Classifications in parentheses are after addition of lime to subgrade material.

TABLE 3

STANDARD ERROR OF THE MEAN–DEFLECTION AND RADIUS OF CURVATURE

Data Run No.	Deflection		Radius of Curvature	
	Crack	Midspan	Crack	Midspan
1	0.000904	0.000911	541	1193
2	0.000818	0.000766	586	935
3	0.000785	0.000781	583	861
4	0.000647	0.000675	1013	1172

Accuracy of Data

In order to qualify the data, it was necessary to compare the accuracy of the measurements by type and position within each test section. The likeness of the data taken from pavement sections of identical design located throughout the state indicates quality data and good experimental technique. The following analyses were made to obtain a measure of the accuracy within a test section and a measure of the accuracy between replicate test sections in the same factorial entry.

Replication Within Test Section—For each individual test section, the standard error of the mean was calculated for deflection and radius of curvature measurements taken at both the crack and midspan positions. The average of these respective measurements was then calculated for each of the four individual runs; the results are given in Table 3. The error within a section presented here is well within the measuring accuracy of the equipment used. The deflection replication within a section is less than 0.001 in. in all cases; this magnitude is considerably less than the resolution of the Benkelman beam (±0.002 in.) (12). The standard errors for the radius of curvature measurements are somewhat larger than the resolution (80 ft) or replication error (250 ft) of the Basin beam (6).

Replication Between Test Sections—To determine the error between equivalent test sections, the standard error of the mean for the test sections within a given factorial block was determined. Only factorial blocks that had replicate sections were used in this analysis, and the number of replicate sections varied from one to two. It should be pointed out that these replicate sections were sometimes in different geographical areas of the state, such as Houston and Tyler. After determining the standard error of the mean for each of the applicable factorial blocks, these values were then averaged for the four data runs. The standard errors found were as follows:

Deflection:

Crack position = ±0.00172 in.
Midspan position = ±0.00127 in.

Radius of curvature:

Crack position = ±1525 ft
Midspan position = ±2079 ft

These results indicate that the error for the data in any factorial block did not significantly exceed the measuring capability of the equipment used. Furthermore, the small error lends credence to assumptions that the test sections were properly classified in the factorial design for this experiment.

ANALYSIS OF DATA

In this section, the data analysis is presented in such a manner that one variable is studied at a time. The radius of curvature data were converted to stress by simple calculation and analyzed in terms of stress rather than the field measurement of radius of curvature. This method of conversion was covered in a previous report on this project (6). The data are presented in bar graph fashion, weighted relative to the total for any type of measurement so that the sum of the four runs is equal to 100 percent.

Controlled Variables

The controlled variables, as previously defined, are the first to be considered in this analysis. The controlled variables are broken into the categories of support properties, concrete properties, and slab thickness and type.

Support Properties—The strength property of the subgrade and its effect on deflection and stress at the crack and midspan position is investigated by comparing data from test sections that were identical except for the subgrade. These comparable sections were taken from the factorial. The weaker subgrade was evaluated in comparison with the better subgrade. There are three basic comparisons for each of the identical sections (except for subbase), i. e., poor to fair, poor to good, and fair to good. The comparisons were made by season or data run and by the total for the four seasons.

Figure 4 shows how the subgrade affected deflection in terms of the percent of the comparisons made. In each of the four seasons the pavements on the weaker subgrade deflected more than comparable pavements on better subgrades. Considering the total comparison, the weaker subgrade deflected more than the better subgrade in 67 percent of the comparisons.

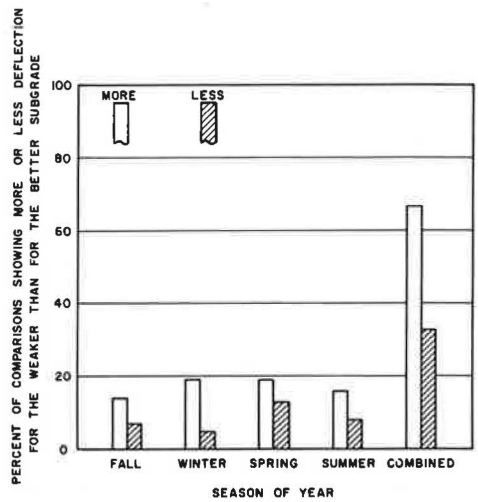

Figure 4. Deflection comparison of a weaker subgrade with a better subgrade.

Figure 5 shows how the subgrade affected concrete pavement stress in terms of the percent of comparisons made. As was the case with deflection, the pavement with the weaker subgrade experienced more stress than one with a better subgrade 60 percent of the time. In all four seasons the pavement with the weak subgrade generally had more stress than one with a better subgrade.

Inspection of Figures 4 and 5 indicates that deflection and stress are directly related to the subgrade support quality, i. e., the better the subgrade, the less deflection and stress there will be. The results for each season indicate this trend. It has been shown that CRCP with poor subgrade deflected 19 and 25 percent more on the average than CRCP with fair and good subgrade respectively. Also pavement with a fair subgrade deflected 9 percent more on the average than did the pavement with the good subgrade.

Calculations show that the CRCP with the poor subgrade had approximately the same stress as did the one with the fair subgrade; however, the pavements with the good subgrade had 15 percent less stress than the CRCP with the poor subgrade.

The subbases that were included in this study were evaluated on a comparative basis with all other variables constant. The deflection of a test section was compared with the deflection on all other types of subbases on the same subgrade class. The results for each subbase type were evaluated for each of the four seasonal data runs. The results for each season followed the same general trend. Figure 6 compares the subbases in terms of deflection on a percentage of comparisons basis (compilation of all four runs). The stabilized subbases appear to be superior to the non-stabilized materials as far as deflection is concerned. The stress analysis showed the same trends with respect to the subbase characteristic (Fig. 7).

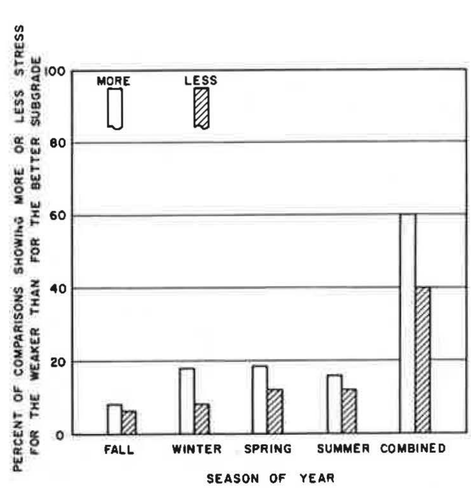

Figure 5. Stress comparison of a weaker subgrade with a better subgrade.

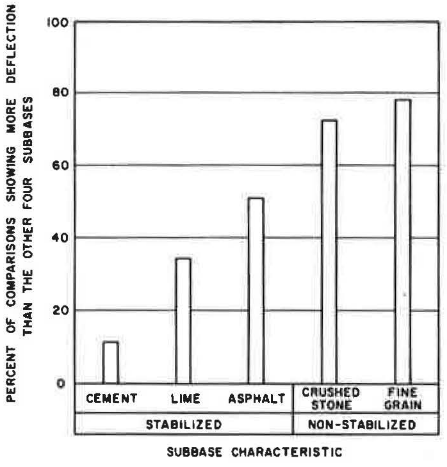

Figure 6. Deflection comparison of each subbase with the other four types.

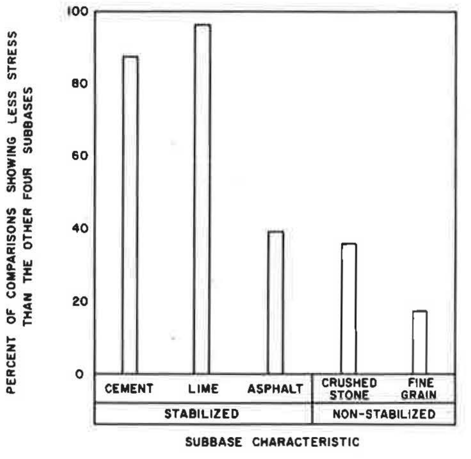

Figure 7. Stress comparison of each subbase with the other four types.

Concrete Properties—The two properties of the concrete that are part of this analysis are the modulus of elasticity and the modulus of rupture or flexural strength. The modulus of elasticity was determined from the type of coarse aggregate in the concrete. Concrete with siliceous river gravel is referred to as high modulus and that with crushed stone is referred to as low modulus of elasticity concrete. In Figure 8, for each data run and all runs combined the deflection is compared on the low and high modulus concrete. On the ordinate the percent of comparisons is plotted in which the low modulus of elasticity concrete deflected more or less than the high modulus of elasticity concrete. For each season except fall the graph has two entries. The cross-hatched bar shows the percent of comparisons made in which the low modulus of elasticty concrete deflected less than the high and the plain bar indicates the comparisons in which low

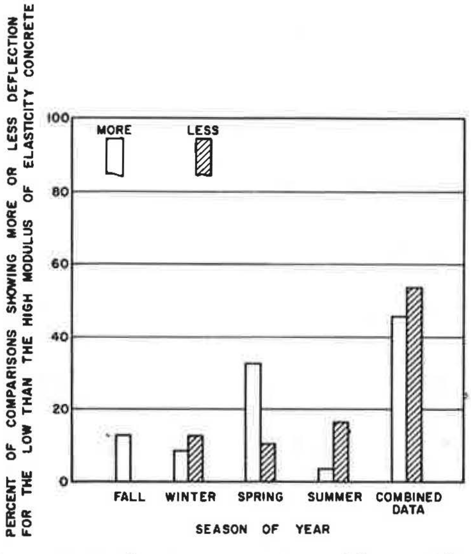

Figure 8. Deflection comparison of low and high modulus of elasticity CRCP.

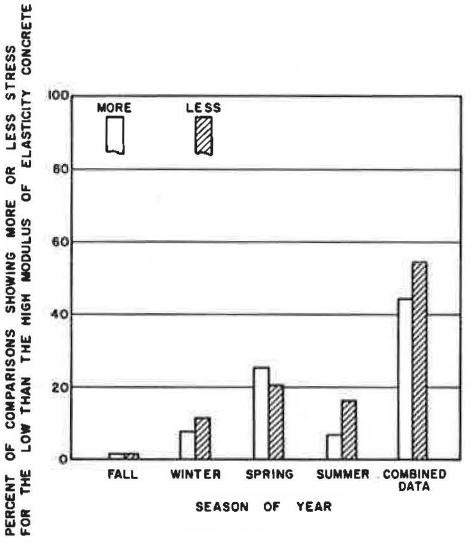

Figure 9. Stress comparison of low and high modulus of elasticity CRCP.

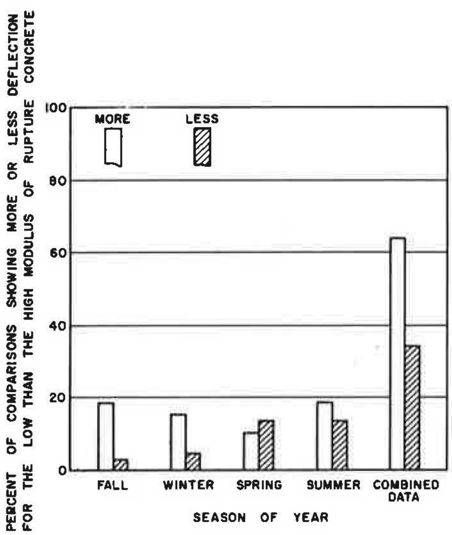

Figure 10. Deflection comparison of low and high modulus of rupture concrete.

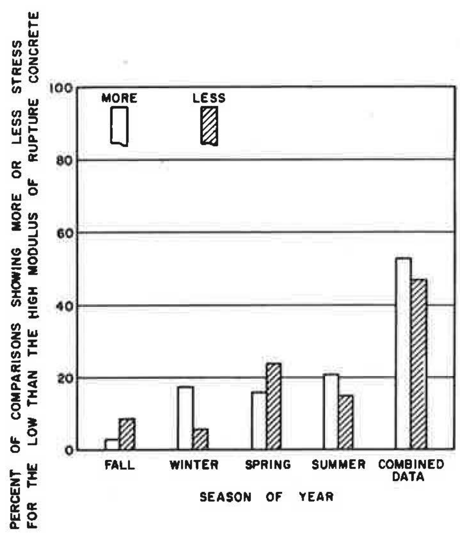

Figure 11. Stress comparison of low and high modulus of rupture concrete.

modulus deflected more than the high modulus of elasticity concrete. The range of modulus of elasticity experiencing the most deflection apparently varies slightly with season. Calculations have shown that, on the average, the lower modulus of elasticity concrete in general deflected 7.4 percent less than the high modulus of elasticity concrete. This finding, although contrary to rational reasoning, is in line with that found in another experiment (7).

Figure 9 is bar graph comparing modulus of elasticity against stress in the concrete slab. The graph structurally is the same as Figure 8 except that it portrays stress in the concrete. Inspection of Figure 9 shows that more comparisons of stress on low and high modulus of elasticity concrete showed less stress in the low than the high modulus concrete. The range of modulus of elasticity experiencing the most stress also varies with season.

The second concrete property considered here is the modulus of rupture. The analysis of the modulus of rupture was made by determining whether the deflections and stresses were more or less for the lower modulus of rupture concrete than the higher modulus of rupture CRCP. The evaluation was made for each season and also the combined data. Figure 10 shows in bar graph style the percentage of comparisons in which deflections on the high modulus of rupture concrete were more or less than those on the low modulus of rupture concrete. Note that the low modulus of rupture concrete deflects more than does the high. This was true for all seasons except for the spring. The combined data also show that the average deflection for all seasons is greater on the low modulus of rupture concrete.

The comparison of stresses on the low and high modulus of elasticity concrete indicate that, on the average, stresses were higher in the low than the high modulus of rupture concrete. Figure 11 shows the percent of comparisons in which the stress was higher or lower than that in the low modulus of rupture concrete.

Slab Thickness and Type—The pavement slab thickness analysis was made by comparing deflection measurements from sections that had identical classifications in the factorial, but different slab thickness. This allows a clean comparison of thickness to deflection and stress.

In each case the smaller thickness of concrete pavement was compared with a greater thickness. The results were combined for all four data runs. The comparison may not be very good because of the small number of sections compared.

TABLE 4

PERFORMANCE OF RIGID PAVEMENT IN TERMS OF THICKNESS, PAVEMENT TYPE, AND LOAD POSITION*

Thickness Comparison	Deflection		Stress	
	Crack or Joint	Midspan	Crack or Joint	Midspan
6-in. CRCP vs 8-in. CRCP	41.1	54.6	11.0	1.1
8-in. CRCP vs 9-in. JCP	-13.1	30.8	-50.2	-11.1
8-in. CRCP vs 10-in. JCP	-38.0	-28.5	-49.6	6.9

*Numbers indicate the average percent difference for the respective condition.

Table 4 is a summary of the results obtained in comparing pavements of different thickness and type. In comparing 6-in. CRCP with 8-in. CRCP, it was found that the 6-in. pavement deflected 41 percent more at the crack position than did the 8-in. CRCP. Comparing 8-in. CRCP with 9-in. JCP, it was found that the CRCP deflected on an average of 13.1 percent less than the JCP. When the 8-in. CRCP was compared to 10-in. JCP, it was found that the CRCP deflected on an average of 38 percent less than the 10-in. JCP.

It has been assumed in the past that 10-in. JCP performance would be very much the same as that of 8-in. CRCP (4). Performance measured in terms of deflection shows that the 8-in. CRCP is superior to the 10-in. JCP. In Figure 12 deflections as computed by the equations developed herein are plotted against deflections measured on comparable 10-in. JCP. The deflections for both pavement types have been corrected to zero temperature differential, and the deflections for CRCP were corrected to an 8-ft crack spacing and a 0.014-in. crack width. The data show a remarkable relation between the two parameters. By forcing the correlation line through zero (a rational approach), the slope of the line indicates that a 10-in. JCP deflects 1.6 times more than an 8-in. CRCP.

Deflection Position—On each test section a midspan deflection (between cracks) was obtained each time a reading was taken at the crack position. Figures 13 through 16 are plots of the average crack deflection versus the midspan deflection for each of the four runs. Although there is an offset on the vertical axis (crack deflection) greater than zero, it may be stated that the edge deflection and crack deflection are approximately equal on any range of support properties with continuous pavements that have 0.5 percent longitudinal steel or greater.

The radius of curvature measurements were also plotted in the same manner as deflection measurements (Figs. 17 through 20). In the case of radius of curvature—in contrast to deflection—the crack position has considerably less magnitude than the midspan position, which means that the concrete at the crack position is experiencing considerably more stress.

In terms of deflection and radius of curvature, it is evident that the aggregate interlock produces adequate load transfer across a crack, but the transverse cracks affect the continuity condition of the slab.

Semi-Controlled Variables

Two factors studied on a semi-controlled basis were the season of the year that the field measurements were taken and the general moisture condition of the soil.

Season—Data were taken on a statewide basis in each of the four seasons of the year. The deflection and radius of curvature data taken during these four seasons were analyzed by comparing each set of data with that taken during the summer. The comparison showed only whether the deflections and stresses were more or less in the fall, winter, and spring than in the summer. In Figure 21 these comparisons showing more or less deflection than the summer data are expressed as percentages. The results indicate that the deflections during fall and winter were generally greater than the summer, whereas the spring deflections were significantly smaller than the summer. Thus the

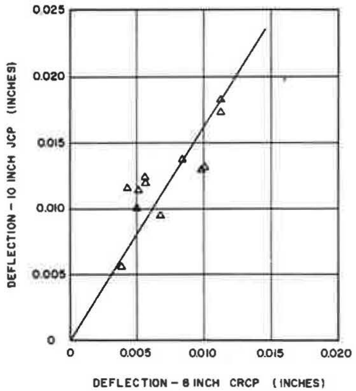

Figure 12. Calculated 8-in. CRCP deflection vs measured 10-in. JCP deflection.

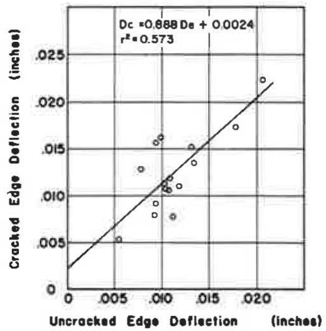

Figure 13. Cracked edge vs uncracked edge deflection—fall.

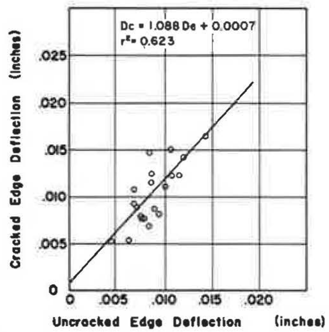

Figure 14. Cracked edge vs uncracked edge deflection—winter.

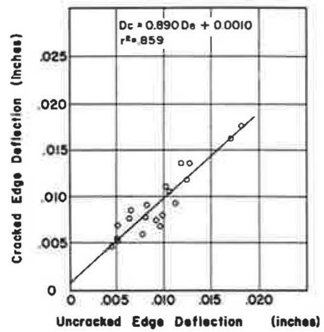

Figure 15. Cracked edge vs uncracked edge deflection—summer.

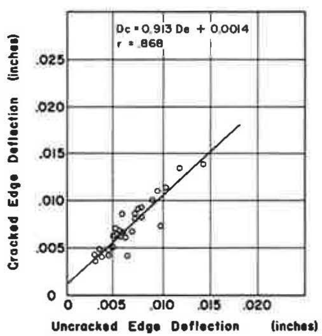

Figure 16. Cracked edge vs uncracked edge deflection—spring.

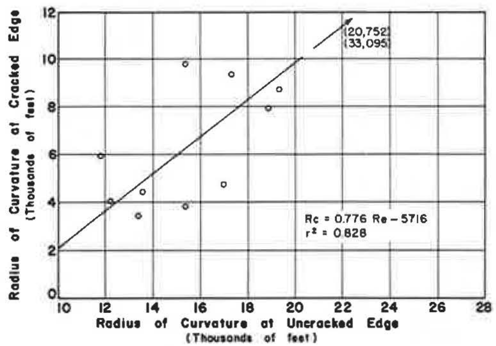

Figure 17. Cracked edge vs uncracked edge radius of curvature—fall.

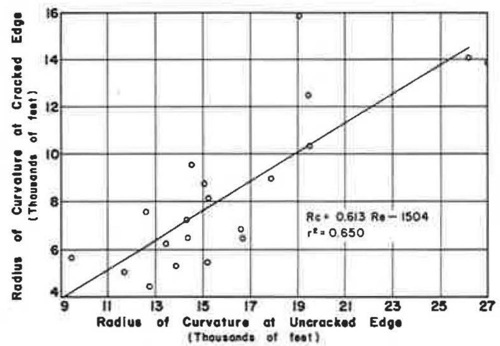

Figure 18. Cracked edge vs uncracked edge radius of curvature—winter.

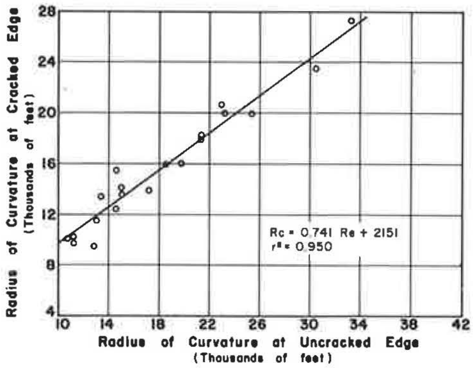

Figure 19. Cracked edge vs uncracked edge radius of curvature—summer.

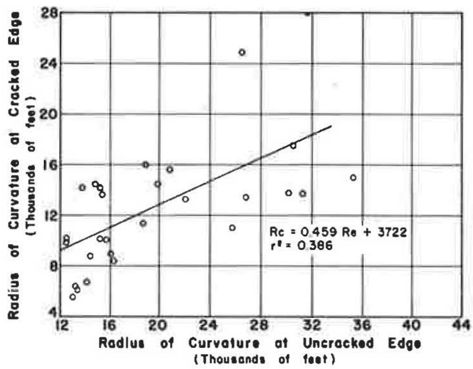

Figure 20. Cracked edge vs uncracked edge radius of curvature—spring.

deflection might in some way be related to the season; however, for the fall and winter there was not very much difference in the data.

The results of the stress analysis shown in Figure 22 indicate that the seasonal comparisons with the summer data are consistent in showing that the pavements experience less stress in the summer than during the other seasons.

Soil Moisture Condition—Each time data were taken on a test section, the general environmental conditions of the soil adjacent to the roadway in a hole 1 ft deep was classified as dry, moist, or wet. As far as the moisture effects are concerned, it was found that the fourth data run, which was the spring run, measured deflections that were much less. During the entire spring run general rains were experienced over the state. Of the four runs, the spring run was by far the wettest.

CORRELATION OF VARIABLES

Deflection

The variables studied that affect deflection are the crack spacing, surface crack width, concrete modulus of elasticity and modulus of rupture, pavement slab thickness, pavement type, strength characteristics of the subgrade and subbase, and moisture conditions. With the exception of the semi-controlled variables and the modulus of rupture, these variables will be correlated into an equation in the following.

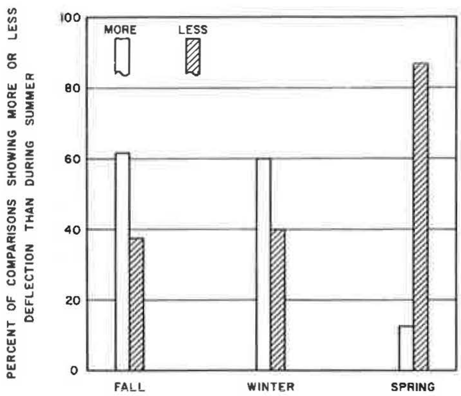

Figure 21. Seasonal comparison of deflection.

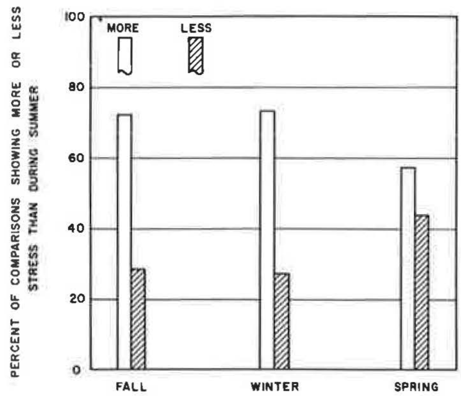

Figure 22. Seasonal comparison of stress.

A model equation was developed which encompassed the variables to be correlated. The model was based on previous work and also on work done at the AASHO Road Test (5, 8). The model chosen to relate the variables is basically an extension of the Road Test model and is of the following form:

$$D_c = \frac{A_0 \, L \, 10^{B_5 \, \Delta X} \, \overline{X}^{B_4}}{D^{1.75} \, E^{B_2} \, SS^{B_3} \, 10^{0.0147 \, T}} \tag{1}$$

where

- L = Load in kips;
- X = Surface crack width in inches;
- $\overline{X}$ = Average crack spacing in feet;
- D = Slab thickness in inches;
- E = Concrete modulus of elasticity, psi;
- SS = Soil support;
- D_c = Deflection at crack position, inches;
- D_e = Deflection at midspan position, inches;
- T = Temperature differential between top and bottom of the slab, degrees F; and

A_0, B_1, B_2, B_3, B_4, and B_5 are constants determined from a regression analysis on the data.

Slab thickness was not truly a full factorial variable, and consequently could not be entered as an independent variable and had to be analyzed separately. All the subsequent regression analyses were performed for the 8-in. pavement thickness factorial. The 1.75 power for the thickness term will be established later.

The soil support term is a combination of the subgrade and subbase strength characteristics. The soil support is a calculated value developed in a previous analysis. In some cases the natural soil was stabilized with lime (generally clay) to facilitate construction operations by providing a working platform.

The soil support is defined as

$$SS = \left(\frac{U_1 + U_2}{T_{sg}}\right) \tag{2}$$

where

- SS = Soil support;
- U = Unconfined compressive strength of subbase and subgrade materials in psi at an age of 7 days;
- T_{sg} = Texas triaxial classification of subgrade material; and
- 1, 2 = Subscripts denoting subbase and stabilized subgrade respectively.

In all subsequent analysis the load, L, will be 18 kips and the pavement slab thickness will be 8 in. The linear form of load used here has been qualified in another report on this project (7) and in studies by others (5). The data from each run were carefully analyzed to screen out what might be considered erroneous.

The power term for the temperature differential term was derived in another report on this overall study (8). The temperature differential, the pavement thickness, and the load terms were not a part of the full factorial experiment, but in order that their effect would be reflected in the A_0 term, constant values for the 8-in. factorial were inserted into the equation for variables not considered in the semi-factorial experiment. The values inserted into the equation were an 18-kip single axle load, 8 in. for pavement thickness, and zero for temperature differential. These factors were then considered as constant and moved to the left of the equation.

A multiple regression analysis was made using the computer on each data run for deflection at the crack position, D_c, and also for deflection midway between cracks, D_e. The constants and the statistics derived from the regression analysis of each of the four runs are given in Table 5.

TABLE 5

COMPUTED CONSTANTS AND STATISTICS FROM REGRESSION ANALYSIS*

Load Position	Data Run No.	Computed Values							
		A_0	B_2	B_3	B_4	B_5	r	r^2	σ
Crack	1	6.664	0.334	0.681	-0.060	3.222	0.698	0.487	±0.0032
	2	0.00256	-0.123	0.526	0.1100	13.437	0.551	0.303	±0.0029
	3	0.1220	0.104	0.690	0.0900	13.911	0.662	0.438	±0.0030
	4	0.1099	0.1249	0.6869	0.0794	13.575	0.694	0.482	±0.0021
Midspan	1	0.0118	-0.0684	0.3211	-0.1936	7.816	0.407	0.166	±0.0035
	2	0.0726	0.0418	0.3434	-0.3294	7.055	0.244	0.060	±0.0032
	3	0.00373	-0.124	0.8709	0.1814	11.798	0.733	0.538	±0.0027
	4	0.0749	0.1026	0.7179	0.1897	4.876	0.515	0.265	±0.0031

*FOR EQUATION 1: r = coefficient of correlation, r^2 = coefficient of determination, σ = standard error of estimate.

The calculated deflection was plotted against the measured deflection for each data run and for each load position. These graphs are shown in Figures 23 through 30. Note the same general pattern for runs 1, 2, and 3 for both the crack and midspan deflections. The deflections at both crack and midspan were very small on run 4, as discussed previously, when compared with the three previous data runs.

In Table 5 note that several values of B_4 are negative. This same result was the case in a previous analysis (8). The crack spacing deflection relationship is a bowl-shaped curve, concave upwards. When the crack spacing is greater than that at the point of zero slope, B_4 is positive, and when it is smaller, B_4 is negative. Figure 31 is an example of the deflection-crack spacing relationship that results in a change of signs on B_4.

Several of the values calculated for B_2 are also negative. B_2 is the exponent on the modulus of elasticity term in the model equation. A negative B_2 would be in disagreement with theoretical concepts. Earlier it was pointed out that the low modulus of elasticity CRCP was deflecting less than the high modulus of elasticity CRCP. Another investigation on an experimental CRCP showed this same factor between lightweight and conventional aggregate concrete (7).

Note that the constants for each variable term generally have approximately the same magnitude, with only a few exceptions. The data from the first three runs were comparable, and therefore they were combined and a regression analysis was run. This resulted in two final equations, one for deflection at the crack position and another for deflection at a point midway between cracks. The computed constants and statistics are given in Table 6. The equation would be applicable to a dry condition; for a wet condition the equation for run 4 would be used. Note that the standard error is only slightly greater than the resolution of the Benkelman beam.

Radius of Curvature

The radius of curvature data have been examined thus far in terms of stress, but the subsequent analysis will be in terms of the radius of curvature data.

TABLE 6

COMPUTED CONSTANTS AND STATISTICS FOR DEFLECTION EQUATIONS

Load Position	Regression Analysis Computations							
	A_0	B_2	B_3	B_4	B_5	r	r^2	σ
Crack	0.3779	0.1683	0.6513	0.0266	6.3407	0.6971	0.486	±0.0028
Midspan	0.1362	0.0977	0.5601	-0.0462	4.1266	0.5544	0.307	±0.0033

Note: r = coefficient of correlation, r^2 = coefficient of determination, σ = standard error of estimate.

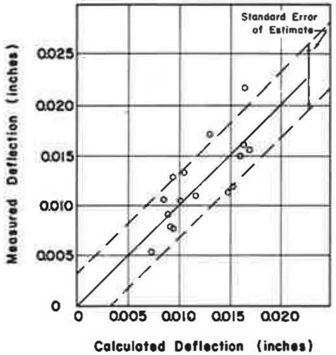

Figure 23. Measured vs calculated deflection at cracked edge—fall.

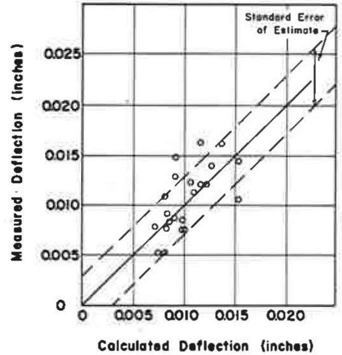

Figure 24. Measured vs calculated deflection at cracked edge—winter.

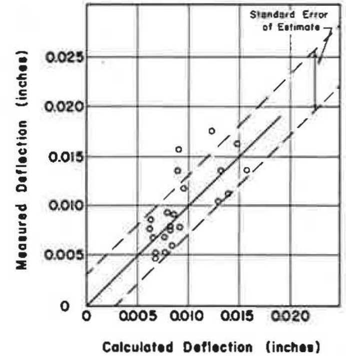

Figure 25. Measured vs calculated deflection at cracked edge—summer.

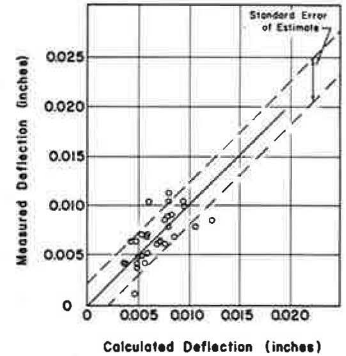

Figure 26. Measured vs calculated deflection at cracked edge—spring.

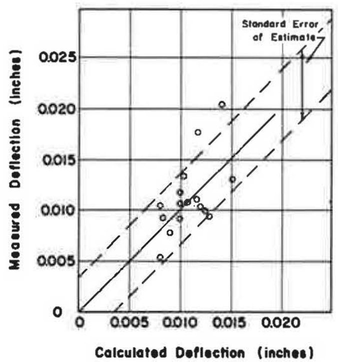

Figure 27. Measured vs calculated deflection at uncracked edge—fall.

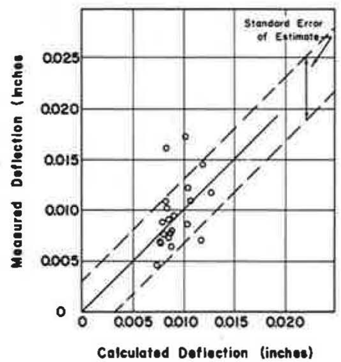

Figure 28. Measured vs calculated deflection at uncracked edge—winter.

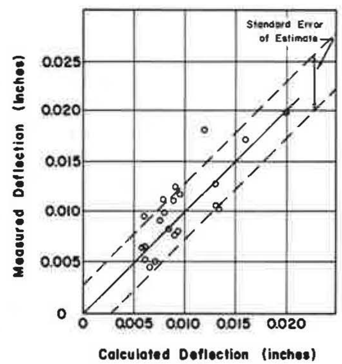

Figure 29. Measured vs calculated deflection at uncracked edge—summer.

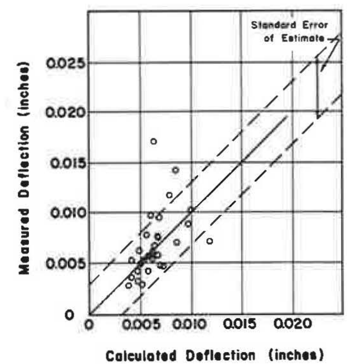

Figure 30. Measured vs calculated deflection at uncracked edge—spring.

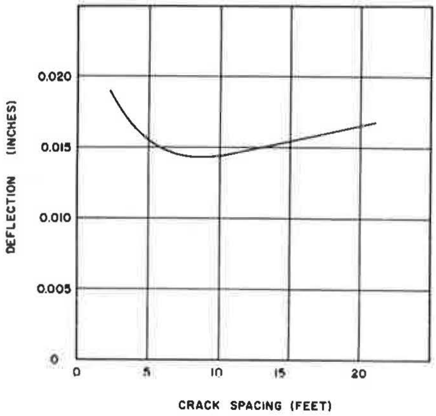

Figure 31. Deflection vs crack spacing.

The variables investigated that might affect the radius of curvature are the average crack spacing, soil support, concrete modulus of elasticity, load, and slab thickness. Thus, radius of curvature is some function of all these variables:

$$R_c, R_e = f(\overline{X}, SS, E, L, D)$$

where

R_c = Radius of curvature at crack position, and

R_e = Radius of curvature at midspan position.

All other terms have been defined previously.

A model equation for radius of curvature was logically derived using the same concept as developed in the deflection equation. The' following is the model with variables considered:

$$R_c = \frac{A_0 \, D^{1.75} \, E^{B_2} \, SS^{B_3} \, \overline{X}^{B_4}}{L} \tag{3}$$

All terms are as previously defined.

In the radius of curvature study the slab thickness again could not be entered as an independent variable because of a shortage of test sections on pavement thinner than 8 in. Thus the same thickness term was used here as in the deflection analysis, $D^{1.75}$.

Although the crack width and temperature differential are not reflected in Eq. 3, they were considered in this study and previous studies. Previous studies indicated that the effect of temperature differential on the radius of curvature was very slight or nonexistent. Therefore, on this basis, the temperature differential term was deleted. With regard to crack width, this term was included in the equation, but it was found that the statistics of correlation were improved by deleting it from the regression equation.

The radius of curvature of the CRCP is studied at two points on the continuous slab, across the volume change crack and midway between the cracks. The crack radius of curvature was analyzed for each data run except the fourth. The individual data runs were analyzed using multiple regression techniques. The regression constants for the model equation are given in Table 7. In order to obtain a more general equation for the radius of curvature at the crack position, the field data were examined and runs 1 and 2 were combined to form the data for the regression that would produce the final equation for radius of curvature at the crack position. Figures 32 through 35 show the measured radius of curvature plotted against the calculated radius of curvature for the crack position for runs 1, 2, and 3 and the combined data. The computed constants and the statistics for the final equation are given in Table 8.

TABLE 7

COMPUTED CONSTANTS AND STATISTICS FROM RADIUS OF CURVATURE ANALYSIS*

Load Position	Data Run No.	Computed Values						
		A_0	B_2	B_3	B_4	r	r^2	σ
Crack	1	0.000832	0.9819	0.6572	-0.2623	0.9518	0.9059	± 962
	2	350.5333	0.1548	0.3429	-0.1766	0.5574	0.3107	±1716
	3	53.4066	0.2898	0.4070	-0.0035	0.6900	0.4762	±2132
Midspan	1	0.0742	0.7395	0.1882	0.0277	0.9527	0.9076	± 868
	2	1779.2667	0.0639	0.3102	0.0863	0.4368	0.1908	±2247
	3	313.4298	0.1736	0.5872	0.0345	0.7503	0.5630	±2798
	4	1337.6603	0.0832	0.2894	0.1147	0.4453	0.1983	±2525

*FOR EQUATION 3: r = coefficient of correlation, r^2 = coefficient of determination, σ = standard error of estimate.

TABLE 8

COMPUTED CONSTANTS AND STATISTICS FOR RADIUS OF CURVATURE EQUATIONS

Load Position	Regression Analysis Computations						
	A_0	B_2	B_3	B_4	r	r^2	σ
Crack	15.3039	0.3312	0.5467	-0.0772	0.6391	0.4085	±1617
Midspan	333.3153	0.1729	0.3579	0.0909	0.5957	0.3548	±2508

Note: r = coefficient of correlation, r^2 = coefficient of determination, σ = standard error of estimate.

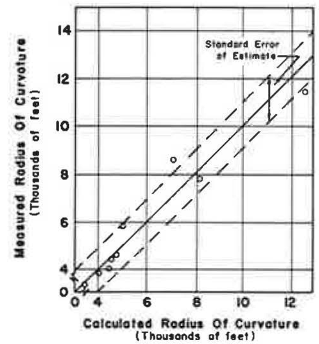

Figure 32. Measured vs calculated radius of curvature at cracked edge—fall.

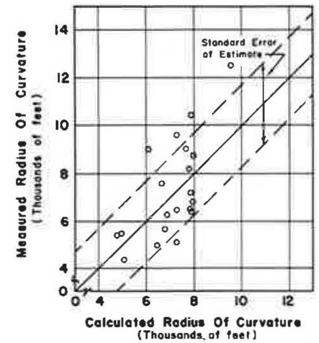

Figure 33. Measured vs calculated radius of curvature at cracked edge—winter.

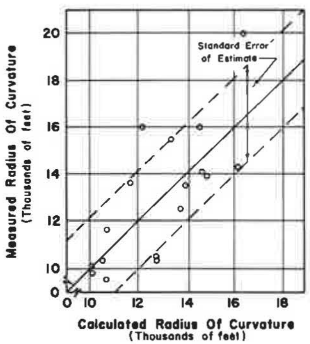

Figure 34. Measured vs calculated radius of curvature at cracked edge—summer.

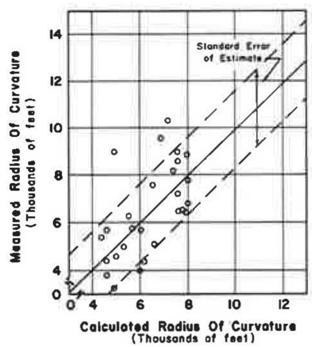

Figure 35. Measured vs calculated radius of curvature—combined data.

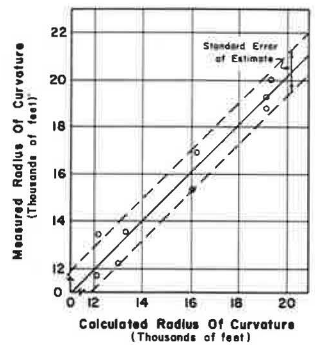

Figure 36. Measured vs calculated radius of curvature at uncracked edge—fall.

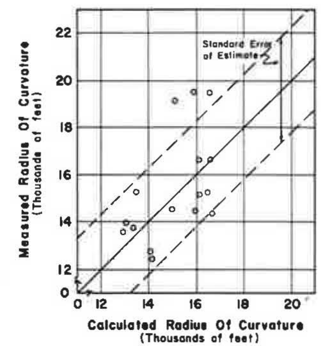

Figure 37. Measured vs calculated radius of curvature at uncracked edge—winter.

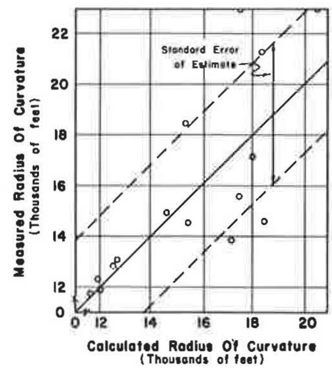

Figure 38. Measured vs calculated radius of curvature at uncracked edge—summer.

The midspan radius of curvature data were analyzed in like manner as the crack radius data; however, here all four data runs were used to relate the parameters studied to radius of curvature. The computed constants and statistics for the four equations are given in Table 8. Figures 36 through 39 show the calculated radius of curvature plotted against the measured midspan radius of curvature.

DISCUSSION OF RESULTS

Deflection

In general, the control variables considered in this study were found to affect the deflection of a CRCP. Their effect follows a pattern that can be expressed by a mathematical expression. Of the semi-controlled variables considered, it was found that the soil moisture condition affected the deflection, although the findings were contrary to the generally accepted criteria of greater deflection for a moist condition. In addition, the findings of this study tend to verify the assumptions used in the design and development of CRCP.

Soil Moisture—The four data runs were made in different seasons over a period of about two years. At the times the data were taken, the general soil moisture conditions were not the same. The fourth run was exceptionally wet, and deflections on this run were all considerably less than they had been on the first three runs. Initially, this discrepancy between the findings and the normal assumption of more deflection for a wet condition caused much concern for errors that might have been made on the fourth run in taking the data. When the weather conditions were the same as on the fourth run, the pavement deflections on approximately one-third of the sections were measured again. As was the case previously, the deflections were small and for all practical purposes identical to those of the fourth run.

It is now believed that when the subgrade and subbase materials are saturated they respond to quick loading as does a soil sample in an undrained triaxial test. The load applied to the pavement is supported partially by the pore water in the pavement foundation rather than the soil grains as is the case where the soil is not saturated (13).

It should also be pointed out that the summer run, where the soil was the dryest, experienced slightly less deflection than periods when the subsoil was partially saturated. Of course, this latter condition could be the result of smaller cracks due to summer temperatures.

Equations—The deflection equations derived herein are extensions of the one developed in an earlier report (8). The previous equation was based on data taken from only two test sections, and those herein are based on 20 pavements with three sets of data from each for the dry condition and one set for the wet run. Table 9 gives a comparison of the equations with the equation developed earlier (8), which was based on crack position data only.

Figures 40 and 41 were prepared to illustrate the capability of the equation for predicting the observed deflection. In each case, the regression equation developed from the data for both the crack position and midspan position was used to calculate the deflection for a given set of conditions on a test section. This calculated deflection was then compared against measured deflections for the test sections as portrayed in the figures. Note the close

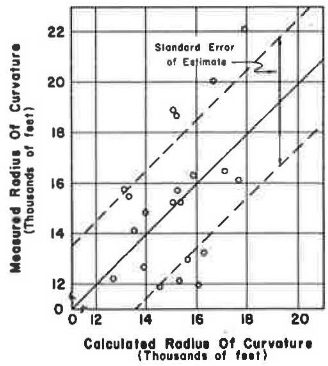

Figure 39. Measured vs calculated radius of curvature at uncracked edge—spring.

agreement, in most cases, between the measured and calculated values. In some cases, both the measured and calculated deflection appear to be out of line with what is to be expected, but these exceptions are normally due to a lime-stabilized subgrade and are so marked on the figures. These figures are typical of all runs, and hence, these observations support the validity of using these equations in design work.

Modulus of Elasticity—The findings in this study in regard to the modulus of elasticity of concrete contradict the generally accepted theory of a lower modulus of elasticity slab deflecting more than a high modulus one for equal conditions. Although the levels of the modulus are not too far apart in magnitude, another experiment on this same research project, wherein the levels were considerably greater through the use of two entirely different coarse aggregate types, indicated the same results. These two separate investigations, along with a limited laboratory investigation,

TABLE 9

COMPARISON OF REGRESSION ANALYSIS CONSTANTS

Constant	Overnight Study	Statewide Study
A_0	0.0106	0.3779
B_2	—	0.1683
B_3	0.8503	0.6513
B_4	0.0994	0.0266
B_5	4.8997	6.3407

$$D_c = \frac{A_0\, L\, 10^{B_5 \Delta X}\, \overline{X}^{B_4}\, T_{sg}^{0.25 B_3}}{D^{1.75}\, E^{B_2}\, U^{0.25 B_3}\, 10^{0.0147 T}}$$

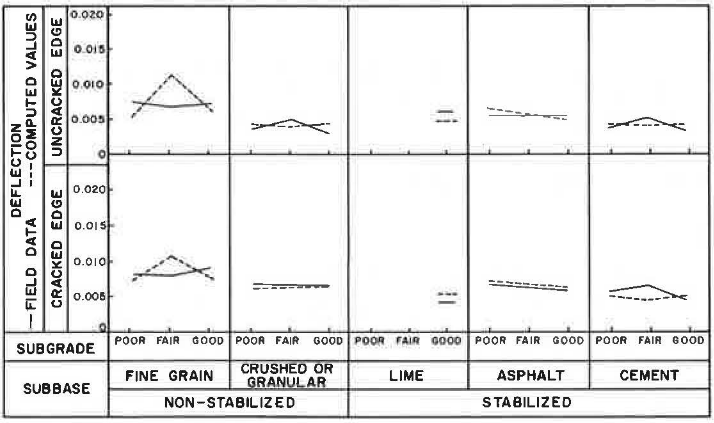

Figure 40. Measured and computed deflections on high modulus of elasticity concrete.

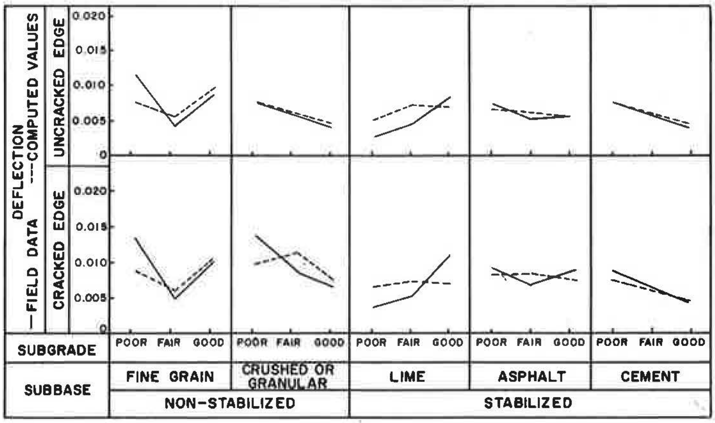

Figure 41. Measured and computed deflections on low modulus of elasticity concrete.

lend credence to the observations of less deflection with a lower modulus of elasticity concrete (14). It should be emphasized, however, that this observation can only be related to CRCP at this time and should not be translated to JCP, which may react differently.

There is a good possibility that this controversial observation attributed to modulus of elasticity could be an indirect effect of a combination of variables not considered in this experiment.

It may be hypothesized that generally speaking, a low modulus of elasticity concrete has a lower coefficient of thermal expansion. In this case the transverse volume change cracks would be smaller, and hence a greater degree of load transfer would be available. Therefore, with a greater load transfer less deflection would be experienced.

Furthermore, in the normal theoretical analyses of this condition, such as those of Westergaard, Pickett, Spangler, etc., the basic assumption is made that the subgrade reaction forces are vertical. An actual pavement on a subgrade deflecting under a wheel load develops a complicated interaction of shear forces and vertical forces, which may result in these field observations rather than those developed in a simplified theoretical approach.

Final Equation—The equations developed contain the term soil support, which was defined by Eq. 2. The soil support term can be eliminated from the deflection equations by substitution of Eq. 2 into Eq. 1. The dry or partially saturated condition was used as the level for selecting the final equation. Thus, the equation for deflection takes the form

$$D_c = \frac{0.3779\ L\ 10^{6.3407\ \Delta X}\ \overline{X}^{0.0266}\ T_{sg}^{0.1628}}{D^{1.75}\ E^{0.1683}\ (U_1 + U_2)^{0.1628}\ 10^{0.0147\ T}}$$

where all terms are as previously defined.

Radius of Curvature

The radius of curvature data show that the average radius of curvature at the cracked edge for all data is about 52 percent less than the radius of curvature at the uncracked edge. The radius of curvature at the crack and midspan was correlated by linear regression analysis for each of the four data runs, and the graphs were shown in Figures 17 through 20.

Figures 42 and 43 show calculated and measured radius of curvatures plotted against the subgrade classifications for each subbase material type that was available.

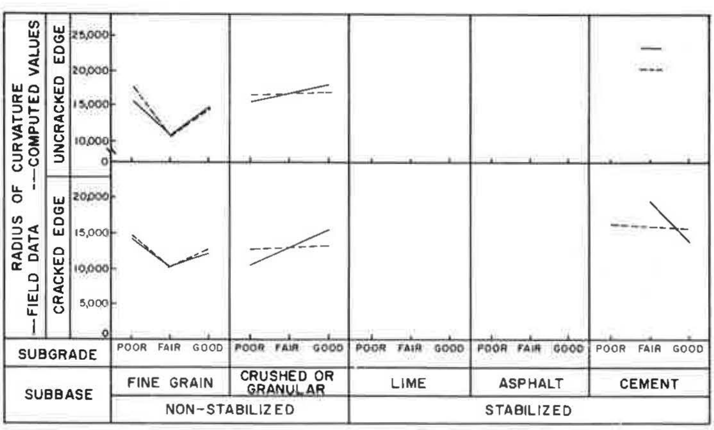

Figure 42. Measured and computed radius of curvatures on high modulus of elasticity concrete.

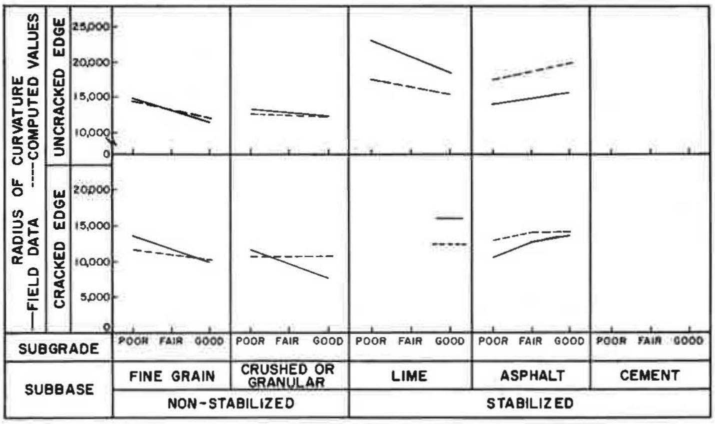

Figure 43. Measured and computed radius of curvatures on low modulus of elasticity concrete.

Final Equation—The radius of curvature equations determined for combined data contained the soil support term. Here again, the definition of soil support can be substituted and the radius of curvature equation will then take the form

$$R_c = \frac{15.3039\ D^{1.75}\ E^{0.3312}\ (U_1 + U_2)^{0.1367}}{L\ T_{sg}^{0.1367}\ \overline{X}^{0.0772}}$$

where all terms are as previously described.

An attempt was made to add the crack width as another variable but the results were such that it would be better not to include the crack width.

Accuracy of Regression Equations

Nineteen sets of deflection and radius of curvature data were analyzed by multiple regression methods. For each analysis a value of r, the correlation coefficient, was obtained. These values of r were checked against a table for their significance for the number of points and degrees of freedom (15). Table 10 gives the results of the r check.

The regression results appear to substantiate the form of the model equations. All checks on the correlation coefficients from the analysis of combined data were above that required to be significant. Previous discussions showed that the standard error of these equations is compatible with the accuracy of the equipment used. Thus the equations are in most cases statistically sound.

TABLE 10

INVESTIGATING THE SIGNIFICANCE OF CORRELATION COEFFICIENTS

Analysis	Crack	Midspan
Deflection:		
Run No. 1	G	F
Run No. 2	G	F
Run No. 3	G	G
Run No. 4	G	G
Combined data	G	G
Radius of Curvature:		
Run No. 1	G	G
Run No. 2	G	F
Run No. 3	G	G
Run No. 4		F
Combined data	G	G

G—The coefficient of correlation is greater than a minimum value required for significance.
F—The coefficient of correlation is less than a minimum value required for significance.

Validation of Design Assumptions

The findings of this study provide validity for the assumptions used in the original design analysis of CRCP. The equal magnitude of deflection at the crack position and midspan position indicates that sufficient granular interlock is provided so that approximately 100 percent load transfer is experienced across a crack. This finding is applicable only where the pavements have 0.5 percent longitudinal steel or more,

although there is a possibility that the lower limit on percent steel may be less than the minimum used in this experiment. Considering these aspects, this finding is applicable over a wide range of support conditions and concrete properties and components.

Furthermore, the use of the Westergaard interior loading conditions for determining the pavement thickness is a satisfactory procedure. The findings of this experiment indicate a 2-in. differential between CRCP and JCP and are in agreement with field performance from a deflection standpoint. This finding also has validity over a wide range of support conditions and concrete properties.

Design Equations

The final equations presented here for both deflection and radius of curvature provide excellent criteria for developing equations to be used in the design of concrete pavements. Although there are numerous factors other than deflection and stress to consider in the design of concrete pavements, this material will present another guideline for a designer to use in selecting the final pavement structure design for a given roadway.

Although percent longitudinal steel and pavement type are not enumerated in these design equations, they may be inserted on the basis of other material and studies developed in connection with this project. These are empirical equations and care should be taken not to extrapolate beyond the limits used in this analysis. The following are some suggested boundary conditions for extrapolation:

D_c = 0.003 in. to 0.030 in.
E = 3×10^6 psi to 6×10^6 psi
D = 6 to 8 in. for CRCP
D = 8 to 10 in. for JCP
$\overline{X}$ = 3 to 12 ft

CONCLUSIONS

This deflection study of CRCP has encompassed a wide variety of conditions and a considerable part of the geographical area of the state. The study was conducted over a 3-year period and over 15,000 separate measurements of various types were used. As a result of this field study and analysis, the following conclusions are warranted:

1. The variables studied herein that were found to affect the deflection of CRCP were concrete modulus of elasticity, modulus of rupture, crack spacing, surface crack width, pavement slab thickness, pavement type, strength characteristics of the subgrade and subbase, and subsurface moisture conditions. An empirical equation was derived using these variables, except modulus of rupture and moisture condition, to predict the deflection of a continuously reinforced concrete pavement under a given wheel load.
2. An equation was also derived from the study that predicts the radius of curvature of a pavement, i.e., related to pavement stress, in terms of the same variables with the exception of crack width.
3. It is recommended that the final equations derived herein be used to develop a nomograph predicting the deflection and radius of curvature for the variables studied. Through the use of this nomograph along with a maximum allowable deflection, pavements may be designed and/or checked in terms of the conditions existing on each project.
4. For the design equation mentioned, the variables of pavement type and percent longitudinal steel may be added to the equation on the basis of the studies herein and previous studies made in connection with this research project.
5. For continuous pavements, longitudinally reinforced with 0.5 percent steel or greater, it was found under a wide variation of support and environmental conditions that the transverse cracks in CRCP are small enough to retain sufficient aggregate interlock to maintain approximately 100 percent load transfer across the crack.
6. The transverse cracks were found to affect the continuity of a CRCP, since measurements indicated that the radius of curvature was smaller, i.e., there was greater stress at the crack than at a midspan point between cracks.
7. From a deflection and stress standpoint, pavements with stabilized subbases are superior in performance to pavements with non-stabilized subbases. All three of the

stabilizing agents considered in this study were found to give excellent performance from a deflection standpoint, but as a result of other studies that will be presented in the future, it is recommended that lime-stabilized subbases be protected with a non-erosive material.

8. From a deflection standpoint, the present practice of using a 2-in. thinner pavement for CRCP in relation to JCP as indicated by current design procedures is correct and conservative. For a given set of conditions, it was found that the deflection for an 8-in. CRCP is equal to or less than for a 10-in. JCP.

9. This study indicated that a reduction in thickness for CRCP had slightly more effect on deflection than an equal reduction in thickness for jointed pavement as found at the AASHO Road Test. Although there is a slight variation, the effect of pavement thickness on deflection as found by (a) this study, (b) the AASHO Road Test, and (c) Westergaard's theoretical analysis are in approximately the same range.

10. The use of a lime-stabilized subgrade, as practiced in Texas, for a working platform or moisture control was found to give an additional benefit of substantially reducing the deflections of a continuous pavement. Under certain conditions, the supporting characteristics of this layer may be considered in design.

11. From a deflection and stress standpoint, the design details presently being used by the Texas Highway Department for CRCP appear to be more than adequate for the conditions found in Texas.

12. This study developed two findings that contradict widely accepted beliefs concerning deflection of concrete pavement: (a) It was found that pavement on moist or saturated foundations deflected less than when the support was dry or partially saturated; These observations were confirmed during two different wet periods and three dry periods. (b) Although the difference is small, deflections and stresses are lower on low modulus CRCP than on high modulus concrete.

ACKNOWLEDGMENTS

The research reported herein was conducted under the supervision of Robert L. Lewis, Research Engineer, and under the general supervision of T. S. Huff, Chief Engineer of Highway Design, Texas Highway Department. The authors wish to extend their thanks to H. D. Swilley, Senior Laboratory Engineer, District 2; B. R. Hunter, Supervising Laboratory Engineer, District 3; Robert L. McKinney, Geologist, District 9; Billy Rudd, Senior Laboratory Engineer, District 10; Franklin J. Shenkir, Senior Laboratory Engineer, District 12; Clarence A. Weise, Supervising Resident Engineer, District 13; Charles W. Baxter, Senior Laboratory Engineer, District 15; Jerry Nemec, Supervising Resident Engineer, District 17; Wilburne C. Gromatsky, Supervising Construction Engineer, District 18; John W. Livingston, Senior Laboratory Engineer, District 19; Warren N. Dudley, Senior Laboratory Engineer, District 20; and Gaston P. Berthelote, Jr., Supervising Resident Engineer, Houston Urban Project, whose cooperation in providing field assistance and basic information made the success of this investigation possible.

The able assistance of various members of the Research Section, Ivan K. Mays, and others who were instrumental in the success of this investigation, is gratefully acknowledged. The field party that gathered the data is also to be commended.

REFERENCES

1. Status Report on Continuously Reinforced Concrete Pavement Built or Under Contract in the U.S. Concrete Reinforcing Steel Institute, July 1966.
2. Shelby, M. D., and McCullough, B. F. Experience in Texas With Continuously Reinforced Concrete Pavement. HRB Bull. 274, p. 1-29, 1960.
3. McCullough, B. F., and Ledbetter, W. B. LTS Design of Continuously Reinforced Concrete Pavements. Jour. Highway Div., Proc. ASCE, Vol. 86, No. HW4, Dec. 1960.
4. AASHO Interim Guide for the Design of Rigid Pavement Structures. AASHO Committee on Design, April 1962.
5. The AASHO Road Test: Report 5, Pavement Research. HRB Spec. Rept. 61E, 1962.

6. McCullough, B. F. Development of Equipment and Techniques for a Statewide Rigid Pavement Deflection Study. Research Rept. No. 46-1, Texas Highway Department, Jan. 1965.
7. McCullough, B. F. Evaluation of Single Axle Load Response on an Experimental Continuously Reinforced Concrete Pavement. Research Rept. No. 46-3, Texas Highway Department, April 1965.
8. McCullough, B. F., and Treybig, H. J. Determining the Relationship of Variables in Deflection of Continuously Reinforced Concrete Pavement. Research Rept. No. 46-4, Texas Highway Department, Aug. 1965.
9. Manual of Testing Procedures, Vol. 1. Texas Highway Department.
10. Design Manual for Controlled Access Highways. Texas Highway Department.
11. Standard Specifications for Road and Bridge Construction. Texas Highway Department, 1962.
12. Hudson, W. R. Value of Single Load Response in Rigid Pavement Design. Paper presented at Texas Section ASCE, May 10, 1963.
13. Taylor, Donald W. Fundamentals of Soil Mechanics (Ninth Printing). John Wiley and Sons, New York, 1956, p. 381-392.
14. McCullough, B. F., and Mays, Ivan K. A Laboratory Study of the Variables That Affect Pavement Deflection. Research Rept. No. 46-6, Texas Highway Department, Aug. 1966.
15. Snedecor, George W. Statistical Methods. Iowa State College Press, Ames, 1946, p. 351.
16. Westergaard, H. M. Stresses in Concrete Pavements Computed by Theoretical Analysis. Public Roads, Vol. 7, No. 2, April 1926.

Editor's Note: The original paper contained six Appendixes pertaining to equipment used, experimental procedure, summaries of data, deflection analysis, and soil support. This material is available from the Highway Research Board at cost of reproduction. When ordering, refer to XS-18, Highway Research Record 239.

Fatigue Tests of Prestressed Concrete Pavements

A. P. CHRISTENSEN and B. E. COLLEY, Paving Development Section,
Portland Cement Association, Skokie, Illinois

The fatigue characteristics of prestressed concrete pavements were studied by repetitive moving load tests on 16 reduced scale prestressed concrete slabs. Each slab was 16 ft long, 12 ft wide, and 1 in. thick. Variables were magnitude of load, amount of longitudinal and transverse prestress, and subgrade strength.

Relationships were established between load magnitude, prestressed pavement properties, and the number of load coverages causing failure. Data from tests on slabs with varying magnitudes of prestress indicate that a minimum prestress of approximately 30 psi in both longitudinal and transverse directions is required to avoid top surface cracking when relatively few moving loads greater than those causing bottom surface cracking are applied repeatedly at interior locations. Data from tests on slabs cast on foundations of different strengths indicated that an increase in the foundation strength resulted in an increase in the number of load coverages causing failure.

•THE LOAD response of prestressed concrete pavements is being studied at the Research and Development Laboratories of the Portland Cement Association. The first published result of this study was a theoretical procedure (1) for determining the magnitude and distribution of stresses and deflections in prestressed concrete pavements for loads beyond cracking of the bottom surface. This procedure is specifically applicable to a centrally loaded infinite slab supported by a "dense liquid" foundation and prestressed equally in longitudinal and transverse directions.

To test the validity of the assumptions made in the theoretical procedure, load tests (2) were conducted on three reduced scale prestressed concrete slabs supported on a coil spring subgrade. Measurements of strain and deflection were made at a number of locations and load increments. Comparisons between test data and theory indicated fair agreement for values of deflection; however, measured strains were significantly smaller than those predicted by theory. The theoretical assumption that the moment-curvature relationship can be represented by two straight lines, an elastic portion with a constant slope followed by a plastic portion in which curvature increases under constant moment, was shown to be conservative for the static type of loading used.

Strain and deflection data were also reported (3) from static load tests conducted on three concrete slabs post-tensioned with steel strands. Each slab was 30 ft long, 12 ft wide, and 5 in. thick. Results again indicated that a prestressed concrete pavement can adequately support an edge or interior load of greater magnitude than that causing bottom surface cracking. Crack patterns were similar to those predicted by the theoretical procedure. Bottom surface cracks extended radially from the center of the load; top surface cracks were approximately circular for interior loads and semicircular for edge loads. However, applications of repeated moving loads cause the development of a random pattern of bottom surface cracks. To obtain information on the fatigue characteristics of prestressed concrete pavements with numerous working bottom surface cracks, a program of repetitive moving load tests was initiated on reduced scale prestressed concrete slabs.

Paper sponsored by Committee on Rigid Pavement Design and presented at the 47th Annual Meeting.

SCOPE AND OBJECTIVES

The test program was designed to study the behavior of 16 prestressed concrete slabs subjected to repetitive moving loads. Variables were magnitude of load, amount of longitudinal and transverse prestress, and subgrade strength. Because it was necessary to test a number of slabs to obtain sufficient data for a fatigue diagram, a reduced scale size was selected for the test slabs and the loading apparatus. The slabs were pretensioned and cast in place on either a clay subgrade, granular subbase, or cement-treated subbase.

The specific objectives of the program were (a) to determine a relationship between the load magnitude and the number of coverages causing pavement failure, (b) to determine the influence of prestress magnitude and foundation strength on fatigue properties of prestressed pavements, and (c) to observe the characteristics of a prestressed pavement failure and determine the factors that cause its development.

TEST FACILITIES AND MATERIALS

Data are reported from load tests on 16 concrete slabs 16 ft long, 12 ft wide, and 1 in. thick. Prestressing was accomplished with pretensioned high-strength steel wire. The slabs were cast in place and tested with a moving load apparatus designed for this program.

Test Area, Subgrade, and Subbase Materials

The prestressed slabs were cast and tested in the area shown in Figure 1. This area is enclosed in a 24-ft wide concrete building equipped with thermostatically controlled heaters to provide uniform temperature during the heating season. The test area was excavated 4 ft below grade to the bottom of the wall footings, and a 5-in. reinforced concrete floor was cast to form an enclosure for a subgrade material. A waterproofing compound was applied to the floor and walls to protect the subgrade from moisture changes. A clay material was compacted into this enclosure to a depth of 4 ft. Properties of the clay subgrade are given in Table 1. The modulus of subgrade reaction, k, is given in Table 5. It will be shown later that the average radius of relative stiffness for the 16 test slabs was 7.3 in. Therefore the subgrade depth was 6.6 times the radius of relative stiffness, and behavior should approximate a subgrade of infinite depth. The radius of relative stiffness, L, is a ratio of the stiffness of the slab to the stiffness of the subgrade (Eq. 3).

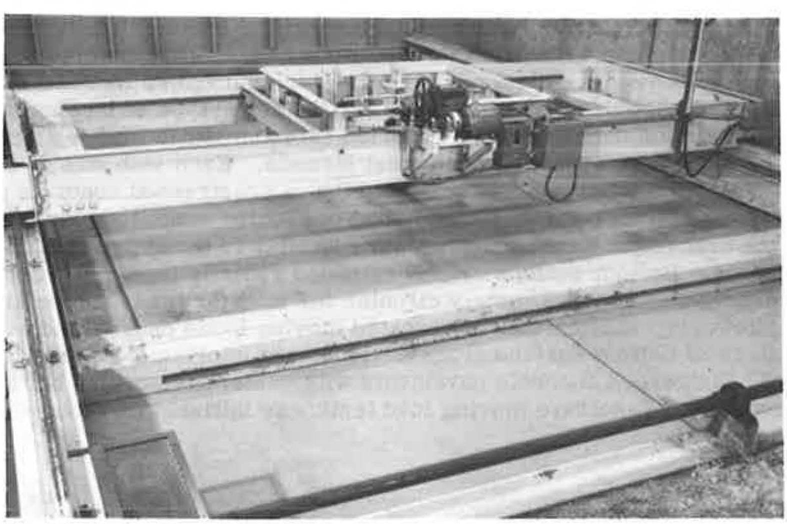

Figure 1. Test area and moving load apparatus.

TABLE 1

SUBGRADE PROPERTIES

Property	Particle Size (mm)	Percent	PCF
Material			
Gravel	76.2 -2.0	0	—
Coarse sand	2.0 -0.42	6	—
Fine sand	0.42 -0.074	8	—
Silt	0.074-0.005	48	—
Clay	smaller than 0.005	38	—
Liquid limit		36	—
Plasticity index		19	—
Maximum dry density (AASHO standard)		—	112
Optimum moisture		16	—

TABLE 2

SUBBASE PROPERTIES

Property	Particle Size (mm)	Percent	PCF
	Granular Material		
Gravel	76.2 -2.0	46	—
Coarse sand	2.0 -0.42	24	—
Fine sand	0.42 -0.074	17	—
Silt	0.074-0.005	10	—
Clay	smaller than 0.005	3	—
Plasticity index		0	—
Maximum dry density (AASHO standard)		—	141
Optimum moisture		7	—
	Cement-Treated Material		
Gravel	76.2 -2.0	27	—
Coarse sand	2.0 -0.42	23	—
Fine sand	0.42 -0.074	32	—
Silt	0.074-0.005	16	—
Clay	smaller than 0.005	2	—
Plasticity index		0	—
Maximum dry density (AASHO standard)		—	125
Optimum moisture		10	—
Cement content		5.5	—

Thirteen of the test slabs were cast on the clay subgrade without a subbase layer. The top surface of the clay was carefully finished to grade with a metal screed to obtain a level casting surface for uniform slab depth. After leveling, the subgrade was covered with two sheets of 4-mil thick polyethylene to retain moisture in the clay subgrade and to reduce stresses resulting from restraint to horizontal slab movement. The clay subgrade was removed to a depth of about 1 ft after each test and the soil was pulverized, reworked to optimum, and recompacted.

A 6-in. granular subbase was used under two of the test slabs, and a 6-in. cement-treated subbase was used under another. The properties of these subbases are given in Table 2. The modulus of subgrade reaction, k, is given in Table 5. For these tests the top 6 in. of clay subgrade was removed and replaced with subbase material. Polyethylene sheets were placed between the subbase and the concrete.

Prestressing

Test slabs were prestressed by the pretensioning method, i.e., the wires were tensioned prior to placing the concrete. After the concrete had attained sufficient strength,

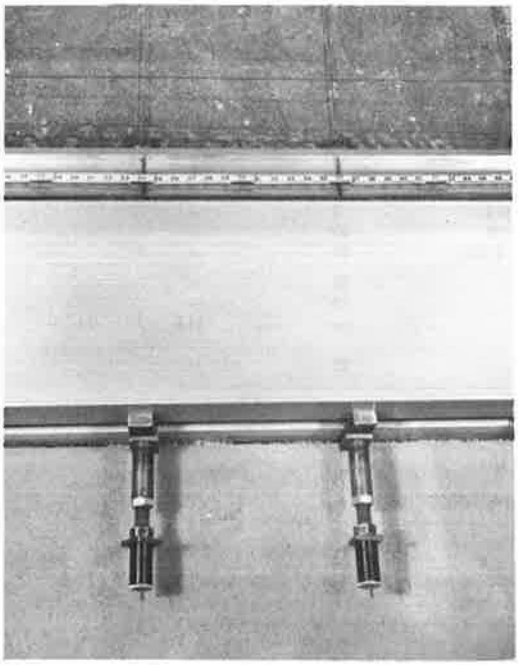

Figure 2. Devices used for tensioning the steel wires.

the wires were released and stress was transferred to the concrete through bond.

Uncoated, stress-relieved No. 12 steel wire was used for applying prestress at the mid-depth of the slabs. Wires in one direction alternated above and below those extending at right angles. The wire diameter was 0.1055 in., area 0.00875 sq. in., modulus of elasticity 27, 600, 000 psi, and ultimate strength 260, 000 psi.

The reaction frame used for tensioning the wires had inside dimensions of 14 by 17 ft. Each side of the frame was formed by a pair of 15-in. steel channels between which the wires were inserted. Bolted moment connections were used at the frame corners. Concrete beams resting on the clay subgrade supported the reaction frame in a horizontal plane at the proper elevation for tensioning the wires at slab mid-depth.

Each prestressing wire was tensioned individually by the extension of a telescoping threaded spacer placed between the wire anchor and the reaction frame (Fig. 2). The force in the wire was measured by a transducer (4) placed between the wire anchor and the reaction frame at the side opposite the spacer. After tensioning the wires, a minimum of one day was allowed before casting the concrete slab. The force in each wire was checked and, if necessary, adjusted to the selected magnitude prior to casting.

To insure full prestress near the slab edges, a 1-in. split steel cube was fastened to each wire at the point where the wire entered the steel side forms. The two halves of the cube were grooved slightly undersize for the wire used and were clamped on the wire by countersunk machine screws.

Casting of Concrete

The cement factor of the concrete was 7.0 sk/cu yd; water-cement ratio was 0.52 by weight, and the sand-aggregate ratio was 0.59 by weight. Type 3 cement was used to obtain a high early strength, and the maximum size of gravel aggregate was ⅜ in. The slump averaged 4.7 in. and vinsol resin was added to provide an average air content of 6.9 percent. Concrete was compacted with a vibrating screed.

After casting, each slab was covered with polyethylene sheeting. The next day, approximately 16 hours later, the sheeting was removed and the top slab surface was coated with a curing compound to reduce moisture losses and thereby minimize curling. Prestressing wires were released after the concrete had cured for 7 days.

Beam specimens 1 by 4 by 22 in. were made at the time of casting from samples of concrete placed in the center portion of each test slab. The beams were cured in a 70 F, 100 percent relative humidity room until tested in flexure with third-point loading on a span of 12 in. It was usually possible to obtain two flexural tests from each beam. A minimum of nine beams was tested for each slab, including three tested when repetitive slab loading was started and three when each failure occurred. Repetitive load tests were started 12 to 14 days after casting. Duration of each test depended on the number of loadings necessary to cause failure and averaged 13 calendar days for all slabs. During the test period, there was relatively little change in the flexural strength of each slab; average values are given in Table 3.

TABLE 3

CONCRETE FLEXURAL STRENGTH

Slab No.	Modulus of Rupture (psi)	Slab No.	Modulus of Rupture (psi)
1	970	9	966
2	880	10	957
3	882	11	970
4	897	12	952
5	952	13	930
6	905	14	963
7	890	15	936
8	916	16	927

A limited number of beams were instrumented with two SR-4 type A9-4 (2-in. length) strain gages on the bottom surface between the third-point loads. Strain measurements during flexural testing of these beams indicated that the average modulus of elasticity for the test slabs was 4, 100, 000 psi.

Load Apparatus

A special load apparatus was constructed for applying repetitive moving loads to the prestressed concrete test slabs. The load apparatus was not designed to simulate traffic operations but rather to develop a random pattern of bottom surface cracks at the interior of each slab. Loads were applied through a single wheel traveling in a number of wheel paths over an interior area 32 in. wide (including the width of the wheel) by 98 in. long. The distances between the loading area and the longitudinal and transverse edges of the 12 by 16-ft slabs were 56 and 47 in. respectively. These edge distances were 7.7 and 6.4 times the average radius of relative stiffness of the test slabs, i.e., sufficient for load behavior to be similar to a slab of infinite surface area.

The equipment used to apply repetitive moving loads is shown in Figure 1. Load was applied through a 16-in. diameter wheel with a 4-in. wide solid rubber tire. The tire had longitudinal and transverse measurements scaled to represent the prototype. The contact area of the tire increased with increasing load as shown in Figure 3.

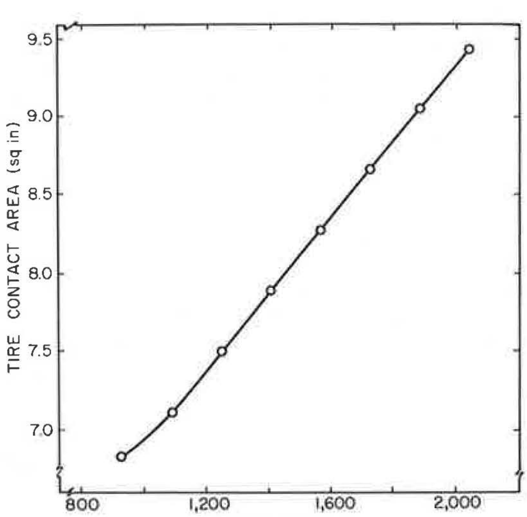

Figure 3. Contact area of solid rubber tire.

The paths traveled by the load wheel during the repetitive moving load tests are shown in Figure 4. Starting at location A, the wheel traveled 98 in. in a longitudinal path to location B. After returning in the same wheelpath to location A, the wheel was driven transversely a distance of 2 in. or half the width of the tire to a second longitudinal wheelpath. After returning to location C, the wheel was again driven transversely a distance of 2 in. to a third wheelpath. During each transverse movement of 2 in. the wheel traveled approximately 10 in. longitudinally. After traveling in 15 longitudinal wheelpaths or a total of 28 in. transversely to location D, the direction of transverse travel was reversed.

The Corps of Engineers (5) defines a load coverage as a sufficient number of vehicle operations or passes to produce

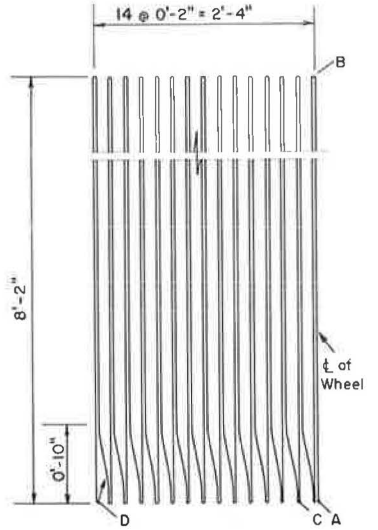

Figure 4. Wheelpaths during load testing.

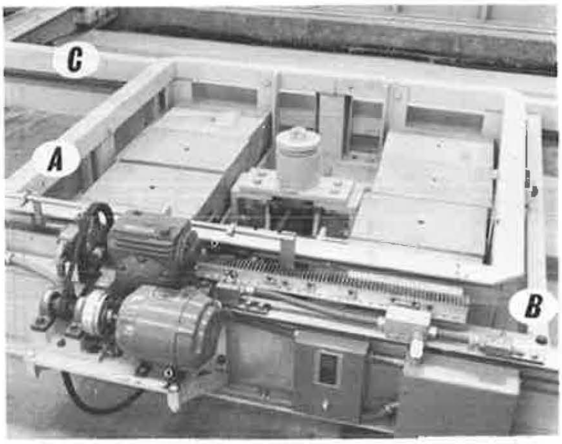

Figure 5. Load box.

statistically one application of the design loading over the entire traffic area. By this definition, 4 load coverages were applied each time the wheel traveled 28 in. transversely or from location A to D. The average wheel speed was 1.68 ft/sec and 106 coverages were applied per hour. Because this rate of loading is greater than that normally encountered on highway and airfield pavements, the data represent conditions more severe than those encountered in actual pavement service.

The load wheel was mounted in the center of a load box. To reduce transverse thrust on the test slabs when the wheel turned to change wheelpaths, the wheel was mounted as a caster with a swivel bearing. A spring mechanism was used to prevent the wheel from rotating 180 degrees on each return trip, as for example, from location B to A.

The load box, as represented by frame A in Figure 5, was made of steel angles welded together to form a frame 4 ft 5 in. by 4 ft 1 in. by 1 ft 5 in. deep. A pair of roller bearings that operated within a vertical channel at the center of each side of the load box enabled it to move freely in the vertical direction within frame B. The desired wheel load was obtained by placing concrete weights inside the load box.

Frame B was designed to move transversely within frame C by means of roller bearings that traveled on transverse bars bolted to the inside of the inside of the span beams of frame A. Power for driving frame B in the transverse direction was supplied by a ½-hp electric motor mounted on frame C. As shown in Figure 5, the motor acted through an electric clutch to drive a pinion gear over a rack mounted on frame B. Length of transverse travel was controlled by a number of stops contacting an electrical switch that regulated current to the clutch.

Frame C had a transverse span of 18 ft and a longitudinal length of 5 ft. A flanged crane wheel mounted near each corner traveled on longitudinal rails that were supported by steel beams independent of the subgrade and prestressing frame. Power for driving frame C in the longitudinal direction was supplied by a 5-hp electric motor. Operating through a gear reducer to obtain proper speed, the motor rotated a transverse steel shaft located near one end of the rails. Two steel drums were mounted on the shaft, one near each end between the flanges of the rail support beams. Each drum pulled a steel cable that traveled around a fixed pulley at the opposite end of the rails. Frame C was attached to the two cables to obtain longitudinal motion when the electric motor was operating. Length of longitudinal travel was controlled by an electrical switch that was activated when the load device passed either of two selected rail locations. This switch disconnected current and applied an electric brake to the motor. By regulating the electric current to the brake, the load device could be smoothly decelerated. An electrical switch on the motor shaft was used to determine when the load device had stopped and to start travel in the opposite longitudinal direction.

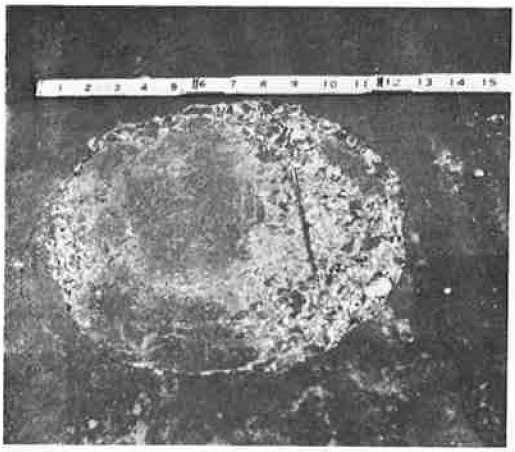

Figure 6. Failure in top surface of slab 2.

Instrumentation

Slab deflections were measured by a resistance bridge deflectometer (6) buried in the clay subgrade 2 ft below the test slabs. The deflectometer was restrained from vertical movement by a steel rod that extended between the deflectometer casing and the concrete slab under the clay subgrade. A second steel rod extended upward from the measurement control pin of the deflectometer to a fitting cast in the slab. An electrical connection between the deflectometer and chart recording equipment enabled deflections to be continuously measured as the load wheel approached and passed over the deflectometer location.

Strains were measured by pairs of SR-4 type A9-4 (2-in. long) strain gages cemented to the top surface of the test slabs, one in the longitudinal and one in the transverse direction at the same location. Strains were also recorded continuously as the load wheel approached and passed over the gages.

TEST RESULTS

Data are reported for load tests on 16 prestressed slabs. The spacing between prestressing wires, amount of tensile force in each wire, and resultant concrete prestress of each test slab are given in Table 4.

Moving loads were applied repeatedly to 15 of the test slabs until failure occurred. Wheel loads and number of coverages at failure are given in Table 5. Failure was characterized by a crumbling of the concrete in the top surface of the slab within a circular area approximately 12 in. in diameter (Fig. 6). These failures occurred very suddenly. Only a few additional load coverages were necessary for the top surface of the slab to deteriorate from the initial cracked condition to the failed condition shown. Failures occurred at random locations within the loaded areas. For most slabs, a thin steel plate was placed over the failed area and repetitive loading was continued until a second failure occurred. A bottom surface view of one of the slabs after a failure had occurred is shown in Figure 7. This photograph shows only a cut out interior portion of the slab where the moving loads were applied. Visual bottom surface cracks were indicated by black ink. Loose concrete was removed at the failure location to expose the prestressing wires. There were no wire failures during any of the load tests. After load testing

TABLE 4

REINFORCEMENT AND PRESTRESS PROPERTIES OF TEST SLABS

Slab No.	Wire Spacing (in.)		Wire Tensile Force (lb)	Concrete Prestress (psi)	
	Long.	Trans.		Long.	Trans.
1-8	12	12	1200	100	100
9	36	36	1200	33	33
10	None	None	0	0	0
11	12	12	140	12	12
12	12	0	1200	100	0
13-16	12	12	1200	100	100

TABLE 5

PROPERTIES OF TEST SLABS

Slab No.	Wheel Load (lb)	Coverages at Failure	h (in.)	k (pci)	L (in.)	a (in.)	α	m_c (in. lb./in.)
1	1730	5730	1.02	70	8.53	1.66	0.195	185
		7270	1.02	70	8.53	1.66	0.195	185
2	1571	2444	1.00	80	8.13	1.62	0.199	165
		3010	1.01	80	8.19	1.62	0.198	168
3	1571	2116	1.01	100	7.75	1.62	0.209	167
		2780	1.02	100	7.80	1.62	0.208	171
4	1410	2098	0.97	100	7.52	1.58	0.210	156
		3816	0.98	100	7.58	1.58	0.208	159
5	1410	25060	1.02	105	7.71	1.58	0.205	182
6	1730	330	0.96	110	7.28	1.66	0.228	155
		342	0.95	110	7.23	1.66	0.230	152
7	1571	472	0.92	120	6.90	1.62	0.235	140
		946	0.93	120	6.96	1.62	0.233	143
8	1571	6160	1.00	120	7.35	1.62	0.220	169
		7700	0.99	120	7.29	1.62	0.222	166
9	1571	7506	1.01	120	7.40	1.62	0.219	170
		8538	1.02	120	7.46	1.62	0.217	173
10	1571	860	1.01	120	7.40	1.62	0.219	163
11	1571	1676	1.02	120	7.46	1.62	0.217	170
12	1571	3226	1.00	120	7.35	1.62	0.220	159
13	Static Load Test		1.02	125	7.38	2.00	0.271	179
14	1730	18500	1.01	170	6.78	1.66	0.245	181
	Static Load Test		1.03	170	6.91	2.00	0.289	188
15	2049	1022	0.97	180	6.49	1.72	0.265	163
		1164	0.98	180	6.53	1.72	0.263	166
16	2206	0 to 14500[a]	1.00	320	5.75	1.76	0.306	171
	3478	14500 to 33700[a]	1.00	320	5.75	1.99	0.246	171

[a]Slab 16 did not fail.

was completed, slab thickness at each failed area was measured with a vernier caliper. Average thicknesses are given in Table 5.

A previous theoretical analysis (1) of prestressed concrete pavements indicated that strength is a function of α and m_c, where

$$\alpha = \frac{a}{L} \tag{1}$$

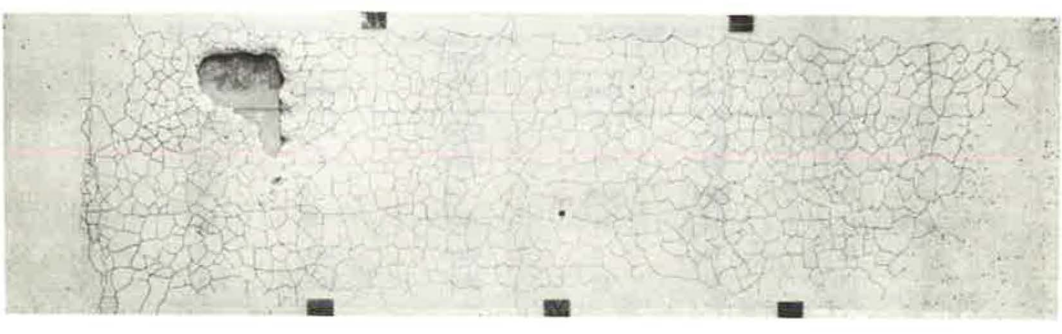

Figure 7. Crack pattern in bottom surface of slab 5.

and

$$m_c = \frac{\sigma_c h^2}{6} \tag{2}$$

in which

L = radius of relative stiffness (in.), i.e.,

$$L = \sqrt[4]{\frac{E h^3}{12 (1 - \mu^2)k}} \tag{3}$$

a = radius of loaded area (in.),
E = concrete elastic modulus (psi),
μ = Poisson's ratio,
h = slab thickness (in.),
k = subgrade modulus (pci),
σ_c = cracking stress (psi) = modulus of rupture plus prestress, and
m_c = cracking moment (in.lb/in. of width).

Computed m_c and α-values for each slab are given in Table 5. The radius of the loaded area, a, used to compute α-values was the radius of a circle having an area equal to that shown in Figure 3 for the loaded tire at the test load. The radius of relative stiffness, L, was computed using the measured value of 4,100,000 psi for the modulus of elasticity, E, and an assumed value of 0.15 for Poisson's ratio. The subgrade modulus, k, was determined with a 30-in. diameter plate at 0.05 in. deflection. The k-value given in Table 5 is the average of the values determined prior to the construction and after the testing of each slab. When computing m_c-values, cracking stresses were assumed to be equal to the summations of the modulus of rupture values given in Table 3 and the prestress values given in Table 4.

Analyses

To analyze the test data given in Table 5 and develop a design method for prestressed pavements, it is necessary to relate m_c and α-values with wheel loads and coverages causing failures. This may be done by using the m_c and α-values to compute either the bottom or the top surface cracking load of each slab, then establishing a relationship between the ratio of such cracking load to applied wheel load and the coverages causing failure.

Bottom Cracking

The following equation, based on Westergaard's (7) theoretical analysis for loads applied in the interior of the area of a panel, can be used to compute the bottom cracking load, P_c:

$$\left.\begin{matrix}\sigma_x \\ \sigma_y\end{matrix}\right\} = \frac{P}{h^2}\left[0.275\,(1+\mu)\log_{10}\frac{Eh^3}{k\left(\frac{a+b}{2}\right)^4} \mp 0.239\,(1-\mu)\frac{a-b}{a+b}\right] \tag{4}$$

where σ_x and σ_y = principal tensile stresses in the directions of x and y at the bottom of the slab under the center of the load, and a and b = semiaxes of an ellipse representing the footprint of a tire. For a circular loading area where a = b and letting μ = 0.15, $L^4 = \frac{Eh^3}{12(1-\mu^2)k}$, $\alpha = \frac{a}{L}$, and $m_c = \frac{\sigma_x h^2}{6}$, Eq. 4 becomes:

$$P_c = \frac{m_c}{0.0527\left(4\log_{10}\frac{1}{\alpha} + 1.069\right)} \tag{5}$$

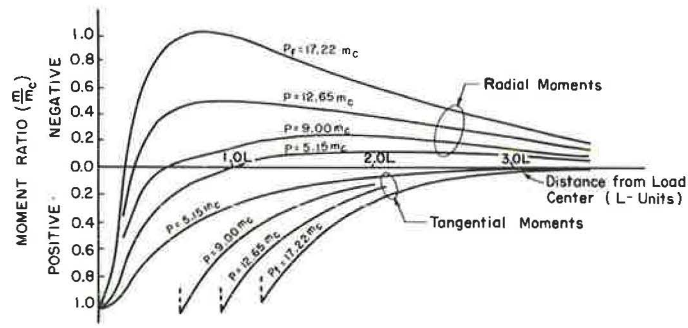

Figure 8. Radial and tangential moment curves—PCA theoretical method for $\alpha = 0.2$.

Top Cracking

The top surface cracking load of a prestressed pavement may be computed by the PCA theoretical method (1). This method is limited to a load applied at an interior position of a slab supported by a dense liquid foundation and prestressed equally in the longitudinal and transverse directions. By use of this method, radial and tangential moment diagrams were developed for loads greater than those causing bottom surface cracking, i.e., beyond conditions to which the elastic theory is applicable. Example moment diagrams for $\alpha = 0.2$ are shown in Figure 8. Bottom surface cracks begin to form under the load when the positive moment, m, equals the cracking moment, m_c, or when $m/m_c = 1$. A small increase in load beyond that initiating bottom cracking will cause these cracks to extend radially from the center of the load. As additional load is applied, there is an increase in the positive tangential moment and negative radial moment. The bottom surface radial cracks become longer, and the point of zero radial moment moves nearer the center of loading. At a load, P_F, equal to 17.22 times the cracking moment, m_c, the negative radial moment equals the cracking moment and a circular crack occurs in the top surface of the slab. Other top surface cracking loads predicted by the PCA method for α-values varying from 0.1 to 0.5 may be determined from the diagram shown in Figure 9.

Another method for computing top surface cracking loads is that used by the Corps of Engineers. Based on the results of previous static load tests on Hydrocal model slabs 16.6 in. square by 0.20 in. thick and supported on a 12-in. thick layer of natural rubber, the following empirical equation was developed (8):

$$P_F = \frac{h^2 (R + R_P)}{6\left[C\frac{M_o}{P_o} - \frac{M_R}{P_o}\right]} \qquad (6)$$

where

P_F = top surface cracking load (lb),
h = slab thickness (in.),
R = flexural strength of the concrete (psi),
R_P = concrete prestress (psi),
C = radial moment correction factor,
M_o/P_o = moment coefficient under center of loaded area, and
M_R/P_o = moment coefficient at point of negative moment cracking.

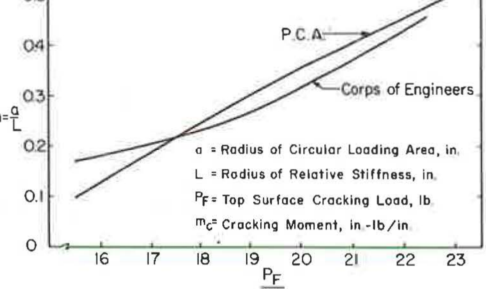

Figure 9. Top surface cracking loads for prestressed concrete pavements.

TABLE 6

DESIGN FACTORS BASED ON TOP CRACKING LOADS

Slab No.	Wheel Load (lb) P	Coverages at Failure	Bottom Cracking Load (lb) P_c	Top Cracking Load (lb) P_F			Fatigue Factors	
				PCA	C of E	Average	$\frac{P}{P_c}$	$\frac{P_F}{P}$
1	1730	5730	898	3170	3080	3125	1.93	1.81
		7270	898	3170	3080	3125	1.93	1.81
2	1571	2444	809	2800	2730	2765	1.94	1.76
		3010	824	2860	2790	2825	1.91	1.80
3	1571	2116	835	2900	2870	2885	1.88	1.84
		2780	855	2950	2910	2930	1.84	1.87
4	1410	2098	784	2730	2700	2715	1.80	1.93
		3816	795	2780	2740	2760	1.77	1.96
5	1410	25060	905	3150	3100	3125	1.56	2.22
6	1730	330	807	2720	2760	2740	2.14	1.58
		342	796	2680	2720	2700	2.17	1.56
7	1571	472	741	2500	2540	2520	2.12	1.60
		946	753	2540	2580	2560	2.09	1.63
8	1571	6160	867	2960	2960	2960	1.81	1.88
		7700	856	2920	2930	2925	1.84	1.86
9	1571	7506	870	2990	2990	2990	1.81	1.90
		8538	881	3060	3000	3030	1.78	1.93
10	1571	860	834	2920	2930	2925	1.88	1.86
11	1571	1676	866	2980	2980	2980	1.81	1.90
12	1571	3226	815	2940	2940	2940	1.93	1.87
13	Static Load Test		1017	3310	3420	3365	—	—
14	1730	18500	978	3260	3340	3300	1.77	1.91
	Static Load Test		1106	3530	3660	3595	—	—
15	2049	1022	916	2980	3080	3030	2.24	1.48
		1164	927	3040	3140	3090	2.21	1.51
16	2206	—[a]	1036	3270	3390	3330	2.13	1.51
	3478	—[a]	1118	3390	3510	3450	3.11	0.99

[a]Slab 16 did not fail.

In using this equation, values of C, M_o/P_o, and M_R/P_o must be obtained from appropriate curves (8). These values are plotted as functions of either A/L^2 or a/L where A is the area of the loaded area, a is the radius of the loaded area, and L is the radius of relative stiffness, so that it is possible to develop a relationship between P_F/m_c and a/L where m_c is equal to $h^2 (R + R_p)/6$. The resultant curve for circular loading areas is compared to the PCA method in Figure 9. It is seen that the two methods are in fair agreement.

Slabs on Clay Subgrade

Data are presented from tests on the nine slabs cast on a clay subgrade and prestressed to 100 psi in both longitudinal and transverse directions. Comparisons will later be made with the four slabs that had reduced amounts of prestress and with the three slabs cast on granular and cement-treated subbases.

Using the m_c and α-values given in Table 5, bottom surface cracking loads were computed by Westergaard's Eq. 5, and top surface cracking loads were computed by both the PCA and Corps of Engineers method using Figure 9. Top cracking loads by the two methods were nearly equal for each slab failure, and average values were used to determine ratios of computed top surface cracking loads divided by repetitive moving wheel loads. Also, ratios of repetitive moving loads divided by bottom surface cracking loads were determined. These ratios are given in Table 6 and in this report are defined as fatigue factors. Fatigue factors are plotted in Figure 10A and 10B vs the number of load coverages causing failure.

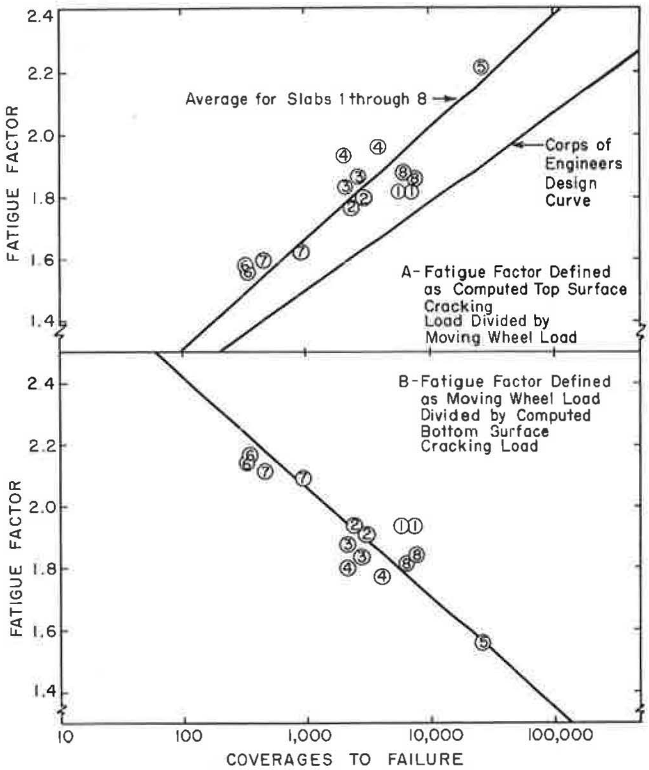

Figure 10. Fatigue relationships for prestressed concrete pavements.

The results of these tests may be compared with data from a similar moving load test program conducted by the Corps of Engineers (5). The essential differences between these two programs were as follows:

Characteristic	Corps of Engineers	PCA
Casting Technique	Precast	Cast in place
Prestressing: Method	Pretensioned	Pretensioned
Amount	250 psi	100 psi
Size of Slab: Length	15 ft	16 ft
Width	6 ft	12 ft
Thickness	1 in.	1 in.
Size of Loaded Area: Length	120 in.	98 in.
Width	24 in.	32 in.
Avg. Conc. Mod. of Rupt.	905 psi	914 psi
Avg. Conc. Elas. Mod.	4,500,000 psi	4,100,000 psi
Avg. Subgrade Modulus	65 pci	105 pci

In analyzing their data, the Corps of Engineers plotted a curve that related a design factor for repetitive loading to the number of load coverages causing failure. Their design factor was defined as the computed top surface cracking load for a single application divided by the repetitive moving wheel load. This curve is shown on the appropriate diagram in Figure 10A. For a given fatigue ratio, it indicates a greater number of coverages at failure than the PCA curve.

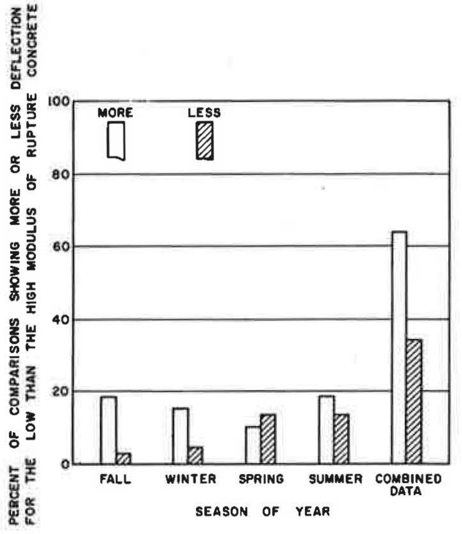

Figure 10. Deflection comparison of low and high modulus of rupture concrete.

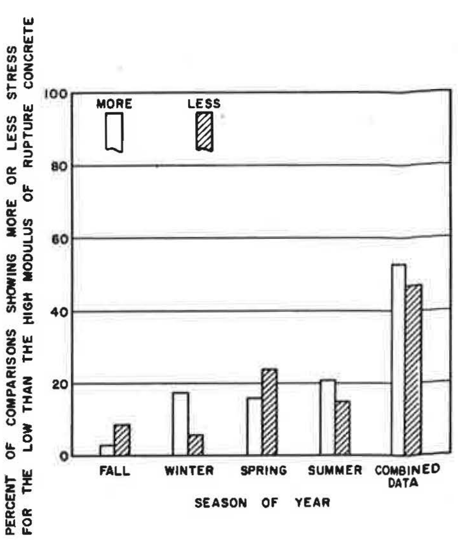

Figure 11. Stress comparison of low and high modulus of rupture concrete.

modulus deflected more than the high modulus of elasticity concrete. The range of modulus of elasticity experiencing the most deflection apparently varies slightly with season. Calculations have shown that, on the average, the lower modulus of elasticity concrete in general deflected 7.4 percent less than the high modulus of elasticity concrete. This finding, although contrary to rational reasoning, is in line with that found in another experiment (7).

Figure 9 is bar graph comparing modulus of elasticity against stress in the concrete slab. The graph structurally is the same as Figure 8 except that it portrays stress in the concrete. Inspection of Figure 9 shows that more comparisons of stress on low and high modulus of elasticity concrete showed less stress in the low than the high modulus concrete. The range of modulus of elasticity experiencing the most stress also varies with season.

The second concrete property considered here is the modulus of rupture. The analysis of the modulus of rupture was made by determining whether the deflections and stresses were more or less for the lower modulus of rupture concrete than the higher modulus of rupture CRCP. The evaluation was made for each season and also the combined data. Figure 10 shows in bar graph style the percentage of comparisons in which deflections on the high modulus of rupture concrete were more or less than those on the low modulus of rupture concrete. Note that the low modulus of rupture concrete deflects more than does the high. This was true for all seasons except for the spring. The combined data also show that the average deflection for all seasons is greater on the low modulus of rupture concrete.

The comparison of stresses on the low and high modulus of elasticity concrete indicate that, on the average, stresses were higher in the low than the high modulus of rupture concrete. Figure 11 shows the percent of comparisons in which the stress was higher or lower than that in the low modulus of rupture concrete.

Slab Thickness and Type—The pavement slab thickness analysis was made by comparing deflection measurements from sections that had identical classifications in the factorial, but different slab thickness. This allows a clean comparison of thickness to deflection and stress.

In each case the smaller thickness of concrete pavement was compared with a greater thickness. The results were combined for all four data runs. The comparison may not be very good because of the small number of sections compared.

TABLE 4

PERFORMANCE OF RIGID PAVEMENT IN TERMS OF THICKNESS, PAVEMENT TYPE, AND LOAD POSITION*

Thickness Comparison	Deflection		Stress	
	Crack or Joint	Midspan	Crack or Joint	Midspan
6-in. CRCP vs 8-in. CRCP	41.1	54.6	11.0	1.1
8-in. CRCP vs 9-in. JCP	-13.1	30.8	-50.2	-11.1
8-in. CRCP vs 10-in. JCP	-38.0	-28.5	-49.6	6.9

*Numbers indicate the average percent difference for the respective condition.

Table 4 is a summary of the results obtained in comparing pavements of different thickness and type. In comparing 6-in. CRCP with 8-in. CRCP, it was found that the 6-in. pavement deflected 41 percent more at the crack position than did the 8-in. CRCP. Comparing 8-in. CRCP with 9-in. JCP, it was found that the CRCP deflected on an average of 13.1 percent less than the JCP. When the 8-in. CRCP was compared to 10-in. JCP, it was found that the CRCP deflected on an average of 38 percent less than the 10-in. JCP.

It has been assumed in the past that 10-in. JCP performance would be very much the same as that of 8-in. CRCP (4). Performance measured in terms of deflection shows that the 8-in. CRCP is superior to the 10-in. JCP. In Figure 12 deflections as computed by the equations developed herein are plotted against deflections measured on comparable 10-in. JCP. The deflections for both pavement types have been corrected to zero temperature differential, and the deflections for CRCP were corrected to an 8-ft crack spacing and a 0.014-in. crack width. The data show a remarkable relation between the two parameters. By forcing the correlation line through zero (a rational approach), the slope of the line indicates that a 10-in. JCP deflects 1.6 times more than an 8-in. CRCP.

Deflection Position—On each test section a midspan deflection (between cracks) was obtained each time a reading was taken at the crack position. Figures 13 through 16 are plots of the average crack deflection versus the midspan deflection for each of the four runs. Although there is an offset on the vertical axis (crack deflection) greater than zero, it may be stated that the edge deflection and crack deflection are approximately equal on any range of support properties with continuous pavements that have 0.5 percent longitudinal steel or greater.

The radius of curvature measurements were also plotted in the same manner as deflection measurements (Figs. 17 through 20). In the case of radius of curvature—in contrast to deflection—the crack position has considerably less magnitude than the midspan position, which means that the concrete at the crack position is experiencing considerably more stress.

In terms of deflection and radius of curvature, it is evident that the aggregate interlock produces adequate load transfer across a crack, but the transverse cracks affect the continuity condition of the slab.

Semi-Controlled Variables

Two factors studied on a semi-controlled basis were the season of the year that the field measurements were taken and the general moisture condition of the soil.

Season—Data were taken on a statewide basis in each of the four seasons of the year. The deflection and radius of curvature data taken during these four seasons were analyzed by comparing each set of data with that taken during the summer. The comparison showed only whether the deflections and stresses were more or less in the fall, winter, and spring than in the summer. In Figure 21 these comparisons showing more or less deflection than the summer data are expressed as percentages. The results indicate that the deflections during fall and winter were generally greater than the summer, whereas the spring deflections were significantly smaller than the summer. Thus the

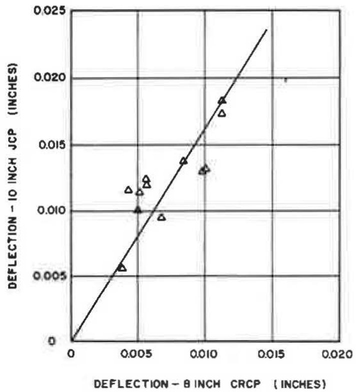

Figure 12. Calculated 8-in. CRCP deflection vs measured 10-in. JCP deflection.

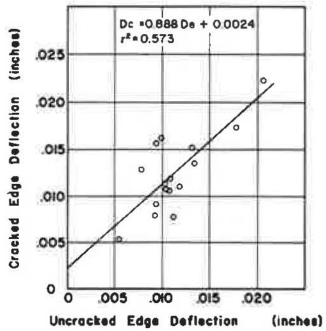

Figure 13. Cracked edge vs uncracked edge deflection—fall.

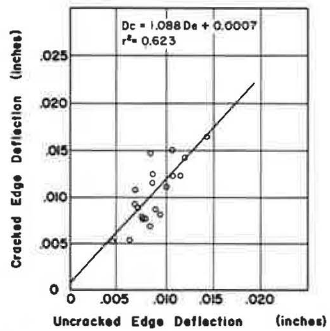

Figure 14. Cracked edge vs uncracked edge deflection—winter.

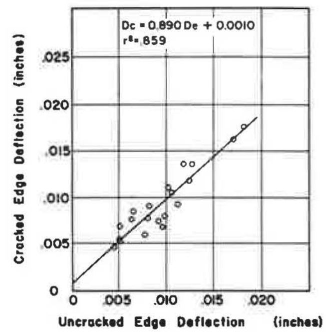

Figure 15. Cracked edge vs uncracked edge deflection—summer.

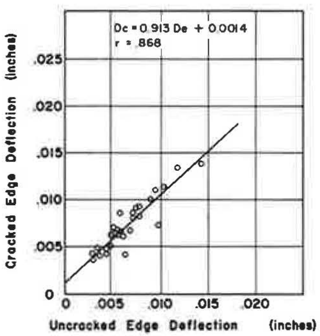

Figure 16. Cracked edge vs uncracked edge deflection—spring.

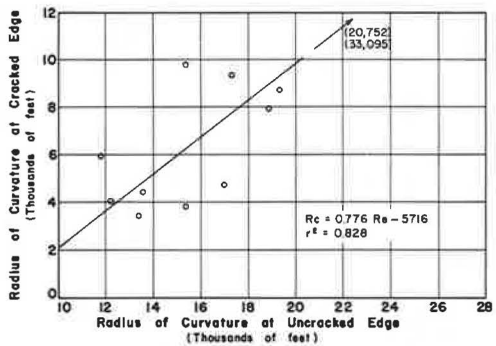

Figure 17. Cracked edge vs uncracked edge radius of curvature—fall.

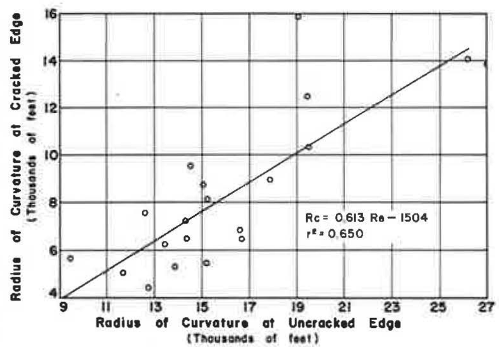

Figure 18. Cracked edge vs uncracked edge radius of curvature—winter.

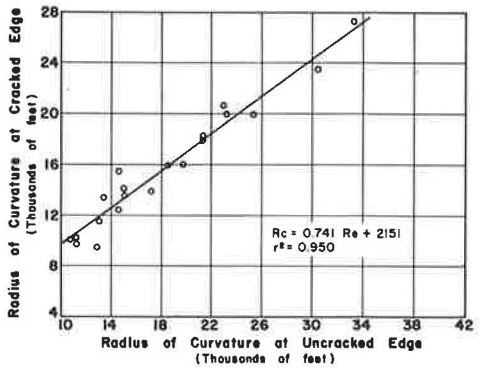

Figure 19. Cracked edge vs uncracked edge radius of curvature—summer.

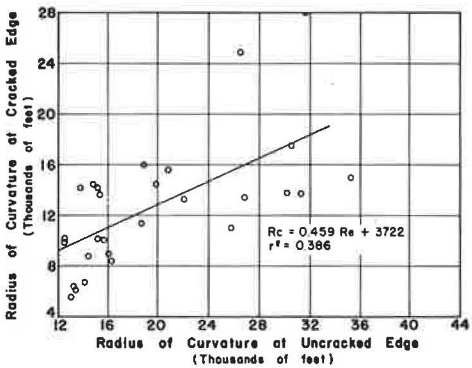

Figure 20. Cracked edge vs uncracked edge radius of curvature—spring.

deflection might in some way be related to the season; however, for the fall and winter there was not very much difference in the data.

The results of the stress analysis shown in Figure 22 indicate that the seasonal comparisons with the summer data are consistent in showing that the pavements experience less stress in the summer than during the other seasons.

Soil Moisture Condition—Each time data were taken on a test section, the general environmental conditions of the soil adjacent to the roadway in a hole 1 ft deep was classified as dry, moist, or wet. As far as the moisture effects are concerned, it was found that the fourth data run, which was the spring run, measured deflections that were much less. During the entire spring run general rains were experienced over the state. Of the four runs, the spring run was by far the wettest.

CORRELATION OF VARIABLES

Deflection

The variables studied that affect deflection are the crack spacing, surface crack width, concrete modulus of elasticity and modulus of rupture, pavement slab thickness, pavement type, strength characteristics of the subgrade and subbase, and moisture conditions. With the exception of the semi-controlled variables and the modulus of rupture, these variables will be correlated into an equation in the following.

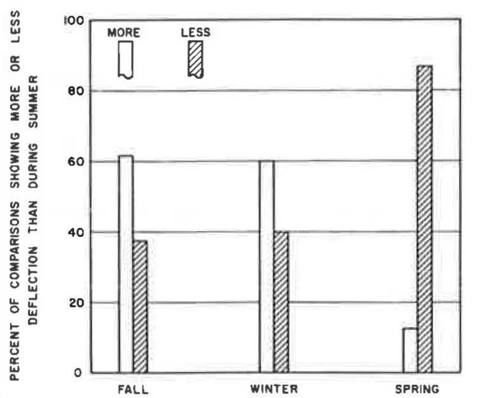

Figure 21. Seasonal comparison of deflection.

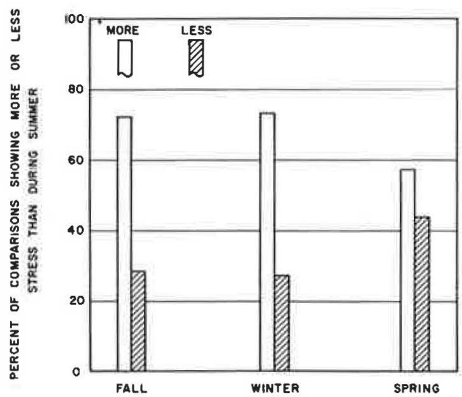

Figure 22. Seasonal comparison of stress.

A model equation was developed which encompassed the variables to be correlated. The model was based on previous work and also on work done at the AASHO Road Test (5, 8). The model chosen to relate the variables is basically an extension of the Road Test model and is of the following form:

$$D_c = \frac{A_0 \, L \, 10^{B_5 \, \Delta X} \, \bar{X}^{B_4}}{D^{1.75} \, E^{B_2} \, SS^{B_3} \, 10^{0.0147 \, T}} \tag{1}$$

where

- L = Load in kips;
- X = Surface crack width in inches;
- $\bar{X}$ = Average crack spacing in feet;
- D = Slab thickness in inches;
- E = Concrete modulus of elasticity, psi;
- SS = Soil support;
- D_c = Deflection at crack position, inches;
- D_e = Deflection at midspan position, inches;
- T = Temperature differential between top and bottom of the slab, degrees F; and A_0, B_1, B_2, B_3, B_4, and B_5 are constants determined from a regression analysis on the data.

Slab thickness was not truly a full factorial variable, and consequently could not be entered as an independent variable and had to be analyzed separately. All the subsequent regression analyses were performed for the 8-in. pavement thickness factorial. The 1.75 power for the thickness term will be established later.

The soil support term is a combination of the subgrade and subbase strength characteristics. The soil support is a calculated value developed in a previous analysis. In some cases the natural soil was stabilized with lime (generally clay) to facilitate construction operations by providing a working platform.

The soil support is defined as

$$SS = \left(\frac{U_1 + U_2}{T_{sg}}\right) \tag{2}$$

where

- SS = Soil support;
- U = Unconfined compressive strength of subbase and subgrade materials in psi at an age of 7 days;
- T_{sg} = Texas triaxial classification of subgrade material; and
- 1, 2 = Subscripts denoting subbase and stabilized subgrade respectively.

In all subsequent analysis the load, L, will be 18 kips and the pavement slab thickness will be 8 in. The linear form of load used here has been qualified in another report on this project (7) and in studies by others (5). The data from each run were carefully analyzed to screen out what might be considered erroneous.

The power term for the temperature differential term was derived in another report on this overall study (8). The temperature differential, the pavement thickness, and the load terms were not a part of the full factorial experiment, but in order that their effect would be reflected in the A_0 term, constant values for the 8-in. factorial were inserted into the equation for variables not considered in the semi-factorial experiment. The values inserted into the equation were an 18-kip single axle load, 8 in. for pavement thickness, and zero for temperature differential. These factors were then considered as constant and moved to the left of the equation.

A multiple regression analysis was made using the computer on each data run for deflection at the crack position, D_c, and also for deflection midway between cracks, D_e. The constants and the statistics derived from the regression analysis of each of the four runs are given in Table 5.

TABLE 5

COMPUTED CONSTANTS AND STATISTICS FROM REGRESSION ANALYSIS*

Load Position	Data Run No.	Computed Values							
		A_0	B_2	B_3	B_4	B_5	r	r^2	σ
Crack	1	6.664	0.334	0.681	-0.060	3.222	0.698	0.487	±0.0032
	2	0.00256	-0.123	0.526	0.1100	13.437	0.551	0.303	±0.0029
	3	0.1220	0.104	0.690	0.0900	13.911	0.662	0.438	±0.0030
	4	0.1099	0.1249	0.6869	0.0794	13.575	0.694	0.482	±0.0021
Midspan	1	0.0118	-0.0684	0.3211	-0.1938	7.816	0.407	0.166	±0.0035
	2	0.0726	0.0418	0.3434	-0.3294	7.055	0.244	0.060	±0.0032
	3	0.00373	-0.124	0.8709	0.1814	11.798	0.733	0.538	±0.0027
	4	0.0749	0.1026	0.7179	0.1897	4.876	0.515	0.265	±0.0031

*FOR EQUATION 1: r = coefficient of correlation, r^2 = coefficient of determination, σ = standard error of estimate.

The calculated deflection was plotted against the measured deflection for each data run and for each load position. These graphs are shown in Figures 23 through 30. Note the same general pattern for runs 1, 2, and 3 for both the crack and midspan deflections. The deflections at both crack and midspan were very small on run 4, as discussed previously, when compared with the three previous data runs.

In Table 5 note that several values of B_4 are negative. This same result was the case in a previous analysis (8). The crack spacing deflection relationship is a bowl-shaped curve, concave upwards. When the crack spacing is greater than that at the point of zero slope, B_4 is positive, and when it is smaller, B_4 is negative. Figure 31 is an example of the deflection-crack spacing relationship that results in a change of signs on B_4.

Several of the values calculated for B_2 are also negative. B_2 is the exponent on the modulus of elasticity term in the model equation. A negative B_2 would be in disagreement with theoretical concepts. Earlier it was pointed out that the low modulus of elasticity CRCP was deflecting less than the high modulus of elasticity CRCP. Another investigation on an experimental CRCP showed this same factor between lightweight and conventional aggregate concrete (7).

Note that the constants for each variable term generally have approximately the same magnitude, with only a few exceptions. The data from the first three runs were comparable, and therefore they were combined and a regression analysis was run. This resulted in two final equations, one for deflection at the crack position and another for deflection at a point midway between cracks. The computed constants and statistics are given in Table 6. The equation would be applicable to a dry condition; for a wet condition the equation for run 4 would be used. Note that the standard error is only slightly greater than the resolution of the Benkelman beam.

Radius of Curvature

The radius of curvature data have been examined thus far in terms of stress, but the subsequent analysis will be in terms of the radius of curvature data.

TABLE 6

COMPUTED CONSTANTS AND STATISTICS FOR DEFLECTION EQUATIONS

Load Position	Regression Analysis Computations							
	A_0	B_2	B_3	B_4	B_5	r	r^2	σ
Crack	0.3779	0.1683	0.6513	0.0266	6.3407	0.6971	0.486	±0.0028
Midspan	0.1362	0.0977	0.5601	-0.0462	4.1266	0.5544	0.307	±0.0033

Note: r = coefficient of correlation, r^2 = coefficient of determination, σ = standard error of estimate.

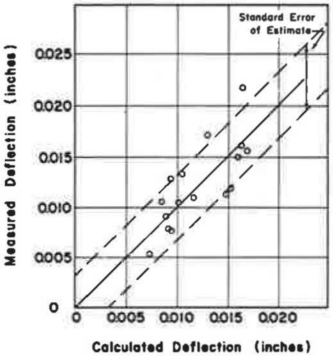

Figure 23. Measured vs calculated deflection at cracked edge—fall.

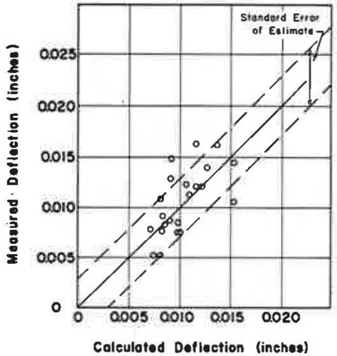

Figure 24. Measured vs calculated deflection at cracked edge—winter.

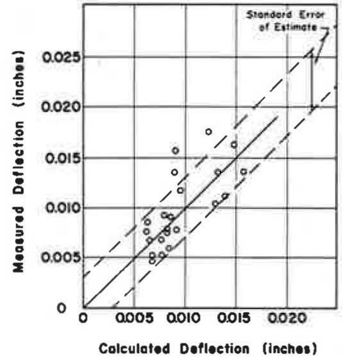

Figure 25. Measured vs calculated deflection at cracked edge—summer.

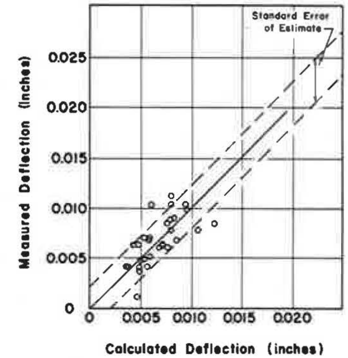

Figure 26. Measured vs calculated deflection at cracked edge—spring.

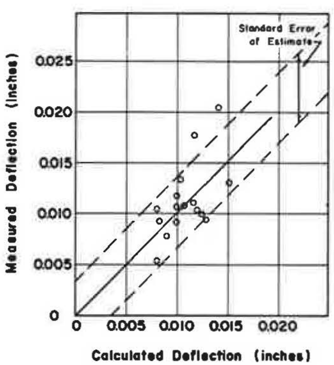

Figure 27. Measured vs calculated deflection at uncracked edge—fall.

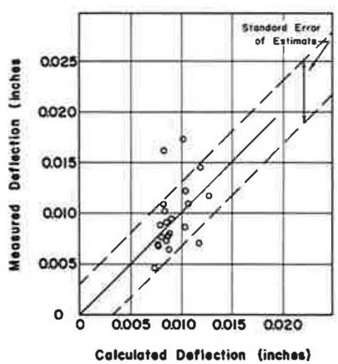

Figure 28. Measured vs calculated deflection at uncracked edge—winter.

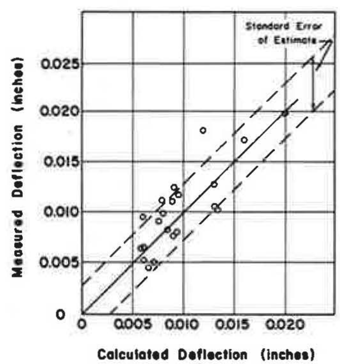

Figure 29. Measured vs calculated deflection at uncracked edge—summer.

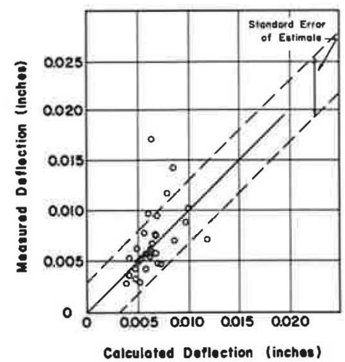

Figure 30. Measured vs calculated deflection at uncracked edge—spring.

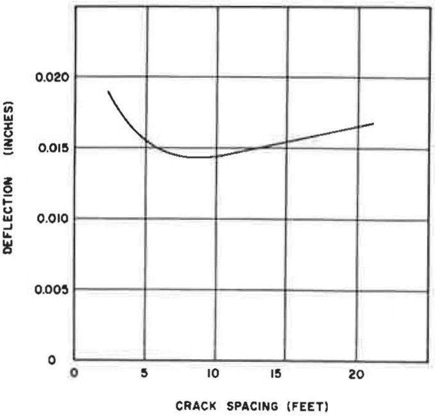

Figure 31. Deflection vs crack spacing.

The variables investigated that might affect the radius of curvature are the average crack spacing, soil support, concrete modulus of elasticity, load, and slab thickness. Thus, radius of curvature is some function of all these variables:

$$R_c,\ R_e = f(\overline{X},\ SS,\ E,\ L,\ D)$$

where

R_c = Radius of curvature at crack position, and

R_e = Radius of curvature at midspan position.

All other terms have been defined previously.

A model equation for radius of curvature was logically derived using the same concept as developed in the deflection equation. The' following is the model with variables considered:

$$R_c = \frac{A_0\, D^{1.75}\, E^{B_2}\, SS^{B_3}\, \overline{X}^{B_4}}{L} \qquad (3)$$

All terms are as previously defined.

In the radius of curvature study the slab thickness again could not be entered as an independent variable because of a shortage of test sections on pavement thinner than 8 in. Thus the same thickness term was used here as in the deflection analysis, $D^{1.75}$.

Although the crack width and temperature differential are not reflected in Eq. 3, they were considered in this study and previous studies. Previous studies indicated that the effect of temperature differential on the radius of curvature was very slight or nonexistent. Therefore, on this basis, the temperature differential term was deleted. With regard to crack width, this term was included in the equation, but it was found that the statistics of correlation were improved by deleting it from the regression equation.

The radius of curvature of the CRCP is studied at two points on the continuous slab, across the volume change crack and midway between the cracks. The crack radius of curvature was analyzed for each data run except the fourth. The individual data runs were analyzed using multiple regression techniques. The regression constants for the model equation are given in Table 7. In order to obtain a more general equation for the radius of curvature at the crack position, the field data were examined and runs 1 and 2 were combined to form the data for the regression that would produce the final equation for radius of curvature at the crack position. Figures 32 through 35 show the measured radius of curvature plotted against the calculated radius of curvature for the crack position for runs 1, 2, and 3 and the combined data. The computed constants and the statistics for the final equation are given in Table 8.

TABLE 7

COMPUTED CONSTANTS AND STATISTICS FROM RADIUS OF CURVATURE ANALYSIS*

Load Position	Data Run No.	Computed Values						
		A_0	B_2	B_3	B_4	r	r^2	σ
Crack	1	0.000832	0.9819	0.6572	-0.2623	0.9518	0.9059	± 962
	2	350.5333	0.1548	0.3429	-0.1766	0.5574	0.3107	±1716
	3	53.4066	0.2898	0.4070	-0.0035	0.6900	0.4762	±2132
Midspan	1	0.0742	0.7395	0.1882	0.0277	0.9527	0.9076	± 868
	2	1779.2667	0.0639	0.3102	0.0863	0.4368	0.1908	±2247
	3	313.4298	0.1736	0.5872	0.0345	0.7503	0.5630	±2798
	4	1337.6603	0.0832	0.2894	0.1147	0.4453	0.1983	±2525

*FOR EQUATION 3: r = coefficient of correlation, r^2 = coefficient of determination, σ = standard error of estimate.

TABLE 8

COMPUTED CONSTANTS AND STATISTICS FOR RADIUS OF CURVATURE EQUATIONS

Load Position	Regression Analysis Computations						
	A_0	B_2	B_3	B_4	r	r^2	σ
Crack	15.3039	0.3312	0.5467	-0.0772	0.6391	0.4085	±1617
Midspan	333.3153	0.1729	0.3579	0.0909	0.5957	0.3548	±2508

Note: r = coefficient of correlation, r^2 = coefficient of determination, σ = standard error of estimate.

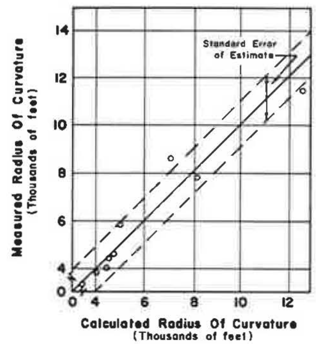

Figure 32. Measured vs calculated radius of curvature at cracked edge—fall.

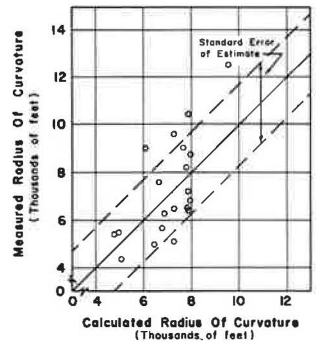

Figure 33. Measured vs calculated radius of curvature at cracked edge—winter.

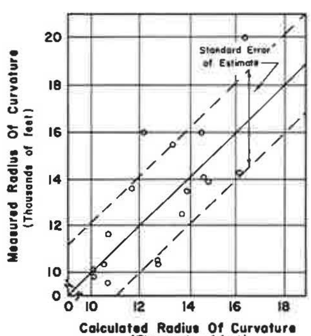

Figure 34. Measured vs calculated radius of curvature at cracked edge—summer.

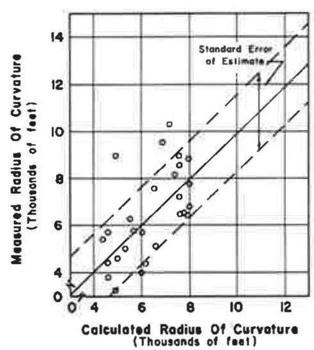

Figure 35. Measured vs calculated radius of curvature—combined data.

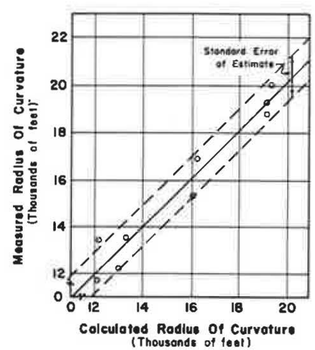

Figure 36. Measured vs calculated radius of curvature at uncracked edge—fall.

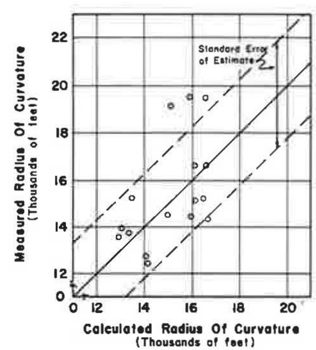

Figure 37. Measured vs calculated radius of curvature at uncracked edge—winter.

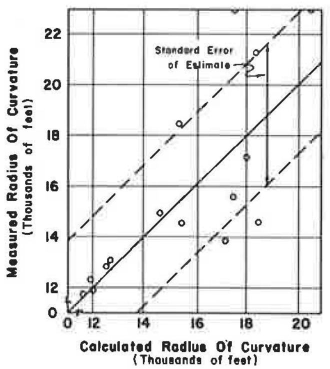

Figure 38. Measured vs calculated radius of curvature at uncracked edge—summer.

The midspan radius of curvature data were analyzed in like manner as the crack radius data; however, here all four data runs were used to relate the parameters studied to radius of curvature. The computed constants and statistics for the four equations are given in Table 8. Figures 36 through 39 show the calculated radius of curvature plotted against the measured midspan radius of curvature.

DISCUSSION OF RESULTS

Deflection

In general, the control variables considered in this study were found to affect the deflection of a CRCP. Their effect follows a pattern that can be expressed by a mathematical expression. Of the semi-controlled variables considered, it was found that the soil moisture condition affected the deflection, although the findings were contrary to the generally accepted criteria of greater deflection for a moist condition. In addition, the findings of this study tend to verify the assumptions used in the design and development of CRCP.

Soil Moisture—The four data runs were made in different seasons over a period of about two years. At the times the data were taken, the general soil moisture conditions were not the same. The fourth run was exceptionally wet, and deflections on this run were all considerably less than they had been on the first three runs. Initially, this discrepancy between the findings and the normal assumption of more deflection for a wet condition caused much concern for errors that might have been made on the fourth run in taking the data. When the weather conditions were the same as on the fourth run, the pavement deflections on approximately one-third of the sections were measured again. As was the case previously, the deflections were small and for all practical purposes identical to those of the fourth run.

It is now believed that when the subgrade and subbase materials are saturated they respond to quick loading as does a soil sample in an undrained triaxial test. The load applied to the pavement is supported partially by the pore water in the pavement foundation rather than the soil grains as is the case where the soil is not saturated (13).

It should also be pointed out that the summer run, where the soil was the dryest, experienced slightly less deflection than periods when the subsoil was partially saturated. Of course, this latter condition could be the result of smaller cracks due to summer temperatures.

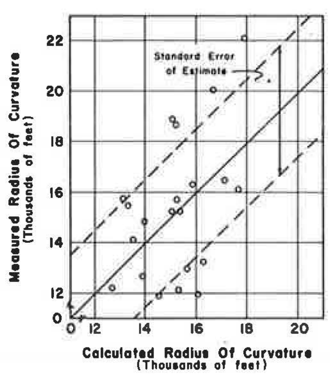

Figure 39. Measured vs calculated radius of curvature at uncracked edge—spring.

Equations—The deflection equations derived herein are extensions of the one developed in an earlier report (8). The previous equation was based on data taken from only two test sections, and those herein are based on 20 pavements with three sets of data from each for the dry condition and one set for the wet run. Table 9 gives a comparison of the equations with the equation developed earlier (8), which was based on crack position data only.

Figures 40 and 41 were prepared to illustrate the capability of the equation for predicting the observed deflection. In each case, the regression equation developed from the data for both the crack position and midspan position was used to calculate the deflection for a given set of conditions on a test section. This calculated deflection was then compared against measured deflections for the test sections as portrayed in the figures. Note the close

agreement, in most cases, between the measured and calculated values. In some cases, both the measured and calculated deflection appear to be out of line with what is to be expected, but these exceptions are normally due to a lime-stabilized subgrade and are so marked on the figures. These figures are typical of all runs, and hence, these observations support the validity of using these equations in design work.

Modulus of Elasticity—The findings in this study in regard to the modulus of elasticity of concrete contradict the generally accepted theory of a lower modulus of elasticity slab deflecting more than a high modulus one for equal conditions. Although the levels of the modulus are not too far apart in magnitude, another experiment on this same research project, wherein the levels were considerably greater through the use of two entirely different coarse aggregate types, indicated the same results. These two separate investigations, along with a limited laboratory investigation,

TABLE 9

COMPARISON OF REGRESSION ANALYSIS CONSTANTS

Constant	Overnight Study	Statewide Study
A_0	0.0106	0.3779
B_2	—	0.1683
B_3	0.8503	0.6513
B_4	0.0994	0.0266
B_5	4.8997	6.3407

$$D_c = \frac{A_0 L\, 10^{B_5 \Delta X}\, \overline{X}^{B_4}\, T_{sg}^{0.25 B_3}}{D^{1.75} E^{B_2} U^{0.25 B_3}\, 10^{0.0147 T}}$$

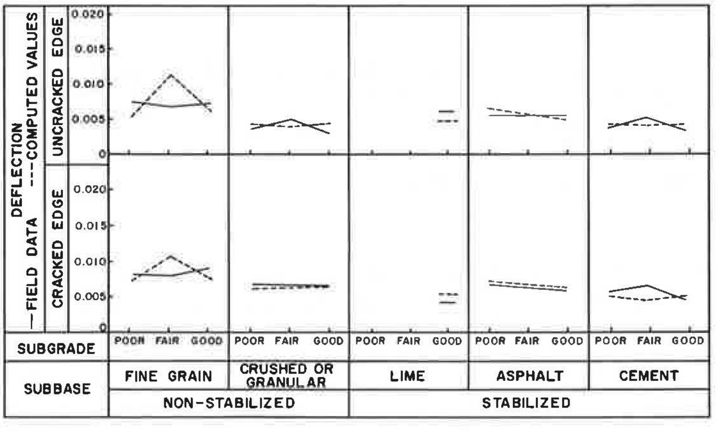

Figure 40. Measured and computed deflections on high modulus of elasticity concrete.

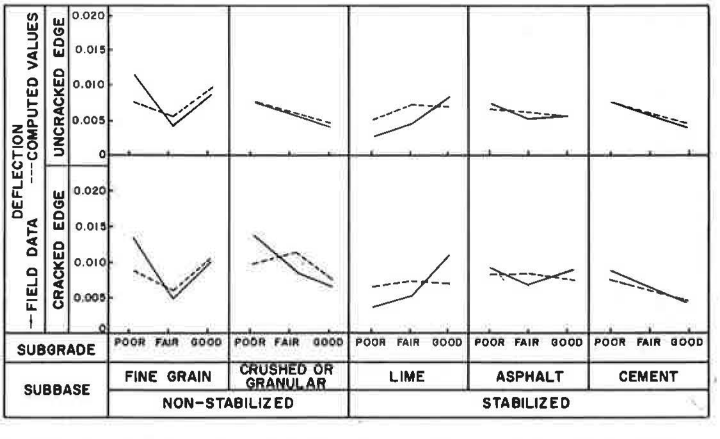

Figure 41. Measured and computed deflections on low modulus of elasticity concrete.

lend credence to the observations of less deflection with a lower modulus of elasticity concrete (14). It should be emphasized, however, that this observation can only be related to CRCP at this time and should not be translated to JCP, which may react differently.

There is a good possibility that this controversial observation attributed to modulus of elasticity could be an indirect effect of a combination of variables not considered in this experiment.

It may be hypothesized that generally speaking, a low modulus of elasticity concrete has a lower coefficient of thermal expansion. In this case the transverse volume change cracks would be smaller, and hence a greater degree of load transfer would be available. Therefore, with a greater load transfer less deflection would be experienced.

Furthermore, in the normal theoretical analyses of this condition, such as those of Westergaard, Pickett, Spangler, etc., the basic assumption is made that the subgrade reaction forces are vertical. An actual pavement on a subgrade deflecting under a wheel load develops a complicated interaction of shear forces and vertical forces, which may result in these field observations rather than those developed in a simplified theoretical approach.

Final Equation—The equations developed contain the term soil support, which was defined by Eq. 2. The soil support term can be eliminated from the deflection equations by substitution of Eq. 2 into Eq. 1. The dry or partially saturated condition was used as the level for selecting the final equation. Thus, the equation for deflection takes the form

$$D_c = \frac{0.3779\ L\ 10^{6.3407}\ \Delta X\ \bar{X}^{0.0266}\ T_{sg}^{0.1628}}{D^{1.75}\ E^{0.1683}\ (U_1 + U_2)^{0.1628}\ 10^{0.0147\ T}}$$

where all terms are as previously defined.

Radius of Curvature

The radius of curvature data show that the average radius of curvature at the cracked edge for all data is about 52 percent less than the radius of curvature at the uncracked edge. The radius of curvature at the crack and midspan was correlated by linear regression analysis for each of the four data runs, and the graphs were shown in Figures 17 through 20.

Figures 42 and 43 show calculated and measured radius of curvatures plotted against the subgrade classifications for each subbase material type that was available.

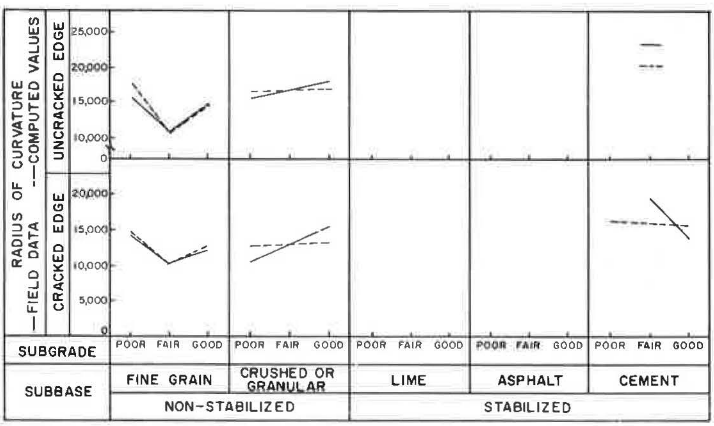

Figure 42. Measured and computed radius of curvatures on high modulus of elasticity concrete.

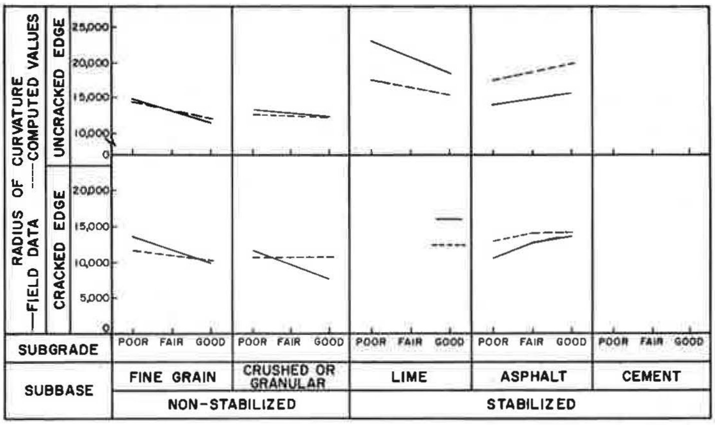

Figure 43. Measured and computed radius of curvatures on low modulus of elasticity concrete.

Final Equation—The radius of curvature equations determined for combined data contained the soil support term. Here again, the definition of soil support can be substituted and the radius of curvature equation will then take the form

$$R_c = \frac{15.3039\ D^{1.75}\ E^{0.3312}\ (U_1 + U_2)^{0.1367}}{L\ T_{sg}^{0.1367}\ \overline{X}^{0.0772}}$$

where all terms are as previously described.

An attempt was made to add the crack width as another variable but the results were such that it would be better not to include the crack width.

Accuracy of Regression Equations

Nineteen sets of deflection and radius of curvature data were analyzed by multiple regression methods. For each analysis a value of r, the correlation coefficient, was obtained. These values of r were checked against a table for their significance for the number of points and degrees of freedom (15). Table 10 gives the results of the r check.

The regression results appear to substantiate the form of the model equations. All checks on the correlation coefficients from the analysis of combined data were above that required to be significant. Previous discussions showed that the standard error of these equations is compatible with the accuracy of the equipment used. Thus the equations are in most cases statistically sound.

Validation of Design Assumptions

The findings of this study provide validity for the assumptions used in the original design analysis of CRCP. The equal magnitude of deflection at the crack position and midspan position indicates that sufficient granular interlock is provided so that approximately 100 percent load transfer is experienced across a crack. This finding is applicable only where the pavements have 0.5 percent longitudinal steel or more,

TABLE 10

INVESTIGATING THE SIGNIFICANCE OF CORRELATION COEFFICIENTS

Analysis	Crack	Midspan
Deflection:		
Run No. 1	G	F
Run No. 2	G	F
Run No. 3	G	G
Run No. 4	G	G
Combined data	G	G
Radius of Curvature:		
Run No. 1	G	G
Run No. 2	G	F
Run No. 3	G	G
Run No. 4		F
Combined data	G	G

G—The coefficient of correlation is greater than a minimum value required for significance.
F—The coefficient of correlation is less than a minimum value required for significance.

although there is a possibility that the lower limit on percent steel may be less than the minimum used in this experiment. Considering these aspects, this finding is applicable over a wide range of support conditions and concrete properties and components.

Furthermore, the use of the Westergaard interior loading conditions for determining the pavement thickness is a satisfactory procedure. The findings of this experiment indicate a 2-in. differential between CRCP and JCP and are in agreement with field performance from a deflection standpoint. This finding also has validity over a wide range of support conditions and concrete properties.

Design Equations

The final equations presented here for both deflection and radius of curvature provide excellent criteria for developing equations to be used in the design of concrete pavements. Although there are numerous factors other than deflection and stress to consider in the design of concrete pavements, this material will present another guideline for a designer to use in selecting the final pavement structure design for a given roadway.

Although percent longitudinal steel and pavement type are not enumerated in these design equations, they may be inserted on the basis of other material and studies developed in connection with this project. These are empirical equations and care should be taken not to extrapolate beyond the limits used in this analysis. The following are some suggested boundary conditions for extrapolation:

D_c = 0.003 in. to 0.030 in.
E = 3×10^6 psi to 6×10^6 psi
D = 6 to 8 in. for CRCP
D = 8 to 10 in. for JCP
$\overline{X}$ = 3 to 12 ft

CONCLUSIONS

This deflection study of CRCP has encompassed a wide variety of conditions and a considerable part of the geographical area of the state. The study was conducted over a 3-year period and over 15,000 separate measurements of various types were used. As a result of this field study and analysis, the following conclusions are warranted:

1. The variables studied herein that were found to affect the deflection of CRCP were concrete modulus of elasticity, modulus of rupture, crack spacing, surface crack width, pavement slab thickness, pavement type, strength characteristics of the subgrade and subbase, and subsurface moisture conditions. An empirical equation was derived using these variables, except modulus of rupture and moisture condition, to predict the deflection of a continuously reinforced concrete pavement under a given wheel load.
2. An equation was also derived from the study that predicts the radius of curvature of a pavement, i.e., related to pavement stress, in terms of the same variables with the exception of crack width.
3. It is recommended that the final equations derived herein be used to develop a nomograph predicting the deflection and radius of curvature for the variables studied. Through the use of this nomograph along with a maximum allowable deflection, pavements may be designed and/or checked in terms of the conditions existing on each project.
4. For the design equation mentioned, the variables of pavement type and percent longitudinal steel may be added to the equation on the basis of the studies herein and previous studies made in connection with this research project.
5. For continuous pavements, longitudinally reinforced with 0.5 percent steel or greater, it was found under a wide variation of support and environmental conditions that the transverse cracks in CRCP are small enough to retain sufficient aggregate interlock to maintain approximately 100 percent load transfer across the crack.
6. The transverse cracks were found to affect the continuity of a CRCP, since measurements indicated that the radius of curvature was smaller, i.e., there was greater stress at the crack than at a midspan point between cracks.
7. From a deflection and stress standpoint, pavements with stabilized subbases are superior in performance to pavements with non-stabilized subbases. All three of the

stabilizing agents considered in this study were found to give excellent performance from a deflection standpoint, but as a result of other studies that will be presented in the future, it is recommended that lime-stabilized subbases be protected with a non-erosive material.

8. From a deflection standpoint, the present practice of using a 2-in. thinner pavement for CRCP in relation to JCP as indicated by current design procedures is correct and conservative. For a given set of conditions, it was found that the deflection for an 8-in. CRCP is equal to or less than for a 10-in. JCP.

9. This study indicated that a reduction in thickness for CRCP had slightly more effect on deflection than an equal reduction in thickness for jointed pavement as found at the AASHO Road Test. Although there is a slight variation, the effect of pavement thickness on deflection as found by (a) this study, (b) the AASHO Road Test, and (c) Westergaard's theoretical analysis are in approximately the same range.

10. The use of a lime-stabilized subgrade, as practiced in Texas, for a working platform or moisture control was found to give an additional benefit of substantially reducing the deflections of a continuous pavement. Under certain conditions, the supporting characteristics of this layer may be considered in design.

11. From a deflection and stress standpoint, the design details presently being used by the Texas Highway Department for CRCP appear to be more than adequate for the conditions found in Texas.

12. This study developed two findings that contradict widely accepted beliefs concerning deflection of concrete pavement: (a) It was found that pavement on moist or saturated foundations deflected less than when the support was dry or partially saturated; These observations were confirmed during two different wet periods and three dry periods. (b) Although the difference is small, deflections and stresses are lower on low modulus CRCP than on high modulus concrete.

ACKNOWLEDGMENTS

The research reported herein was conducted under the supervision of Robert L. Lewis, Research Engineer, and under the general supervision of T. S. Huff, Chief Engineer of Highway Design, Texas Highway Department. The authors wish to extend their thanks to H. D. Swilley, Senior Laboratory Engineer, District 2; B. R. Hunter, Supervising Laboratory Engineer, District 3; Robert L. McKinney, Geologist, District 9; Billy Rudd, Senior Laboratory Engineer, District 10; Franklin J. Shenkir, Senior Laboratory Engineer, District 12; Clarence A. Weise, Supervising Resident Engineer, District 13; Charles W. Baxter, Senior Laboratory Engineer, District 15; Jerry Nemec, Supervising Resident Engineer, District 17; Wilburne C. Gromatsky, Supervising Construction Engineer, District 18; John W. Livingston, Senior Laboratory Engineer, District 19; Warren N. Dudley, Senior Laboratory Engineer, District 20; and Gaston P. Berthelote, Jr., Supervising Resident Engineer, Houston Urban Project, whose cooperation in providing field assistance and basic information made the success of this investigation possible.

The able assistance of various members of the Research Section, Ivan K. Mays, and others who were instrumental in the success of this investigation, is gratefully acknowledged. The field party that gathered the data is also to be commended.

REFERENCES

1. Status Report on Continuously Reinforced Concrete Pavement Built or Under Contract in the U.S. Concrete Reinforcing Steel Institute, July 1966.
2. Shelby, M. D., and McCullough, B. F. Experience in Texas With Continuously Reinforced Concrete Pavement. HRB Bull. 274, p. 1-29, 1960.
3. McCullough, B. F., and Ledbetter, W. B. LTS Design of Continuously Reinforced Concrete Pavements. Jour. Highway Div., Proc. ASCE, Vol. 86, No. HW4, Dec. 1960.
4. AASHO Interim Guide for the Design of Rigid Pavement Structures. AASHO Committee on Design, April 1962.
5. The AASHO Road Test: Report 5, Pavement Research. HRB Spec. Rept. 61E, 1962.

6. McCullough, B. F. Development of Equipment and Techniques for a Statewide Rigid Pavement Deflection Study. Research Rept. No. 46-1, Texas Highway Department, Jan. 1965.
7. McCullough, B. F. Evaluation of Single Axle Load Response on an Experimental Continuously Reinforced Concrete Pavement. Research Rept. No. 46-3, Texas Highway Department, April 1965.
8. McCullough, B. F., and Treybig, H. J. Determining the Relationship of Variables in Deflection of Continuously Reinforced Concrete Pavement. Research Rept. No. 46-4, Texas Highway Department, Aug. 1965.
9. Manual of Testing Procedures, Vol. 1. Texas Highway Department.
10. Design Manual for Controlled Access Highways. Texas Highway Department.
11. Standard Specifications for Road and Bridge Construction. Texas Highway Department, 1962.
12. Hudson, W. R. Value of Single Load Response in Rigid Pavement Design. Paper presented at Texas Section ASCE, May 10, 1963.
13. Taylor, Donald W. Fundamentals of Soil Mechanics (Ninth Printing). John Wiley and Sons, New York, 1956, p. 381-392.
14. McCullough, B. F., and Mays, Ivan K. A Laboratory Study of the Variables That Affect Pavement Deflection. Research Rept. No. 46-6, Texas Highway Department, Aug. 1966.
15. Snedecor, George W. Statistical Methods. Iowa State College Press, Ames, 1946, p. 351.
16. Westergaard, H. M. Stresses in Concrete Pavements Computed by Theoretical Analysis. Public Roads, Vol. 7, No. 2, April 1926.

Editor's Note: The original paper contained six Appendixes pertaining to equipment used, experimental procedure, summaries of data, deflection analysis, and soil support. This material is available from the Highway Research Board at cost of reproduction. When ordering, refer to XS-18, Highway Research Record 239.

Fatigue Tests of Prestressed Concrete Pavements

A. P. CHRISTENSEN and B. E. COLLEY, Paving Development Section, Portland Cement Association, Skokie, Illinois

The fatigue characteristics of prestressed concrete pavements were studied by repetitive moving load tests on 16 reduced scale prestressed concrete slabs. Each slab was 16 ft long, 12 ft wide, and 1 in. thick. Variables were magnitude of load, amount of longitudinal and transverse prestress, and subgrade strength.

Relationships were established between load magnitude, prestressed pavement properties, and the number of load coverages causing failure. Data from tests on slabs with varying magnitudes of prestress indicate that a minimum prestress of approximately 30 psi in both longitudinal and transverse directions is required to avoid top surface cracking when relatively few moving loads greater than those causing bottom surface cracking are applied repeatedly at interior locations. Data from tests on slabs cast on foundations of different strengths indicated that an increase in the foundation strength resulted in an increase in the number of load coverages causing failure.

•THE LOAD response of prestressed concrete pavements is being studied at the Research and Development Laboratories of the Portland Cement Association. The first published result of this study was a theoretical procedure (1) for determining the magnitude and distribution of stresses and deflections in prestressed concrete pavements for loads beyond cracking of the bottom surface. This procedure is specifically applicable to a centrally loaded infinite slab supported by a "dense liquid" foundation and prestressed equally in longitudinal and transverse directions.

To test the validity of the assumptions made in the theoretical procedure, load tests (2) were conducted on three reduced scale prestressed concrete slabs supported on a coil spring subgrade. Measurements of strain and deflection were made at a number of locations and load increments. Comparisons between test data and theory indicated fair agreement for values of deflection; however, measured strains were significantly smaller than those predicted by theory. The theoretical assumption that the moment-curvature relationship can be represented by two straight lines, an elastic portion with a constant slope followed by a plastic portion in which curvature increases under constant moment, was shown to be conservative for the static type of loading used.

Strain and deflection data were also reported (3) from static load tests conducted on three concrete slabs post-tensioned with steel strands. Each slab was 30 ft long, 12 ft wide, and 5 in. thick. Results again indicated that a prestressed concrete pavement can adequately support an edge or interior load of greater magnitude than that causing bottom surface cracking. Crack patterns were similar to those predicted by the theoretical procedure. Bottom surface cracks extended radially from the center of the load; top surface cracks were approximately circular for interior loads and semicircular for edge loads. However, applications of repeated moving loads cause the development of a random pattern of bottom surface cracks. To obtain information on the fatigue characteristics of prestressed concrete pavements with numerous working bottom surface cracks, a program of repetitive moving load tests was initiated on reduced scale prestressed concrete slabs.

Paper sponsored by Committee on Rigid Pavement Design and presented at the 47th Annual Meeting.

SCOPE AND OBJECTIVES

The test program was designed to study the behavior of 16 prestressed concrete slabs subjected to repetitive moving loads. Variables were magnitude of load, amount of longitudinal and transverse prestress, and subgrade strength. Because it was necessary to test a number of slabs to obtain sufficient data for a fatigue diagram, a reduced scale size was selected for the test slabs and the loading apparatus. The slabs were pretensioned and cast in place on either a clay subgrade, granular subbase, or cement-treated subbase.

The specific objectives of the program were (a) to determine a relationship between the load magnitude and the number of coverages causing pavement failure, (b) to determine the influence of prestress magnitude and foundation strength on fatigue properties of prestressed pavements, and (c) to observe the characteristics of a prestressed pavement failure and determine the factors that cause its development.

TEST FACILITIES AND MATERIALS

Data are reported from load tests on 16 concrete slabs 16 ft long, 12 ft wide, and 1 in. thick. Prestressing was accomplished with pretensioned high-strength steel wire. The slabs were cast in place and tested with a moving load apparatus designed for this program.

Test Area, Subgrade, and Subbase Materials

The prestressed slabs were cast and tested in the area shown in Figure 1. This area is enclosed in a 24-ft wide concrete building equipped with thermostatically controlled heaters to provide uniform temperature during the heating season. The test area was excavated 4 ft below grade to the bottom of the wall footings, and a 5-in. reinforced concrete floor was cast to form an enclosure for a subgrade material. A waterproofing compound was applied to the floor and walls to protect the subgrade from moisture changes. A clay material was compacted into this enclosure to a depth of 4 ft. Properties of the clay subgrade are given in Table 1. The modulus of subgrade reaction, k, is given in Table 5. It will be shown later that the average radius of relative stiffness for the 16 test slabs was 7.3 in. Therefore the subgrade depth was 6.6 times the radius of relative stiffness, and behavior should approximate a subgrade of infinite depth. The radius of relative stiffness, L, is a ratio of the stiffness of the slab to the stiffness of the subgrade (Eq. 3).

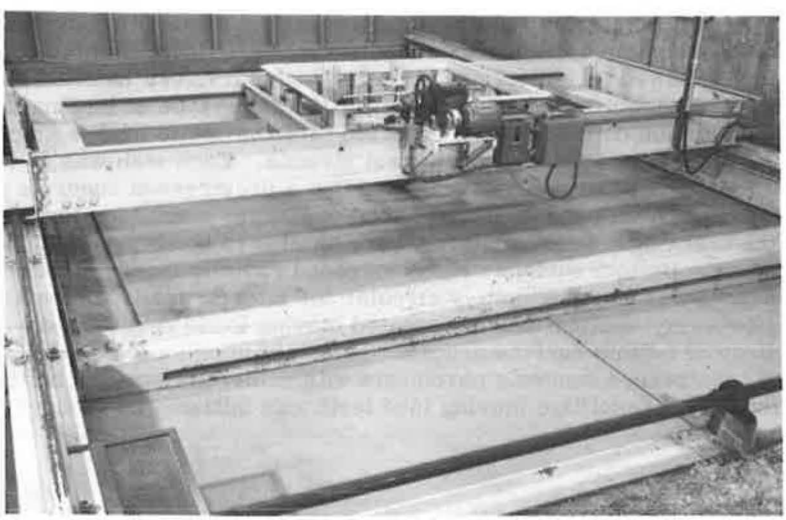

Figure 1. Test area and moving load apparatus.

TABLE 1

SUBGRADE PROPERTIES

Property	Particle Size (mm)	Percent	PCF
Material			
Gravel	76.2 -2.0	0	—
Coarse sand	2.0 -0.42	6	—
Fine sand	0.42 -0.074	8	—
Silt	0.074-0.005	48	—
Clay	smaller than 0.005	38	—
Liquid limit		36	—
Plasticity index		19	—
Maximum dry density (AASHO standard)		—	112
Optimum moisture		16	—

TABLE 2

SUBBASE PROPERTIES

Property	Particle Size (mm)	Percent	PCF
	Granular Material		
Gravel	76.2 -2.0	46	—
Coarse sand	2.0 -0.42	24	—
Fine sand	0.42 -0.074	17	—
Silt	0.074-0.005	10	—
Clay	smaller than 0.005	3	—
Plasticity index		0	—
Maximum dry density (AASHO standard)		—	141
Optimum moisture		7	—
	Cement-Treated Material		
Gravel	76.2 -2.0	27	—
Coarse sand	2.0 -0.42	23	—
Fine sand	0.42 -0.074	32	—
Silt	0.074-0.005	16	—
Clay	smaller than 0.005	2	—
Plasticity index		0	—
Maximum dry density (AASHO standard)		—	125
Optimum moisture		10	—
Cement content		5.5	—

Thirteen of the test slabs were cast on the clay subgrade without a subbase layer. The top surface of the clay was carefully finished to grade with a metal screed to obtain a level casting surface for uniform slab depth. After leveling, the subgrade was covered with two sheets of 4-mil thick polyethylene to retain moisture in the clay subgrade and to reduce stresses resulting from restraint to horizontal slab movement. The clay subgrade was removed to a depth of about 1 ft after each test and the soil was pulverized, reworked to optimum, and recompacted.

A 6-in. granular subbase was used under two of the test slabs, and a 6-in. cement-treated subbase was used under another. The properties of these subbases are given in Table 2. The modulus of subgrade reaction, k, is given in Table 5. For these tests the top 6 in. of clay subgrade was removed and replaced with subbase material. Polyethylene sheets were placed between the subbase and the concrete.

Prestressing

Test slabs were prestressed by the pretensioning method, i.e., the wires were tensioned prior to placing the concrete. After the concrete had attained sufficient strength,

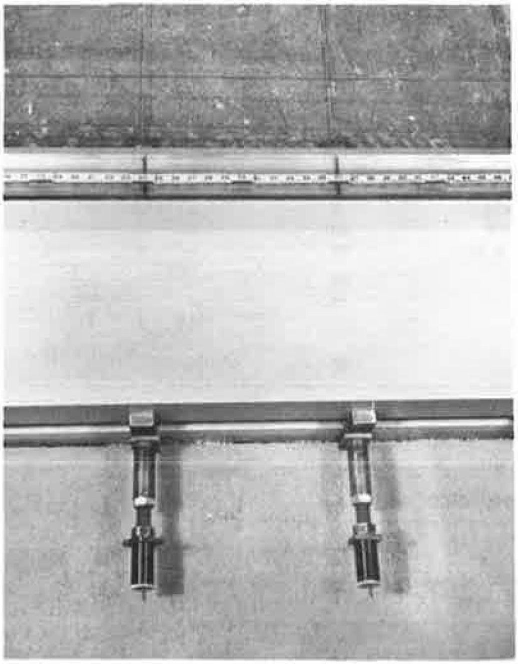

Figure 2. Devices used for tensioning the steel wires.

the wires were released and stress was transferred to the concrete through bond.

Uncoated, stress-relieved No. 12 steel wire was used for applying prestress at the mid-depth of the slabs. Wires in one direction alternated above and below those extending at right angles. The wire diameter was 0.1055 in., area 0.00875 sq. in., modulus of elasticity 27,600,000 psi, and ultimate strength 260,000 psi.

The reaction frame used for tensioning the wires had inside dimensions of 14 by 17 ft. Each side of the frame was formed by a pair of 15-in. steel channels between which the wires were inserted. Bolted moment connections were used at the frame corners. Concrete beams resting on the clay subgrade supported the reaction frame in a horizontal plane at the proper elevation for tensioning the wires at slab mid-depth.

Each prestressing wire was tensioned individually by the extension of a telescoping threaded spacer placed between the wire anchor and the reaction frame (Fig. 2). The force in the wire was measured by a transducer (4) placed between the wire anchor and the reaction frame at the side opposite the spacer. After tensioning the wires, a minimum of one day was allowed before casting the concrete slab. The force in each wire was checked and, if necessary, adjusted to the selected magnitude prior to casting.

To insure full prestress near the slab edges, a 1-in. split steel cube was fastened to each wire at the point where the wire entered the steel side forms. The two halves of the cube were grooved slightly undersize for the wire used and were clamped on the wire by countersunk machine screws.

Casting of Concrete

The cement factor of the concrete was 7.0 sk/cu yd; water-cement ratio was 0.52 by weight, and the sand-aggregate ratio was 0.59 by weight. Type 3 cement was used to obtain a high early strength, and the maximum size of gravel aggregate was 3/8 in. The slump averaged 4.7 in. and vinsol resin was added to provide an average air content of 6.9 percent. Concrete was compacted with a vibrating screed.

After casting, each slab was covered with polyethylene sheeting. The next day, approximately 16 hours later, the sheeting was removed and the top slab surface was coated with a curing compound to reduce moisture losses and thereby minimize curling. Prestressing wires were released after the concrete had cured for 7 days.

Beam specimens 1 by 4 by 22 in. were made at the time of casting from samples of concrete placed in the center portion of each test slab. The beams were cured in a 70 F, 100 percent relative humidity room until tested in flexure with third-point loading on a span of 12 in. It was usually possible to obtain two flexural tests from each beam. A minimum of nine beams was tested for each slab, including three tested when repetitive slab loading was started and three when each failure occurred. Repetitive load tests were started 12 to 14 days after casting. Duration of each test depended on the number of loadings necessary to cause failure and averaged 13 calendar days for all slabs. During the test period, there was relatively little change in the flexural strength of each slab; average values are given in Table 3.

TABLE 3

CONCRETE FLEXURAL STRENGTH

Slab No.	Modulus of Rupture (psi)	Slab No.	Modulus of Rupture (psi)
1	970	9	966
2	880	10	957
3	882	11	970
4	897	12	952
5	952	13	930
6	905	14	963
7	890	15	936
8	916	16	927

A limited number of beams were instrumented with two SR-4 type A9-4 (2-in. length) strain gages on the bottom surface between the third-point loads. Strain measurements during flexural testing of these beams indicated that the average modulus of elasticity for the test slabs was 4, 100, 000 psi.

Load Apparatus

A special load apparatus was constructed for applying repetitive moving loads to the prestressed concrete test slabs. The load apparatus was not designed to simulate traffic operations but rather to develop a random pattern of bottom surface cracks at the interior of each slab. Loads were applied through a single wheel traveling in a number of wheel paths over an interior area 32 in. wide (including the width of the wheel) by 98 in. long. The distances between the loading area and the longitudinal and transverse edges of the 12 by 16-ft slabs were 56 and 47 in. respectively. These edge distances were 7.7 and 6.4 times the average radius of relative stiffness of the test slabs, i.e., sufficient for load behavior to be similar to a slab of infinite surface area.

The equipment used to apply repetitive moving loads is shown in Figure 1. Load was applied through a 16-in. diameter wheel with a 4-in. wide solid rubber tire. The tire had longitudinal and transverse measurements scaled to represent the prototype. The contact area of the tire increased with increasing load as shown in Figure 3.

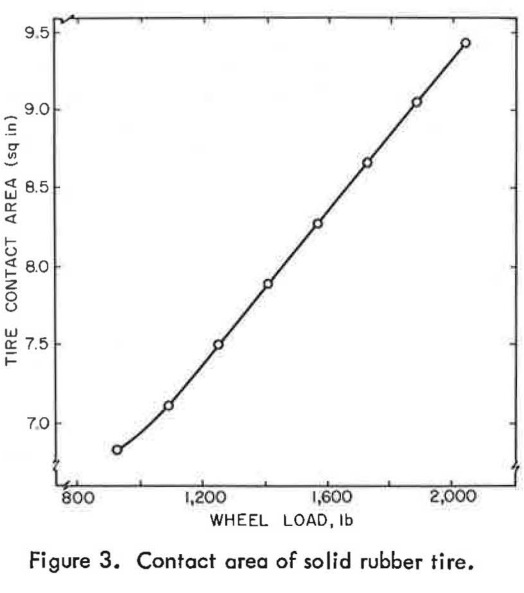

Figure 3. Contact area of solid rubber tire.

The paths traveled by the load wheel during the repetitive moving load tests are shown in Figure 4. Starting at location A, the wheel traveled 98 in. in a longitudinal path to location B. After returning in the same wheelpath to location A, the wheel was driven transversely a distance of 2 in. or half the width of the tire to a second longitudinal wheelpath. After returning to location C, the wheel was again driven transversely a distance of 2 in. to a third wheelpath. During each transverse movement of 2 in. the wheel traveled approximately 10 in. longitudinally. After traveling in 15 longitudinal wheelpaths or a total of 28 in. transversely to location D, the direction of transverse travel was reversed.

The Corps of Engineers (5) defines a load coverage as a sufficient number of vehicle operations or passes to produce

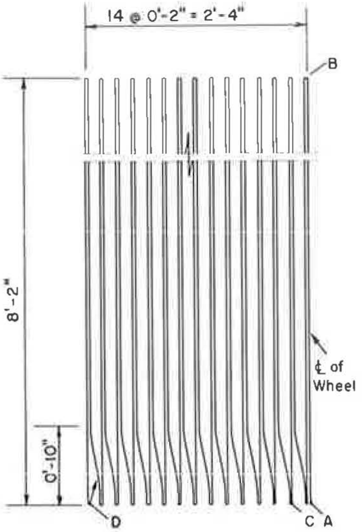

Figure 4. Wheelpaths during load testing.

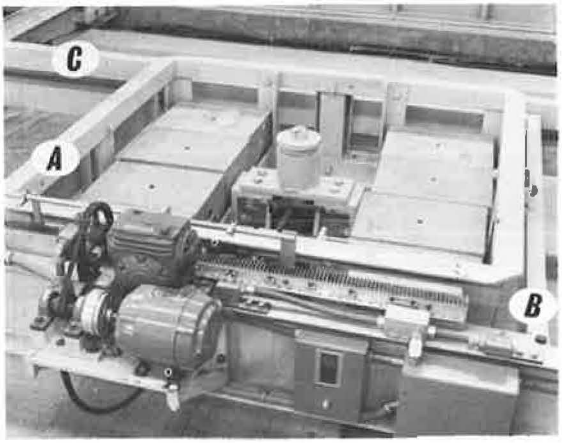

Figure 5. Load box.

statistically one application of the design loading over the entire traffic area. By this definition, 4 load coverages were applied each time the wheel traveled 28 in. transversely or from location A to D. The average wheel speed was 1.68 ft/sec and 106 coverages were applied per hour. Because this rate of loading is greater than that normally encountered on highway and airfield pavements, the data represent conditions more severe than those encountered in actual pavement service.

The load wheel was mounted in the center of a load box. To reduce transverse thrust on the test slabs when the wheel turned to change wheelpaths, the wheel was mounted as a caster with a swivel bearing. A spring mechanism was used to prevent the wheel from rotating 180 degrees on each return trip, as for example, from location B to A.

The load box, as represented by frame A in Figure 5, was made of steel angles welded together to form a frame 4 ft 5 in. by 4 ft 1 in. by 1 ft 5 in. deep. A pair of roller bearings that operated within a vertical channel at the center of each side of the load box enabled it to move freely in the vertical direction within frame B. The desired wheel load was obtained by placing concrete weights inside the load box.

Frame B was designed to move transversely within frame C by means of roller bearings that traveled on transverse bars bolted to the inside of the inside of the span beams of frame A. Power for driving frame B in the transverse direction was supplied by a ½-hp electric motor mounted on frame C. As shown in Figure 5, the motor acted through an electric clutch to drive a pinion gear over a rack mounted on frame B. Length of transverse travel was controlled by a number of stops contacting an electrical switch that regulated current to the clutch.

Frame C had a transverse span of 18 ft and a longitudinal length of 5 ft. A flanged crane wheel mounted near each corner traveled on longitudinal rails that were supported by steel beams independent of the subgrade and prestressing frame. Power for driving frame C in the longitudinal direction was supplied by a 5-hp electric motor. Operating through a gear reducer to obtain proper speed, the motor rotated a transverse steel shaft located near one end of the rails. Two steel drums were mounted on the shaft, one near each end between the flanges of the rail support beams. Each drum pulled a steel cable that traveled around a fixed pulley at the opposite end of the rails. Frame C was attached to the two cables to obtain longitudinal motion when the electric motor was operating. Length of longitudinal travel was controlled by an electrical switch that was activated when the load device passed either of two selected rail locations. This switch disconnected current and applied an electric brake to the motor. By regulating the electric current to the brake, the load device could be smoothly decelerated. An electrical switch on the motor shaft was used to determine when the load device had stopped and to start travel in the opposite longitudinal direction.

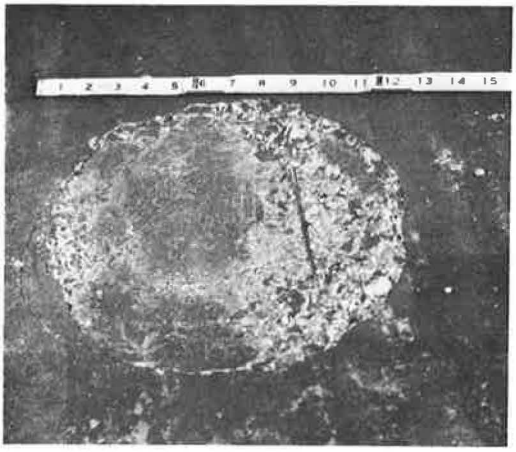

Figure 6. Failure in top surface of slab 2.

Instrumentation

Slab deflections were measured by a resistance bridge deflectometer (6) buried in the clay subgrade 2 ft below the test slabs. The deflectometer was restrained from vertical movement by a steel rod that extended between the deflectometer casing and the concrete slab under the clay subgrade. A second steel rod extended upward from the measurement control pin of the deflectometer to a fitting cast in the slab. An electrical connection between the deflectometer and chart recording equipment enabled deflections to be continuously measured as the load wheel approached and passed over the deflectometer location.

Strains were measured by pairs of SR-4 type A9-4 (2-in. long) strain gages cemented to the top surface of the test slabs, one in the longitudinal and one in the transverse direction at the same location. Strains were also recorded continuously as the load wheel approached and passed over the gages.

TEST RESULTS

Data are reported for load tests on 16 prestressed slabs. The spacing between prestressing wires, amount of tensile force in each wire, and resultant concrete prestress of each test slab are given in Table 4.

Moving loads were applied repeatedly to 15 of the test slabs until failure occurred. Wheel loads and number of coverages at failure are given in Table 5. Failure was characterized by a crumbling of the concrete in the top surface of the slab within a circular area approximately 12 in. in diameter (Fig. 6). These failures occurred very suddenly. Only a few additional load coverages were necessary for the top surface of the slab to deteriorate from the initial cracked condition to the failed condition shown. Failures occurred at random locations within the loaded areas. For most slabs, a thin steel plate was placed over the failed area and repetitive loading was continued until a second failure occurred. A bottom surface view of one of the slabs after a failure had occurred is shown in Figure 7. This photograph shows only a cut out interior portion of the slab where the moving loads were applied. Visual bottom surface cracks were indicated by black ink. Loose concrete was removed at the failure location to expose the prestressing wires. There were no wire failures during any of the load tests. After load testing

TABLE 4

REINFORCEMENT AND PRESTRESS PROPERTIES OF TEST SLABS

Slab No.	Wire Spacing (in.)		Wire Tensile Force (lb)	Concrete Prestress (psi)	
	Long.	Trans.		Long.	Trans.
1-8	12	12	1200	100	100
9	36	36	1200	33	33
10	None	None	0	0	0
11	12	12	140	12	12
12	12	0	1200	100	0
13-16	12	12	1200	100	100

TABLE 5

PROPERTIES OF TEST SLABS

Slab No.	Wheel Load (lb)	Coverages at Failure	h (in.)	k (pci)	L (in.)	a (in.)	α	m_c (in. lb./in.)
1	1730	5730	1.02	70	8.53	1.66	0.195	185
		7270	1.02	70	8.53	1.66	0.195	185
2	1571	2444	1.00	80	8.13	1.62	0.199	165
		3010	1.01	80	8.19	1.62	0.198	168
3	1571	2116	1.01	100	7.75	1.62	0.209	167
		2780	1.02	100	7.80	1.62	0.208	171
4	1410	2098	0.97	100	7.52	1.58	0.210	156
		3816	0.98	100	7.58	1.58	0.208	159
5	1410	25060	1.02	105	7.71	1.58	0.205	182
6	1730	330	0.96	110	7.28	1.66	0.228	155
		342	0.95	110	7.23	1.66	0.230	152
7	1571	472	0.92	120	6.90	1.62	0.235	140
		946	0.93	120	6.96	1.62	0.233	143
8	1571	6160	1.00	120	7.35	1.62	0.220	169
		7700	0.99	120	7.29	1.62	0.222	166
9	1571	7506	1.01	120	7.40	1.62	0.219	170
		8538	1.02	120	7.46	1.62	0.217	173
10	1571	860	1.01	120	7.40	1.62	0.219	163
11	1571	1676	1.02	120	7.46	1.62	0.217	170
12	1571	3226	1.00	120	7.35	1.62	0.220	159
13	Static Load Test		1.02	125	7.38	2.00	0.271	179
14	1730	18500	1.01	170	6.78	1.66	0.245	181
	Static Load Test		1.03	170	6.91	2.00	0.289	188
15	2049	1022	0.97	180	6.49	1.72	0.265	163
		1164	0.98	180	6.53	1.72	0.263	166
16	2206	0 to 14500[a]	1.00	320	5.75	1.76	0.306	171
	3478	14500 to 33700[a]	1.00	320	5.75	1.99	0.246	171

[a]Slab 16 did not fail.

was completed, slab thickness at each failed area was measured with a vernier caliper. Average thicknesses are given in Table 5.

A previous theoretical analysis (1) of prestressed concrete pavements indicated that strength is a function of α and m_c, where

$$\alpha = \frac{a}{L} \tag{1}$$

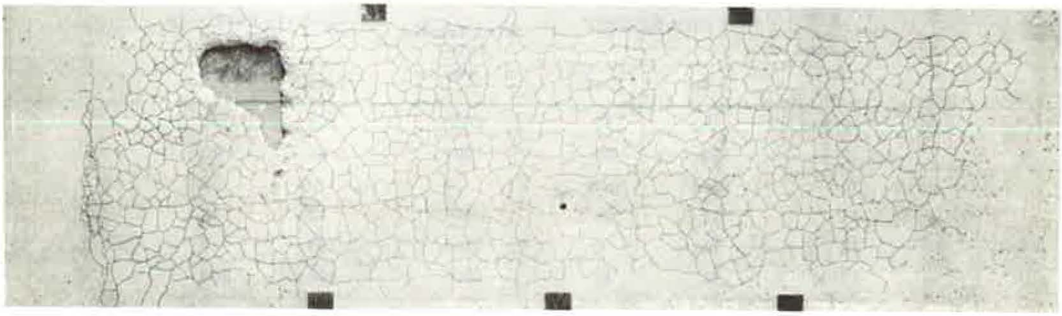

Figure 7. Crack pattern in bottom surface of slab 5.

and

$$m_C = \frac{\sigma_C h^2}{6} \tag{2}$$

in which

L = radius of relative stiffness (in.), i.e.,

$$L = \sqrt[4]{\frac{E h^3}{12 (1 - \mu^2)k}} \tag{3}$$

a = radius of loaded area (in.),
E = concrete elastic modulus (psi),
μ = Poisson's ratio,
h = slab thickness (in.),
k = subgrade modulus (pci),
σ_C = cracking stress (psi) = modulus of rupture plus prestress, and
m_C = cracking moment (in.lb/in. of width).

Computed m_C and α-values for each slab are given in Table 5. The radius of the loaded area, a, used to compute α-values was the radius of a circle having an area equal to that shown in Figure 3 for the loaded tire at the test load. The radius of relative stiffness, L, was computed using the measured value of 4,100,000 psi for the modulus of elasticity, E, and an assumed value of 0.15 for Poisson's ratio. The subgrade modulus, k, was determined with a 30-in. diameter plate at 0.05 in. deflection. The k-value given in Table 5 is the average of the values determined prior to the construction and after the testing of each slab. When computing m_C-values, cracking stresses were assumed to be equal to the summations of the modulus of rupture values given in Table 3 and the prestress values given in Table 4.

Analyses

To analyze the test data given in Table 5 and develop a design method for prestressed pavements, it is necessary to relate m_C and α-values with wheel loads and coverages causing failures. This may be done by using the m_C and α-values to compute either the bottom or the top surface cracking load of each slab, then establishing a relationship between the ratio of such cracking load to applied wheel load and the coverages causing failure.

Bottom Cracking

The following equation, based on Westergaard's (7) theoretical analysis for loads applied in the interior of the area of a panel, can be used to compute the bottom cracking load, P_C:

$$\left.\begin{matrix}\sigma_x \\ \sigma_y\end{matrix}\right\} = \frac{P}{h^2}\left[0.275\,(1+\mu)\log_{10}\frac{Eh^3}{k\left(\frac{a+b}{2}\right)^4} \mp 0.239\,(1-\mu)\,\frac{a-b}{a+b}\right] \tag{4}$$

where σ_x and σ_y = principal tensile stresses in the directions of x and y at the bottom of the slab under the center of the load, and a and b = semiaxes of an ellipse representing the footprint of a tire. For a circular loading area where a = b and letting $\mu = 0.15$, $L^4 = \frac{Eh^3}{12(1-\mu^2)k}$, $\alpha = \frac{a}{L}$, and $m_C = \frac{\sigma_x h^2}{6}$, Eq. 4 becomes:

$$P_C = \frac{m_C}{0.0527\left(4\log_{10}\frac{1}{\alpha} + 1.069\right)} \tag{5}$$

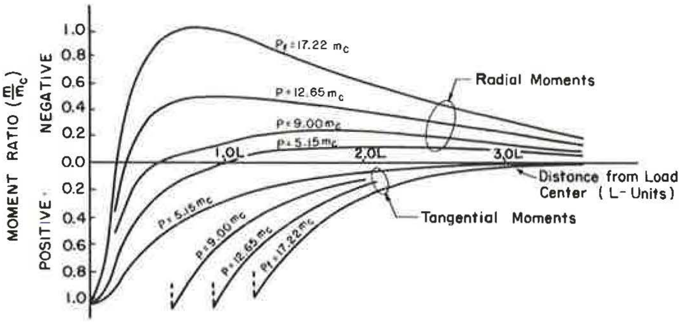

Figure 8. Radial and tangential moment curves—PCA theoretical method for $\alpha = 0.2$.

Top Cracking

The top surface cracking load of a prestressed pavement may be computed by the PCA theoretical method (1). This method is limited to a load applied at an interior position of a slab supported by a dense liquid foundation and prestressed equally in the longitudinal and transverse directions. By use of this method, radial and tangential moment diagrams were developed for loads greater than those causing bottom surface cracking, i.e., beyond conditions to which the elastic theory is applicable. Example moment diagrams for $\alpha = 0.2$ are shown in Figure 8. Bottom surface cracks begin to form under the load when the positive moment, m, equals the cracking moment, m_c, or when $m/m_c = 1$. A small increase in load beyond that initiating bottom cracking will cause these cracks to extend radially from the center of the load. As additional load is applied, there is an increase in the positive tangential moment and negative radial moment. The bottom surface radial cracks become longer, and the point of zero radial moment moves nearer the center of loading. At a load, P_F, equal to 17.22 times the cracking moment, m_c, the negative radial moment equals the cracking moment and a circular crack occurs in the top surface of the slab. Other top surface cracking loads predicted by the PCA method for α-values varying from 0.1 to 0.5 may be determined from the diagram shown in Figure 9.

Another method for computing top surface cracking loads is that used by the Corps of Engineers. Based on the results of previous static load tests on Hydrocal model slabs 16.6 in. square by 0.20 in. thick and supported on a 12-in. thick layer of natural rubber, the following empirical equation was developed (8):

$$P_F = \frac{h^2 (R + R_P)}{6\left[C\frac{M_O}{P_O} - \frac{M_R}{P_O}\right]} \qquad (6)$$

where

P_F = top surface cracking load (lb),
h = slab thickness (in.),
R = flexural strength of the concrete (psi),
R_P = concrete prestress (psi),
C = radial moment correction factor,
M_O/P_O = moment coefficient under center of loaded area, and
M_R/P_O = moment coefficient at point of negative moment cracking.

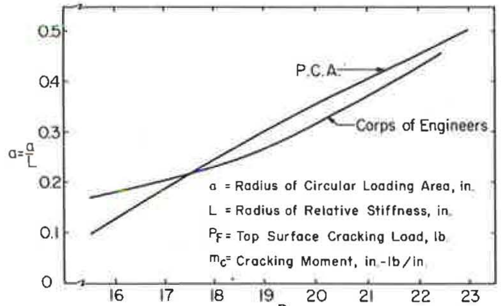

Figure 9. Top surface cracking loads for prestressed concrete pavements.

TABLE 6

DESIGN FACTORS BASED ON TOP CRACKING LOADS

Slab No.	Wheel Load (lb) P	Coverages at Failure	Bottom Cracking Load (lb) P_c	Top Cracking Load (lb) P_F			Fatigue Factors	
				PCA	C of E	Average	$\frac{P}{P_c}$	$\frac{P_F}{P}$
1	1730	5730	898	3170	3080	3125	1.93	1.81
		7270	898	3170	3080	3125	1.93	1.81
2	1571	2444	809	2800	2730	2765	1.94	1.76
		3010	824	2860	2790	2825	1.91	1.80
3	1571	2116	835	2900	2870	2885	1.88	1.84
		2780	855	2950	2910	2930	1.84	1.87
4	1410	2098	784	2730	2700	2715	1.80	1.93
		3816	795	2780	2740	2760	1.77	1.96
5	1410	25060	905	3150	3100	3125	1.56	2.22
6	1730	330	807	2720	2760	2740	2.14	1.58
		342	796	2680	2720	2700	2.17	1.56
7	1571	472	741	2500	2540	2520	2.12	1.60
		946	753	2540	2580	2560	2.09	1.63
8	1571	6160	867	2960	2960	2960	1.81	1.88
		7700	856	2920	2930	2925	1.84	1.86
9	1571	7506	870	2990	2990	2990	1.81	1.90
		8538	881	3060	3000	3030	1.78	1.93
10	1571	860	834	2920	2930	2925	1.88	1.86
11	1571	1676	866	2980	2980	2980	1.81	1.90
12	1571	3226	815	2940	2940	2940	1.93	1.87
13	Static Load Test		1017	3310	3420	3365	—	—
14	1730	18500	978	3260	3340	3300	1.77	1.91
	Static Load Test		1106	3530	3660	3595	—	—
15	2049	1022	916	2980	3080	3030	2.24	1.48
		1164	927	3040	3140	3090	2.21	1.51
16	2206	—[a]	1036	3270	3390	3330	2.13	1.51
	3478	—[a]	1118	3390	3510	3450	3.11	0.99

[a]Slab 16 did not fail.

In using this equation, values of C, M_o/P_o, and M_R/P_o must be obtained from appropriate curves (8). These values are plotted as functions of either A/L^2 or a/L where A is the area of the loaded area, a is the radius of the loaded area, and L is the radius of relative stiffness, so that it is possible to develop a relationship between P_F/m_c and a/L where m_c is equal to $h^2 (R + R_P)/6$. The resultant curve for circular loading areas is compared to the PCA method in Figure 9. It is seen that the two methods are in fair agreement.

Slabs on Clay Subgrade

Data are presented from tests on the nine slabs cast on a clay subgrade and prestressed to 100 psi in both longitudinal and transverse directions. Comparisons will later be made with the four slabs that had reduced amounts of prestress and with the three slabs cast on granular and cement-treated subbases.

Using the m_c and α-values given in Table 5, bottom surface cracking loads were computed by Westergaard's Eq. 5, and top surface cracking loads were computed by both the PCA and Corps of Engineers method using Figure 9. Top cracking loads by the two methods were nearly equal for each slab failure, and average values were used to determine ratios of computed top surface cracking loads divided by repetitive moving wheel loads. Also, ratios of repetitive moving loads divided by bottom surface cracking loads were determined. These ratios are given in Table 6 and in this report are defined as fatigue factors. Fatigue factors are plotted in Figure 10A and 10B vs the number of load coverages causing failure.

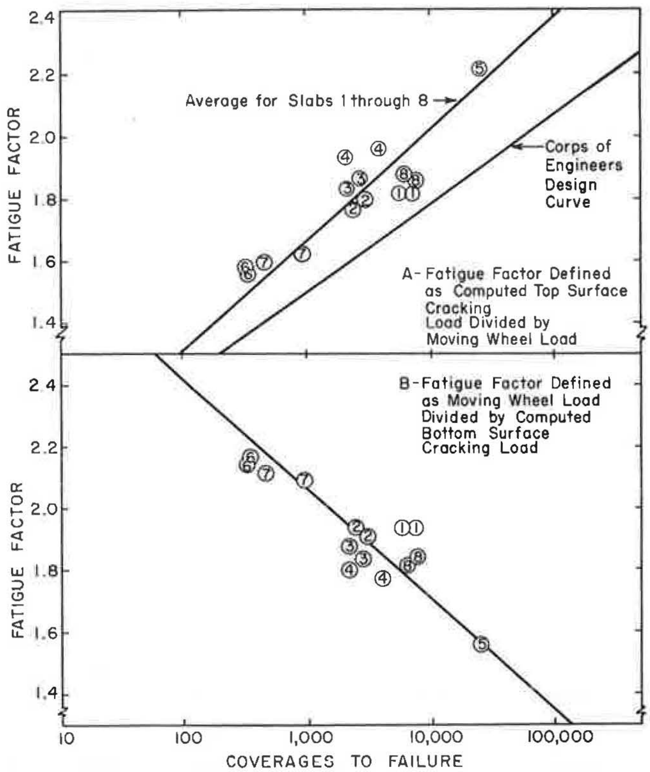

Figure 10. Fatigue relationships for prestressed concrete pavements.

The results of these tests may be compared with data from a similar moving load test program conducted by the Corps of Engineers (5). The essential differences between these two programs were as follows:

Characteristic	Corps of Engineers	PCA
Casting Technique	Precast	Cast in place
Prestressing: Method	Pretensioned	Pretensioned
Amount	250 psi	100 psi
Size of Slab: Length	15 ft	16 ft
Width	6 ft	12 ft
Thickness	1 in.	1 in.
Size of Loaded Area: Length	120 in.	98 in.
Width	24 in.	32 in.
Avg. Conc. Mod. of Rupt.	905 psi	914 psi
Avg. Conc. Elas. Mod.	4,500,000 psi	4,100,000 psi
Avg. Subgrade Modulus	65 pci	105 pci

In analyzing their data, the Corps of Engineers plotted a curve that related a design factor for repetitive loading to the number of load coverages causing failure. Their design factor was defined as the computed top surface cracking load for a single application divided by the repetitive moving wheel load. This curve is shown on the appropriate diagram in Figure 10A. For a given fatigue ratio, it indicates a greater number of coverages at failure than the PCA curve.

TABLE 7

CRACKING LOADS FROM PREVIOUS STATIC LOAD TEST PROGRAM (2)

Slab No.	α	m_c (in. lb./in.)	Measured Cracking Loads (lb)		Theoretical Cracking Loads (lb)	
			Bottom	Top	Bottom	Top
1	0.315	155	880	4140	900	2950
2	0.525	155	1220	4820	1270	3570
3	0.315	130	850	4180	780	2470

In designing a prestressed pavement using the data shown in Figure 10A and 10B, the fatigue factor may be based on either the top or bottom cracking load. However, it will be shown that top cracking loads measured during static load tests on prestressed pavements are usually greater than those predicted by either the PCA or Corps of Engineers method, whereas measured bottom cracking loads can be accurately predicted by elastic theory analysis. Also, to measure the strength of an in-service prestressed pavement, the bottom cracking load can be more readily determined by a static load test than the top cracking load, which would result in permanent damage to the pavement. Therefore, in analyzing the remaining data in this report, fatigue factors will be based only on the bottom surface cracking loads.

Static Load Tests

A previously reported (2) program of static load tests on prestressed concrete slabs indicated that the PCA theoretical method (1) provided conservative top surface cracking loads. In that program, reduced scale slabs, 8 ft by 8 ft by 1 in. thick, were loaded through centrally located circular plates while supported on a coil spring subgrade. A summary of bottom and top surface cracking loads from these tests is given in Table 7. Measured and theoretical bottom cracking loads were in agreement but measured top cracking loads were an average of 46 percent greater than theoretical values.

The theory assumed that the moment-curvature relationship could be represented by two straight lines, i.e., an elastic portion with a constant slope, followed by a plastic portion where curvature increased at a constant maximum moment equal to the cracking moment. The experimental slabs did not react in accordance with this assumption; moments greater than the initial cracking moment occurred after bottom surface cracking. This was the major reason that experimental top cracking loads were greater than those predicted theoretically.

The theory also assumed that bottom surface cracks extend radially from the center of the loaded area as load is increased. This assumption was confirmed by experimental data for static loading. However, under traffic load conditions the radial cracking is altered, and the assumed theoretical moment-curvature relationship may possibly be more appropriate. To study the effects of a random pattern of bottom surface cracks on load behavior, static load tests were conducted on slabs 13 and 14. The only test conducted on slab 13 was with a static load, so that the slab was in an uncracked condition prior to loading. The static load test on slab 14 was made after one failure had occurred from applications of repetitive moving load. The static load was applied through a 2-in. radius steel plate in 500-lb increments until top surface cracking occurred. A ½-in. thick rubber pad was placed between the plate and slab to aid in obtaining uniform load distribution. Both slabs were instrumented to measure maximum deflection at the load as well as radial and tangential strains at the load and at locations 7, 10, and 13 in. from the load.

Stresses were computed from the measured strains using

$$\sigma_r = \frac{E}{1 - \mu^2} (\epsilon_r + \mu \epsilon_t) \tag{7}$$

$$\sigma_t = \frac{E}{1 - \mu^2} (\epsilon_t + \mu\epsilon_r) \tag{8}$$

in which

σ_r = radial stress,
σ_t = tangential stress,
ϵ_r = measured radial strain,
ϵ_t = measured tangential strain,
E = concrete modulus of elasticity, 4,100,000 psi, and
μ = Poisson's ratio, assumed 0.15.

Maximum top surface compressive stresses resulting from positive moment at the center of the loaded area and maximum top surface tensile stresses resulting from negative radial moment beyond the point of contraflexure were determined for each load increment. These stresses together with maximum deflections are plotted in Figures 11 and 12.

Experimental top surface compressive stresses at the load center were used to determine the bottom surface cracking load for slab 13. Assuming that, before cracking occurred, top surface compressive stresses equaled bottom surface tensile stresses and that the cracking stress was 1030 psi, the experimental data indicated a bottom cracking load of 960 lb for slab 13. At this load, there was a slight change in the slope of the experimental load-stress curve. In comparison, the theoretical bottom cracking load as determined by Westergaard's analysis using Eq. 5 was 1018 lb for slab 13. Before bottom cracking, there was good agreement between experimental and theoretical stresses for slab 13; however, for slab 14 experimental stresses were approximately 40 percent greater than theoretical stresses. This expected difference was due to the extensive bottom surface cracking that had already occurred in slab 14 during 18,500 coverages of a 1730-lb moving wheel load.

For the PCA theoretical method, curves shown in Figure 13 indicate the relationship between maximum theoretical deflection, y, subgrade modulus, k, radius of relative stiffness, L, cracking moment m_c, radius of loaded area, a, and applied load, P. The curves in Figure 14 indicate the relationship between maximum theoretical negative radial moment, m_n, radius of relative stiffness, L, cracking moment, m_c, radius of loaded area, a, and applied load, P. Using these curves and the slab properties given in Table 5, maximum theoretical deflections and maximum theoretical top surface tensile stresses resulting from negative radial moments were determined for loads less than theoretical top cracking loads. Theoretical curves are compared with experimental data in Figures 11 and 12.

Experimental and theoretical deflections were in good agreement, but experimental top surface tensile stresses were generally greater than theoretical values. As a result, experimental top surface cracking loads were 4300 and 5000 lb for slabs 13 and 14, respectively, or an average of 36 percent greater than theoretical top cracking loads of 3310 and 3530 lb. Also, measured radii of the top surface cracks were an average of 10 in. compared with a theoretical average of 7 in. There did not appear to be any reduction in either top surface tensile stresses or top cracking loads as a result of the bottom surface cracking that occurred in slab 14 during repetitive moving load testing prior to the static test.

From these data it was concluded that, by existing methods of analysis for prestressed concrete pavement, bottom cracking loads can be more accurately predicted than top cracking loads. Therefore, for a prestressed pavement it appears more rational to base a fatigue factor for traffic load conditions on the bottom cracking load.

Influence of Prestress

The influence of magnitude and distribution of prestress on the load behavior of prestressed concrete pavements was studied by reducing the prestress in four of the test slabs. As shown in Table 4, all slabs except 9, 10, 11, and 12 had a concrete prestress of 100 psi in both longitudinal and transverse directions. In slab 9, the spacing

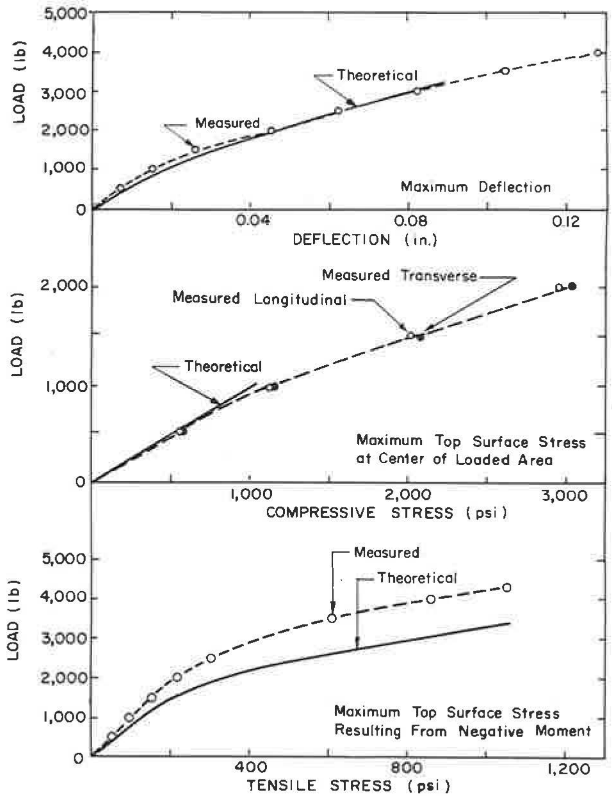

Figure 11. Static load test data—slab 13 (no prior loading).

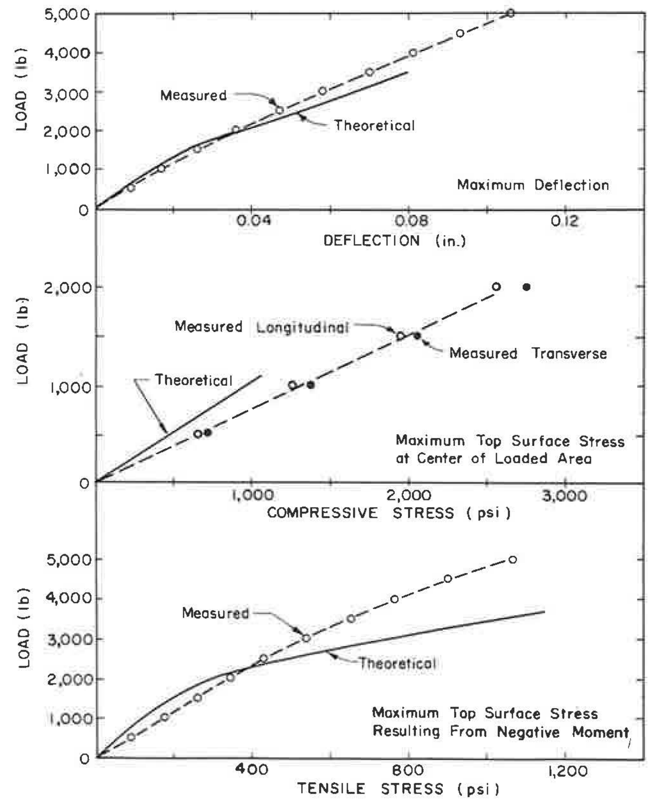

Figure 12. Static load test data—slab 14 (after repeated loading).

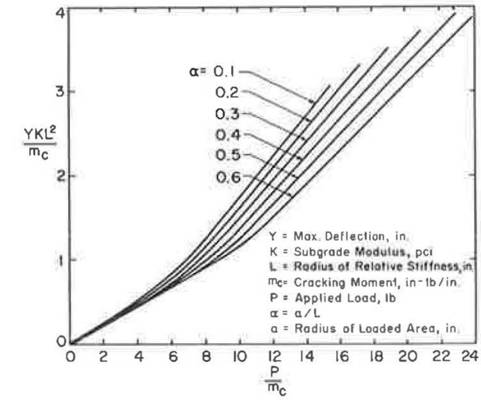

Figure 13. Relationship established by PCA theoretical analysis for deflections.

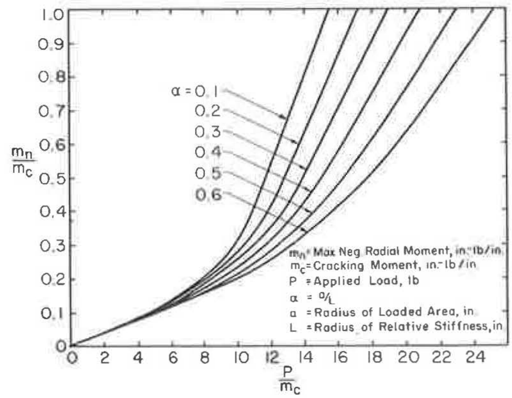

Figure 14. Relationship established by PCA theoretical analysis for moments.

of the steel wires was tripled from 12 to 36 in.; with a force of 1200 lb on each wire, the resulting prestress was reduced from 100 to 33 psi. Slab 10 did not contain any steel wires and was therefore neither reinforced nor prestressed. In slab 11, a spacing of 12 in. was used for the steel wires. However, the force on each wire was reduced to that needed for straightening the wires. This force was 140 lb on each wire and resultant prestress was 12 psi. Slab 12 did not contain any transverse steel wires; longitudinal wires were spaced 12 in. apart and had a force of 1200 lb on each wire, resulting in a longitudinal prestress of 100 psi.

Slabs 9 to 12 were tested with a 1571-lb repetitive moving wheel load until at least one slab failure occurred. Slabs 10 and 12 did not fail in the same manner as the other slabs, i.e., with a sudden crumbling of the concrete in the top surface of the slab. Slab 10 with neither reinforcement nor prestress showed distress earlier than the other test slabs, and top surface cracking developed over the entire loaded area after only a few load coverages, although it required 860 coverages before failure. Slab 12, with only longitudinal prestress, developed a longitudinal crack over each wire in the loaded area after a few hundred load coverages, although 3226 coverages were required before failure. Therefore, it was concluded that two-way prestress is required to avoid top surface cracking when relatively few moving loads greater than those causing bottom surface cracking are applied repeatedly at interior locations.

Fatigue factors were determined for slabs 9 and 11 by dividing the 1571-lb wheel load by the bottom cracking load computed from Westergaard's equation (Eq. 5). These fatigue factors are given in Table 6 and are plotted in Figure 15 as a function of the number of load coverages causing failure. Data from slab 9 (33 psi, 2-way prestress) were in better agreement than slab 11 (12 psi, 2-way prestress) with the curve determined from tests on slabs 1 through 8 (100 psi, 2-way prestress). Because of this it was considered that a prestress of 33 psi is approximately the minimum required for prestressed concrete pavements to support repeated moving loads greater than those causing bottom surface cracking.

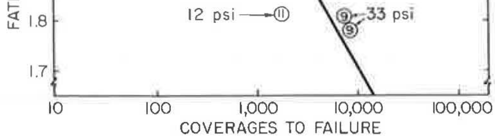

Figure 15. Effect of magnitude of prestress on fatigue.

Influence of Foundation Strength

The influence of foundation strength on the load behavior of prestressed concrete

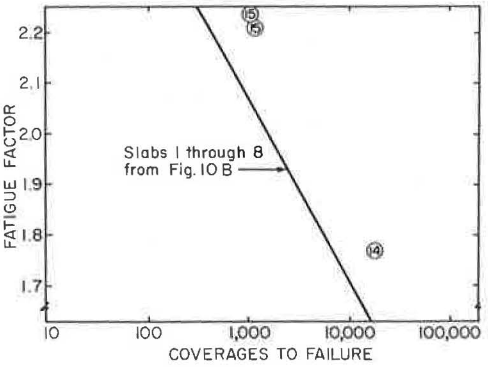

Figure 16. Effect of foundation strength on fatigue.

pavements was studied by casting three of the test slabs on 6-in. thick subbases. A granular subbase was used under slabs 14 and 15, and a cement-treated subbase was used under slab 16.

Slabs 14 and 15 failed in the same manner as slabs 1 through 8, i.e., with a sudden crumbling of the concrete in the top surface of the slab. Fatigue factors were determined by dividing the applied moving wheel load by the bottom cracking load computed from Westergaard's equation (Eq. 5). These fatigue factors are given in Table 6 and are plotted in Figure 16 as a function of the number of load coverages causing failure. Results are compared with the curve determined for slabs 1 through 8. Each of these slabs was prestressed to 100 psi in both longitudinal and transverse directions. However, the average subgrade modulus of the clay subgrade under slabs 1 through 8 was 100 pci compared to the modulus of 175 pci for the granular subbase under slabs 14 and 15. As would be expected, the curve determined for slabs 1 through 8 predicted a conservative number of load coverages for slabs 14 and 15 with the stronger foundation.

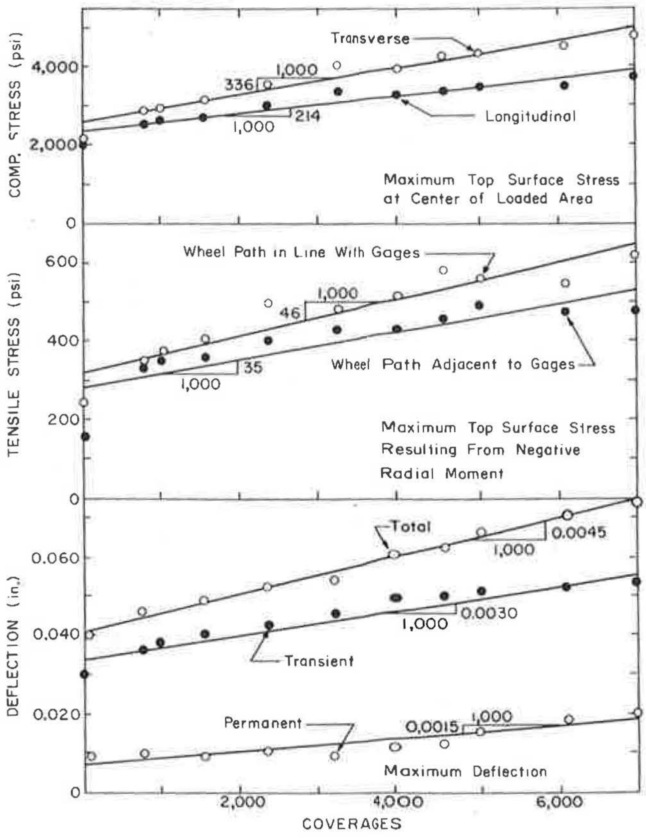

Figure 17. Typical stress and deflection values—slab 8.

Slab 16, cast on a cement-treated subbase with a modulus of 320 pci, did not fail after 14, 500 coverages of a 2206-lb load. The load was then increased to 3478 lb, or approximately that predicted by the PCA theoretical method as the top surface cracking load for a single, static application. After 19, 200 additional coverages, failure of the slab had not occurred and the test was discontinued. This demonstrates the advantage of a high-strength subbase under thin pavements. Stresses and deflections of slab 16 were much less than those predicted by theory. Measured strains at the load center indicated a bottom surface cracking load of 1570 lb as compared to the 1035-lb load predicted by Eq. 5. Therefore, the load behavior of slab 16 was not in agreement with Westergaard's theoretical analysis.

Strain and Deflection Data

Strain gages and deflectometers were connected to chart recording equipment to obtain continuous measurements as the load wheel approached and passed over their locations. At intervals of approximately 1000 moving load coverages on each slab, strains and deflections were continuously recorded as the load wheel traversed the entire loaded area. From these recordings, it was possible to determine (a) the maximum longitudinal and transverse compressive strain as the load wheel passed over the strain gages, (b) the maximum longitudinal tensile strain resulting from negative radial moment as the load wheel approached the strain gages, (c) the maximum transverse tensile strain resulting from negative radial moment as the load wheel passed the strain gages in an adjacent wheelpath, and (d) the maximum deflection as the load wheel passed over the deflectometer location. Stresses were computed from the measured strains using Eqs. 7 and 8.

Typical stress and deflection diagrams are shown in Figure 17. During the initial moving load coverage on slab 8, the top surface compressive stresses when the load wheel passed over the strain gages were 2000 and 2160 psi in the longitudinal and transverse directions respectively. These stresses were both greater than the theoretical value of 1880 psi computed by Westergaard's equation. Measured and theoretical values for the other test slabs are given in Table 8. As all slabs were loaded beyond elastic conditions, the measured values except for slab 16 were, as expected, greater than those computed by Westergaard's equations based on elastic theory. As previously discussed, the load behavior of slab 16 on the cement-treated subbase was not in agreement with Westergaard's theoretical analysis. Maximum top surface radial tensile stresses during the initial moving load coverage on slab 8 (Fig. 17) were 240 psi when the load wheel was in line with the strain gages and 156 psi when the load wheel was adjacent to the strain gages. These stresses were both less than the theoretical value of 246 psi computed by the PCA method using the relationships shown in Figure 14. Measured values for the other test slabs, as given in Table 8, were also generally less than the theoretical values with the exception of slab 10, which was unreinforced, and slab 12, which had only longitudinal prestress.

The initial measured deflection of slab 8 was 0.030 in., compared with a theoretical deflection of 0.037 in. computed by the PCA method using the relationships shown in Figure 13. Measured and theoretical deflections for the other test slabs are given in Table 8. As expected, measured moving load deflections were generally less than theoretical values based on static load conditions.

It can also be seen in Figure 17 that stresses and deflections increased with the number of load coverages. The average rate of increase was determined by computing the slope of the best-fit straight line for each set of data. For example, deflections of slab 8 increased at an average rate of 0.003 in. per 1000 load coverages until failure occurred. Rates of increase for the other test slabs are given in Table 8. These rates of increase were compared with fatigue factors computed by dividing the moving wheel load by the bottom surface cracking load of each slab. As shown in Figure 18, slabs tested at greater fatigue factors had generally greater rates of stress and deflection increases. It is also seen that the rates of increase for slabs 10 through 12 were much greater than those for slabs 1 through 9. Slab 10 was unreinforced, slab 11 had 12 psi, two-way prestress, and slab 12 had only longitudinal prestress, whereas slabs 1 through

TABLE 8

STRESSES AND DEFLECTIONS MEASURED DURING INITIAL COVERAGE OF MOVING LOAD

Slab No.	Wheel Load (lb)	Top Surface Compressive Stress at Load Center					Max. Top Surface Tensile Stress From Negative Radial Moment					Max. Transient Deflection		
		Measured (psi)		Theor. (psi)	Increase (psi/1000 cov.)		Measured (psi)		Theor. (psi)	Increase (psi/1000 cov.)		Measured (in.)	Theor. (in.)	Increase (in. /1000 cov.)
		Long.	Trans.		Long.	Trans.	In Line	Adj.		In Line	Adj.			
1	1730	2500	2940	2050	282	226	244	147	260	10	48	0. 051	0. 053	0. 008
2	1571	2050	2170	1910	534	723	206	210	240	319	188	0. 051	0. 046	0. 012
3	1571	2970	3590	1830	1057	515	131	189	230	28	172	0. 043	0. 039	0. 003
4	1410	2210	2450	1780	385	650	101	105	220	13	37	N. G.	0. 037	N. G.
5	1410	1930	1800	1640	17	140	156	110	190	6	63	0. 028	0. 031	0. 001
6	1730	2600	3160	2160	6140	4980	391	269	340	361	563	0. 051	0. 049	0. 080
7	1571	2490	2420	2090	1712	1692	298	214	320	148	257	0. 038	0. 044	0. 024
8	1571	2000	2160	1880	214	336	240	156	240	46	35	0. 030	0. 037	0. 003
9	1571	2240	2980	1790	193	276	160	210	230	37	63	0. 034	0. 035	0. 006
10	1571	2390	4030	1810	1990	2650	357	436	240	618	1240	0. 036	0. 037	0. 022
11	1571	2100	1820	1780	1328	1930	260	198	230	511	295	0. 029	0. 035	0. 014
12	1571	1960	1900	1840	858	3520	252	341	250	266	1300	0. 031	0. 038	0. 011
13	Static Load Test													
14	1730	2080	2040	1880	84	68	134	227	260	11	15	0. 029	0. 033	0. 001
15	2049	2940	2850	2310	1150	1700	332	357	430	122	207	0. 044	0. 045	0. 025
16	2206	1560	1320	2110	14	19	101	88	410	2	11	0. 016	0. 034	0. 004

N.G. = Deflectometer inoperable.

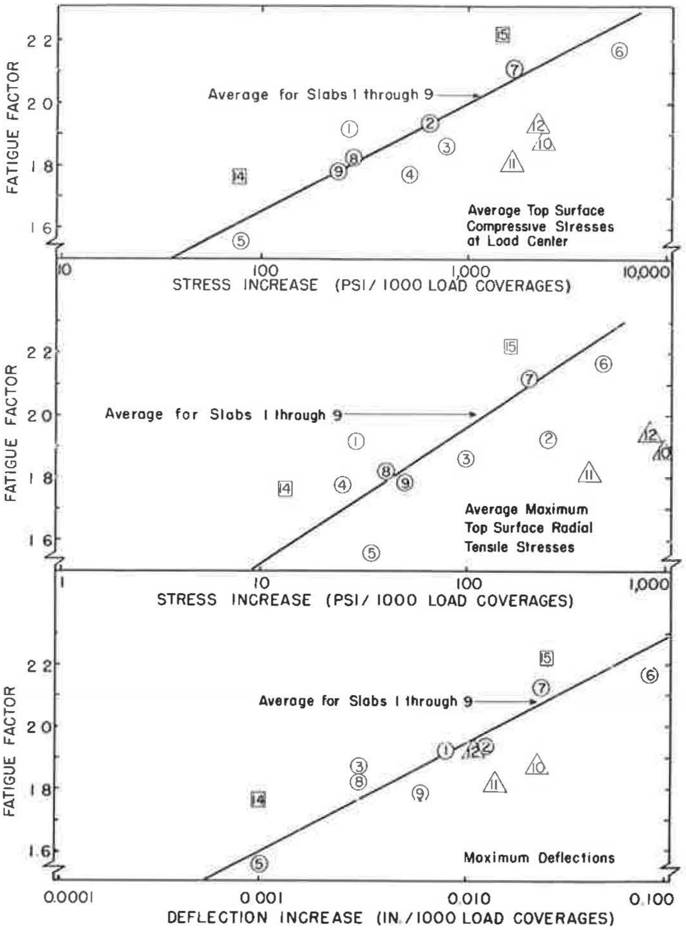

Figure 18. Effect of fatigue factor on rate of increase of slab stresses and deflections.

9 contained at least 33-psi, two-way prestress. In contrast, the rates of increase for slabs 14 and 15 were much less than those for slabs 1 through 9. These slabs were cast on a 6-in. thick granular subbase with an average k-value of 175 pci, whereas slabs 1 through 9 were cast on a clay subgrade with an average k-value of 100 pci.

Test data from all slabs were studied to determine the causes of prestressed concrete pavement failures. As shown in Table 8, none of the top surface tensile stresses resulting from negative radial moment was more than half the cracking stress during initial moving load applications. Therefore, slab failures were probably not caused by fatigue of the concrete in the top surface of the slab due to a repetition of radial tensile stresses. Rather, there appeared to be a progressive deterioration of the pavements caused by bottom surface cracks extending upward toward the top surface accompanied by increased deflections and a reduction in the concrete area needed to resist externally applied moments.

Relationship Between Model and Prototype

The model-size prestressed slabs used in this test program were purposely overloaded to obtain early failures. To indicate the degree of overloading, a comparison is made with a prototype prestressed concrete pavement. The following loading conditions and pavement properties are considered:

Load = 50, 000 lb applied repeatedly at interior locations,
Loaded area = 267 sq in.,
Slab thickness = 6 in.,
Concrete strength = 700 psi,
Minimum concrete prestress = 100 psi longitudinally and transversely,
Elastic modulus = 4, 000, 000 psi,
Poisson's ratio = 0.15, and
Subgrade modulus = 120 pci.

This prototype pavement has a radius of relative stiffness, L = 28.0 in., radius of loaded area, a = 9.2 in., $\alpha = a/L = 0.328$, and cracking moment, m_c = 4800 in. lb/in. From Eq. 5, where $m_c = 0.0527\ P_c(4 \log_{10} 1/\alpha + 1.069)$, the bottom cracking load, P_c, equals 30,200 lb and the fatigue factor, P/P_c, equals 1.66. From the curve in Figure 10B, approximately 13,500 coverages can be applied before failure occurs. Maximum deflections for initial load applications can be determined from Figure 13, because deflections predicted by these curves were in good agreement with measured deflections. For P/m_c = 10.4 and α = 0.328, the deflection, y, equals 0.077 in.

In this comparison, it should be noted that the fatigue curve shown in Figure 10B is based on an ultimate failure caused by loads applied at interior locations. A safety factor should be included in a practical design method for prestressed concrete pavements.

SUMMARY

To obtain information on the fatigue characteristics of prestressed concrete pavements, 16 pretensioned, cast-in-place slabs were load tested. The slabs were purposely overloaded to cause failure under repeated loading. The results are summarized in the following:

1. Moving loads with magnitudes greater than those causing bottom surface cracking were applied repeatedly to an interior area of 15 of the test slabs until failure occurred. Failure was characterized by a crumbling of the concrete in the top surface of the slab. For slabs that had sufficient longitudinal and transverse prestress, failures occurred soon after top surface cracking became visible. Only a few additional load coverages were necessary for the top slab surface to deteriorate from an uncracked to a complete failure condition. Relationships were established between load magnitude, prestressed pavement properties, and the number of coverages causing failure.
2. Strain and deflection data indicated that failures from the application of repeated moving loads were probably not caused by fatigue of the concrete in the top surface of the slab due to a repetition of radial tensile stresses. Rather, there appeared to be a progressive deterioration of the pavements caused by bottom surface cracks extending upward toward the top surface accompanied by increased deflections and a reduction in the concrete area needed to resist externally applied moments.
3. Static loads sufficient to cause top surface cracking were applied to two of the test slabs. Measured bottom surface cracking loads were accurately predicted by Westergaard's equation based on elastic theory. However, measured top surface cracking loads were greater than those predicted by existing methods of analysis for prestressed pavements.
4. Data from tests on slabs with varying magnitudes of prestress indicated that two-way prestress is required to avoid top surface cracking when relatively few moving loads greater than those causing bottom surface cracking are applied repeatedly at interior locations. Also, the minimum prestress required for prestressed concrete pavements to support repeated moving loads greater than those causing bottom surface cracking is approximately 30 psi.
5. Data from exploratory tests on slabs cast on foundations of different strengths indicated that an increase in the foundation strength resulted in an increase in the number of load coverages causing failure.
6. A fatigue factor, defined as moving wheel load divided by computed bottom surface cracking load, is suggested for evaluation of fatigue life of prestressed concrete

pavements. In practical design, this fatigue factor should be augmented by a suitable safety factor.

REFERENCES

1. Osawa, Y. Strength of Prestressed Concrete Pavements. Jour. Struct. Div., ASCE, Proc. Paper 3308, Vol. 88, No. ST5, p. 143-164, Oct. 1962; also, PCA Development Dept. Bulletin D57.
2. Christensen, A. P., and Janes, R. L. Load Tests on Thin Pretensioned Pavement Slabs. Highway Research Record 60, p. 77-94, 1964; also, PCA Development Dept. Bulletin D87.
3. Christensen, A. P. Load Tests on Post-Tensioned Pavement Slabs. Highway Research Record 60, p. 95-115, 1964; also, PCA Development Dept. Bulletin D88.
4. Hanson, N. W. Load Cells for Structural Testing. Jour. PCA RandD Labs., Vol. 1, No. 1, p. 40-44, 1959; also, PCA Development Dept. Bulletin D33.
5. Carlton, P. F., and Behrmann, R. M. Repetitive Loading Model Tests of Prestressed Rigid Pavement on a Low-Strength Subgrade. Corps of Engineers, Ohio River Div. Labs., Tech. Rept. No. 4-28, 1964.
6. Nowlen, W. J. Techniques and Equipment for Field Testing of Pavements. Jour. PCA R and D Labs., Vol. 6, No. 3, p. 43-52, Sept. 1964; also, PCA Development Dept. Bulletin D83.
7. Westergaard, H. M. New Formulas for Stresses in Concrete Pavements of Airfields. ASCE Proc. Vol. 75, p. 687-701, 1947.
8. Carlton, P. F. Small-Scale Model Studies of Prestressed Rigid Pavements for Military Airfields. Part II, Single-Wheel Loadings and Pre-Tensioned and Post-Tensioned Slabs. Corps of Engineers, Ohio River Div. Labs., Tech. Rept. No. 4-25, 1962.

PCA R and D Ser. 1317-1

A Twenty-Year Report on the Illinois Continuously Reinforced Pavement

JOHN E. BURKE and JAGAT S. DHAMRAIT, Illinois Division of Highways

THE possibility that continuous reinforcement could serve in portland cement concrete pavements as a means for eliminating or greatly reducing the numbers of transverse joints and open cracks that too often have become points of weakness in otherwise sound pavements was suggested many years ago. Continuous reinforcement was used as early as 1921 in the Columbia Pike experimental pavement near Washington, D.C. The next recorded use was in an experimental pavement built on US 40 west of Indianapolis in 1938.

With this background of experience to draw upon, the Illinois Division of Highways, in cooperation with the U.S. Bureau of Public Roads, in 1946 undertook an experimental study to develop more definite information on the relationships between performance and slab dimensions and steel amounts of continuously reinforced pavements. The establishment of the project in Illinois was generated largely through the efforts of W. R. Wooley of the Bureau of Public Roads and J. D. Lindsay of the Illinois Division of Highways.

The Illinois study has centered on an experimental continuously reinforced pavement constructed in 1947 and 1948 on US 40 west of Vandalia. The study was first described by Russell and Lindsay in a 1947 report (1). A second and third report were subsequently published (2, 3). The present paper, which covers a 20-year span of service of the pavement, is intended to be the final report of the study. While most of the experimental pavement is structurally capable of continuing to serve the heavy traffic now being served, the construction of paralleling pavements on the Interstate system soon will divert all but local traffic from the experimental pavement.

Construction of the Illinois experimental pavement began on September 25, 1947, and was completed on May 20, 1948. It was opened to traffic immediately upon completion. The experimental section of continuously reinforced pavement is 5½ miles long and divided into eight test sections, six of which are about 3500 ft long and two of which are about 4200 ft long. The pavement is 22 ft wide, and placed directly on natural fine-grained soil. The longitudinal reinforcement is continuous through each test section but not between sections. It consists of round deformed bars (ASTM 305-47T) meeting the requirements of ASTM designation A 16 for rail-steel bars. Transverse reinforcement consists of round deformed bars meeting ASTM designation A 15 for intermediate grade billet steel, chosen to permit welding of supporting steel to the bars. The transverse bars extend through the entire width of the pavement and the customary center joint has been omitted. Various details of the test sections, including the size and spacing of the steel reinforcement, are given in Table 1. The results of mill tests of the reinforcing steel are given in Table 2.

Four of the test sections are uniformly 7 in. thick and four are 8 in. in thickness. Four percentages of longitudinal steel, 0.3, 0.5, 0.7, and 1.0 percent, based on the gross cross-sectional area of the pavement, were used with each thickness of pavement. Both bar size and spacing were varied to obtain the different percentages of steel. The reinforcement bars were assembled as a continuous mat on the subgrade by means of chairs extending upward to approximately 3 in. below the finished surface of the pavement. Splice laps were maintained at a length equivalent to 30 bar diameters. Air-entrained concrete was deposited to full pavement thickness in a single operation and finished by means of a conventional spreader and finishing machine followed by the usual hand operations.

Paper sponsored by Committee on Rigid Pavement Design and presented at the 47th Annual Meeting.

TABLE 1

TEST SECTION DETAILS

Section	Length (ft)	Thickness (in.)	Longitudinal Steel		
			Diameter (in.)	Spacing (in.)	Percent
1	3504	7	$^3/_8$	$5^1/_4$	0.3
2	3504	7	$^1/_2$	$5^9/_{16}$	0.5
3	3504	7	$^5/_8$	$6^1/_4$	0.7
4	3504	8	$^3/_8$	$4^9/_{16}$	0.3
5	3504	8	$^1/_2$	$4^{13}/_{16}$	0.5
6	3508	8	$^5/_8$	$5^7/_{16}$	0.7
7	4233	8	$^3/_4$	$5^7/_{16}$	1.0
8	4233	7	$^3/_4$	$6^1/_4$	1.0

Note: Transverse reinforcement $^3/_8$-in. diameter round deformed bars at 12-in. centers in half of each section and at 18-in. centers in other half.

TABLE 2

RESULTS OF MILL TESTS OF REINFORCING STEEL

Bar No.*	No. of Tests	Yield Point (psi)	Tensile Strength (psi)	Elongation (%)
(a) Longitudinal Reinforcement				
3	6	78,701	119,469	14.3
4	14	66,223	107,355	14.5
5	17	70,778	127,759	12.5
6	21	70,157	124,888	11.7
(b) Transverse Reinforcement				
3	7	43,498	77,356	21.5

*Normal diameters of $^3/_8$, $^1/_2$, $^5/_8$, $^3/_4$ in., respectively.

A conventional concrete pavement constructed immediately west of the experimental pavement at about the same time and carrying approximately the same traffic has been used as a control section. This pavement was built to the Illinois standard design of the period and consists of a 10-in. slab reinforced with welded wire fabric at the rate of 78 lb per 100 sq ft, with doweled contraction joints spaced at 100-ft intervals and no expansion joints. Unlike the continuously reinforced pavement, which was placed directly on the natural fine-grained soil, the conventional pavement was placed on a 6-in. thickness of granular subbase.

The continuously reinforced pavement has been the subject of many observations and measurements from the time of its construction, and a relatively thorough record of its performance has been obtained. Certain pertinent observations and measurements have also been made on the adjoining conventional pavement.

TRANSVERSE CRACKING

Characteristic of continuously reinforced pavement are stress-relieving transverse cracks that develop at very close intervals. Crack development begins shortly after placement of the concrete as shrinkage takes place during setting and drying. It is an essential feature in the design of continuously reinforced pavement that the longitudinal steel reinforcement be properly distributed and of sufficient area to maintain the structural integrity of the slab by preventing the cracks from opening excessively during contraction of the concrete.

The crack frequencies near the free ends of long, continuously reinforced slabs would be expected to be similar to those in conventionally reinforced slabs. This proved to be

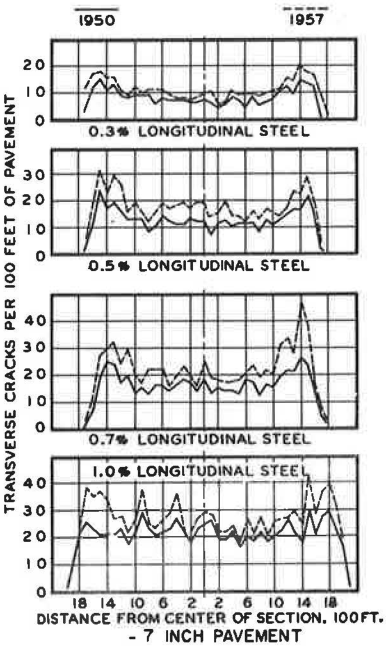

Figure 1. Crack frequency.

the case in the Illinois experiment and has been described in the earlier reports. The crack frequency was found to increase gradually away from the ends up to a distance of about 500 ft, to decrease over the next few hundred feet, then to become fairly stable through the longer center portion of the pavement. This is demonstrated in Figure 1.

Two relationships are of special significance in the consideration of transverse cracking of continuously reinforced pavements. One of these is that which exists between crack frequency and age, the other is that between crack frequency and steel percentage. Both are shown in Figures 2 and 3 for the 20-year period that the pavement has been under observation. With regard to the crack frequency and age relationship, it will be seen that the average crack interval decreased rather rapidly during the first 3 or 4 years following construction, after which the rate of decrease became and stayed very slow through the remainder of the 20 years of observation. It will be noted also that the rate of decrease has been slowest for the higher steel percentages.

A definite relationship between crack frequency and steel content is also obvious from Figures 2 and 3. At all ages at which observations of crack frequency have been made up to 20 years, the average crack frequency is consistently higher for each incremental increase in steel percentage. This relationship is in accord with theory regarding the behavior of long, continuously reinforced slabs subjected to temperature and moisture changes.

The magnitudes of the average crack intervals and of the changes in the average intervals that have taken place through the years are of interest. In Figures 2 and 3 it will be seen that, with the exception of the 0.3 percent steel sections, which have proven to be inadequate, average crack intervals ranged from about 5 to 9 ft at the end of 4 years and from about 5 to 8 ft at the end of 20 years.

Transverse Crack Width

It is essential that the steel reinforcement of continuously reinforced pavements hold the cracks to a narrow width if these pavements are to function properly. Open cracks can be expected to destroy the continuity afforded by aggregate interlock, a continuity

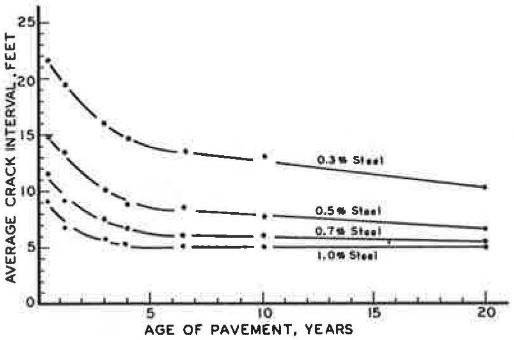

Figure 2. Relationship between crack interval and age, 7-in. pavements.

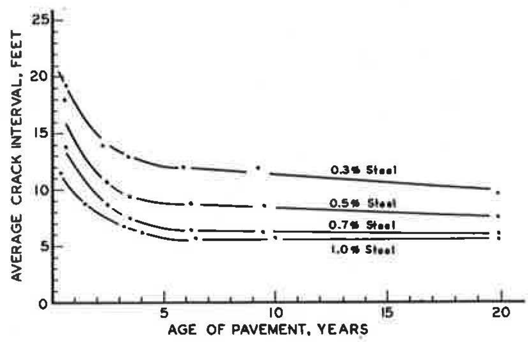

Figure 3. Relationship between crack interval and age, 8-in. pavements.

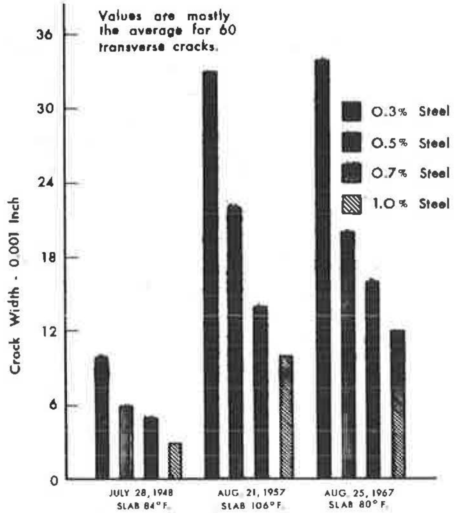

Figure 4. Crack width data, 7-in. pavements.

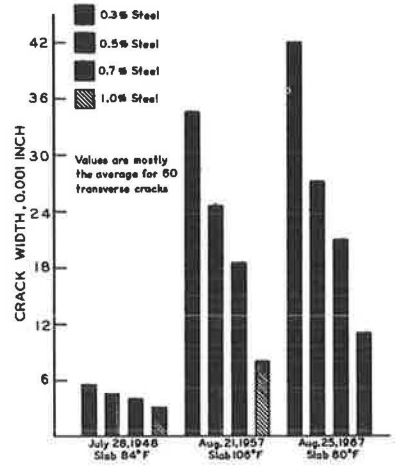

Figure 5. Crack width data, 8-in. pavements.

that is needed to prevent excessive flexing under traffic with resultant spalling of the concrete and rupture of the steel. Excessive openings can lead also to the infiltration of incompressible material, causing spalling and blowups; and to the entrance of water to reduce subgrade support and cause rusting of the steel. Failures that have taken place at some of the construction joints on the experimental project give ample evidence of the importance of aggregate interlock and the need for narrow crack openings.

Transverse crack openings in continuously reinforced pavements have been found to be not the same width for the entire thickness of the pavement and are difficult to measure. The apparent width observed by looking at the surface of the pavement is characteristically greater than the width through most of the depth of the crack.

Early in the study 60 transverse cracks were selected from each test section for periodic measurements of crack width with a measuring microscope capable of measuring to 0.001 in. Ten cracks were selected to represent the cracks at each end of each test section, another 10 to represent those at each quarter point, and 20 to represent those at the center of each section. The first crack width readings were made in July 1948.

In an attempt to obtain width readings most nearly representative of the true width of the cracks, the microscope was focused some distance down the crack. While the method is not considered to be extremely accurate, it is believed to have given fairly reliable results, although the widths may be somewhere in between those visible at the surface and the actual widths through the major portion of the pavement depth.

Average crack width data for the transverse cracks measured in each section are shown in Figure 4 for the 7-in. sections and in Figure 5 for the 8-in. sections for the years 1948, 1957, and 1967. Averages are for 60 cracks measured in each section, except for the 1967 measurements in which some patching and resurfacing removed a few cracks in the 0.3 percent steel sections from the observation. It will be noted that a correlation has existed between crack width and the percentage of longitudinal steel through 20 years of observation of the experimental pavement. Crack widths become progressively smaller as the percent of steel increases. It is also apparent that crack openings have become wider with time. The rate of increase, however, seems to have decreased with time.

The 7-in. sections, except for the 1.0 percent steel section, in 1948 showed somewhat wider crack openings than did the 8-in. sections. In 1967 this trend had become reversed. No explanation for these observed conditions is apparent.

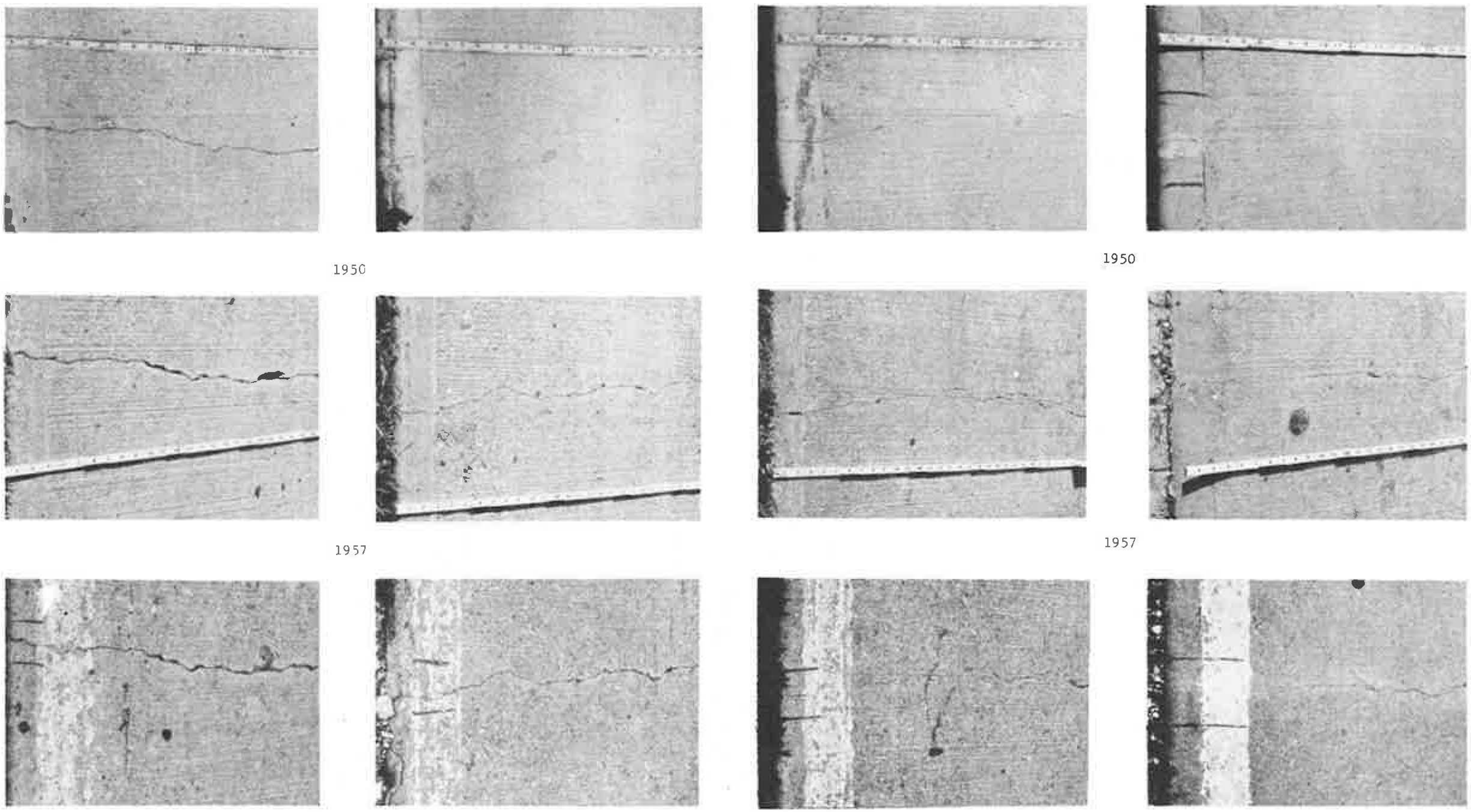

Figure 6. Typical transverse cracks in 7-in. sections.

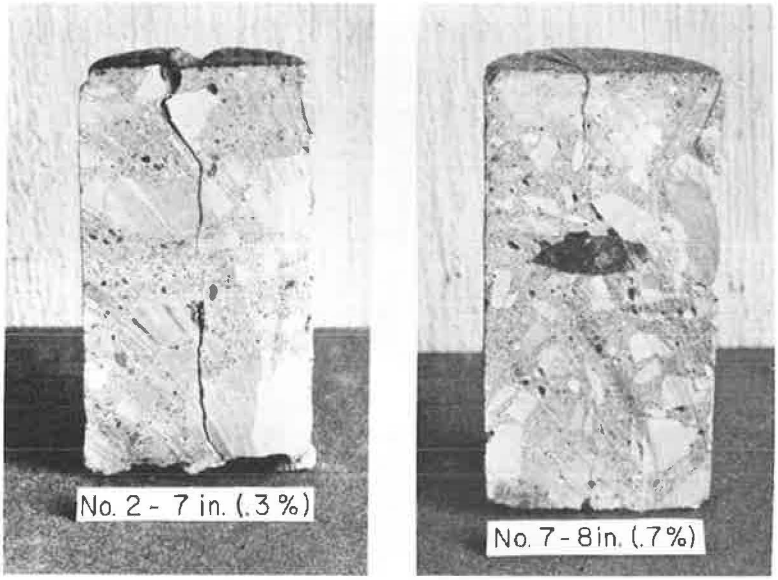

Figure 7. Condition of transverse cracks as seen in cores sawed to expose clean face of concrete.

The pavement surface at most of the cracks now shows occasional slight spalling. The amount and severity of the spall is related to the percentage of longitudinal reinforcement, and is most pronounced in the sections having 0.3 percent of steel. Little increase in spall has taken place after the first few years, and that which is visible after 20 years of service does not detract appreciably from the general appearance of the pavement, nor require any maintenance. The cracks are not visible to occupants of vehicles traveling the pavement at ordinary speeds. Photographs of a typical transverse crack in each of the sections of 7-in. pavement taken in 1950, 1957, and 1967 are shown in Figure 6.

The performance of the pavement at transverse cracks is considered to have been satisfactory except at a few locations in the 0.3 percent longitudinal steel sections, at two isolated locations in the 0.5 percent steel section of 7-in. thickness, and at cracks associated with the joints that have failed. Structural continuity at these locations obviously was lost; elsewhere, it has been maintained. While the crack openings are such that evidence of the infiltration of very fine material that might be speculated to have been moisture-deposited has been found, no signs of serious structural damage attributable to this source have been observed.

Photographs of cores taken through typical transverse cracks in 1967 are shown in Figure 7. It is apparent in the photographs that the crack openings become very fine a short distance below the surface, at about the level of the steel reinforcement, and remain fine to the bottom of the pavement. An examination of the cores showed a discoloration of the slab faces at the cracks, indicative of the infiltration of fine material. An examination of the condition of the steel reinforcement in the cores showed only a negligible amount of rusting.

The need to remove a portion of the experimental pavement in 1965 as part of a new construction contract provided an opportunity to observe closely the condition of the steel of a continuously reinforced pavement after 18 years of service. The new construction required the removal of 957 lineal feet of section 7, which is the 8-in. pavement with 1.0 percent of longitudinal steel.

The pavement of section 7 was considered to be in excellent condition at the time of removal. Transverse cracks appeared to be tight and showed only a minor amount of spalling at the edges. The longitudinal cracks that had formed through most of the section in the absence of a constructed center joint were somewhat wider than the transverse joints and showed somewhat more spalling.

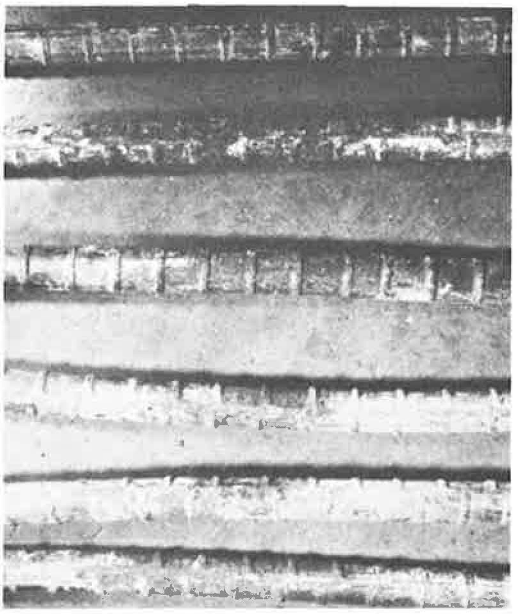

Figure 8. Condition of longitudinal reinforcement bars in the vicinity of transverse cracks.

Removal of the concrete confirmed previous observations that transverse cracks assume hair-like widths below the surface of the pavement. It was evident, too, that a thin layer of soil accumulates in most cracks.

Very slight rusting was found commonly to occur on the surface of the steel at transverse cracks. The rust stains imprinted on removed concrete appeared generally to progress no more than from 1 to 3 in. beyond the cracks. Beyond this point, no rust stain was evident. Observations of the condition of the steel deformation imprints in the concrete showed no evidence of slip between steel and concrete. No evidence of slippage was found in lap areas. The degree of rusting of the longitudinal steel at the transverse cracks was considered to be minor. Typical conditions of bars removed at transverse cracks are shown in Figure 8.

LONGITUDINAL CRACKS

As stated previously, the conventional center joint was omitted from the Illinois experimental continuously reinforced pavement. The No. 3 round deformed bars that were used as transverse reinforcement were extended across the entire width of the pavement spaced at 12-in. centers in half of each test section and at 18-in. centers in the other half.

Longitudinal cracks began to form in some of the test sections soon after construction and now involve most of the experimental pavement. Most of the longitudinal cracking does not coincide with the center of the pavement; however, it rarely meanders more than 3 ft away from the center. In a few instances two parallel longitudinal cracks are present; more rarely, there are three present.

Previous reports have described a relationship that appeared to exist between the time of year of construction and the extent of longitudinal cracking. The pavement constructed during the fall of 1947 showed a much earlier development of longitudinal cracking than did that constructed in the spring of 1948. As will be seen from Table 3, this relationship was still apparent at the end of 10 years. At the end of 20 years, longitudinal cracking has progressed to the extent that the relationship becomes less distinct. No explanation can be offered for the slower development of longitudinal cracks in the spring construction. No other consistent relationships between longitudinal cracking and the variables under consideration, including the two spacings of transverse steel, have been observable.

A considerable amount of surface spall is visible at some of the longitudinal cracks, and the cracks have the general appearance of being open wider than most of the transverse cracks.

In the removal of pavement from section 7 mentioned previously, the concrete was found to have been less protective of the steel, both transverse and longitudinal, at the longitudinal cracks. Transverse bars were often found to be quite severely rusted and sometimes broken at the longitudinal cracks. A "necking down" of the bars and an accompanying fracture in the form of a cup and cone noted in many instances indicate the possibility of tensile deformation before fracture. The stage of rusting of the fracture faces indicated in many instances that the steel had been broken for some time. Longitudinal bars exposed by the formation of longitudinal cracks also showed some rusting. An example appears in Figure 9.

TABLE 3

LONGITUDINAL CRACKING IN TEST SECTIONS

Pavement Thickness (in.)	Section No.	Dates Constructed (inclusive)	Longitudinal Steel (%)	Percent of Section Length Showing Longitudinal Cracking			
				March 1948	Dec. 1948	Sept. 1957	June 1967
7	1	9/25/47 9/30/47	0.3	0	22	57	77
	2	9/30/47 10/ 3/47	0.5	0	30	81	91
	3	10/ 3/47 10/ 7/47	0.7	0	39	63	76
	8	10/14/47 10/17/47	1.0	44	72	81	92
8	4	4/30/48 5/20/48	0.3	—	0	6	56
	5	4/26/48 4/30/48	0.5	—	0	6	84
	6	11/ 6/47 12/ 3/47 4/22/48 4/26/48	0.7	—	0	13	52
	7	10/14/47 10/17/47	1.0	48	68	76	87

The concrete that was removed was found to be of good quality and uniformly well consolidated around the steel. No durability defects were evident. Experience with the formation of longitudinal cracks and the subsequent behavior of the pavement at these cracks indicates that the center joint used in conventional pavement should be used also in continuously reinforced pavement.

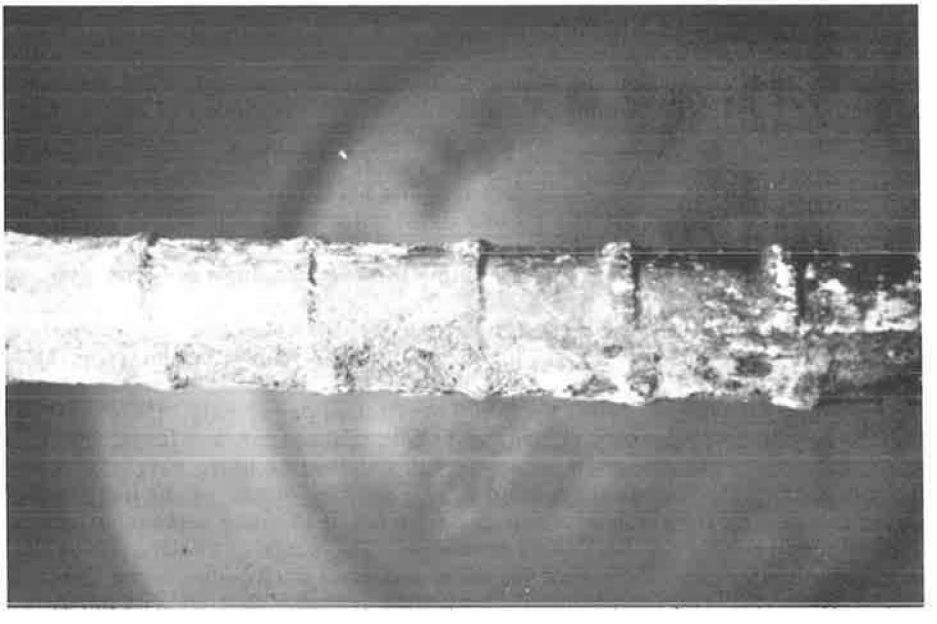

Figure 9. Condition of longitudinal reinforcement bar in the vicinity of a longitudinal crack.

PAVEMENT PUMPING

When the Illinois experimental continuously reinforced pavement was being planned over 20 years ago, it was believed that the absence of joints at closely spaced intervals, the tightness of the cracks, and an inherent flexibility, which would allow the pavement to adjust to minor subgrade movement, would be sufficient to control pumping of fine-grained soils and eliminate the need for a granular subbase. This was of special interest in reducing the total cost of construction. The pavement was therefore constructed on the natural fine-grained subgrade to test this belief. Most of the subgrade soils of the project are of the A-7-4, A-4, A-4-2, and A-6 groups, all known to be capable of pumping under the rainfall conditions (about 38 in. average annual precipitation) that exist at the location of the experimental project. The anticipated volume of heavy truck traffic is sufficient to produce pumping of conventional pavements.

At the time of preparation of the 10-year report, serious pumping had been noted at the expansion joints that were placed between the experimental sections, and at most of the construction joints placed at the end of each day's run in the sections with 0.3 and 0.5 percent steel. The construction joints in sections with 0.7 and 1.0 percent steel showed neither pumping nor faulting. The pumping, where found, was associated with considerable pavement distress that made patching necessary. Pumping also has been excessive at wide transverse cracks in the low-steel-content sections where the longitudinal reinforcement obviously had fractured.

A small amount of edge pumping not associated with joints or open transverse cracks has been observed on the 0.3 and 0.5 percent steel sections. No pavement failures have been observed that can be attributed to this pumping.

The expansion joints were installed in the pavement as part of the experimentation to assure that each test section would act independently. This usage would not be a part of normal construction of continuously reinforced pavement. However, the inherent weakness that is present at unprotected slab ends needs to be recognized when designing terminal systems at such locations as bridges and the ends of construction projects.

Construction work was terminated each day by the placing of a wood header. When concrete placement was resumed, the header was removed and the new concrete placed against the older concrete. No longitudinal reinforcement in addition to that of the normal design of the section was placed at these joints.

Pumping that was visible at construction joints in the 0.3 and 0.5 percent reinforcement sections at the time of the 10-year survey (at all construction joints in the 0.3 percent steel sections and two of seven in the 0.5 percent steel sections) has led subsequently to failure of the pavement at most of these locations, making patching necessary. The joints in the 0.7 and 1.0 percent reinforcement sections are still in good condition after 20 years of service.

The behavior of the pavement at the construction joints is interpreted as indicating a need for additional reinforcement at construction joints if performance equal to that away from the joints is to be achieved.

It has long been known that even slight pumping is likely to progress to a severe stage, and cannot be depended on to remain slight through the ordinary life of a pavement. Although pumping of serious consequence has been confined principally to joints and open cracks in the sections in which the steel content might be considered inadequate, it would appear prudent to include a protective subbase with continuously reinforced pavement where the use of a subbase would seem warranted with conventional pavement.

CHANGE IN LENGTH

The 4-in. expansion joints that were installed between test sections allowed each considerable freedom to change length. In the early years following construction, seasonal movements of 1 to 2 in. between summer and winter, with the sections being larger in the summer, were recorded. By the summer of 1957 all of the joints that were 4 in. wide when constructed were tightly closed. Large spalls indicative of excessive compression were observable at several of the joints and major repairs were required. Subsequently, patching has been required at almost all of these joints.

The cause of the growth of the pavement cannot be stated with certainty. Growth of the concrete itself cannot be excluded entirely as a possibility. However, some readings taken in 1957 between gage plugs which were not influenced by transverse cracks did not show much variation from initial readings, giving indication that growth of the concrete was not a major factor. The most logical explanation of the growth seems to be an incomplete closure of transverse cracks once they form. The finding of slight coatings of soil in crack openings supports this explanation.

The experience gained on this research project, where expansion joints were placed at 3,500 to 4,200-foot intervals, has not been sufficient to allow prediction of the behavior of larger runs, or of the requirements for expansion space. Nor can predictions be made of the amount of restraint that would be required to prevent growth of the pavement. Theoretical considerations suggest that considerable restraint is already present.

STRESSES IN LONGITUDINAL STEEL

For successful performance of continuously reinforced pavements, stresses in the steel must remain below the yield point; otherwise, the cracks would become excessively wide.

During the construction of the Illinois experimental pavement, SR-4 strain gages were mounted on selected longitudinal bars in the 7- and 8-in. sections containing 0.7 percent steel. Many stress readings were taken during the first month following construction, and periodically but less frequently thereafter.

In the fall 1947 construction, a maximum average stress of 62,400 psi was measured at a preformed transverse crack in January 1948. This is within a critical range of the 70, 000-psi yield point of the rail steel bars of the section. Stresses away from the crack never measured higher than 10,000 psi. In the spring 1948 construction, a maximum average stress of 42,000 psi was recorded the following January.

The strain gages became inoperable in a relatively short period of time and did not yield usable data beyond one season of contraction. During their period of operation, the gages showed that the tensile stress of the steel bears an inverse relationship to slab temperature, being high when the temperature is low and low when the temperature is high. The stress in the steel was seen to respond rapidly to daily changes in temperature, and to show considerable variation in a 24-hour period.

The strain gage study is reported in more detail in earlier reports, particularly in the 3-year performance report.

RIDING QUALITY

The Illinois experimental continuously reinforced pavement was judged from the beginning by Illinois Division of Highways engineers to offer better-than-average riding quality. As the years passed, it was agreed generally that the pavement was retaining this characteristic. Roughness measurements that were begun in 1957 when the Division of Highways acquired a Bureau of Public Roads-type roughometer have confirmed the earlier judgments.

The results of roughometer measurements made in 1957, and again in 1962, 1964, and 1967, are given in Table 4. Each value of the roughness index shown is the average for measurements made in each of the four wheelpaths of the two-lane pavement. It will be noted that, with the exception of the roughness index reading of 92 recorded for section 1 (7-in. thick, 0. 3 percent steel) in 1967, all readings, including those for the conventional pavement, indicate riding surfaces in the "smooth" and "very smooth" categories. It will be noted also that, with the exception of section 1, little change in riding quality has taken place during the 10 years that roughometer measurements have been made. Most of the experimental sections have been, and have remained, somewhat smoother than the conventional pavement.

PERFORMANCE

Carey and Irick (4) describe a system for estimating pavement ratings of serviceability and for determining performance by summarizing the serviceability record over

TABLE 4

ROUGHNESS INDEXES FOR EXPERIMENTAL PAVEMENT AND ADJOINING CONVENTIONAL PAVEMENT

Test Section	Steel Content (%)	Pavement Thickness (in.)	Roughness Index (in. per mi)			
			1957	1962	1964	1967
1	0.3	7	73	87	78	92
2	0.5	7	70	81	72	74
3	0.7	7	68	70	79	70
4	0.3	8	71	75	74	78
5	0.5	8	74	79	73	80
6	0.7	8	79	79	76	81
7	1.0	8	71	71	71	70
8	1.0	7	70	70	71	75
Conventional pavement			81	85	78	81

Note: Illinois Adjective Ratings for Roughness of Rigid Pavements:

Roughness Index Range	Adjective Rating
Less than 75	Very smooth
75-89	Smooth
90-124	Slightly rough
125-169	Rough
170-219	Very rough
220 or more	Unsatisfactory

a period of time. The system, for concrete pavements, involves measurements of riding quality, cracking, and patching.

Under the serviceability performance concept, the term "present serviceability" was chosen to represent how well a pavement is serving high-volume, high-speed, mixed truck and passenger vehicle traffic at a specific time. A mathematical index (present serviceability index) was developed for estimating subjective ratings of present serviceability through objective measurements taken on the pavement. The relationship, modified to make use of the roughness index as provided by the Illinois roughometer, can be expressed as follows:

$$P = 12.0 - 4.27 \log \overline{RI} - 0.09 \sqrt{C + P}$$

where

P = Present serviceability index;
$\overline{RI}$ = Roughness index in inches per mile as obtained by the Illinois roughometer;
C = Cracking in lineal feet per 1000 sq ft of pavement area, considering only those cracks that are open or spalled at the surface to a width of ¼ in. or more for at least half the crack length, and sealed cracks; and
P = Bituminous patching in square feet per 1000 sq ft of pavement area.

Under the present serviceability concept, the present serviceability rating is expressed on a scale between 0 and 5 as follows:

5
Very good
4
Good
3
Fair
2
Poor
1
Very poor
0

TABLE 5

PRESENT SERVICEABILITY PERFORMANCE OF EXPERIMENTAL PAVEMENT AND ADJOINING CONVENTIONAL PAVEMENT

Test Section	Steel Content (%)	Pavement Thickness (in.)	Year	Cracking (lin. ft/ 1000 sq ft)	Patching (sq ft/ (1000 sq ft)	Roughness Index (in./mi)	Present Serviceability Index
1	0.3	7	1962	0.3	143.6	87	2.6
			1964	14.3	172.5	78	2.7
			1967	45.4	153.0	92	2.4
2	0.5	7	1962	3.9	50.2	81	3.2
			1964	4.6	50.2	72	3.4
			1967	6.8	50.2	74	3.3
3	0.7	7	1962	0.0	0.0	70	4.0
			1964	0.0	0.0	69	4.2
			1967	3.7	0.0	70	4.0
4	0.3	8	1962	8.6	1.7	75	3.7
			1964	15.1	2.8	74	3.6
			1967	34.0	7.6	78	3.3
5	0.5	8	1962	0.5	0.0	79	3.8
			1964	0.3	0.5	73	4.0
			1967	6.3	0.2	80	3.6
6	0.7	8	1962	0.0	0.0	79	3.9
			1964	0.0	5.8	76	3.8
			1967	1.4	11.9	81	3.5
7	1.0	8	1962	0.0	0.0	71	4.1
			1964	0.0	0.3	71	4.1
			1967	0.4	1.9	70	4.0
8	1.0	7	1962	0.0	0.0	70	4.1
			1964	0.0	0.3	71	4.1
			1967	0.0	1.2	75	3.9
Conventional pavement			1962	0.3	0.0	85	3.7
			1964	3.2	0.1	78	3.8
			1967	4.0	0.2	81	3.7

Illinois highway engineers consider a present serviceability index (PSI) of 2.0 or lower to indicate a need for reconstruction or replacement of a two-lane pavement on the primary system.

The results of measurements made in 1962, 1964, and 1967 to compute the PSI's of the experimental pavements, and the computed PSI's, are given in Table 5. The computations and the PSI's for the conventional pavement are also presented.

As mentioned previously, failures in the continuously reinforced pavement sections other than a few that occurred in the 0.3 percent steel content sections and in the 0.5 percent steel section of 7-in. thickness (two isolated occurrences in the latter), have been confined to small areas associated with transverse joints. Evidences that total failure is imminent have been a widening of crack openings, spall at cracks and joints, excessive slab deflection, faulting, and pumping. A series of closely spaced transverse cracks usually becomes involved as failure progresses. If repairs are not made within a reasonable period of time, the individual slabs between cracks, or between cracks and joints when joints are involved, become broken into smaller sections and are pushed into the subgrade soil by passing traffic. The failures not associated with transverse joints that have occurred in the lower steel content sections have been similar except for the absence of joints.

Defects in the conventional pavement have been confined to a very limited number of transverse cracks that are of more than a simple stress-relieving nature and to some spalling at the edged full-depth metal plate contraction joints.

No pavement maintenance has been required in the sections of continuously reinforced pavement of higher steel content except in the few instances where joint weakness has been involved. Maintenance of the conventional control pavement has been limited almost entirely to a twice-yearly application of joint and crack seal. Maintenance cost records are not adequate for use in the study.

TABLE 6

VOLUME AND CHARACTER OF TRAFFIC ON EXPERIMENTAL PAVEMENT AND ADJOINING CONVENTIONAL PAVEMENT

Vehicle Type	Average Daily Traffic						
	1950	1953	1956	1959	1962	1965	1967
Passenger cars	2,060	3,100	2,885	3,000	3,400	4,500	4,810
Single-unit trucks	305	340	335	390	400	525	702
Multiple-unit trucks	300	760	1,030	1,210	1,100	1,475	1,768
Cumulative 18,000-lb single-axle equivalent loadings	207,000	737,000	1,400,000	2,178,000	2,889,000	3,524,000	4,273,000

It will be noted in Table 5 that during the past five years all of the experimental sections with the exception of section 1 (0.3 percent steel), and also the conventional pavement, have rated as "Good" or "Very Good" under the present serviceability concept. Section 1 has rated as "Fair." A fairly consistent relationship exists between steel content and PSI, with pavements of higher steel content showing higher PSI's. The relationship between pavement thickness and PSI is less consistent.

With the possible exception of the 7-in. section having 0.3 percent steel content, all experimental sections and the conventional pavement used as a control are continuing to offer satisfactory service 20 years after construction. Some of the experimental pavements may be providing slightly better service than the conventional pavement; some appear to be providing a slightly lesser degree of service. In general, the sections of greater steel content and greater thickness are providing the better service.

It will be recalled that the conventional pavement was placed on granular subbase while the experimental continuously reinforced pavements were placed on the natural fine-grained soil subgrade. It is also to be remembered that the principal failures in the continuously reinforced pavements took place at expansion joints installed only because of the experimental nature of the project, and at construction joints where the weakness undoubtedly can be overcome through the use of additional steel.

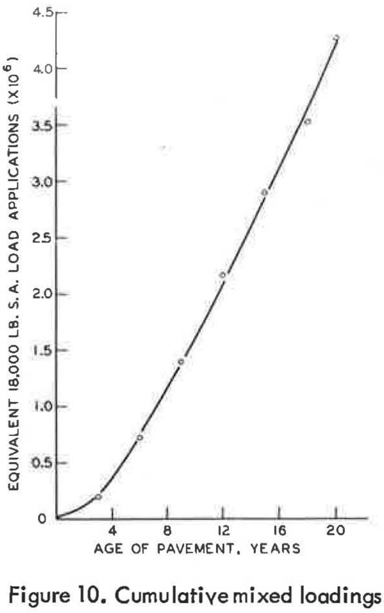

Figure 10. Cumulative mixed loadings.

TRAFFIC

The traffic that the experimental pavements have carried through the years is typical in volume and character of the traffic on many primary highways serving a high percentage of through truck traffic. Average daily traffic volumes for representative years, based on manual and machine counts, and shown separately for passenger cars, single-unit trucks, and multiple-unit trucks, are given in Table 6.

To evaluate the performance of a pavement in relation to the axle loadings to which it has been subjected, it is convenient to represent the varying axle loadings a pavement receives to a single loading having the same effect on the pavement structure. The AASHO performance equations are often used to accomplish this purpose.

Engineers of the Illinois Division of Highways and others have made use of loadometer data and traffic volume count and classification data in conjunction with the AASHO Road Test performance equations to estimate equivalent numbers of a standard axle loading to represent mixed loadings applied to pavements. Usually, the equivalency is established on the basis

of an 18,000-lb single-axle loading. The system used in Illinois was reported by Chastain (5).

Equivalent 18,000-lb single-axle loadings have been computed by Illinois procedures to represent cumulative mixed loadings applied to the experimental pavements beginning with the opening of the pavement to traffic. The results of these computations are shown in Figure 10.

SUMMARY OF PRINCIPAL FINDINGS

Observation of the behavior of the Illinois experimental continuously reinforced pavement and an adjacent conventional control pavement over a 20-year service period indicates the following:

1. Transverse cracks begin to develop at closely spaced intervals in continuously reinforced concrete pavements soon after construction. The number of cracks increases with age, but at a very slow rate after the first few years. Crack frequency increases with the amount of longitudinal steel.
2. For the sections under study, no strong differences occurred between the behavior of the 7-in. and 8-in. thicknesses of pavements.
3. Crack width is an important factor in the behavior of continuously reinforced pavements. Narrow cracks are essential to the maintenance of structural integrity of the pavement system. Crack width is a function of steel content, with lesser width being associated with higher steel content. Crack width increases slowly with age.
4. Slight spall begins to occur at transverse cracks in continuously reinforced pavement soon after construction. The spall increases with age and is related in amount inversely to the amount of longitudinal steel. Within the 20 years of service of the experimental pavements, spall at transverse cracks has not become a defect requiring maintenance.
5. Meandering longitudinal cracks will occur in a continuously reinforced pavement constructed wider than one lane without a center joint. Within the transverse steel contents investigated (No. 3 bars at 12- and 18-in. centers), the longitudinal cracks can become unsightly and a source of structural weakness within the expected life of a pavement.
6. Construction joints are potential sources of weakness at longitudinal steel contents of less than 0.7 percent.
7. When longitudinal movement is unrestrained, seasonal movements of continuously reinforced pavements can be expected, and also permanent increases in length with age. The cause of the growth was not apparent from examination of the existing experimental pavements.
8. Continuously reinforced pavements can be designed and constructed to serve at least as effectively as conventional pavements, and have the potential of overcoming the basic weakness that occurs at transverse joints of conventional pavements.
9. Continuously reinforced pavements can be built to, and can retain for long periods of time (at least 20 years), a high standard of surface smoothness.
10. While pumping has not been a major cause of failure of the experimental pavement during 20 years of service, it has nevertheless been sufficient in amount to indicate that continuous reinforcement is not a positive protection against pumping.

DESIGN RECOMMENDATIONS

Considering the traffic loadings to which the experimental continuously reinforced pavement has been subjected, it would appear that:

1. A 7-in. thickness of pavement will probably be adequate. However, unless future loadings can be predicted with a fair degree of certainty, conservatism would suggest an 8-in. thickness.
2. The selection of the amount of longitudinal steel requires considerable judgment. The general appearance of the 0.3 percent longitudinal steel sections after 20 years suggests that satisfactory performance through many more years cannot be expected.

The 0.5 percent steel sections are still performing well, and this steel content can be considered a minimum. The 0.7 percent steel sections have a generally better overall appearance (slightly less spall at transverse cracks), but to date can be said not to be performing significantly better. Again, conservatism would suggest a longitudinal steel content of perhaps 0.6 percent.

3. The extent and condition of the longitudinal cracks that developed in the absence of a center joint leave no doubt as to the need for a center joint.

4. The magnitude of the movement that has taken place at unrestrained section ends suggests that some further study of the control of slab ends is needed. Whether some form of restraint needs to be provided, or whether an improved expansion joint that will provide a positive means of load transfer or of slab support is needed, is not known.

5. Some form of subbase to control pumping is suggested.

REFERENCES

1. Russell, H. W., and Lindsay, J. D. An Experimental Continuously Reinforced Concrete Pavement in Illinois. HRB Proc., Vol. 27, p. 42-52, 1947.
2. Russell, H. W., and Lindsay, J. D. Three-Year Performance Report on Experimental Continuously Reinforced Concrete Pavement in Illinois. HRB Proc., Vol. 30, p. 45-61, 1950.
3. Lindsay, J. D. A Ten-Year Report on the Illinois Continuously Reinforced Pavement. HRB Bull. 214, p. 22-40, 1959.
4. Carey, W. N., Jr., and Irick, P. E. The Pavement Serviceability-Performance Concept. HRB Bull. 250, p. 40-58, 1960.
5. Chastain, W. E., Sr. Application of Road Test Formulas in Structural Design of Pavement. HRB Spec. Rept. 73, p. 299-313, 1962.

A Thickness Design Method for Concrete Pavements

A. C. ESTEP, Engineer of Design, and
PAUL I. WAGNER, Assistant Engineer of Design,
California Division of Highways

The thickness of portland cement concrete pavement and the underlying cement-treated layer was formerly based on California's Traffic Index, which was developed for use in flexible pavement design. Because the Traffic Index is computed from all predicted truck axle loadings, its use is not necessarily valid for rigid pavement designs. A design method was adapted from previous design work published by the Portland Cement Association, and adjusted empirically to fit past experience with satisfactory concrete pavements. A new method of predicting truck traffic from loadometer data and classified truck counts was developed. The design method is sensitive to variation in support value of the underlying soil, thickness of granular subbase, thickness of cement-treated base, modulus of rupture of the concrete, and truck traffic predicted for the design life of the pavement.

•THE design of pavements and their supporting layers is recognized as a gray area inhabited by specters of uncertainty and ghosts of old broken pavements. The only guiding light is past experience, which may be partially obscured by incomplete records of road life and maintenance.

Uncertainties result because it is often cheaper to overdesign instead of investing a large sum in an exhaustive soil survey. Engineers know that it is uneconomical to process natural deposits until aggregates have the uniformity of a factory product. They have experienced the frustrations that occur when trying to get uniform compaction on a project with varying soil types, bad weather, or inexperienced personnel.

The worst uncertainty is the prediction of future traffic that will use the pavement during its design life. Even if reliable classified truck counts are available on existing highways in the area, there are problems of assignment of this traffic to the new facility and expansion of the assigned traffic to the total volumes expected during the design period.

Despite the difficulties cited, it is not believed desirable to leave the determination of the structural elements of the roadbed entirely to rules in a manual or to the judgment of individuals. Engineering judgment is a necessary element in all good design, but in the interest of consistency and uniformity a definite design method should be used as a basic tool. Departures from the results of the strict use of a design process will have to be made on some individual projects, but such modifications should be justified in each instance.

California has adhered to these principles for many years in the design of flexible pavements, but the thicknesses of portland cement concrete pavements have been selected by a set of rules. In recent years, thicknesses were chosen that corresponded

Paper sponsored by Committee on Rigid Pavement Design.

to the depths of standard side forms. With almost all concrete pavement construction in the state now being performed by the slip-form method, there is no reason to be limited to any particular pavement thickness.

Previously, concrete pavement thickness and depth of cement-treated base was determined by rule from California's Traffic Index. The Traffic Index is calculated from total 5000-lb equivalent wheel loads, and this total is computed from estimated future truck traffic using axle weights of all trucks. This is an acceptable process in flexible pavement design, but it is not necessarily valid for rigid pavement determinations, which should be based only on those loads that produce a stress ratio in excess of 0.50. In this context, stress ratio is the stress produced by a given load divided by the modulus of rupture of the concrete determined by third-point loading at 28 days.

In the selection of concrete pavement thickness from the Traffic Index, no adjustment was made for variation in the support value of the natural soils encountered unless they were expansive. When the soils were expansive, the granular subbase layer was increased to provide sufficient weight in the total structural section to prevent future expansion of the underlying material with resulting loss in stability.

A design method was desired that would be sensitive to the support value of any natural materials that might be found when the soil survey was made for each project, and also would show the increase in support provided by the use of subbases and cement-treated bases. A minimum 0.50-ft thickness of granular subbase has been used when the R-value of the underlying soil is less than 40. Cement-treated bases have been used under nearly all concrete pavements for about 20 years. The purpose was to prevent erosion of the subgrade by pumping, and to provide extra support at the joints.

Another objective was to have a design method that would use the same loadometer data, soil survey reports, and classified truck counts used for flexible designs. Such a method would not be limited in range, and could result in either thicker or thinner designs than were previously considered. This would enhance the validity of the economic comparison made to determine the choice between rigid and flexible pavement for a given project.

After review of the literature, it was concluded that the simplest approach to developing a concrete design method would be to adapt the design data previously published by the Portland Cement Association to the traffic and soil survey information available for all California highway projects. It was also indicated that one or more factors in the new design method would have to be empirically adjusted to correlate the new designs and past experience with satisfactory concrete pavements.

DESIGN METHOD DEVELOPMENT

Fordyce and Packard (1) proposed a concrete highway pavement design procedure based on three major elements: analysis of stress due to moving loads, fatigue resulting from stress ratios exceeding 0.50, and load safety factors. They had prepared charts for single and tandem axle loads that gave stress relationships to axle loads, k-values (Westergaard's modulus of subgrade reaction), and slab depths. These charts were based on influence charts developed by Pickett and Ray (2) from Westergaard's theoretical analysis of concrete slab behavior. In order to use these stress charts, it was proposed to develop a procedure for determining k-values from the soil survey data obtained for each project. This will be discussed later in detail. The stress charts reproduced here as Figure 4 and Figure 5 have been redrawn with slab thickness lines for 0.05-ft increments instead of ½-in. increments. This was done to correspond to our standard practice of designing depths of flexible pavements and the underlying layers to the nearest 0.05 ft. This eliminates the need of converting inches to feet in quantity, profile, and construction staking calculations.

Fordyce and Packard (1) had proposed a new PCA fatigue curve for concrete pavements subject to flexural stresses. From this curve they had prepared a table of allowable stress repetitions to failure vs stress ratio as previously defined. This table was extended from the curve and used without further modification. It is presented here as Table 1.

TABLE 1

ALLOWABLE LOAD REPETITIONS FOR VARIOUS STRESS RATIOS

Stress Ratio	Allowable Repetitions	Stress Ratio	Allowable Repetitions
0.51	400,000	0.71	1,500
0.52	300,000	0.72	1,100
0.53	240,000	0.73	850
0.54	180,000	0.74	650
0.55	130,000	0.75	490
0.56	100,000	0.76	360
0.57	75,000	0.77	270
0.58	57,000	0.78	210
0.59	42,000	0.79	160
0.60	32,000	0.80	120
0.61	24,000	0.81	90
0.62	18,000	0.82	70
0.63	14,000	0.83	50
0.64	11,000	0.84	40
0.65	8,000	0.85	30
0.66	6,000	0.86	23
0.67	4,500	0.87	17
0.68	3,500	0.88	13
0.69	2,500	0.89	10
0.70	2,000	0.90	8

A later publication by the Portland Cement Association titled "Thickness Design for Concrete Pavements" (3) defined the entire design procedure.

R-Value vs k-Value

Soil surveys are made for all major projects with samples being obtained from various depths in the proposed cuts. R-values are determined for all of the soil types encountered using the Hveem Stabilometer and the procedures described in test method No. Calif. 301-F.

It was desired to establish a relationship between R-value and k-value for various soils in order to use the data normally available, and to avoid making plate bearing tests.

Such a relationship is shown in chart form in Figure 9 on page 36 of the "PCA Soil Primer" (4), but it is believed that this chart was constructed by comparing k-value and R-value with California Bearing Ratio (CBR). An investigation to establish a direct relationship was considered desirable, and there was no literature available indicating that this had ever been done.

This investigation was sponsored by the Bureau of Public Roads. The Portland Cement Association cooperated by sending their truck-mounted plate bearing test equipment to California from their laboratory at Skokie, Illinois. They performed tests and established k-values of basement soils at 20 locations. The test sites were compacted embankments with a minimum height of 6 ft, all located on going California highway contracts.

Standard ASTM D1196-64 procedure with static loading for highways was used with the preload modification used at the AASHO Road Test. The preload was sufficient to produce 0.01-in. deflection and was repeated four times. The Ames dials were then set with no load, and test loading procedure commenced.

R-value tests were performed on samples from each test site by the Materials and Research Department; k-values of the clay soils were corrected for eventual saturation by factors developed from consolidometer tests. The method used was Corps of Engineers Military Standard 621 A, Method 104.

When k-value was plotted vs R-value, no direct correlation was found as had been predicted. However, we were able to develop a curve which lies at or below the minimum k-values measured for various R-values. This curve is shown in Figure 1.

The use of this curve in the design of the structural sections for rigid pavements was consistent with our use of minimum R-values for flexible designs. The proposed method was not extremely sensitive to variations in k-value and any inaccuracies would result in more conservative designs.

Design k-Value

It was still necessary to develop a method of obtaining a design k-value which would indicate the increase in support provided by the use of granular subbases and cement-treated bases. The PCA published two charts for this purpose based on Burmister's method for analysis of two-layered systems (5). Both charts are conservative with respect to laboratory and field data. These charts were recomputed and redrawn so that they could be read to the nearest 0.05 ft in line with our other design practices. They are shown as Figures 2 and 3.

These charts are used one at a time to raise the k-value of the underlying soil to a new value at the top of the subbase, and then raise this value to the design k-value at

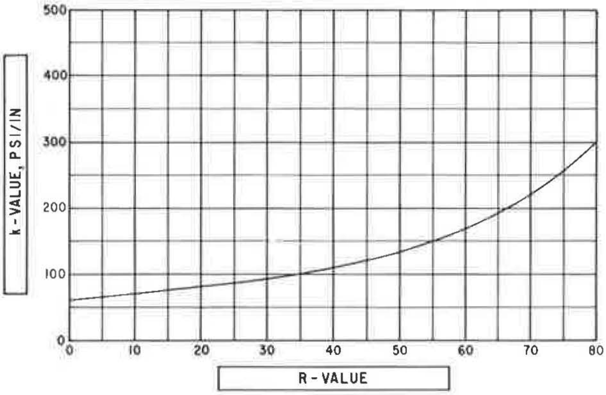

Figure 1. k-value vs R-value.

the top of the cement-treated base. If no subbase is used because of high k-value for the basement soil, just the second chart (Fig. 3) is used to obtain the design k-value.

Estimated Axle Load Repetitions

Loadometer surveys are made every year in California and truck counts, classified by the number of axles, are also made on a statewide basis.

Data from these two sources are used to compute total estimated 5000-lb equivalent wheel loads (EWL) for each project for a 20-year design period extending ahead from the estimated date of project completion. Traffic index is derived from this total EWL figure and used in the design of flexible pavements.

In developing EWL constants from loadometer data, it had been found expedient to use California Table W-4, All Main Rural and Urban (reproduced in the Appendix as Table 2), because the differences in truck traffic patterns between main rural and urban were insignificant for state highways. It also had been determined that despite

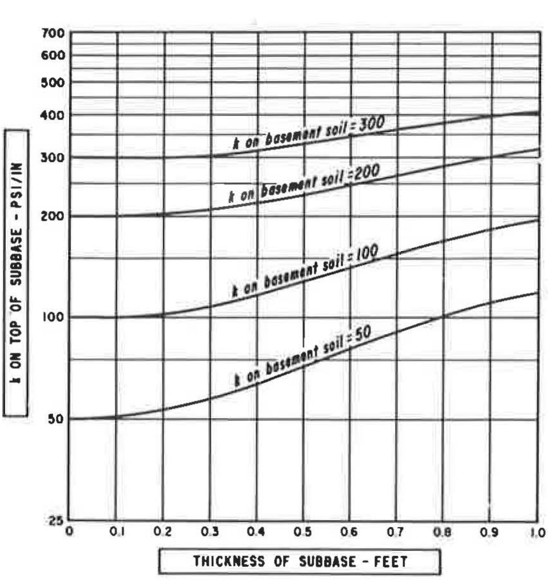

Figure 2. Effect of various thicknesses of granular subbases on k-values.

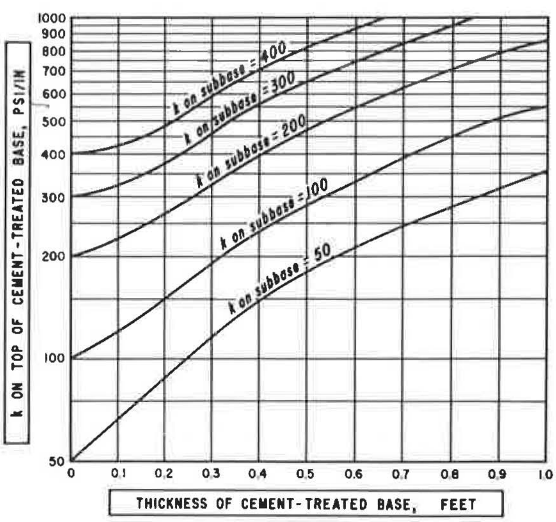

Figure 3. Effect of various thicknesses of cement-treated bases on k-values.

annual variation, averaging the last three years of loadometer data resulted in constants that had very little variation from year to year. Using four-, five-, and six-year averages did not make any significant difference, and one set of constants could be used for several years.

Truck traffic data are expanded to give the estimated average daily truck traffic for each axle type for the midyear of the design period for each project. These figures are multiplied by EWL constants to give the EWL for each truck type and these products are added to give the total EWL for the midyear of the design period. This total multiplied by the number of years gives the total EWL for the design period.

For rigid pavement design, it was logical to make use of the same estimated average daily truck figures. It also was desirable to use the same latest three years of loadometer data to develop constants for computing the total number of axle load repetitions expected during the design life period. These constants would have to be separated by axle classification to use the same traffic data, and by weight of axle increments to use the PCA stress charts.

The method developed for computing the repetition constants is outlined step by step as follows:

1. The numbers of axles weighed shown in each column of the loadometer sheets are expanded to the probable number by the ratio of axles counted to axles weighed. This is done for each weight category for both single and tandem axles.
2. All of the columns for each truck classification for three years are added across to give the total probable number of axles in each weight category for each truck type.
3. The proportion that each weight category bears to each truck type total for single axles is computed, and the same process is repeated for tandem axles.
4. The proportional figures for single axles in each truck type are multiplied by the ratio of number of single axles to number of trucks counted. The same type of computation is made for tandem axles.
5. To use the constants with average daily truck traffic figures, they are multiplied by 365 to give the repetitions for one year.
6. Because the traffic counts are reported for two-way traffic, the above figures are divided by two.
7. The final step is to multiply all the figures by 20 or whatever number of years is to be covered by the design life period.

An example of this computation is shown in detail for three-axle trucks in the Appendix. The final constants are shown in Table 4 in the Appendix, which is used to compute the total estimated axle load repetitions for each 2000-lb weight category for single and for tandem axles.

EVALUATION AND ADJUSTMENT

At this point, a complete design method had been developed, but it was necessary to evaluate the results and make any necessary empirical adjustments. Current data were obtained for four projects from each of the 11 highway districts. Considering inside and outside lanes separately where there were more than two lanes in each direction, it was possible to make 57 designs for comparison with results by the old procedure, asphalt concrete designs based on the same data, and the designs of existing satisfactory portland cement concrete pavements.

As previously mentioned, a minimum 0.50-ft thickness of granular subbase had been used when the R-value of the underlying soil was less than 40. This provides extra support, improved drainage, and a layer of material less susceptible to pumping than the basement soil. It was decided to continue this practice.

A 0.35-ft depth of cement-treated base was considered the practical minimum, and it was decided to use this value in the design process. A nominal thickness of 0.45 ft will be shown on the plans to take care of allowable construction tolerances. Variation in the depths of subbase and base can be accommodated by the method to take care of unusual situations, but these two depths were used in the comparisons.

Safety factors are usually used in concrete pavement design, and these have been referred to as load impact factors. Fordyce and Packard (1) suggest that in reality they are load safety factors and that term is used here. They suggested values ranging from 1.0 to 1.2 depending on the type of street or highway and the expected truck traffic characteristics. These same load safety factors are shown in the PCA's "Thickness Design for Concrete Pavements" (3).

These load safety factors were used in the first trial designs to evaluate the new method. The comparison showed lighter designs than had been used in pavements with a satisfactory road life of 20 to 35 years before resurfacing or replacement. An adjustment had to be made, and it was decided that changing the load safety factors was the best way to accomplish this since these factors are empirical judgments.

The load safety factors and types of facility finally were designated as follows:

LSF = 1.3 for the outside lanes of Interstate highways and other multilane projects with high predicted truck traffic;

LSF = 1.2 for the inside lanes of Insterstate highways and other multilane projects with high predicted truck traffic, and for all lanes of projects with moderate predicted truck traffic; and

LSF = 1.1 for minor highways, frontage roads or streets with low predicted truck traffic.

In the PCA publications, the 1.0 value is suggested for residential streets or rural roads carrying similar traffic. This category is outside state highway practice, and our adjustment expanded the two higher traffic categories to three classifications.

Another adjustment was made in the axle load values used to enter the stress charts. Originally the average value of the load increment was used, but this did not result in designs as heavy as past experience indicated were necessary. Using the top value of the increment, as shown in the PCA method, gave the desired results when combined with the increases in the load safety factors.

The final comparison indicated close agreement with many past designs using 0.75-ft depth of concrete pavement. In the heaviest traffic patterns for which 0.67-ft thickness had been used, the new method indicated 0.75-ft despite a 0.10-ft increase in the depth of cement-treated base. For the heaviest truck traffic reported, the new depth of pavement would be 0.80 ft. Finally, the new method provided a procedure for designing thinner pavements for lighter traffic patterns than had been considered previously for the use of portland cement concrete pavement.

DESIGN PROCEDURE

The project data required for the design process are the type of facility, number of lanes, minimum R-value of the basement soil, expected modulus of rupture of the concrete, and estimated average daily trucks for the midyear of the design period. With these data, the design procedure consists of the following steps, listed in order:

1. Determine the k-value of the basement soil.
2. Find the increased k-value due to the use of a granular subbase.
3. Determine the k-value at the top of the cement-treated base.
4. Choose a load safety factor and apply it to the design axle loads.
5. Select a trial thickness of pavement, and determine the stresses for each axle load for both single and tandem axle loads.
6. Compute the stress ratios by dividing each stress value by the modulus of rupture of the concrete.
7. Record the allowable axle load repetitions for each stress ratio.
8. Compute the estimated numbers of axle load repetitions for the design period.
9. Determine the percent each estimated number of repetitions bears to the allowable repetitions, and add these values to obtain the total percent fatigue resistance used.

Several pavement thicknesses should be tried and that trial thickness selected which shows the nearest to 100 percent fatigue used, but not to exceed 125 percent. The 125 percent upper limit is allowed because a change of 0.05 ft in pavement thickness results in a large change in percent fatigue used, and also because a conservative approach was used throughout the development of the method. Examples of this are the use of minimum k-values, the determination of modulus of rupture from 28-day specimens with third-point loading, and the use of high load safety factors.

To make it easy to follow the design procedure, an example is worked out in detail in the Appendix.

SUMMARY

This new method of portland cement concrete pavement design is sensitive to all of the variables now reflected in California's flexible pavement designs. It uses the same soil survey data, predicted truck traffic, and loadometer survey data. It provides structural sections that result in more valid economic comparisons with flexible designs for selection of pavement type. It produces designs that are nearer optimum and this should result in some economies. It provides extra thickness where unusual conditions of foundation or traffic are encountered.

It is believed that the adoption of this method of rigid pavement design eliminates the inadequacies of designing by arbitrary rules and raises the professional level of California's structural design activities.

REFERENCES

1. Fordyce, Phil, and Packard, R. G. Concrete Pavement Design. Presented to AASHO Committee on Design, October 22-25, 1963.
2. Pickett, Gerald, and Ray, Gordon K. Influence Charts for Concrete Pavements. Trans. ASCE, Paper No. 2425, Vol. 116, p. 49-73, 1951.
3. Thickness Design for Concrete Pavements. Concrete Information, HB 35, Portland Cement Association, 1966.
4. PCA Soil Primer. SC10-3, Portland Cement Association, 1962.
5. Burmister, D. M. The Theory of Stresses and Displacements in Layered Systems and Applications to Design of Airport Runways. HRB Proc. Vol. 23, p. 126-148, 1943.

Appendix

PROCEDURE FOR COMPUTING LOAD REPETITION CONSTANTS

The following example, which is shown for three-axle trucks only, illustrates the procedure for computing load repetition constants. The expansion of loadometer data is further limited to the year 1965, but the method is the same for each year of loadometer data used.

1. A portion of a loadometer Table W-4, All MR and U, is reproduced here, designated as Table 2. All three-axle truck columns are used and these are marked (A), (B), and (C). The numbers of axles weighed in the current column are expanded by the ratio of axles counted to axles weighed. In column (A), this would be 2805 divided by 765 equals 3.66667 for both single and tandem axles. This probable number factor is multiplied by the sum of the numbers of axles under 16 kips and each following number in the column. The figures are entered in column (7) on the work sheet designated Table 3. The same computation is made for tandem axles and the process is repeated for columns (B) and (C), using the appropriate probable number factors, and entered in columns (8) and (9). The same type of calculation was made for the years 1963 and 1964 and entered in columns (1) to (6) in Table 3.

2. The horizontal lines are added across to give the total probable numbers of axles in each weight category. These sums are recorded in column (10).

3. The proportion that each weight category of single axles bears to each single axle truck type total is computed, and the same process is repeated for tandem axles. In column (10), the first figure, 30,807.6, is divided by 32,586.0, and the quotient, 0.94542, is recorded as the first figure in column (11). This is repeated for every figure in column (10) for single axles. For tandem axles the divisor would be 6687.0.

4. The proportional figures for single axles in each truck type are multiplied by the ratio of number of single axles to number of trucks counted. In this example from column (10), 32,586 would be divided by 15,320 to give a factor of 2.12702. This factor multiplied by the proportional figures in column (11) gives the products recorded in column (12) for each weight category. The same type of computation is made for tandem axles, dividing 6687 by 15,320.

5. To use the constants with average daily truck traffic figures, they are multiplied by 365 to give the repetitions for one year.

6. Because the traffic counts are reported for two-way traffic, the figures are divided by two. Steps 5 and 6 are combined and all of the figures in column (12) are multiplied by 365 divided by 2 and recorded in column (13).

7. The final step is to multiply all of the figures by 20 or whatever number of years is to be covered by the design life period. These final constants are shown in column (14).

The final constants for all truck types and weight categories are shown in Table 4, which is used to compute the total estimated axle load repetitions for each 2-kip increment of axle loading.

DESIGN PROCEDURE

The design procedure is illustrated by an example with basic data assumed as follows:

- Minimum R-value of basement soil = 10
- Modulus of rupture of the concrete = 550 psi
- Outside lanes of Interstate 8-lane divided construction
- Expanded average daily trucks as tabulated below:

Vehicle Type	Outside Lanes
2-axle trucks	1870
3-axle trucks	1090
4-axle trucks	460
5-axle trucks	3480
6-axle trucks	110

1. Determine the k-value of the basement soil from Figure 1. Intersect the vertical line for an R-value of 10 with the curve, and read the k-value of 70 on the vertical scale reading to the nearest 5 units.

2. Assuming that there will be no problems with expansion, a 0.50-ft thickness of subbase will be used. In Figure 2, the k-value of 70 determined for the basement soil is interpolated logarithmically on the vertical line for 0.50 ft. The new k-value of 90 is read horizontally to the left on the vertical scale.

3. Determine the final design k-value from Figure 3. Using the k-value of 90 determined previously and the minimum cement-treated base thickness of 0.35 foot, a design k-value of 195 is read from the vertical scale on the left.

TABLE 2

S I N G L E   A X L E S

AXLE LOADS IN POUNDS AND 18 KIP AXLE EQUIVALENCY ITEMS	18 KIP AXLE EQUIVALENCY FACTOR RIGID PAVEMENT P=2.5 D=9	FLEXIBLE PAVEMENT P=2.5 SN=5	SINGLE UNIT TRUCKS: PANEL - PICKUP (UNDER ONE TON) CUR	PRI	2 - AXLE, 4 - TIRE CUR	PRI	2 - AXLE, 6 - TIRE CUR	PRI	(A) 3 - AXLE CUR	PRI	4 - AXLE CUR	PRI	SINGLE UNIT TRUCKS TOTAL PROBABLE NOS. CURRENT	PRIOR	TRACTOR (B) 3 - AXLE CUR	PRI	4 - CUR
UNDER 3000	0.0002	0.0002	7042	4781	293	411	621	419	5	1			116430	106930	13	3	9
3000- 6999	0.005	0.005	966	487	220	234	4849	3414	242	149			41357	33423	917	669	332
7000- 7999	0.026	0.032	4	2	2	5	550	361	135	119			3025	2834	371	268	197
8000-11999	0.082	0.087	1	2	4		1106	720	276	195			5990	5327	720	504	378
12000-15999	0.341	0.360	1				418	301	89	47		4	2189	2057	349	269	172
1 16000 18000	0.783	0.796			1		139	97	15	19			688	676	109	93	107
18001-20000	1.260	1.240					44	25	3	2			206	161	30	24	23
20001-21999	1.926	1.826					1	5		1			4	35	2		1
22000-23999	2.818	2.513						2						12			1
24000-25999	3.976	3.533															
26000-29999	6.289	5.389															
30000-34999	11.395	9.432															
~~UNKNOWN~~													~~12~~				
TOTAL SINGLE AXLES WEIGHED			8014	5272	520	650	7728	5344	765	533		4			2511	1830	1220
TOTAL SINGLE AXLES COUNTED			22952	11624	9990	5014	34142	32224	2805	2579	12	14	169901	151455	10662	10515	5624

1/CALIF LEGAL LIMIT. SINGLE AXLE 18000 POUNDS

T A N D E M   A X L E S

AXLE LOADS IN POUNDS AND 18 KIP AXLE EQUIVALENCY ITEMS	18 KIP AXLE EQUIVALENCY FACTOR RIGID PAVEMENT P=2.5 D=9	FLEXIBLE PAVEMENT P=2.5 SN=5	SINGLE UNIT TRUCKS: PANEL - PICKUP (UNDER ONE TON) CUR	PRI	2 - AXLE, 4 - TIRE CUR	PRI	2 - AXLE, 6 - TIRE CUR	PRI	3 - AXLE CUR	PRI	4 - AXLE CUR	PRI	SINGLE UNIT TRUCKS TOTAL PROBABLE NOS. CURRENT	PRIOR	TRACTOR 3 - AXLE CUR	PRI	4 - CUR
UNDER 6000	0.010	0.010							5	2			18	10			16
6000-11999	0.010	0.010							266	167			976	808			219
12000-17999	0.062	0.044							224	146			821	706			118
18000-23999	0.253	0.148							74	72			271	349			122
24000-29999	0.729	0.426							94	62			345	300			93
2 30000-32000	1.305	0.753							68	51			249	246			30
32001-33999	1.700	0.970							28	25			103	121			7
34000-35999	2.165	1.230							6	4			22	20			2
36000-37999	2.721	1.533															2
38000-39999	3.373	1.885								1		2		11			1
40000-41999	4.129	2.289								1				5			
42000-43999	4.997	2.749								1				5			
44000-45999	5.987	3.001															
46000-49999	7.725	4.170								1				5			
50000-54999	10.160	5.100															
~~UNKNOWN~~													~~4~~				
TOTAL TANDEM AXLES WEIGHED									765	533		2					610
TOTAL TANDEM AXLES COUNTED									2805	2579	6	7	2811	2586			2812

2/CALIF LEGAL LIMIT. TANDEM AXLES 32000 POUNDS

A L L   A X L E S

AXLE LOADS IN POUNDS AND 18 KIP AXLE EQUIVALENCY ITEMS	18 KIP AXLE EQUIVALENCY FACTOR RIGID PAVEMENT P=2.5 D=9	FLEXIBLE PAVEMENT P=2.5 SN=5	SINGLE UNIT TRUCKS: PANEL - PICKUP (UNDER ONE TON) CUR	PRI	2 - AXLE, 4 - TIRE CUR	PRI	2 - AXLE, 6 - TIRE CUR	PRI	3 - AXLE CUR	PRI	4 - AXLE CUR	PRI	SINGLE UNIT TRUCKS TOTAL PROBABLE NOS. CURRENT	PRIOR	TRACTOR - 3 - AXLE CUR	PRI	4 - AX CUR
UNDER 3000			7042	4781	293	411	621	419	26	8			116507	106964	13	3	45
3000- 6999			966	487	220	234	4849	3414	904	559			43785	35407	917	669	871
7000- 7999			4	2	2	5	550	361	291	220			3596	3322	371	268	264
8000-11999			1	2	4		1106	720	581	445			7109	6537	720	504	697
12000-15999			1				418	301	385	259		4	3274	3082	349	269	382
1 16000 18000					1		139	97	98	95			992	1045	109	93	148
18001-20000							44	25	10	6		4	232	194	30	24	30
20001-21999							1	5		5			4	54	2		1
22000-23999								2		2				22			1
24000-25999																	
26000-29999																	
30000-34999																	1

S T A T E OF C A L I F O R N I A

ABLE W-4 (ALL MR AND U)-- NUMBER OF AXLE LOADS OF VARIOUS MAGNITUDES OF LOADED AND EMPTY TRUCKS AND TRUCK COMBINATIONS OF EACH TYPE WEIGHED, THE PROBABLE NUMBER OF SUCH LOADS, AND THE EIGHTEEN KIP AXLE EQUIVALENTS OF EACH GENERAL TYPE AND OF ALL TYPES COUNTED AT 19 STATIONS FROM JUN. 15 TO AUG. 5, 1965, COMPARED TO CORRESPONDING DATA FOR 1964

S I N G L E A X L E S

- SEMITRAILER COMBINATIONS							TRUCK AND TRAILER COMBINATIONS												T W O - T R A I L E R C O M					
AXLE	5 - AXLE		6 - AXLE OR MORE		TRACTOR-SEMI-TRAILER TOTAL PROBABLE NOS.		(C) 3 - AXLE		4 - AXLE		5 - AXLE		6 - AXLE OR MORE		TRUCK-TRAILER TOTAL PROBABLE NOS.		4 - AXLE		5 - AXLE		6 - AXLE	7
PRI	CUR	PRI	CUR	PRI	CUR	PRI	CUR	PRI	CUR	PRI	CUR	PRI	CUR	PRI	CUR	PRI	CUR	PRI	CUR	PRI	CUR	PRI		
3	8	1		1	140	45			16	4	10	6	2		193	75	1		67	12	4	5		
275	132	106	3	8	6163	6071	7	1	65	63	892	658	14	17	5545	5192	3		2679	2080	51	33		
168	394	284		1	4609	4396	1		17	11	283	232	9	5	1641	1696	2		1085	869	22	16		
259	1402	1037	6	15	12417	11493	2	1	24	24	794	609	42	34	4382	4634			1506	1191	49	30		
135	23	11	1		2408	2338	2		22	17	257	194	10	15	1642	1554	5		1150	1064	20	17		
67	2	1		1	966	902		1	9	11	701	525	1	1	3515	3745	1		1757	1526	2	6		
26	1				239	276			3	6	235	175			1177	1236			299	220		2		
1					13	5					2	1			10	7			5	5		1		
					5															1				
934	1962	1440	10	26			12	3	156	136	3174	2400	78	72			12		8548	6968	148	110		
4960	10586	9933	88	118	26960	25526	984	270	1346	1164	15552	16248	223	457	18105	18139	132	56	53442	51164	790	734		

T A N D E M A X L E S

- SEMITRAILER COMBINATIONS							TRUCK AND TRAILER COMBINATIONS												T W O - T R A I L E R C O M					
XLE	5 - AXLE		6 - AXLE OR MORE		TRACTOR-SEMI-TRAILER TOTAL PROBABLE NOS.		3 - AXLE		4 - AXLE		5 - AXLE		6 - AXLE OR MORE		TRUCK-TRAILER TOTAL PROBABLE NOS.		4 - AXLE		5 - AXLE		6 - AXLE	7
PRI	CUR	PRI	CUR	PRI	CUR	PRI	CUR	PRI	CUR	PRI	CUR	PRI	CUR	PRI	CUR	PRI	CUR	PRI	CUR	PRI	CUR	PRI		
9	33	17		1	253	170							2	3	5	20					1	2		
166	1033	667	3	9	6646	5523				1	347	260	28	20	1771	1910			3	1	14	7		
99	582	466	3	6	3731	3767					100	72	14	5	526	520					10	6		
88	412	298		4	2800	2541			1	1	26	28	17	12	174	288					7	6		
73	891	740	3	4	5295	5510			3		249	183	13	24	1258	1396					6	12		
21	548	405	1	1	3123	2909					238	184	4	4	1175	1272			2		2	1		
5	276	178		1	1531	1259					81	59			396	400			1			1		
5	66	76			368	551					12	9		1	59	67								
1	21	16			123	116					7	5			34	34								
	3	4			21	27																		
	5	2			27	14																		
	3	1			16	7																		
	4				22																			
	2				11																			
467	3879	2870	10	26					4	2	1060	800	78	69					6	1	40	35		
2480	21067	19796	88	118	23967	22394			9	38	5184	5416	205	453	5398	5907			9	3	241	212		

A L L A X L E S

SEMITRAILER COMBINATIONS							TRUCK AND TRAILER COMBINATIONS										T W O - T R A I L E R C O M							
LE	5 - AXLE		6 - AXLE OR MORE		TRACTOR-SEMI-TRAILER TOTAL PROBABLE NOS.		3 - AXLE		4 - AXLE		5 - AXLE		6 - AXLE OR MORE		TRUCK-TRAILER TOTAL PROBABLE NOS.		4 - AXLE		5 - AXLE		6 - AXLE	7
PRI	CUR	PRI	CUR	PRI	CUR	PRI	CUR	PRI	CUR	PRI	CUR	PRI	CUR	PRI	CUR	PRI	CUR	PRI	CUR	PRI	CUR	PRI		
24	124	64	1	3	944	600			16	4	15	8	8	9	228	148	1		67	12	7	10		
661	2681	1861	8	29	22521	20322	7	1	65	65	1694	1245	79	60	9613	9484	3		2685	2082	84	50		
252	764	544	3	4	6962	6649	1		17	11	341	279	18	9	1940	2044	2		1085	869	31	21		
481	2566	1910	10	28	20276	18752	2	1	28	26	903	709	84	65	5040	5543			1506	1191	66	48		
313	2546	2026	7	10	17114	17227	2		26	17	1110	828	42	60	5922	6145	5		1153	1064	38	39		
104	884	675	1	4	5948	5761		1	9	11	962	737	3	6	4788	5216	1		1760	1526	2	9		
37	124	89			938	922			3	6	270	193		1	1346	1366			299	220		2		
1	16	9			100	67					4	1			19	7			5	5		1		
	12				70						1				5					1				
	2	2			11	14																		
	1				5																			
					5																			

TABLE 3

CALCULATIONS OF CONSTANTS FOR LOAD REPETITIONS FOR 20 YEARS FOR ONE VEHICLE - ADT (TRUCKS)

	LOADOMETER SURVEY DATA, TABLE W-4, ALL MR & U, PROBABLE NUMBERS (1)	(2)	(3)	(4)	(5)	(6)	(7)	(8)	(9)	(10)	(11)	(12)	(13)	(14)
TRUCK CLASS	3-AXLE									TOTAL	PRO-PORTION	× 2.12702	× 365/2	× 20
YEAR	1963			1964			1965							
PROB. NO. FACTOR	2.58531	2.31034	2.41667	4.60549	5.72792	73.00000	3.66667	4.24612	82.00000					
SINGLE AXLE LOADS-Kips: Under 16	1191.8	3890.6	84.6	2583.7	9124.6	146.0	2739.0	10063.8	984.0	30807.6	0.94542	2.01093	366.9947	7339.894
16-18	5.2	247.2	—	87.5	469.7	73.0	55.0	462.8	—	1400.4	0.04298	0.09142	16.6842	333.684
18-20	—	83.2	2.4	9.2	131.7	—	11.0	127.4		364.9	0.01120	0.02382	4.3472	86.944
20-22		—	—	4.6	—		—	8.5		13.1	0.00040	0.00085	0.1551	3.102
22-24				—				—		—	—	—	—	—
24-26														
26-28														
28-30														
30-32														
32-34														
34-35														
TOTAL PROBABLE NO.	1197.0	4221.0	87.0	2685.0	9726.0	219.0	2805.0	10662.0	984.0	32586.0	1.00000	2.12702	388.1812	7763.624
PROB. NO. FACTOR	2.58531	—	—	4.60549	—	—	3.66667	—	—	—	—	× 0.43649	—	—
TANDEM AXLE LOADS-Kips: Under 24	873.8	—	—	2031.0	—	—	2086.3	—	—	4991.1	0.74639	0.32579	59.4567	1189.134
24-26	47.4			96.7			114.9			259.0	0.03873	0.01691	3.0861	61.722
26-28	47.4			96.7			114.9			259.0	0.03873	0.01691	3.0861	61.722
28-30	47.4			96.7			114.9			259.0	0.03873	0.01690	3.0843	61.686
30-32	106.0			216.5			249.3			571.8	0.08551	0.03732	6.8109	136.218
32-34	54.3			106.0			102.7			263.0	0.03933	0.01717	3.1335	62.670
34-36	12.9			23.0			22.0			57.9	0.00866	0.00378	0.6898	13.796
36-38	2.6			—			—			2.6	0.00039	0.00017	0.0310	0.620
38-40	2.6			4.6						7.2	0.00108	0.00047	0.0858	1.716
40-42	2.6			4.6						7.2	0.00108	0.00047	0.0858	1.716
42-44	—			4.6						4.6	0.00069	0.00030	0.0548	1.096
44-46				—						—	—	—	—	—
46-48				2.3						2.3	0.00034	0.00015	0.0274	0.548
48-50				2.3						2.3	0.00034	0.00015	0.0274	0.548
TOTAL PROBABLE NO.	1197.0	—	—	2685.0	—	—	2805.0	—	—	6687.0	1.00000	0.43649	79.6596	1593.192
TOTAL AXLES										45960				
TOTAL VEHICLES										15320				

TABLE 4

CALCULATION OF 20-YEAR AXLE LOAD REPETITIONS

Dist.-Co.-Rte. 00-XX-00 P.M. 0.0/00.0 Exp. Auth. 000000 Inside Lanes ______ Outside Lanes X

Axle Loads Kips	2-Axle ADTT = 1870 Constant	Repetitions	3-Axle ADTT = 1090 Constant	Repetitions	4-Axle ADTT = 460 Constant	Repetitions	5-Axle ADTT = 3480 Constant	Repetitions	6-Axle ADTT = 110 Constant	Repetitions	Total 20-year Repetitions
SINGLE AXLE 35							0.09	313			313
34							0.17	592			592
32							0.17	592	—	—	592
30							—	—	14.3	1,573	1,573
28							—	—	14.3	1,573	1,573
26	—	—			—	—	—	—	28.7	3,157	3,157
24	1.75	3,273	—	—	3.72	1,711	0.44	1,531	—	—	6,515
22	5.91	11,052	3.10	3,379	9.20	4,232	6.28	21,854	27.4	3,014	43,531
20	40.4	75,548	86.9	94,721	202.	92,920	419.	1,458,120	60.4		
18	128.		334.		611.		2060.		349.		
TANDEM AXLE 50			0.55	600			0.55	1,914			2,514
48			0.55	600			0.55	1,914			2,514
46			—	—			1.50	5,220			5,220
44			1.10	1,199			1.75	6,090			7,289
42			1.72	1,875	—	—	3.80	13,224			15,099
40			1.72	1,875	5.66	2,604	3.29	11,449	—	—	15,928
38			0.62	676	9.09	4,181	22.6	78,648	28.8	3,168	86,673
36			13.8	15,042	12.1	5,566	78.3	272,484	61.4	6,754	299,846
34			62.7	68,343	35.4	16,284	262.	911,760	62.9		
32			136.		145.		576.		272.		
30			61.7		164.		292.		462.		
28			61.7		164.		292.		462.		
26			61.7		164.		292.		462.		

4. For this example, a load safety factor of 1.3 is appropriate for outside lanes. On the work sheet (Table 5), the axle load designations in column (1) are multiplied by 1.3 and the resulting figures are entered to the nearest 0.1 kip in column (2).

5. Stresses are determined from Figure 4 (a) for single axle loads and Figure 4 (b) for tandem axle loads. A trial thickness of pavement is first selected and then the charts are entered with each axle load in column (2) of the work sheets. The load line is followed to the horizontal line for the design k-value, thence vertically to the trial thickness line, and then horizontally to the stress scale on the left. The stress values are entered in column (3) of the work sheet to the nearest 5 psi.

To illustrate from the example, a trial depth of 0.75 ft was chosen for the outside lanes. The first axle load in column (2) is 45.5 kips. This value is interpolated in Figure 4 (a) and followed up to the combined k-value of 195 which also must be interpolated. From this point proceed vertically to an intersection with the 0.75-ft curve, thence horizontally left to the scale where a stress of 370 psi is read and recorded on the work sheet. Stresses are determined for each axle load in column (2) for single axles, and in the same manner for tandem axles using Figure 4(b).

TABLE 5
WORK SHEET

Dist.-Co.-Rte. 00-XX-00 P.M. 0.0 / 00.0

Outside Lanes 2 Inside Lanes — Exp. Auth. 000000

Load Safety Factor (L.S.F.) 1.3 Basement Soil R-Value 10

Subbase Depth 0.50' Cement-treated Base Depth 0.45'

k-Values: Basement 70 Subbase 90 C.T.B. 195

Modulus of Rupture (M.R.) 550 Trial Depth PCC 0.75'

(1) Axle Load Kips	(2) Axle Load x L.S.F. Kips	(3) Stress psi	(4) Stress Ratio Col. 3 / M.R.	(5) Allowable Repetitions No.	(6) Estimated Repetitions No.	(7) Fatigue Resistance Used %
SINGLE AXLE LOADS						
35	45.5	370	0.67	4,500	313	7
34	44.2	360	0.65	8,000	592	7
32	41.6	345	0.63	14,000	592	4
30	39.0	330	0.60	32,000	1,573	5
28	36.4	315	0.57	75,000	1,573	2
26	33.8	300	0.55	130,000	3,157	2
24	31.2	280	0.51	400,000	6,515	2
22	28.6	260	< 0.50	—	—	—
20	26.0					
18	23.4					
TANDEM AXLE LOADS						
50	65.0	340	0.62	18,000	2,514	14
48	62.4	330	0.60	32,000	2,514	8
46	59.8	320	0.58	57,000	5,220	9
44	57.2	310	0.56	100,000	7,289	7
42	54.6	295	0.54	180,000	15,099	8
40	52.0	285	0.52	300,000	15,928	5
38	49.4	275	0.50	—	—	—
36	46.8					
34	44.2					
32	41.6					
30	39.0					
28	36.4					
				Total % Fatigue Used		80

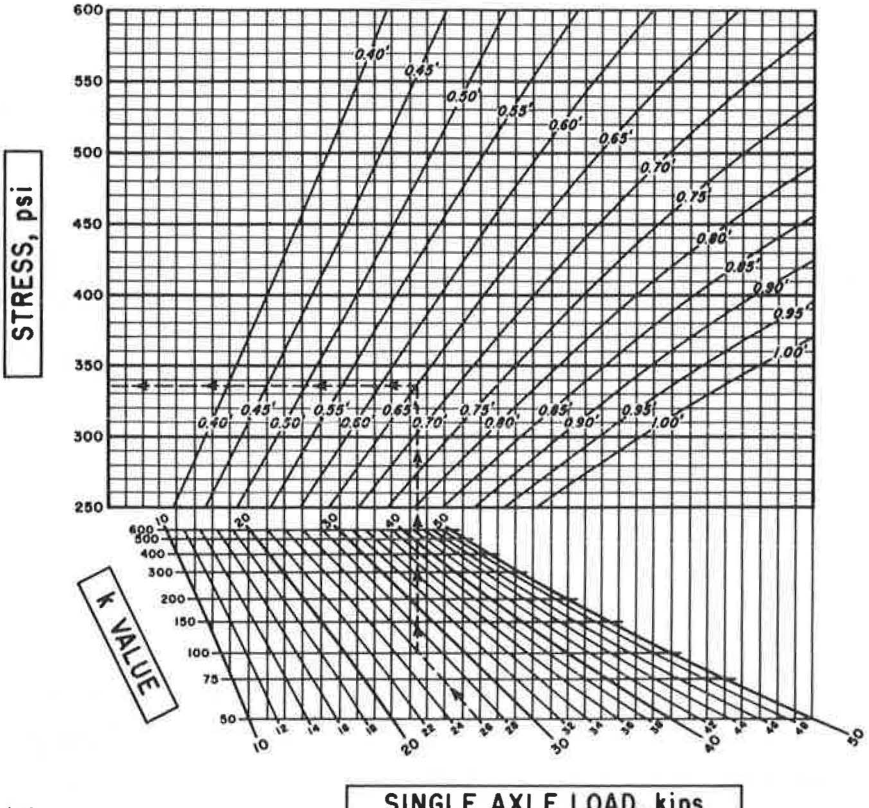

(a)

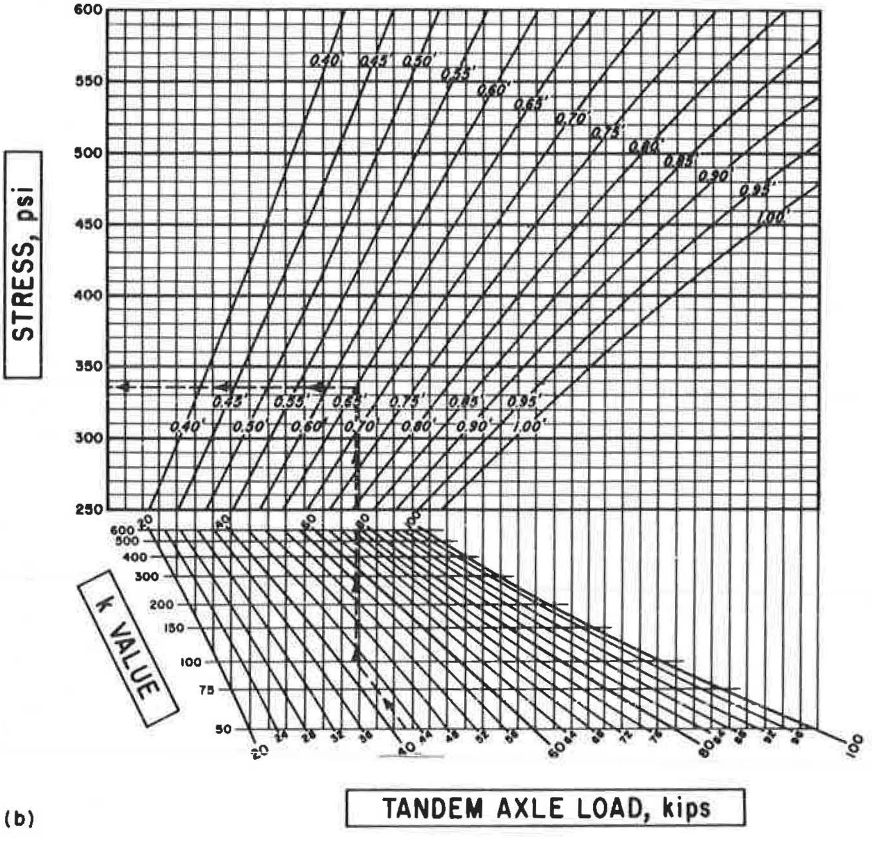

(b)

Figure 4. (a) Stress chart for single axle loads and (b) stress chart for tandem axle loads.

6. Each stress value is divided by the modulus of rupture (MR) and the ratios recorded to the nearest 0.01 in column (4) of the work sheet. No values less than 0.51 are used because allowable repetitions are unlimited for stress ratios of 0.50 or less. It can be seen from this that no stress values less than half the modulus of rupture need be determined in the preceding step.

7. Allowable repetitions are taken from Table 1 for each stress ratio and recorded in column (5).

8. Estimated numbers of axle load repetitions for 20 years are calculated on the form represented by Table 4. For this example, the expanded average daily trucks for each vehicle type are entered in the column headings. The average daily truck figure for each vehicle type is multiplied by each constant for that type and the repetition figure entered to the right of the constant. By adding the repetition figures on each horizontal line, the probable number of repetitions for each weight classification is obtained. The total 20-year repetitions are then entered in column (6) on the work sheet, Table 5.

9. For the final step, the estimated repetitions in column (6) are divided by the allowable repetitions in column (5) and multiplied by 100, which gives the percent fatigue resistance used. These figures are recorded to the nearest one percent in column (7) of the work sheet. Column (7) is totaled and the total percent fatigue used is recorded. Several thicknesses are tried and that trial thickness is selected which shows the nearest to 100 percent fatigue used but not to exceed 125 percent. With experience only two trials are necessary.

In this example, only the calculations for the finally selected design thickness of 0.75 ft for the outside lanes are shown to illustrate the method. A trial thickness of 0.70 ft also was used, but this lesser thickness showed a "fatigue resistance used" far in excess of 125 percent.